이학박사 학위논문

High order post-Newtonian computation of Orbits and Gravitational waves of Compact binaries with Spin and Eccentricity

자전과 이심률을 가지는 밀집 쌍성계의 궤도와 중력파에 대한 고차 포스트-뉴토니안 계산

2020년 8월

서울대학교 대학원

물리·천문학부 물리학전공

조 기 혁

High order post-Newtonian computation of Orbits and Gravitational waves of Compact binaries with Spin and Eccentricity

by

Gihyuk Cho
(whrlsos@snu.ac.kr)

A dissertation submitted in partial fulfillment of the requirements for the degree of

Doctor of Philosophy

in

Physics

in

Physics Program
Department of Physics and Astronomy
Seoul National University

Committee:

Professor	Sung-Chul Yoon
Professor	Woong-Tae Kim
Professor	Sunghoon Jung
Professor	Hyung Mok Lee
Doctor	Gungwon Kang

To my parents

ABSTRACT

Extracting accurate gravitational waveforms quickly is important work both in theory and in observation. Until now post-Newtonian (PN) theory is the unique framework to provide analytic expressions for equations of motion of binaries and corresponding gravitational waveforms. However, it is not trivial to solve the non-integrable PN equations of motion for a long duration. In order to resolve this problem, quasi-Keplerian parametrization with the variation of constants method is widely adopted. In this thesis, we present the derivation of the quasi-Keplerain parametrizations and the efficient algorithm to compute gravitational waveforms for the following three cases.

First, we derive fourth order post-Newtonian (4PN) contributions to Keplerian-type parametric solution for describing dynamics of non-spinning compact binaries in eccentric orbits. The underlying compact binary dynamics is described by the 4PN accurate near-zone local-in-time Arnowitt-Deser-Misner (ADM) Hamiltonian. We provide explicit expressions up to 4PN order for various orbital elements and functions of our parametric solution in terms of the conserved orbital energy, angular momentum, and the symmetric mass ratio. The resulting parametric solution is employed to obtain an updated inspiral, merger and ring-down waveform family to model the coalescence of non spinning black hole binaries in moderately eccentric orbits.

Second, we derive a fully analytic Keplerian-type parametrization solution to conservative motion of spinning binary in ADM gauge. This solution is able to describe the three-dimensional motion of binaries of arbitrary eccentricity, mass ratio, and initial configuration of spin angular momentum up to the leading order of post-Newtonian(PN) approximation and a linear order in a spin. Based on our results waveforms can be quickly computed with high accuracy.

Third, we derive third post-Newtonian (3PN) accurate the keplerian-type parametric solution to describe PN-accurate dynamics of non-spinning compact binaries in hyperbolic

orbits. The orbital elements and functions of the parametric solution are obtained in terms of the conserved 3PN accurate conserved orbital energy and angular momentum both in ADM and modified harmonic coordinates. Elegant checks are provided that include a modified analytic continuation prescription to obtain our independent hyperbolic parametric solution from its eccentric version. A prescription to model gravitational-wave polarization states for hyperbolic compact binaries experiencing 3.5PN-accurate orbital motion is presented that employs our 3PN-accurate parametric solution.
Finally we discuss the possible ways of improving these results in obtaining waveforms of compact binaries with various initial conditions.

Keywords: Post-Newtonian theory − Dynamics of compact binaries − Gravitational waves

Student Number: 2014-21341

Contents

List of Figures

List of Tables

Chapter 1

Introduction

The existence of gravitational waves (GWs), which had been a controversial issue for a quite long time, was first unraveled by Bondi et al. (1962) and Sachs (1962) by showing that Bondi-mass of asymptotically flat spacetime always decreases when spacetime is governed by the Einstein's field equations. Although Bodi-Sachs formalism proves the existence of gravitational radiation without relying on any approximation, it does not provide an explicit description of sources and corresponding gravitational waveform. After many attempts had been made, the first satisfying success to find explicit expressions for entire spacetime and gravitationally radiating systems was given by Blachet & Damour (1986) and Blanchet(1987) in the scheme of multipolar post-Minkowskian (MPM) approximation augmenting post-Newtonian (PN) approximation so as to cover the entire spacetime and finally model compact binary systems. (See Fig. 2.2). This particular framework is called *Blanchet-Damour-Iyer* (BDI) approach, which will be reviewed in Chapter 2. The mathematical foundation of BDI formalism had been achieved (See Blanchet (1993, 1998); Poujade and Blanchet (2002)) and the successive herculean efforts for extracting out explicit analytic expressions of dynamics of compact binaires have been made. (Most recent 4PN progresses are found in Marchand et al. (2017); Bernard et al. (2017); Marchand et al. (2020)). Besides BDI formalism, there are other approaches (*e.g.* Hamilotnian formalism

in Arnowitt-Deser-Misner (ADM) gauge (Schäfer and Jaranowski (2018)), and Effective field theory approach (Porto (2016)) in post-Newtonian efforts. Despite of technical differences in these approaches, every post-Newtonian efforts could be roughly seen as collective procedures where dynamics of interacting gravitational field and compact objects reduces down to dynamics of compact objects only, in the power series around $\frac{1}{c} = 0$.[1] The formal expansion in powers of $\frac{1}{c}$ corresponds to the following physical restrictions,

1. Distant from the objects, $\frac{Gm}{c^2 r} \ll 1$.[2]

2. Slowness of the objects, $\frac{v^2}{c^2} \ll 1$.

As a result, relative accelaration of a (non-spinning) compact binary is given in algebraically closed forms of relations of relative positions $\mathbf{x}$ and relative velocities $\dot{\mathbf{x}}$,

$$\ddot{\mathbf{x}} = \ddot{\mathbf{x}}_{\mathrm{N}}(\mathbf{x}) + \frac{1}{c^2}\ddot{\mathbf{x}}_{\mathrm{1PN}}(\mathbf{x}, \dot{\mathbf{x}}) + \frac{1}{c^4}\ddot{\mathbf{x}}_{\mathrm{2PN}}(\mathbf{x}, \dot{\mathbf{x}}) + \frac{1}{c^5}\ddot{\mathbf{x}}_{\mathrm{2.5PN}}(\mathbf{x}, \dot{\mathbf{x}}) + \frac{1}{c^6}\ddot{\mathbf{x}}_{\mathrm{3PN}}(\mathbf{x}, \dot{\mathbf{x}}) \cdots . \quad (1.1)$$

Therein, $\frac{1}{c^n}$ order term is called '$\frac{n}{2}$ PN contribution'. And note that there are no terms of $\frac{1}{c}$ and $\frac{1}{c^3}$ orders. Solving the PN equations of motion and getting $\mathbf{x}(t)$ should be the last task and which is the subject of this thesis. There are three different ways of treating the PN equations of motion as described below.

1. The first way should be a direct numerical integration using standard integrators. Note that the PN equations of motion are generally *non-linear* and *non-integrable*,[3] which leads

---

[1] c stands for the speed of light. And actually $\ln c$ terms arise in high order terms.

[2] G is Newton constant, m is a mass of the object and r is the cooridinate distance from the location of the compac object. Thus, getting too close to the object gives rise to divergence and breaks the convergence of the series. For example, blackholes in PN theory do not have apparent horizon.

[3] We call some ordinary/partial differential equations *integrable systems* when there is a systematic construction for value of a solution $f(t)$ at an arbitrary time t only by initial values $f(t_0)$. Otherwise, it is called *non-integrable*, i.e. $f(t - dt)$ must be needed (in the case of the first order ordinary differential equations).

to moderately high sensitivity on initial values, and hence loss of predictabiliy in long-time evolution. Additionally, since there is none of *first-integrals*, there is no way to have accumulating numerical errors under control, and which means that results of numerical integration are hardly reliable. Even though the integrability is restored if one is interested in the conservative part of the acceleration,[4] we must emphasize that the conservative acceleration is *not integrable* as an exact expression. It permits the conserved quantities only perturbatively. For the purpose of illustration, let $\mathcal{E}(\mathbf{x},\dot{\mathbf{x}}) = \mathcal{E}_{\rm N}(\mathbf{x},\dot{\mathbf{x}}) + \frac{1}{c^2}\mathcal{E}_{\rm 1PN}(\mathbf{x},\dot{\mathbf{x}})$ and $\ddot{\mathbf{x}} = \ddot{\mathbf{x}}_{\rm N}(\mathbf{x},\dot{\mathbf{x}}) + \frac{1}{c^2}\,\ddot{\mathbf{x}}_{\rm 1PN}(\mathbf{x},\dot{\mathbf{x}})$ be the 1PN accurate energy and acceleration expressions, and then a direct time derivation of $\mathcal{E}$ reveals that the energy (and angular momentum) conservation holds as long as the higher order ($\frac{1}{c^4}$ here) terms are consistently ignored,

$$\begin{aligned}
\frac{d\mathcal{E}}{dt} &= \frac{\partial\mathcal{E}}{\partial\mathbf{x}}\cdot\dot{\mathbf{x}} + \frac{\partial\mathcal{E}}{\partial\dot{\mathbf{x}}}\cdot\ddot{\mathbf{x}}\,,\\
&= \Big(\frac{\partial\mathcal{E}_{\rm N}}{\partial\mathbf{x}} + \frac{1}{c^2}\frac{\partial\mathcal{E}_{\rm 1PN}}{\partial\mathbf{x}}\Big)\cdot\dot{\mathbf{x}} + \Big(\frac{\partial\mathcal{E}_{\rm N}}{\partial\dot{\mathbf{x}}} + \frac{1}{c^2}\frac{\partial\mathcal{E}_{\rm 1PN}}{\partial\dot{\mathbf{x}}}\Big)\cdot\big(\ddot{\mathbf{x}}_{\rm N} + \frac{1}{c^2}\ddot{\mathbf{x}}_{\rm 1PN}\big)\,,\\
&= \underbrace{\Big(\frac{\partial\mathcal{E}_{\rm N}}{\partial\mathbf{x}}\cdot\dot{\mathbf{x}} + \frac{\partial\mathcal{E}_{\rm N}}{\partial\dot{\mathbf{x}}}\cdot\ddot{\mathbf{x}}_{\rm N}\Big) + \frac{1}{c^2}\Big(\frac{\partial\mathcal{E}_{\rm 1PN}}{\partial\mathbf{x}}\cdot\dot{\mathbf{x}} + \frac{\partial\mathcal{E}_{\rm 1PN}}{\partial\dot{\mathbf{x}}}\cdot\ddot{\mathbf{x}}_{\rm N}\Big)}_{=0} + \underbrace{\frac{1}{c^4}\frac{\partial\mathcal{E}_{\rm 1PN}}{\partial\dot{\mathbf{x}}}\cdot\ddot{\mathbf{x}}_{\rm 1PN}}_{\neq 0}\,,\\
&\neq 0\,.
\end{aligned} \tag{1.2}$$

When a standard integrator (*e.g.* Runge-Kutta scheme) integrates the PN equations of motion, it works as if the equations are exact and hence, non-integrable and less predictable. This feature gives rise to the overall error proportional to square of integration time $\sim t^2$. (See Lubich et al. (2010); Huang and Mei (2019) and there, the special numerical treatments have been considered.) What is even worse is that the dissipative part (*i.e.* not conservative), is completely non-integrable. Practically, we are interested in the

[4] In the case of non-spinning binaries, the conservative part is only given by picking up the even order contributions $\frac{1}{c^{2n}}$ in the acceleration. From 4PN order $\sim \frac{1}{c^8}$, the even order terms also include non-integrable contributions (or, non-linear dissipative part). If it is the case of non-spinning binaries, conservative precession of spinning binaries is not integrable except the leading order of spin-orbit interaction. See Cho and Lee (2019) for the first-integrals.

long-time evolution where the dissipation effects become very significant. Thus, we need to seek more efficient and accurate methodology to solve the PN equations of motion.

2. Another treatment could be getting regular perturbative solutions. Schemaically, putting the regular perturbative ansatz $\mathbf{x} = \mathbf{x}^R$,

$$\mathbf{x}^R(t) = \mathbf{x}_{\rm N}(t) + \frac{1}{c^2}\mathbf{x}_{\rm 1PN}(t) + \frac{1}{c^4}\mathbf{x}_{\rm 2PN}(t) + \frac{1}{c^5}\mathbf{x}_{\rm 2.5PN}(t) + \cdots , \tag{1.3}$$

into Eq. (1.1) and solve it order by order. This procedure looks formally simple and may reduce the complexity of equations than treating the whole equations. However, this method actually does not work. The failure is that the disspative terms of $\mathbf{x}^R(t)$, for instance $\frac{1}{c^5}\mathbf{x}_{\rm 2.5PN}(t)$, do not remain small but will bring a huge deviation from the leading order orbit $\mathbf{x}_{\rm N}(t)$ when one is interested in time evolution longer than *radiative-reaction* time scale, *i.e.* $t \sim \frac{\mathcal{E}}{\dot{\mathcal{E}}}$ even before the PN equation of motion gets divergent. This means that the regular perturbative series must diverge after a short time duration. Thus, we should abandon this regular perturbative scheme.

3. Finally, we introduce the osculating quasi-Keplerian parametrized orbital elements method which is adopted throughout this thesis. (The details could be found in Damour et al. (2004); Königsdörffer and Gopakumar (2006); Tanay et al. (2016). Here, we provide illustrative explanations for relatively low orders dynamics (< 5PN).) This method is designed to maximize the integrability of PN equations of motion, and first starts from a thorough classification of the post-Newtonian acceleration, into (perturbatively integrable) conservative part $\ddot{\mathbf{x}}_{\rm con}$ and (non-integrable) dissipative one $\ddot{\mathbf{x}}_{\rm diss}$,

$$\ddot{\mathbf{x}} = \ddot{\mathbf{x}}_{\rm con}(\mathbf{x}, \dot{\mathbf{x}}) + \epsilon\, \ddot{\mathbf{x}}_{\rm diss}(\mathbf{x}, \dot{\mathbf{x}}) \,, \tag{1.4}$$

where $\epsilon = \frac{\omega^2}{\dot{\omega}} \sim \mathcal{O}(1/c^5) \ll 1$,[5] a dimensionless parameter introduced to define a slow time $\hat{t} := \epsilon\, t$. As mentioned earlier, since $\ddot{\mathbf{x}} = \ddot{\mathbf{x}}_{\rm con}$ is integrable, let us assume that we

[5] where ω is an orbital speed of a binary.

have its solution as a function the coordinate time t, the energy $\mathcal{E}$ and the orbital angular momentum $\mathcal{J}$,

$$\mathbf{x}(t) = \mathbf{x}_{\rm con}\big(t,\, \mathcal{E},\, \mathcal{J},\, \frac{1}{c}\big) + \mathbf{c}\,, \tag{1.5a}$$

$$\dot{\mathbf{x}}(t) = \frac{\partial}{\partial t}\mathbf{x}_{\rm con}\big(t,\, \mathcal{E},\, \mathcal{J},\, \frac{1}{c}\big)\,, \tag{1.5b}$$

with a new vectorial constant $\mathbf{c}$ corresponding to initial positions. And allowing the constants to vary in the slow time $\hat{t}$ enables us to write the solution $\mathbf{x}^t, \dot{\mathbf{x}}^t$ of $\ddot{\mathbf{x}} = \ddot{\mathbf{x}}_{\rm con}(\mathbf{x}, \dot{\mathbf{x}}) + \epsilon\, \ddot{\mathbf{x}}_{\rm diss}(\mathbf{x}, \dot{\mathbf{x}})$ schematically as

$$\mathbf{x}^t(t) = \mathbf{x}_{\rm con}\big(t,\, \mathcal{E}(\hat{t}),\, \mathcal{J}(\hat{t}),\, \frac{1}{c}\big) + \mathbf{c}(\hat{t})\,, \tag{1.6a}$$

$$\dot{\mathbf{x}}^t(t) = \frac{\partial}{\partial t}\mathbf{x}_{\rm con}\big(t,\, \mathcal{E}(\hat{t}),\, \mathcal{J}(\hat{t}),\, \frac{1}{c}\big)\,. \tag{1.6b}$$

A direct derivative reveals that $\mathbf{x}^t(t)$ and $\dot{\mathbf{x}}^t(t)$ are really the solutions of the original differential equation

$$\begin{aligned}\ddot{\mathbf{x}}^t = \frac{d}{dt}\dot{\mathbf{x}}^t(t) &= \frac{\partial^2 \mathbf{x}_{\rm con}}{\partial t^2} + \epsilon\left(\frac{\partial^2 \mathbf{x}_{\rm con}}{\partial t\, \partial \mathcal{E}}\,\frac{d\mathcal{E}}{d\hat{t}} + \frac{\partial^2 \mathbf{x}_{\rm con}}{\partial t\, \partial \mathcal{J}}\,\frac{d\mathcal{J}}{d\hat{t}}\right), \\ &= \ddot{\mathbf{x}}_{\rm con}(\mathbf{x}^t, \dot{\mathbf{x}}^t) + \epsilon\, \ddot{\mathbf{x}}_{\rm diss}(\mathbf{x}^t, \dot{\mathbf{x}}^t)\,, \end{aligned} \tag{1.7}$$

by invoking the fact that $\frac{\partial^2 \mathbf{x}_{\rm con}}{\partial\, t^2} = \ddot{\mathbf{x}}_{\rm con}(\mathbf{x}^t, \dot{\mathbf{x}}^t)$ and $\frac{\partial^2 \mathbf{x}_{\rm con}}{\partial t \partial \mathcal{E}}\frac{dE}{d\hat{t}} + \frac{\partial^2 \mathbf{x}_{\rm con}}{\partial t \partial \mathcal{J}}\frac{dJ}{d\hat{t}} = \ddot{\mathbf{x}}_{\rm diss}(\mathbf{x}^t, \dot{\mathbf{x}}^t)$ hold by the construction. Thus it is assured that $\mathbf{x}^t$ provides the very solution of Eq. (1.4) as long as $\frac{d\mathbf{c}}{d\hat{t}} = -\frac{\partial \mathbf{x}_{\rm con}}{\partial \mathcal{E}}\frac{d\mathcal{E}}{d\hat{t}} - \frac{\partial \mathbf{x}_{\rm con}}{\partial \mathcal{J}}\frac{d\mathcal{J}}{d\hat{t}}$ holds additionally. To see further advatanges, we formally expand $\mathbf{x}_{\rm con}$ in powers of $1/c^2$ (no odd order terms appear here) preventing the slow time $\hat{t} \sim \frac{t}{c^5}$ from expanded,

$$\mathbf{x}^t = \mathbf{x}_{\rm N}(t, \mathcal{E}(\hat{t}),\, \mathcal{J}(\hat{t})) + \frac{1}{c^2}\mathbf{x}_{\rm 1PN}(t, \mathcal{E}(\hat{t}),\, \mathcal{J}(\hat{t})) + \frac{1}{c^4}\mathbf{x}_{\rm 2PN}(t, \mathcal{E}(\hat{t}),\, \mathcal{J}(\hat{t})) + \cdots\,. \tag{1.8}$$

This ansatz allows us to solve integrable differential equations order by order, and results in analytic solutions (*i.e.* quasi-Keplerian parametrizations) only via elementary functions. This perturbation series does not break down even after long time evolution as long as the

PN equations of motion Eq.(1.1) hold. (See Eqs. (3.21). Every PN corrections there are in the form of $\sin n\nu$, and hence only oscillate around the Newtonian order contribution.) Furthermore, another advantage is seen when solving $\frac{d\mathcal{E}}{d\hat{t}} = \frac{d\mathcal{E}}{d\hat{t}}(\mathcal{E}, \mathcal{J})$ and $\frac{d\mathcal{J}}{d\hat{t}} = \frac{d\mathcal{J}}{d\hat{t}}(\mathcal{E}, \mathcal{J})$ to get $\mathcal{E}(\hat{t})$ and $\mathcal{J}(\hat{t})$ for incorporating (adiabatic) radiation-reactive effects. The evolution of the first-integrals is less sensitive than the direct integration of the disspative accelerations $\mathbf{x}_{\rm diss}$ to initial values as seen in Fig.(1.1). One can find that a smalll difference (1%) of initial position leads to a big difference of final positions caused by 2.5PN radiation reaction after radiation-reaction time scale. On the other hand, time evolution of the difference of two eccentricities remains small during the same period. And this could be also verified by the fact that adiatbatic process of radiation reaction permits a first integral, *i.e.* it is an integrable system. For instance, let us consider the Newtonian dissipative coupled equations of ω and e,[6]

$$\frac{d\omega}{dt} = \eta\,\frac{\omega^{11/3}}{5\,(1-e^2)^{7/2}}\big(96 + 292\,e^2 + 37\,e^4\big)\,, \tag{1.9a}$$

$$\frac{de}{dt} = -\eta\,\frac{\omega^{8/3}\,e}{15\,(1-e^2)^{5/2}}\big(304 + 121\,e^2\big)\,. \tag{1.9b}$$

Despite of ignorance of closed form solutions, at least one is able to find that the following quantity is conserved,

$$\frac{\omega\,(304 + 121\,e^2)^{1305/2299}\,e^{18/19}}{(1-e^2)^{3/2}}\,. \tag{1.10}$$

Hence, we can conclude that solving radiation reaction effects in terms of time-evolution of conserved quantities rather than in terms of orbital variables (such as positions, velocities) will maximize the integrability and minimize the sensitivity of systems on initial values , and hence keep the systems predictable as far as possible.

---

[6] ω is a secular orbital frequency of a binary and e is an eccetricity.

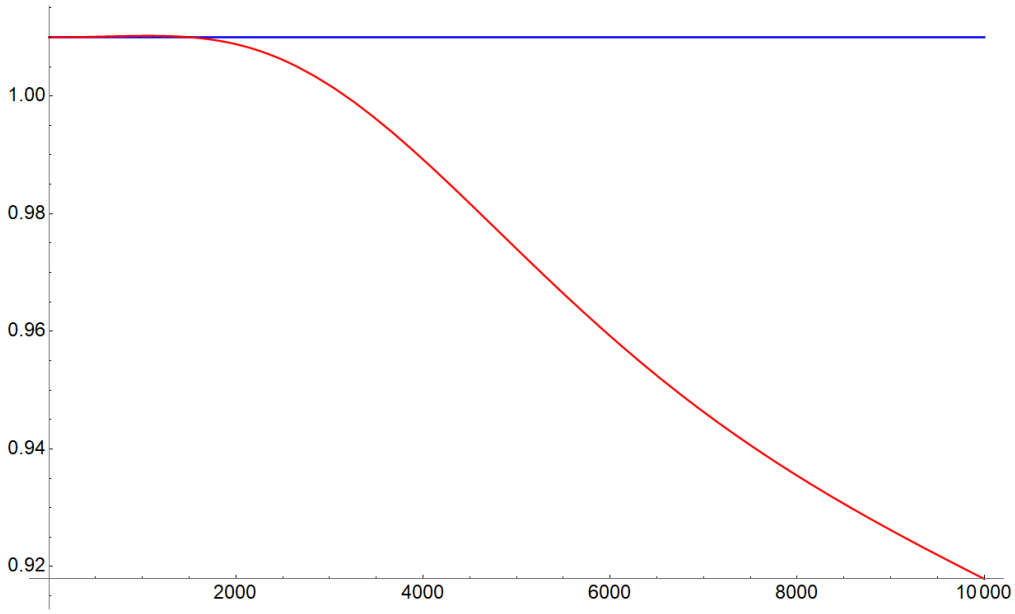

Figure 1.1 The ratios of two dissipative solutions with 1% difference in intial values are presented. The red line represents the ratio of x component of two solutions of 2.5PN term of Eq.(1.1) . It is clearly shown that 1% of initial difference gets magnified and sensitive to intial values. On the other hand, the blue line which is the ratio of two time dependences of eccentiricity with 1% of initial difference keeps 1% difference all the time.

This thesis presents state-of-the-art applications of the third method. We derive quasi-Keplerian parametrizations and present the results for three cases: (1) Elliptical bounded motion of non-spinning binaries, (2) precession of generally spinning binaries and (3) hyperbolic encounter of two compact objects. In Chapter 2, we review how Einstein's field equations are reduced down to PN equations of motion of compact binaries, and how the entire spacetime solution is constructed and hence GW are generated in the perspective of the so-called *Blanchet-Damour-Iyer approach*. In Chapter 3, we derive and present quasi-Keplerian parametrizations for elliptic motions up to 4PN accurate order. In Chpater 4, we derive and present the first analytic expression for precessional and orbital motion

of spinning compact binaries in elliptic orbits up to leading order of spin-orbit coupling. And in Chapter 5, the derivation of hyperbolic QKP and how the dissipative effects get involved are presented, and exact phase evolution is computed. Finally, we provides how the burst GW waveforms are generated during hyperbolic encounters.

Chapter 2

Post-Newtonian Theory: Blanchet-Damour-Iyer Approach[1]

In order to build reliable and accurate GW waveforms with an efficient manner, post-Newtonian formalism is of the most importance. The PN efforts are two-fold: (1) Reducing Einstein's field equations to PN equations of motion, and (2) Solving the PN equations and getting GW waveforms. Before presenting our efforts on the latter in this thesis, we provide a fundamental formalism where modeling of the system of our interest is rigoroulsy constructed and every subsequent computations get algorithmic and systemetic so that both of the PN efforts could be enabled as concrete programs. Especially, we review Blanchet-Damour-Iyer approach of the fundamental theory for constructing solutions of Einstein's field equations. And also we introduce nomenclatures which will be used throughout this thesis. This chapter could be seen as an organized review of the following historic references and I mostly follow the terminologies used there (See Blanchet and Damour (1986); Blanchet (1987, 1998); Poujade and Blanchet (2002); Blanchet (2014)).

Before delving into the concrete formalism, it must be mentioned that what kind of sys-

[1] The formalism in this chapter is mainly from Blanchet (2014) with re-edition.

tems we are interested in. We are trying to describe an asymptotic flat spacetime where every gravitating matter source is gathering around near the origin $\mathbf{x} = \{0, 0, 0\}$. By gravitation, the source gets highly energetic and radiates GWs out to the infinity. Thus what we need to know is explicit expressions of dynamics of the source and the propagation of GWs. Please see the Fig. 2.1.

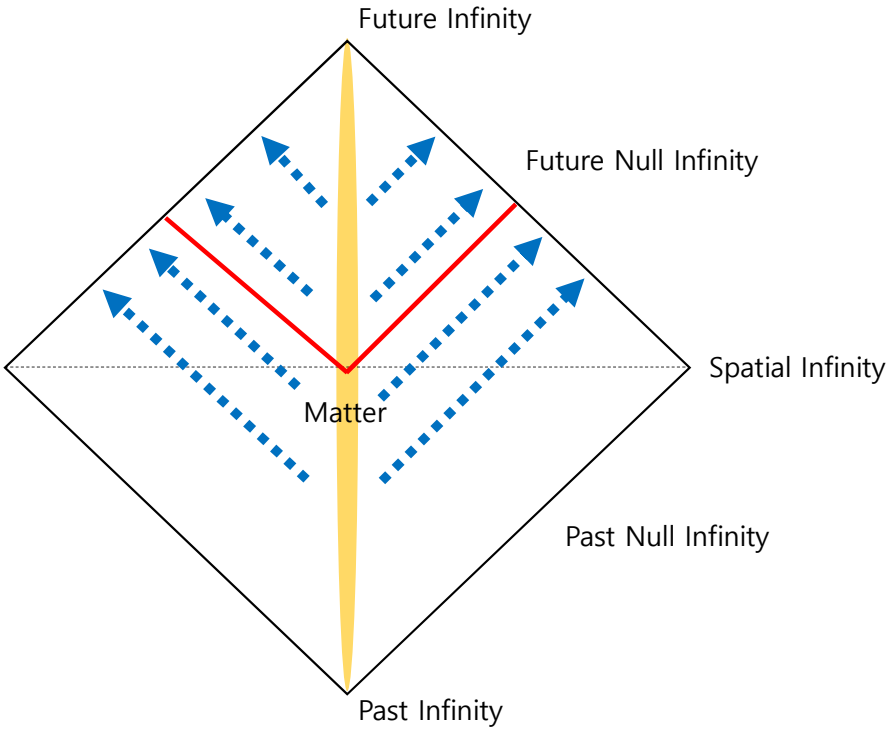

Figure 2.1 Penrose diagram of spacetime of our interest. The yellow region represents matter fields only composed of massive particles and the blue arrows represent gravitational radiation. Note that asymptotic expansion $r \to \infty$ near past null infinity starts from $\frac{1}{r^2}$ *i.e.* no-incoming waves while outgoing waves propagate away to future null infinity. Redline represents a null-like hypersurface of early inspiral, where post-Newtonian description is valid enough. See Fig.2.2 for pictorial description.

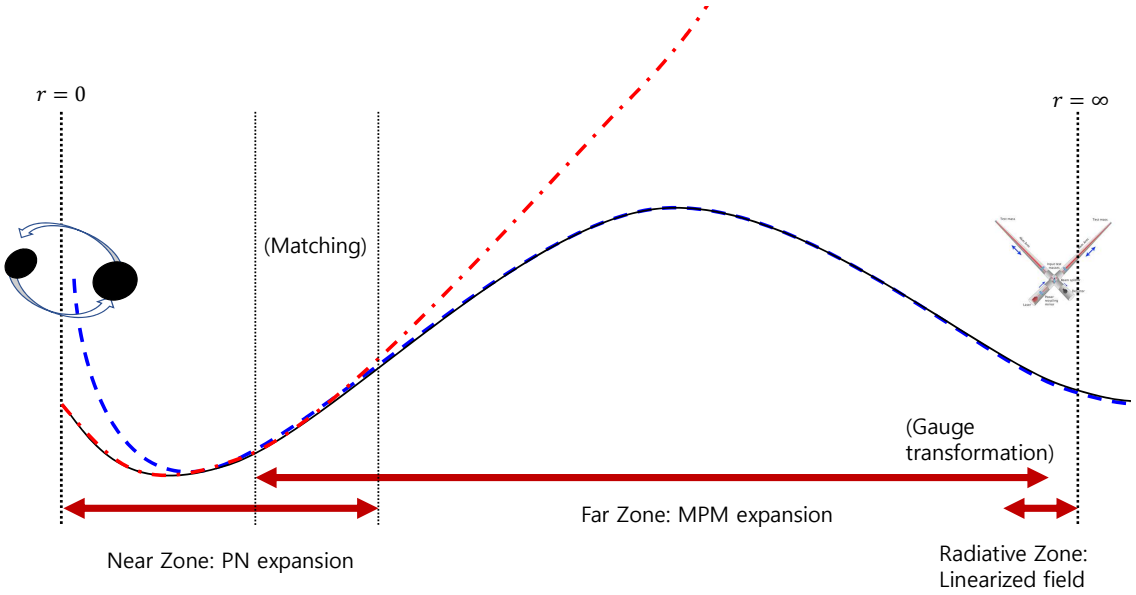

Figure 2.2 This is a schematic structure for showing how PN and MPM theories construct an entire solution and hence how to relate the motion of binaries with asymptotic gravitational waveform. The black solid line represents the exact solution while the red dashed line refers to post-Newtonian solution. PN solution is valid only with a radius of characteristic wave-length (near zone) while MPM soution(blue dashed line) covers vacuum far zone and diverges at $r = 0$ since it is a multipole expansion.

Here are some nomenclatures. First, if indices of a tensor are written in Greek alphabets such as $\mu, \nu, \rho, \cdots$ it means that the tensor is defined on 4-dimensional spacetime. But if indices are written in Latin alphabets such as $i, j, k \cdots$ it means that the tensor is restricted to a 3-dimensional spatial splice of whole spacetime. Secondly, $\mathbf{x} = \{x^1, x^2, x^3\}$ means a spatial position in Cartesian coordinates and $x = \{x^0, x^1, x^2, x^3\}$ means a position

in spacetime with $x^0 = c\,t$. Please note that although the first coordinate x^0 is not same with coordinate time t, $x^0 \neq t$, we often use, for instance, $h(t, \mathbf{x}) = h(x)$ instead of $h(x)$ which is actually an abbreviation of $h(x^0, \mathbf{x})$. Thirdly, if there is no ambiguity, we often omit indices when writing tensors, for example, h refers to $h^{\mu\nu}$, for convenience.

2.1 Relaxed Einstein's field equations

Everything starts from Einstein's field equations

$$G^{\mu\nu}[g](x) = \frac{8\,\pi\,G}{c^4}\,T^{\mu\nu}[g, \phi](x)\,, \tag{2.1}$$

where ϕ stands for (unspecified) matter field and g for the gravitational field. Einstein tensor $G^{\mu\nu}$ is a functional of the single field g and the stress-energy tensor $T^{\mu\nu}$ is a functional of both ϕ and g. With a change of variables

$$h^{\mu\nu} := \sqrt{-g}\,g^{\mu\nu} - \eta^{\mu\nu}\,, \tag{2.2}$$

where g is the determinant of $g_{\mu\nu}$ (not $g^{\mu\nu}$) and $\eta^{\mu\nu} := \mathrm{diag}(-1, 1, 1, 1)$ and by making use of gauge symmetry in General Relativity such as

$$\partial_\mu\,h^{\mu\nu} = 0\,, \tag{2.3}$$

which is called the *harmonic* gauge condition, then Eq.(2.1) is reduced into a kind of d'Almebertian equation,

$$\Box\,h^{\mu\nu}(x) = \frac{16\,\pi\,G}{c^4}\tau^{\mu\nu}[\phi(x), g(x)]\,, \tag{2.4}$$

where $\Box := \eta^{\mu\nu}\partial_\mu\partial_\nu$ and τ is the pseudo stress-energy tensor which is also a functional of the matter and the gravitational field. The pseudo stress-energy tensor τ is decomposed into two parts,

$$\tau[\phi, g] = |g|T[\phi, g] + \frac{c^4}{16\pi G}\Lambda[g]\,, \tag{2.5}$$

where

$$\begin{aligned}\Lambda^{\alpha\beta} = &-h^{\mu\nu}\partial^2_{\mu\nu}h^{\alpha\beta} + \partial_\mu h^{\alpha\nu}\partial_\nu h^{\beta\mu} + \frac{1}{2}g^{\alpha\beta}g_{\mu\nu}\partial_\lambda h^{\mu\tau}\partial_\tau h^{\nu\lambda} \\ &- g^{\alpha\mu}g_{\nu\tau}\partial_\lambda h^{\beta\tau}\partial_\mu h^{\nu\lambda} - g^{\beta\mu}g_{\nu\tau}\partial_\lambda h^{\alpha\tau}\partial_\mu h^{\nu\lambda} + g_{\mu\nu}g^{\lambda\tau}\partial_\lambda h^{\alpha\mu}\partial_\tau h^{\beta\nu} \\ &+ \frac{1}{8}\big(2\,g^{\alpha\mu}\,g^{\beta\nu} - g^{\alpha\beta}\,g^{\mu\nu}\big)\big(2g_{\lambda\tau}\,g_{\epsilon\pi} - g_{\tau\epsilon}\,g_{\lambda\pi}\big)\partial_\mu\,h^{\lambda\pi}\partial_\nu\,h^{\tau\epsilon}\,. \end{aligned} \tag{2.6}$$

Note that T is assumed to have *compact support*, which means there is a finite radius such that T is zero outside of it, while the non-linear source Λ has no compact support.

2.1.1 Stationary-past Assumption

Let us assume that the (new) gravitational field h was stationary before a remote past. That is, a finite $-\mathcal{T} < 0$ exists such that

$$\partial_t h(x) = 0 \quad \text{whenever} \quad t < -\mathcal{T}\,. \tag{2.7}$$

This assumption is equivalent to assuming the integro-differential expression,

$$h^{\mu\nu}(x) = \frac{16\,\pi\,G}{c^4}\Box^{-1}_{\rm ret}[\tau^{\mu\nu}](x)\,, \tag{2.8}$$

where the retarded integration is given by

$$\Box^{-1}_{\rm ret}[\tau](x) = -\frac{1}{4\pi}\int \frac{d^3\mathbf{x}'}{|\mathbf{x}-\mathbf{x}'|}\,\tau(t - \frac{|\mathbf{x}-\mathbf{x}'|}{c}, \mathbf{x}')\,. \tag{2.9}$$

Roughly speaking, the condition imposes no incoming wave hence GWs are only out-going from the sources to infinity.

2.2 Linearized Theory of Gravitational Wave

Before considering entire spacetime solution, let us think about linearized field and properties of GW itself. This is equivalent with assuming that $h \ll 1$ and there is no matter souce. Then keeping only terms linear in $h = h_{(1)}$, (2.4) becomes

$$\Box h_{(1)} = 0\,, \tag{2.10a}$$

$$\partial_\mu h^{\mu\nu}_{(1)} = 0\,. \tag{2.10b}$$

2.2.1 Multipolar General solution of linearized theory

In ths subsection, we present a general solution of Eq.(2.10) in multipole expanded form. This is crucial for BDI formalism in that it is a link of post-Newtonian solution and multipolar-post-Minkowskian (MPM) constructed solution as well as it initiates MPM construction starts. The following (retarded) general expressions of $h_{(1)}$ solve the above Eq.(2.10) with 6 symmetric tracefree (STF)[2] tensors $\{I_L, J_L, W_L, X_L, Y_L, Z_L\}$ unspecified,

$$h^{\mu\nu}_{(1)} = k^{\mu\nu} + \partial^\mu\varphi^\nu + \partial^\nu\varphi^\mu - \eta^{\mu\nu}\partial_\lambda\varphi^\lambda\,, \tag{2.11a}$$

with

$$k^{00} = -\frac{4}{c^2}\sum_{l=0}\frac{(-)^l}{l!}\partial_L\left(\frac{I_L(t-\frac{r}{c})}{r}\right)\,, \tag{2.11b}$$

$$k^{0i} = \frac{4}{c^3}\sum_{l=1}\frac{(-)^l}{l!}\partial_{L-1}\left\{\frac{I^{(1)}_{iL-1}(t-\frac{r}{c})}{r} + \frac{l}{l+1}\epsilon_{iab}\partial_a\left(\frac{J_{bL-1}(t-\frac{r}{c})}{r}\right)\right\}\,, \tag{2.11c}$$

$$k^{ij} = -\frac{4}{c^4}\sum_{l=2}\frac{(-)^l}{l!}\partial_{L-2}\left\{\frac{I^{(2)}_{ijL-2}(t-\frac{r}{c})}{r} + \frac{2l}{l+1}\partial_a\left(\frac{\epsilon_{ab(i}J^{(1)}_{j)L-2}(t-\frac{r}{c})}{r}\right)\right\}\,, \tag{2.11d}$$

$$\varphi^0 = \frac{4}{c^3}\sum_{l=0}\frac{(-)^l}{l!}\partial_L\left(\frac{W_L(t-\frac{r}{c})}{r}\right)\,, \tag{2.11e}$$

$$\varphi^i = -\frac{4}{c^4}\sum_{l=0}\frac{(-)^l}{l!}\partial_{iL}\left(\frac{X_L(t-\frac{r}{c})}{r}\right)\,, \tag{2.11f}$$

---

[2] A STF tensor F_L is an abbreviation of $F_L = F_{i_1 i_2\cdots i_l}$ with two properites that

$$F_{i_1 i_2\cdots i_j\cdots i_k i_l} = F_{i_1 i_2\cdots i_k\cdots i_j i_l} \quad \text{symmetric}$$

and

$$\delta^{i_j i_k} F_{i_1 i_2\cdots i_j\cdots i_k i_l} = 0 \quad \text{tracefree.}$$

$$-\frac{4}{c^4}\sum_{l=1}\frac{(-)^l}{l!}\partial_{L-1}\left\{\frac{Y^{(1)}_{iL-1}(t-\frac{r}{c})}{r}+\frac{l}{l+1}\epsilon_{iab}\,\partial_a\left(\frac{Z_{bL-1}(t-\frac{r}{c})}{r}\right)\right\}.$$

Note that since φ term is corresponding to gauge transformation, hence only k is equivalent with the entire expression. However, that equivalence only holds at the linear order and two expressions go unequivalent when non-linear contributions get involved in. Thus whenever distinguishing them is required, we will use the terminology such as $h_{(1)}[I,J,W,X,Y,Z]$ and $h_{(1)}[M,S,0,0,0,0]$(or, just $h_{(1)}[M,S]$). Specifically, the latter one is called *canonical* linearized field and hence $\{M_L,S_L\}$ *canonical multipole moments*, while $\{I_L,J_L,W_L,X_L,Y_L\,Z_L\}$ is called *source multipole moments*.

2.2.2 Predictablity of Gravitational Waves

In this subsection, let us consider how the theoretical prediction and observation meet. In the small region very far from sources of interest, the lineaized field can be decomposed into Fourier modes,

$$h^{\mu\nu}_{(1)}(x)=A^{\mu\nu}(k)\exp[i\,k_\rho\,x^\rho]\,, \tag{2.12}$$

with $\eta^{\mu\nu}k_\mu k_\nu=0$ and $A^{\mu\nu}k_\mu=0$. It is easily shown that this monochromatic plane wave solution solves (2.10). By virtue of general covariance, another physically equivlaent solution $h'^{\mu\nu}=h^{\mu\nu}+\partial\xi^{\mu\nu}$ will satisfy Einstein's field equations up to linear order with any vector ξ^ν, where $\partial\xi^{\mu\nu}:=\partial^\mu\xi^\nu+\partial^\mu\xi^\nu-\eta^{\mu\nu}\partial_\lambda\xi^\lambda$. This gauge symmetry makes it difficult to connect observation data and prediction from theory. Traceless-transverse part of linear field is where they could meet.

Any symmetric tensor $A^{\mu\nu}$ is decompsed into

$$A^{00}=A\,, \tag{2.13a}$$

$$A^{0i}=\rho^i+\partial^i S\,, \tag{2.13b}$$

$$A^{ij}=\delta^{ij}P+(\partial^iP^j+\partial^jP^i)+(\partial_{ij}-\frac{1}{3}\delta^{ij}\nabla)\sigma\,+\sigma^{ij}, \tag{2.13c}$$

where ρ^i is transverse part of A^{0i} as $\partial_i \rho^i = 0$ while P is the trace part of A^{ij} and P^i and σ stand for longitudinal part with $\partial_i P^i = 0$. And also $\partial_j \sigma^{ij} = \delta_{ij}\sigma^{ij} = 0$ (thus TT part). Now let us a gauge transformation expression of the linearized theory. With an arbitrary vector ξ^μ

$$h^{\mu\nu} \to h^{\mu\nu} + \partial\xi^{\mu\nu}\,,$$

whre $\partial\xi^{\mu\nu} := \partial^\mu\xi^\nu + \partial^\mu\xi^\nu - \eta^{\mu\nu}\partial_\lambda\xi^\lambda$. Its decomposition is

$$\partial\xi^{00} = \partial^0(2\,\xi^0) + \partial_\lambda\xi^\lambda\,, \tag{2.14a}$$

$$\partial\xi^{0i} = \partial^0\xi^i + \partial^i\xi^0 = \partial^0(\xi^i - \nabla^{-1}\partial_{ij}\xi^j) + \partial^i(\xi^0 + \nabla^{-1}\partial_{0j}\xi^j)\,, \tag{2.14b}$$

$$\partial\xi^{ij} = \delta^{ij}(-\partial_\mu\xi^\mu + \frac{2}{3}\partial_k\xi^k) + (\partial^i K^j + \partial^j K^i) + (\partial_{ij} - \frac{1}{3}\delta^{ij}\nabla)(2\,\nabla^{-1}\partial_k\xi^k), \tag{2.14c}$$

where $K^i := \xi^i - \partial_i(\nabla^{-1}\partial_k\xi^k)$, a divergenceless vector. In $\partial\,\xi$, there is nothing corresponding to the transverse-traceless part σ^{ij} of the general expression. Thus we find that the spatial metric $\partial\xi^{ij}$ has no transverse-traceless part. Or, we can see that the transvese-traceless part of the spatial h^{ij} is a *gauge invariant* up to the linear approximation and hence this TT part is *predictable* by theory. On the other hand, we can even be in a frame where every components vanish other than TT component. Let us take a particular choice of $\xi^\mu := -i\,C^\mu \exp[i\,k_\rho\,x^\rho]$ as

$$C^0 = \frac{\delta_{ij}A^{ij}}{2\,k_0} - \frac{k_i\,A^{0i}}{2\,k_0^2}\,, \tag{2.15a}$$

$$C^i = \frac{A^{0i}}{k_0} + \frac{\delta^{ij}k_j}{k_0}\,C^0\,. \tag{2.15b}$$

Then it holds that $\partial_\mu h'^{\mu\nu} = 0$ and $h'^{0i} = \delta_{ij}\,h'^{ij} = 0$. Also it follows that $h'^{00} = 0$. (Hereafter we use h symbol for h'.) Since this kind of coordinate change only leaves transverse-traceless(TT) part while we have seen that TT part is gauge invariant in the previous section. Thus we can conclude that the particular expression of TT part of the gravitational field constructed all through PN expansion and multipolar post-Minkowskian construction, is exactly the same with the linear metric in TT frame. Thus those who are

trying to obseverve GWs is recommended to be in the TT frame, or to have information of transformation rules from TT frame at least.

2.3 Post-Newtonian approximation in the Near Zone

In this section, we are going to find approximation of the exact solution h of Eq.(2.4). To do this, we introduce a formal post-Newtonian (PN) expansion of h with upper line,

$$\bar{h}^{\mu\nu}(x,c) = \sum_{m=2}^{\infty} \frac{1}{c^m} h^{\mu\nu(m)}(x, \ln c)\,. \tag{2.16}$$

By the word 'formal', we mean that the above summation should be seen as a sequence of symbols not numerical summation. (thus '+' does not have to be the numerical operation 'addition'). But we expect that *numerically* the summation converges to the exact solution $h(x)$ if $|\mathbf{x}| \ll \mathcal{R}$ which is called *near zone*. $\mathcal{R}$ stands for characteristic wave-length of the system out of which PN expansion does not give correct answer since expanding with respect to $\frac{1}{c}$ breaks finit speed of propagation of gravitational field. Schematically, any retarded function

$$F(t - \frac{r}{c}) \simeq F(t) - \frac{r}{c}F'(t) + \frac{1}{2}(\frac{r}{c})^2 F''(t) + \cdots\,, \tag{2.17}$$

becomes a power series of r/c so that large values of r eventually breaks down the validity of PN exapnsion.

On the other hand, τ is a functional of h and suppose that ϕ is somehow determined. By expanding $\tau[\bar{h}]$ we get another formal series $\bar{\tau}$ converging to $\tau[h]$ only within the near zone.

$$\bar{\tau}(x,c) = \sum_{m=-2}^{\infty} \frac{1}{c^m} \tau^{(m)}(x, \ln c)\,. \tag{2.18}$$

If we had the exact solution h and hence exact τ, then the retarded integration of τ, $\Box^{-1}_{\rm ret}\tau[h]$ would be convergent and give arise to h repeatedely again. However, we only have an approximation thus after integration the result $\Box^{-1}_{\rm ret}\bar{\tau}[\bar{h}]$ must be different from

$\Box^{-1}_{\rm ret}\tau[h]$. Actually, it is not even convergent because PN expansion makes fields singular at the spatial infinity. A naive retarded integration of singular field causes another divergence.

2.3.1 Finite part regularization

In many cases, the retarded integration diveges since the particular expressions of sources must be given as infinite series in practical. In our case, it will be two kinds: *Post-Newtonian expansion* and *Multipole expansion*. The former involves divergences at $r = \infty$ while the latter at $r = 0$. Before tackling this problem directly let us look into some examples. Firstly, consider the following radial integration,

$$I = \int_1^\infty dr\, r^2\,. \tag{2.19}$$

A naive integration yields $I = \frac{r^3}{3}|_1^\infty = \infty - \frac{1}{3}$. Thus, we introduce a complex number B such that

$$I(B) := \int_1^\infty dr\, r^{B+2}\,. \tag{2.20}$$

Then the integration is $I(B) = [\frac{r^{B+3}}{B+3}]_1^\infty$. If we are interested in the area where $\mathrm{Re}(B) < -3$, then $I(B) = -\frac{1}{B+3}$ and this expression converges except for $B = -3$. Thus by the argument of analytic continuation, at $B = 0$, $I(0) = -\frac{1}{3}$. We will call this *finite part* (FP) regularization. Thus we write $\mathrm{FP}\cdot I = -\frac{1}{3}$. The second example is $I = \int_0^2 \frac{dr}{r} = \ln 2 - \ln 0 = -\infty$.

$$\begin{aligned} I(B) &= \int_0^2 r^{B-1} dr = \frac{2^B}{B} \quad \text{if} \quad \mathrm{Re}(B) > 0\,, \\ &= \frac{2}{B} + \ln 2 + \mathcal{O}(B). \end{aligned} \tag{2.21}$$

Getting rid of $\frac{2}{B}$ yields that $\mathrm{FP}\cdot I = \ln 2$.

Now consider the retarded integration $\Box^{-1}_{\rm ret}[r^B\,\Lambda]$. Let $I(B)$ be an analytic continuatio of $\Box^{-1}_{\rm ret}[r^B\,\Lambda]$. As seen in the previous examples, the analytic continuation $I(B)$ could be

divergent at $B = 0$. Thus after Laurent expansion, $I(B) = \sum_{p=p_0\leq 0} B^p I^{(p)}$. Then by performing d'Alembert operation again,

$$\Box\, I(B) = \sum_{p=p_0\leq 0} B^p \Box I^{(p)} = r^B\, \Lambda\,. \tag{2.22}$$

Because Laurent series of $r^B\,\Lambda$ does not contain negative powers of B. So we conclude that $I^{(p)}$ when $p_0 \leq p \leq -1$ are homogeneous solutions *i.e.*$\Box\, I^{(p)} = 0$ for $p_0 \leq p \leq -1$. Hence we can get rid of them in the process of finding a particular solution. Hereafter, we are going to use the following symbol for representing the *finite part* particular solution, which has gotten through what we have seen as

$$\mathrm{FP}\cdot\, \Box^{-1}_{\mathrm{ret}}[\Lambda](\mathbf{x},t) := I^{(0)}(\mathbf{x},t)\,. \tag{2.23}$$

What should be noticed

When it comes to the finite part regularization, exchanges of the expansion operators with the finite part operation are not allowed. But the expansion structure remains. Since we used to be confused about them, in order to make it clear, we leave some relations as

$$M(\Box^{-1}_{\mathrm{ret}}[\varphi]) = \Box^{-1}_{\mathrm{ret}}[M(\varphi)]\,, \tag{2.24a}$$

$$\overline{\Box^{-1}_{\mathrm{ret}}[\varphi])} = \Box^{-1}_{\mathrm{ret}}[\bar{\varphi}]\,, \tag{2.24b}$$

$$M(\Box^{-1}_{\mathrm{ret}}[\varphi]) \neq \mathrm{FP}\cdot \Box^{-1}_{\mathrm{ret}}[M(\varphi)]\,, \tag{2.24c}$$

$$M(\mathrm{FP}\cdot \Box^{-1}_{\mathrm{ret}}[M(\varphi)]) = \mathrm{FP}\cdot \Box^{-1}_{\mathrm{ret}}[M(\varphi)]\,, \tag{2.24d}$$

$$\overline{\Box^{-1}_{\mathrm{ret}}[\varphi]} \neq \mathrm{FP}\cdot \Box^{-1}_{\mathrm{ret}}[\bar{\varphi}]\,, \tag{2.24e}$$

$$\overline{\mathrm{FP}\cdot \Box^{-1}_{\mathrm{ret}}[\bar{\varphi}]} = \mathrm{FP}\cdot \Box^{-1}_{\mathrm{ret}}[\bar{\varphi}]\,. \tag{2.24f}$$

2.3.2 General solution of post-Newtonian metric

In this subsection, we are going to find the general expression of post-Newtonian metric. Unlike the exact solution case, the differential equation $\Box\bar{h} = \frac{16\,\pi\, G}{c^4}\bar{\tau}$ is not equivalent

with $\bar{h} = \frac{16\pi G}{c^4}\mathrm{FP}\cdot\Box^{-1}_{\mathrm{ret}}[\bar{\tau}]$ because $\mathrm{FP}\cdot\Box^{-1}_{\mathrm{ret}}[\bar{\tau}] \neq \overline{\mathrm{FP}\cdot\Box^{-1}_{\mathrm{ret}}[\tau]}$. Instead we write

$$\bar{h}^{\mu\nu} = \mathrm{FP}\cdot\Box^{-1}_{\mathrm{ret}}[\bar{\tau}^{\mu\nu}] - \frac{4G}{c^4}\sum_{l=0}^{\infty}\partial_L\Big\{\frac{\overline{R_L^{\mu\nu}(t-r/c) - R_L^{\mu\nu}(t+r/c)}}{2\,r}\Big\}\,, \tag{2.25}$$

where the each term comes explicitly as

$$\mathrm{FP}\cdot\Box^{-1}_{\mathrm{ret}}[\bar{\tau}](x) = -\frac{1}{4\pi}\sum_{m=0}^{\infty}\frac{(-)^m}{m!}\Big(\frac{\partial}{c\,\partial t}\Big)^m\,\mathrm{FP}\cdot\int d^3x'|\mathbf{x}-\mathbf{x}'|^{m-1}\,\bar{\tau}(t,\mathbf{x}')\,, \tag{2.26}$$

$$R_L^{\mu\nu}(t) := \mathrm{FP}\cdot\int d^3\mathbf{x}\,\hat{x}_L\int_1^{+\infty}dz\,\gamma_l(z)\,M(\tau^{\mu\nu})(t-zr/c,\mathbf{x})\,, \tag{2.27}$$

where $\gamma_l(z) = -\frac{(2l+1)!!}{2^l\,l!}(1-z^2)^l$ and $M(\varphi)$ stands for multipole expansion of φ *i.e.* $M(\varphi(t,\mathbf{x})) = \sum_{l=0}^{\infty}a_l(t,r)\,\varphi^{(l)}(\theta,\phi)\,(r\neq 0)$. Now the partial expression $\bar{h} = \mathrm{FP}\cdot\Box^{-1}_{\mathrm{ret}}[\bar{\tau}[\bar{h}]]$ is compeleted in that it is a relation of one variable $\bar{h}$ and allow us to solve it iteratively. However, this happens only up to 3.5PN. Starting from 4PN order we need to consider the second part which is an anti-symmetric homogeneous solution so that the general solution expression gaurantees that $\Box\bar{h} = \bar{\tau}$, and furthermore is supposed to be regular at $r = 0$ because PN expansion does not have singularity at $r = 0$ and also must be numerically equal to the exact solution h in the near zone. Thus as being restricted within near zone, obviously we cannot determine the entire solution especially because of lack of R (non-linear radiation reaction term) only by PN iterations.

Now let us prove Eq.(2.25). Consider $\Delta_1(x,t) := \Box^{-1}_{\mathrm{ret}}[\tau](x,t) - \mathrm{FP}\cdot\Box^{-1}_{\mathrm{ret}}[\bar{\tau}](x,t)$. Since the first term is regular and convergent, we can rewrite it as

$$\begin{aligned}
\Delta_1 &= \mathrm{FP}\cdot\Box^{-1}_{\mathrm{ret}}[\tau] - \mathrm{FP}\cdot\Box^{-1}_{\mathrm{ret}}[\bar{\tau}]\,, \qquad (2.28)\\
&= \mathrm{FP}\cdot\Box^{-1}_{\mathrm{ret}}[\tau-\bar{\tau}] = \mathrm{FP}\cdot\Box^{-1}_{\mathrm{ret}}[M(\tau-\bar{\tau})]\,, \quad \because \text{ it is vanishing in near zone}\\
&= \mathrm{FP}\cdot\Box^{-1}_{\mathrm{ret}}[M(\tau)]\,, \quad \because \text{finite part involving } M(\bar{\tau}) \text{ is zero}^3\\
&= \mathrm{FP}\cdot\Bigg(\sum_l\int_{-r}^{r}ds\,\hat{\partial}_L\Big(\frac{\mathcal{R}_L^B(\frac{s+r}{2},t-s/c)}{r}\Big) - \frac{1}{4\pi}\sum_l\frac{(-)^l}{l!}\hat{\partial}_L\Big(\frac{R_L^B(t-r/c)-R_L^B(t+r/c)}{2r}\Big)\Bigg)\,,
\end{aligned}$$

according to Appendix.5.4 and Eq.(2.100).

Because the second term is a homogeneous solution let us focus on the first term, which is a part of retarded solution of $\Box^{-1}_{\rm ret}[r^B\,M(\tau)]$, thus can be written in the form of general retarded solution,

$$\sum_l \int_{-r}^{r} ds\,\partial_L\Big(\frac{\mathcal{R}^B_L(\frac{s+r}{2}, t-s/c)}{r}\Big) = W(B) + \partial_L\Big(\frac{C^B_L(t-r/c) + D^B_L(t+r/c)}{r}\Big)\,, \tag{2.29}$$

where $W(B)$ stands for a particular solution ($\Box W(B) = r^B M(\tau)$). When $r \to 0$, it is proportional to r^B,

$$\sum_l \int_{-r}^{r} ds\hat{\partial}_L\Big(\frac{\mathcal{R}^B_L(\frac{s+r}{2}, t-s/c)}{r}\Big) \sim \sum_{p,q,l} r^p\,\hat{n}_L\,\frac{d^q}{dr^q}\frac{\mathcal{R}^B_L(r, t-r/c)}{r}|_{r=0} \sim r^B\,, \tag{2.30}$$

while the homogenous part $\partial_L(\frac{C^B_L(t-r/c)+D^B_L(t+r/c)}{r})$ cannot be proportioanl to r^B, since B is only involved with time components through $C^B(t)$, $D^B(t)$ and their time derivatives when $r \to 0$. Thus we can conclude $C^B_L = D^B_L = 0$ and subsequently

$$\bar{\Delta}_1 = \overline{\mathrm{FP}\cdot W(B)} + \mathrm{FP}\cdot\Big(-\frac{1}{4\pi}\sum_l \frac{(-)^l}{l!}\partial_L\Big(\frac{\overline{R^B_L(t-r/c) - R^B_L(t+r/c)}}{2r}\Big)\Big)\,, \tag{2.31}$$

On the other hand, by definition of Δ_1, PN expansion of Δ_1 does not have the particular solution part

$$\Box[\bar{\Delta}_1] = \bar{\tau} - \bar{\tau} = 0\,, \tag{2.32}$$

and hence $\overline{\mathrm{FP}\cdot W(B)} = 0$. Finally we have arrived at the proof of Eq.(2.25)\,,

$$\bar{\Delta}_1 = \overline{\Box^{-1}_{\rm ret}[\tau]}(=\bar{h}) - \mathrm{FP}\cdot\Box^{-1}_{\rm ret}[\bar{\tau}] = -\frac{1}{4\pi}\sum_l \frac{(-)^l}{l!}\partial_L\Big(\frac{\overline{R_L(t-r/c) - R_L(t+r/c)}}{2r}\Big)\,. \tag{2.33}$$

---

[3] $M[\bar{\tau}] = \sum_{0\le l<\infty, -\infty<m<\infty} \hat{n}_L\,r^m\,F_{L,m}(t)$. Thus after angular integration and z, it becomes

$$\sim \int_0^\infty dr r^{B+a} = \int_D^\infty dr\,r^{B+a} + \int_0^D dr\,r^{B+a} = -\frac{D^{B+a+1}}{B+a+1}|_{\mathrm{Re}(B)\gg 1} + \frac{D^{B+a+1}}{B+a+1}|_{\mathrm{Re}(B)\ll 1} = 0\,(\text{as}\quad B\to 0).$$

2.4 Multipolar-post-Minkowskian(MPM) solutions

2.4.1 General Structure of Multipole expansion of the exact metric

Let $M(h)$ be the multipole expansion of h. Outside of the matter source $|\mathbf{x}| > a$ where $T = 0$, it holds that $\Box\, M(h) = \frac{16\,\pi\,G}{c^4}\tau[M(h)] = \Lambda[M(h)] =: M(\Lambda)$ (Since Λ is a functional only dependent on h) . In order to find general structure of $M(h)$, let us think about the difference $\Delta_2(x) := h(x) - \mathrm{FP}\cdot\Box^{-1}_{\mathrm{ret}}[M(\Lambda)](x)$. Finite part is introduced because the mulitpole expanded source is singular at $r = 0$, which makes the naive integrations divegent. Since $h = \frac{16\,\pi\,G}{c^4}\Box^{-1}_{\mathrm{ret}}[\tau]$,

$$\Delta_2 = \frac{16\,\pi\,G}{c^4}\Box^{-1}_{\mathrm{ret}}[\tau] - \mathrm{FP}\cdot\Box^{-1}_{\mathrm{ret}}[M(\Lambda)]\,. \tag{2.34}$$

the first term is convergent so finite part could be attached without changing anything. Thus

$$\Delta_2 = \mathrm{FP}\cdot\Box^{-1}_{\mathrm{ret}}[\frac{16\,\pi\,G}{c^4}\tau - M(\Lambda)](x,t)\,. \tag{2.35}$$

Note that $\frac{16\,\pi\,G}{c^4}\tau - M(\Lambda) = 0$ at $|\mathbf{x}| > a$ (outside of matter source) thus has a compact support. In Appendix.5.4.1, I derived the general form of multipole expansion of retarded integration of compact support sources. Introducing STF tensors F_L, the multipole expansion of Δ_2 is

$$M(\Delta_2) = -\frac{4\,G}{c^4}\sum_{l=0}^{\infty}\frac{(-)^l}{l!}\partial_L\big\{\frac{F_L(u)}{r}\big\}\,, \tag{2.36}$$

where $F_L(u) = \mathrm{FP}\cdot\int d^3x'\hat{x}'_L\int_{-1}^{+1}dz\delta_l(z)\big(\tau - M(\tau)\big)(u + zr'/c, \mathbf{x}')$. Since inside source, PN expansion does not change its numerical value we can rewrite F

$$F_L(t) = \mathrm{FP}\cdot\int d^3\mathbf{x}'\,|\mathbf{x}'|^B\,\hat{x}'_L\int_{-1}^{+1}dz\,\delta_l(z)\,\big(\bar{\tau} - \overline{M(\tau)}\big)(t + zr'/c, \mathbf{x}') \tag{2.37}$$

but since $\overline{M(\tau)}$ diverges both $r = 0$ and $r = \infty$ thus it has no contribution after performing the finite part operation. Thus finally we can express F only in terms of $\bar{\tau}$ as

$$F_L = \mathrm{FP}\cdot\int d^3x'\hat{x}'_L\int_{-1}^{+1}dz\delta_l(z)\,\bar{\tau}(u + zr'/c, \mathbf{x}')\,. \tag{2.38}$$

Also since $M(\Delta) = M(h) - M(\mathrm{FP}\cdot\Box^{-1}_{\mathrm{ret}}[M(\tau)](x,t))$, we finally arrive at the general expression of the multipole expansion of the exact solution:

$$M(h) = \mathrm{FP}\cdot\Box^{-1}_{\mathrm{ret}}[M(\Lambda)] - \frac{4\,G}{c^4}\sum_{l=0}^{\infty}\frac{(-)^l}{l!}\partial_L\{\frac{F_L(u)}{r}\}\,. \tag{2.39}$$

2.4.2 General Structure of MPM vacuum solutions

Although at the end of the previous subsection we saw the general structure of $M(h)$, the explicit expression is not known yet. Thus in this section multipolar-post-Minkowskian (MPM) iteration will be introduced to get particular expressions of *multipole-expanded vacuum* solution.

$$M(h) = \sum_{n=1}^{\infty} G^n h_{(n)}\,, \tag{2.40}$$

to solve

$$\Box M(h) = M(\Lambda[h])\,. \tag{2.41}$$

2.4.3 Identification of linear order term and higher order terms

Because MPM solution is a kind of multipole expansion of the exact solution, we can equate Eq.(2.39) and Eq.(2.40),

$$\sum_{n=1}^{\infty} G^n\, h^{\mu\nu}_{(n)} = \mathrm{FP}\cdot\Box^{-1}_{\mathrm{ret}}[M(\Lambda^{\mu\nu})] - \frac{4G}{c^4}\sum_{l}^{\infty}\frac{(-1)^l}{l!}\partial_L\{\frac{F^{\mu\nu}_L(t-\frac{r}{c})}{r}\}\,, \tag{2.42}$$

where $M(\Lambda)[h] = \Lambda[M(h)]$. It is our aim to equate $h^{\mu\nu}_{(n)}(x)$ which arises in practical computations with a part of the general structure.

Firstly, let $u^{\mu\nu} \equiv \mathrm{FP}\cdot\Box^{-1}_{\mathrm{ret}}[M(\Lambda^{\mu\nu})]$, then because $\partial_\mu M(h^{\mu\nu}) = 0$ (the harmonic gauge condtion), we get a numerical equality of

$$\partial_\nu u^{\mu\nu} = \frac{4G}{c^4}\sum_{l}^{\infty}\frac{(-1)^l}{l!}\partial_\nu\partial_L\{\frac{F^{\mu\nu}_L(t-\frac{r}{c})}{r}\}. \tag{2.43}$$

Thus we can find that $\partial_\nu u^{\mu\nu}$ is a homogeneous solution *i.e.* $0 = \Box\partial_\nu u^{\mu\nu}$ and also time depndence should be given in terms of $t - \frac{r}{c}$. Thus it can be parametrizied by vectorial STF tensors,

$$\partial_\nu u^{\mu\nu} =: \frac{4\,G}{c^4}\sum_l^\infty \frac{(-)^l}{l!}\partial_L\{\frac{G_L^\mu(t-r/c)}{r}\}. \tag{2.44}$$

By direct integration we get $v^{\mu\nu}(t,x)$ which satisfies $\partial_\nu(u^{\mu\nu}+v^{\mu\nu})=0$ and $\Box\, v = 0$.

$$v^{00} = \frac{4G}{c^4}\left\{-\frac{c}{r}\int G^0 + \partial_a(\frac{1}{r}\left[c\int G_a^0 + c^2\int\int G^a - G_{ab}^b\right])\right\}, \tag{2.45a}$$

$$\begin{aligned} v^{0i} = \frac{4G}{c^4}\Big\{ &-\frac{1}{r}\left[c\int G^i - \frac{1}{c}\dot{G}_{ai}^a\right] + \frac{c}{2}\partial_a\left(\frac{1}{r}[\int G_a^i - \int G_i^a]\right) \\ &-\sum_{l\geq 2}\frac{(-)^l}{l!}\hat{\partial}_{L-1}\left(\frac{1}{r}G_{iL-1}^0\right)\Big\}, \end{aligned} \tag{2.45b}$$

$$\begin{aligned} v^{ij} = \frac{4G}{c^4}\Bigg\{ &\frac{1}{r}G_{j)}^{(i} + 2\sum_{l\geq 3}\frac{(-)^l}{l!}\hat{\partial}_{L-3}\left(\frac{1}{rc^2}\ddot{G}_{ijaL-3}^a\right) \\ &+\sum_{l\geq 2}\frac{(-)^l}{l!}\Big[\partial_{L-2}(\frac{1}{rc}\dot{G}_{ijL-2}^a) + \partial_{aL-2}(\frac{1}{r}G_{ijL-2}^a) + 2\,\delta_{ij}\hat{\partial}_{L-1}(\frac{1}{r}G_{aL-1}^a) \\ &-4\partial_{L-2(i}\left(\frac{1}{r}G_{j)aL-2}^a\right) - 2\partial_{L-1}\left(\frac{1}{r}G_{j)L-1}^{(i}\right)\Big]\Bigg\}, \end{aligned} \tag{2.45c}$$

where $\int G := \int_{-\infty}^u dv G(v)$. Thus if the STF tensor G_L is determined then $v^{\mu\nu}$ is determined. Now let us rewrite the general MPM solution as

$$M(h) = u + v - v - \frac{4G}{c^4}\sum_l^\infty \frac{(-1)^l}{l!}\partial_L\{\frac{F_L^{\mu\nu}(t-\frac{r}{c})}{r}\}. \tag{2.46}$$

As the construction each $u+v$ and $-v-\frac{4G}{c^4}\sum_l^\infty\frac{(-1)^l}{l!}\partial_L\{\frac{F_L^{\mu\nu}(t-\frac{r}{c})}{r}\}$ satisfy the harmonicity condition. Thus, the linearized potential can be assigned as

$$G\,h_{(1)}^{\mu\nu}(t,\,x) = -\frac{4G}{c^4}\sum_l^\infty\frac{(-1)^l}{l!}\partial_L\{\frac{F_L^{\mu\nu}(t-\frac{r}{c})}{r}\} - v^{\mu\nu}\,, \tag{2.47}$$

$$\sum_{m=2}^{\infty} G^m \, h^{\mu\nu}_{(m)}(t,\, x) = u^{\mu\nu} + v^{\mu\nu} \,. \tag{2.48}$$

In order to complete $h^{\mu\nu}_{(1)}(t,\, x)$, one needs an explicit expression of v for linear order. Since by definition $u^{\mu\nu}$ has no linear contribution $\sim G^1$, it is needed that

$$\frac{4G}{c^4} \sum_{l}^{\infty} \frac{(-1)^l}{l!} \partial_\nu \partial_L \Big\{ \frac{F^{\mu\nu}_L(t - \frac{r}{c})}{r} \Big\} = \sum_{l}^{\infty} \frac{(-1)^l}{l!} \partial_L \Big\{ \frac{G^{\mu}_L(t - r/c)}{r} \Big\} \tag{2.49}$$

which gives us the explict expression of G_L, and also $v^{\mu\nu}$ via Eq.(2.45)s as the follow

$$G^{\mu}_L(t - \frac{r}{c}) = \mathrm{FP} \cdot \int d^3y \, B|y|^{B-2} \, \hat{y}_L \, y_j \int_{-1}^{+1} dz \, \delta_l(z) \, \bar{\tau}^{j\mu}(t - \frac{r}{c} + \frac{z|y|}{c}, y^i). \tag{2.50}$$

Please see section.5.5 for the derivation.

Higher order Non-Linear Contributions

Now we know how the linear contribution $h_{(1)}$ can be constructed in terms of PN sources. A succesive MPM iteation determines the second order $h^{(2)\mu\nu}(t,\, x)$ as the following algorithm:

1. Put $G\, h^{(1)\mu\nu}(t,\, x)$ into $u = \mathrm{FP} \cdot \Box^{-1}_{\mathrm{ret}} M(\Lambda)[h]$.

2. Expand and get G^2 order term of u such as $u = G^2\, u^{(2)} + O(G^3)$.

3. Calculate G_L from Eq.(2.44) and $u = G^2\, u^{(2)}$ up to the second order.

4. Get $v^{(2)}$ via eq.(2.45).

5. Determine $h^{(2)} := u^{(2)} + v^{(2)}$.

The higher order terms are also determined by through exactly same algorithm.

2.4.4 Source mulitpole moments in terms of PN sources[4]

Now we are in the position of expressing the 6 STF parameters $\{I, J, W, X, Y, Z\}$ of linear metric, in terms of PN sources by equating

$$-\frac{4G}{c^4}\sum_l^\infty \frac{(-1)^l}{l!}\hat{\partial}_L\Big\{\frac{F_L^{\mu\nu}(t-\frac{r}{c})}{r}\Big\} - v^{\mu\nu} = G\,k^{\mu\nu} + G(\partial^\mu\varphi^\nu + \partial^\nu\varphi^\mu - \eta^{\mu\nu}\partial_\lambda\varphi^\lambda)\,. \quad (2.51)$$

By lengthy but straightforward inversion of Eq. (2.51), one can arrive the closed expressions of the source moments in terms of post-Newtonian sources:

$$\begin{aligned}
I_L(u) &= \mathrm{FP}\cdot\int d^3\mathbf{y}\int_{-1}^1 dz\left\{\delta_l\hat{y}_L\overline{\Sigma} - \frac{4(2l+1)}{c^2(l+1)(2l+3)}\delta_{l+1}\hat{y}_{iL}\dot{\overline{\Sigma}}_i\right.\\
&\qquad\left.+\frac{2(2l+1)}{c^4(l+1)(l+2)(2l+5)}\delta_{l+2}\hat{y}_{ijL}\ddot{\overline{\Sigma}}_{ij}\right\}(u+z|\mathbf{y}|/c,\mathbf{y})\ ,\\
J_L(u) &= \varepsilon_{ab<i_l}\mathrm{FP}\cdot\int d^3\mathbf{y}\int_{-1}^1 dz\left\{\delta_l\hat{y}_{L-1>a}\overline{\Sigma}_b\right.\\
&\qquad\left.-\frac{2l+1}{c^2(l+2)(2l+3)}\delta_{l+1}\hat{y}_{L-1>ac}\dot{\overline{\Sigma}}_{bc}\right\}(u+z|\mathbf{y}|/c,\mathbf{y})\ . \quad (2.52a)
\end{aligned}$$

$$\begin{aligned}
W_L(u) &= \mathrm{FP}\cdot\int d^3\mathbf{y}|\int_{-1}^1 dz\left\{\frac{2l+1}{(l+1)(2l+3)}\delta_{l+1}\hat{y}_{iL}\overline{\Sigma}_i\right.\\
&\qquad\left.-\frac{2l+1}{2c^2(l+1)(l+2)(2l+5)}\delta_{l+2}\hat{y}_{ijL}\dot{\overline{\Sigma}}_{ij}\right\}(u+z|\mathbf{y}|/c,\mathbf{y})\ ,\\
X_L(u) &= \mathrm{FP}\cdot\int d^3\mathbf{y}\int_{-1}^1 dz\left\{\frac{2l+1}{2(l+1)(l+2)(2l+5)}\delta_{l+2}\hat{y}_{ijL}\overline{\Sigma}_{ij}\right\}(u+z|\mathbf{y}|/c,\mathbf{y})\ ,\\
Y_L(u) &= \mathrm{FP}\cdot\int d^3\mathbf{y}\int_{-1}^1 dz\left\{-\delta_l\hat{y}_L\overline{\Sigma}_{ii} + \frac{3(2l+1)}{(l+1)(2l+3)}\delta_{l+1}\hat{y}_{iL}\dot{\overline{\Sigma}}_i\right.\\
&\qquad\left.-\frac{2(2l+1)}{c^2(l+1)(l+2)(2l+5)}\delta_{l+2}\hat{y}_{ijL}\ddot{\overline{\Sigma}}_{ij}\right\}(u+z|\mathbf{y}|/c,\mathbf{y})\ ,\\
Z_L(u) &= \mathrm{FP}\cdot\int d^3\mathbf{y}\int_{-1}^1 dz\left\{-\frac{2l+1}{(l+2)(2l+3)}\varepsilon_{ab<i_l}\delta_{l+1}\hat{y}_{L-1>bc}\overline{\Sigma}_{ac}\right\}(u+z|\mathbf{y}|/c,\mathbf{y})\ .
\end{aligned}$$

[4] This subsection mostly comes from Section 4.4. of Blanchet (2014) without significant modifications.

(2.52b)

where

$$\overline{\Sigma} = \frac{\overline{\tau}^{00} + \overline{\tau}^{ii}}{c^2} , \tag{2.53a}$$

$$\overline{\Sigma}_i = \frac{\overline{\tau}^{0i}}{c} , \tag{2.53b}$$

$$\overline{\Sigma}_{ij} = \overline{\tau}^{ij} . \tag{2.53c}$$

2.5 Asymptotic Gravitational Waveform

2.5.1 Radiative multipole moments

Around the future infinity, because h must be small linearized theory is totally enough. That is, there must be a set of multipole moments $\{\mathcal{U}_L, \mathcal{V}_L\}$ such that

$$G\, h_{(1)}[\mathcal{U}_L, \mathcal{V}_L]|_{\frac{1}{r}} = M(h)|_{\frac{1}{r}} , \tag{2.54}$$

where now $M(h)$ refers the MPM constructed solution started from the canonical linearized field,

$$M(h) := \sum_{n=1}^{\infty} G^n\, h_{(n)}[M_L, S_L] , \tag{2.55}$$

not just a general multipole expansion of the exact solution. By comparing $\frac{1}{r}$ one can specify $\{\mathcal{U}_L, \mathcal{V}_L\}$ in terms of $\{M_L, S_L\}$. However, the leading asymptotic order of $M(h)$ has logarithm terms in the non-linear contributions. To see this let us consider the second order. Because the linear contribution has the following large r structure,

$$h_{(1)} = \sum_{1\le k\le\infty,\, 0\le l\le\infty} \frac{\hat{n}_L}{r^k} F_{k,L}(u) . \tag{2.56}$$

$\mathrm{FP}\cdot\Box^{-1}\Lambda_{(2)}[h_{(1)}]$ requires the following integrals with any STF tensors K and P

$$a := \mathrm{FP}\cdot\Box^{-1}_{\mathrm{ret}}[\frac{\hat{n}_L}{r^2} K_L(u)] = -\frac{\hat{n}_L}{r}\int_r^{\infty} dz\, Q_l(\frac{z}{r})\, K_L(t-\frac{z}{c}) , \tag{2.57}$$

$$\mathrm{FP}\cdot\Box^{-1}_{\mathrm{ret}}[\frac{\hat{n}_L}{r^k}P_L(u)]=\sum_{i=3}^{\infty}\hat{n}_L\sum_{j=0}^{i-3}\frac{c_{jil}}{r^{j+1}}(\frac{d}{du})^{i-3-j}P_L(u)\quad(k\geq 3)\,,$$

where c_{jkl} are some numerical coefficients and $Q_l(x)$ is Legendre function of the second kind. The a-type integration gives us aymptotic lograthms since

$$\lim_{x\to 1}Q_l(x)\to-\frac{1}{2}\log(\frac{x-1}{2}). \tag{2.58}$$

Thus it is written down that $\{\mathcal{U}_L[M(u),S(u),\log r],\mathcal{V}_L[M(u),S(u),\log r]\}$ such as each radiative multipole moments are functionals of $M(u),S(u)$ and $\log r$. This is mathematically ridiculous because $\{\mathcal{U}_L(u),\mathcal{V}_L(u)\}$ must be functions of retarded time u. To resolve this discrephancy let us consider the future null infinity in harmonic gauge. Let null hypersurface $U(x)=$ const, which is desirable to parametrize the future null infinity and x is harmonic coordinate. Let us compute this up to linear order. By defintion of null hypersurface,

$$0\equiv\frac{\partial U}{\partial x^\mu}\frac{\partial U}{\partial x^\nu}g^{\mu\nu}=\frac{\partial U^{(0)}}{\partial x^\mu}\frac{\partial U^{(0)}}{\partial x^\nu}\eta^{\mu\nu}+G\left(2\frac{\partial U^{(1)}}{\partial x^\mu}\frac{\partial U^{(0)}}{\partial x^\nu}\eta^{\mu\nu}+\frac{\partial U^{(0)}}{\partial x^\mu}\frac{\partial U^{(0)}}{\partial x^\nu}h^{\mu\nu}_{(1)}\right)+O(G^2) \tag{2.59}$$

where $U^{(0)}:=t-\frac{r}{c}=u$. The G order equation is written as

$$\frac{\partial U^{(1)}}{\partial u}+c\frac{\partial U^{(1)}}{\partial r}=\frac{1}{2}\left(-h^{00}_{(1)}+2\frac{x^i}{r}h^{0i}_{(1)}-\frac{x^ix^j}{r^2}h^{ij}_{(1)}\right)=\sum_{k=1,l=0}\frac{\hat{n}_L}{r^k}\tilde{F}_{k,L}(u) \tag{2.60}$$

Since we are only interseted in $r\to\infty$ region, only $k=1$ the monopole contribution does matter. Thus $U^{(1)}$ has leading $\log r$ contribution as

$$U=u+G\,U^{(1)}=t-\frac{r}{c}-\frac{2\,G\,M}{c^3}\log(r/r_0)+O(r^0,G^2)\,. \tag{2.61}$$

This show us that the harmonic retarded time u was not good coordinate for the future null infinity but instead U should be involved. We can infer that every logarithm terms are absorbed into M and S as

$$\{\mathcal{U}_L[M(u),S(u),\log r],\mathcal{V}_L[M(u),S(u),\log r]\}\to\{\mathcal{U}_L[M(U),S(U)],\mathcal{V}_L[M(U),S(U)]\}.$$

Practically, new *radiative multipole moments* $\{\mathrm{U}_L, \mathrm{V}_L\}$ are widely used instead of $\{\mathcal{U}_L, \mathcal{V}_L\}$, which is defined as

$$\mathrm{U}_L := (\frac{d}{dU})^l \mathcal{U}_L \tag{2.62}$$

$$\mathrm{V}_L := (\frac{d}{dU})^l \mathcal{V}_L \,. \tag{2.63}$$

In terms of the radiative multipole moments, gravitational waveform is written as

$$h_{ij}^{\mathrm{TT}}(U, \mathbf{x}) = \frac{4G}{c^2 r} \mathcal{P}_{ijab}(\boldsymbol{n}) \sum_{l=2}^{+\infty} \frac{1}{c^l l!} \left\{ n_{L-2} \mathrm{U}_{abL-2}(U) - \frac{2l}{c\,(l+1)} n_{cL-2} \epsilon_{cd(a} \mathrm{V}_{b)dL-2}(U) \right\} + \mathcal{O}\left(\frac{1}{r^2}\right) . \tag{2.64}$$

where $\mathcal{P}_{ijab} = \mathcal{P}_{ia}\mathcal{P}_{jb} - \frac{1}{2}\mathcal{P}_{ij}\mathcal{P}_{ab}$ ($\mathcal{P}_{ij} = \delta_{ij} - n_i\, n_j$) is the transverse-tranceless (TT) projection which will be defined in. And the energy flux $\mathcal{F}$ and angular momentum fluxe $\mathcal{G}^i$ are given as (Blanchet (2014))

$$\mathcal{F} = \sum_{l=2}^{+\infty} \frac{G}{c^{2l+1}} \left\{ \frac{(l+1)(l+2)}{(l-1)ll!(2l+1)!!} \mathrm{U}_L^{(1)} \mathrm{U}_L^{(1)} + \frac{4l(l+2)}{c^2(l-1)(l+1)!(2l+1)!!} \mathrm{V}_L^{(1)} \mathrm{V}_L^{(1)} \right\}, \tag{2.65a}$$

$$\mathcal{G}_i = \epsilon_{iab} \sum_{l=2}^{+\infty} \frac{G}{c^{2l+1}} \left\{ \frac{(l+1)(l+2)}{(l-1)l!(2l+1)!!} \mathrm{U}_{aL-1} \mathrm{U}_{bL-1}^{(1)} + \frac{4l^2(l+2)}{c^2(l-1)(l+1)!(2l+1)!!} \mathrm{V}_{aL-1} \mathrm{V}_{bL-1}^{(1)} \right\}. \tag{2.65b}$$

2.6 Summary

We have gone through the foundation for constructing the solution of Einstein's field equatons with post-Newtonian approximation and multipolar-post-Minkowskian approximation. In this section, we summarize only the resulting algorithm for the computations. (The examples presented here are from Faye et al. (2012).)

1. Solve the PN constructed equation Eq.(2.25) order by order, and get $\bar{h}$ and finally $\bar{\tau}$.[5]

[5] Since $\bar{\tau}$ (Eq.2.5) includes both the matter source part T, and non-linear gravitational source part Λ which

2. Via Eqs.(2.52), one can compute explicit expressions for the source multipole moments $\{I, J, W, X, Y, Z\}$ from $\bar{\tau}$. This is a starting point of MPM construction since the linearized field $h^{(1)}$ is given in terms $\{I, J, W, X, Y, Z\}$ of via Eqs.(2.11a).

3. Follow the algorithm presented in the subsection 2.4.3. One can construct the higher order terms $h^{(2)}, h^{(3)}, \cdots$.

4. By equating two differently constructed MPM solutions starting from two linearized field $h_{(1)}[I, J, W, X, Y, Z]$ and $h_{(1)}[M, S]$, one can find the explicit canonical multipole moment $\{M, S\}$ in terms of $\{I, J, W, X, Y, Z\}$. For example,

$$M_{ij} = I_{ij} + \frac{4G}{c^5}\big[W^{(2)}\, I_{ij} - W^{(1)}\, I^{(1)}_{ij}\big] + \mathcal{O}(1/c^4)\,. \tag{2.66}$$

5. From the MPM solution constructed from $h_{(1)}[M, S]$, one can compute the radiative multipole moments $\{\mathrm{U}, \mathrm{V}\}$ and which determine GW waveform Eq.(2.64) and fluxes Eqs.(2.65). For example,

$$\mathrm{U}_{ij}(u) = \frac{d^2}{du^2} M_{ij}(u) + \frac{2GM}{c^3}\int_0^{+\infty} d\tau \left[\ln\frac{c\,\tau}{2\,r_0} + \frac{11}{12}\right]\frac{d^4}{du^4} M_{ij}(u-\tau) + \mathcal{O}(1/c^4)\,. \tag{2.67}$$

2.7 Appendix to Chapter 2

2.7.1 Multipole expansion of retarded solutions

In this section let us find a STF expression of a retarded solution

$$\phi(t, \mathbf{x}) := -4\pi\, \Box^{-1}_{\mathrm{ret}}[\rho](t, \mathbf{x})\,, \tag{2.68}$$

---

arises at high orders and the homogeneous part $-\frac{4G}{c^4}\sum_{l=0}^{\infty} \partial_L \big\{ \overline{\frac{R^{\mu\nu}_L(t-r/c) - R^{\mu\nu}_L(t+r/c)}{2\,r}} \big\}$ in Eq.(2.25) also arises from 4PN order, we can neglect them in the low-order computation and thus, starting from well-defined matter source T, we can compute low order of $\bar{h}$. And inputing $\bar{h}$ in Λ yield the higher-order of $\bar{\tau}$ and $\bar{h}$.

or

$$\phi(\mathbf{x},t) = \int d^4x' G_R(x-x')\,\rho(x'), \tag{2.69}$$

where

$$\begin{aligned} G_R(x-x') &= \frac{\delta(t-t'-|\mathbf{x}-\mathbf{x}'|)}{|\mathbf{x}-\mathbf{x}'|} \\ &= \frac{\delta(t-t'-\sqrt{r^2+r'^2-2rr'\vec{n}\cdot\vec{n}'})}{\sqrt{r^2+r'^2-2rr'\vec{n}\cdot\vec{n}'}}\,. \end{aligned} \tag{2.70}$$

Hence it satisfies

$$\Box\,\phi(t,\mathbf{x}) = -4\pi\,\rho(t,\mathbf{x}). \tag{2.71}$$

We want to find multipole expansion of ϕ, $M[\phi]$. First, consider that

$$F(\vec{n}\cdot\vec{n}') = \frac{1}{2}\sum_{l=0}^{+\infty}\frac{(2l+1)!!}{l!}\hat{n}_L\hat{n}'_L\int_{-1}^{+1}dz F(z)P_l(z), \tag{2.72}$$

This formula comes from the fact that

$$\hat{n}_L\hat{n}'_L = \frac{l!}{(2l-1)!!}P_l(\vec{n}\cdot\vec{n}'). \tag{2.73}$$

Now, expand retarded Green function,

$$G_R(x-x') = \frac{1}{2}\sum_{l=0}^{+\infty}\frac{(2l+1)!!}{l!}\hat{n}_L\hat{n}'_L\int_{-1}^{+1}dz\frac{\delta(t-t'-\sqrt{r^2+r'^2-2rr'z})}{\sqrt{r^2+r'^2-2rr'z}}P_l(z) \tag{2.74}$$

$$= \frac{\Theta(t-t')\Theta(1-\nu^2)}{2}\sum_{l=0}^{+\infty}\frac{(2l+1)!!}{l!}\hat{n}_L\hat{n}'_L\int_{-1}^{+1}dz\frac{\delta(z-\nu)}{rr'}P_l(z)$$

$$= \frac{\Theta(t-t')\Theta(1-\nu^2)}{2rr'}\sum_{l=0}^{+\infty}\frac{(2l+1)!!}{l!}\hat{n}_L\,\hat{n}'_L\,P_l(\nu),$$

where $\nu(r') = \frac{r'^2+r^2-(t-t')^2}{2rr'}$. Thus the multipolar retarded solution $M(\phi)(x)$ becomes

$$M(\phi)(x) = \int d^4x'\frac{\Theta(t'-t)\Theta(1-\nu^2)}{2rr'}\sum_{k=0}^{+\infty}\frac{(2k+1)!!}{k!}\hat{n}_K\hat{n}'_K P_k(\nu)\rho(x')\,, \tag{2.75}$$

$$= 4\pi \int dt'dr' \frac{\Theta(t'-t)\Theta(1-\nu^2)}{2r} r' \sum_{k=0}^{+\infty} \hat{n}_K P_k(\nu)\sigma_K(t',r')\,,$$

$$= \frac{\pi}{r}\hat{n}_L \int dt'dr' \Theta(t'-t)\Theta(1-\nu^2)\, r'\, P_l(\nu)\sigma_L(t',r')\,,$$

In the second line, we used the following identities,

$$\int d\Omega(\vec{n})\hat{n}_L\hat{n}_K = \frac{4\pi l!}{(2l+1)!!}\,\delta_{lk}\,, \tag{2.76}$$

more generally, for multipole expansion, $f(\vec{n}) = \sum_{l=0}^{\infty} f_L \hat{n}_L$,

$$\sigma_L(t,r) := \frac{(2l+1)!!}{4\pi l!}\int d\Omega\, \hat{n}_L\, \rho(t,\mathbf{x}). \tag{2.77}$$

In the last line, the variables have been changed as $u = t - r$, $v = t + r$. And the domain is $D = \{u', v' | u' < u, u < v' < v\}$. Using the result of *Koepf*, the Legendre function can be written as

$$P_l(\nu) = \sum_{k=0}^{l} \frac{l(l-1)\cdots(l-k+1)}{k!}\frac{(-l-1)(-l-2)\cdots(-l-k)}{k!}(\frac{1-\nu}{2})^k \tag{2.78}$$

$$= \sum_{k=0}^{l} \frac{(-)^k(l+k)!}{(l-k)!(k!)^2}(\frac{(u'-u)(v'-v)}{(v'-u')(v-u)})^k$$

$$= \sum_{k=0}^{l} \frac{(-)^k(l+k)!}{(l-k)!(k!)^2}(\frac{(u'-u)}{(v'-u')(v-u)})^k((v'-u')+(u'-v))^k$$

$$= \sum_{k=0}^{l} \frac{(-)^k(l+k)!}{(l-k)!(k!)^2}(\frac{(u'-u)}{(v'-u')(v-u)})^k \sum_{s=0}^{k}\frac{k!}{s!(k-s)!}(v'-u')^{k-s}(u'-v)^s$$

$$= \sum_{k=0}^{l}\sum_{s=0}^{k} \frac{(-)^k(l+k)!}{(l-k)!k!s!(k-s)!}\frac{(u'-u)^k(u'-v)^s}{(v-u)^k(v'-u')^s}$$

$$= \sum_{s=0}^{l}\sum_{k=s}^{l} \frac{(-)^k(l+k)!}{(l-k)!k!s!(k-s)!}\frac{(u'-u)^k(u'-v)^s(v-u)^{l-k}}{(v-u)^l(v'-u')^s}$$

$\because$ (changing the order of summation)

$$= \sum_{k=0}^{l} \frac{1}{k!(v-u)^l(v'-u')^k} \sum_{s=k}^{l} \frac{(-)^s(l+s)!}{(l-s)!s!(s-k)!}(u'-u)^s(u'-v)^k(v-u)^{l-s}$$

$$= \sum_{k=0}^{l} \frac{1}{k!(v-u)^l(v'-u')^k} \sum_{s=0}^{l-k} \frac{(-)^{k+s}(l+k+s)!}{(l-s-k)!(s+k)!(s)!}(u'-u)^{s+k}(u'-v)^k(v-u)^{l-k-s}$$

$$= \sum_{k=0}^{l} \frac{1}{k!(v-u)^l(v'-u')^k} \sum_{s=0}^{l-k} \sum_{t=0}^{l-k-s} \frac{(-)^{k+s+t}(l+k+s)!}{(l-s-k-t)!(s+k)!t!s!}(u'-u)^{l-t}(u'-v)^{k+t}.$$

On the other hand, another identity $\mathcal{I}_1$ holds:

$$\frac{(-1)^l}{l!}\frac{(v'-u')^{l+1}}{(v-u)^l}(\frac{\partial}{\partial u'})^l\Big\{\frac{(u'-u)^l(u'-v)^l}{(v'-u')^{l+1}}\Big\} \tag{2.79}$$

$$= \frac{(-)^l}{l!}\frac{(v'-u')^{l+1}}{(v-u)^l}\sum_{k=0}^{l}\frac{l!}{k!(l-k)!}(\frac{\partial}{\partial u'})^k(v'-u')^{-l-1}(\frac{\partial}{\partial u'})^{l-k}[(u'-u)^l(u'-v)^l]$$

$$= \frac{(-)^l}{l!}\sum_{k=0}^{l}\frac{(l+k)!}{k!(l-k)!}\frac{1}{(v'-u')^k(v-u)^l}(\frac{\partial}{\partial u'})^{l-k}[(u'-u)^l(u'-v)^l]$$

$$= \frac{(-)^l}{l!}\sum_{k=0}^{l}\frac{(l+k)!}{k!(l-k)!}\frac{1}{(v'-u')^k(v-u)^l}\sum_{t=0}^{l-k}\frac{(l-k)!}{t!(l-k-t)!}\frac{l!}{(l-t)!}\frac{l!}{(k+t)!}(u'-u)^{l-t}(u'-v)^{k+t}$$

$$= \sum_{k=0}^{l}\frac{(-)^l(l+k)!}{k!(l-k)!}\frac{1}{(v'-u')^k(v-u)^l}\sum_{t=0}^{l-k}\frac{l!(l-k)!}{t!(l-k-t)!(k+t)!(l-t)!}(u'-u)^{l-t}(u'-v)^{k+t}$$

$$= \sum_{k=0}^{l}\frac{1}{k!(v-u)^l(v'-u')^k}\sum_{t=0}^{l-k}\frac{(-)^l(l+k)!(l-k)!l!}{(l-k)!(k+t)!(l-t)!t!(l-k-t)!}(u'-u)^{l-t}(u'-v)^{k+t}.$$

And also the following identity $\mathcal{I}_2$ is used,

$$\sum_{k=0}^{l} \frac{1}{k!(v-u)^l(v'-u')^k} \sum_{t=0}^{l-k} \sum_{s=0}^{l-k-t} \frac{(-)^{k+s+t}(l+k+s)!}{(l-s-k-t)!(s+k)!t!s!}(u'-u)^{l-t}(u'-v)^{k+t} \tag{2.80}$$

$$= \sum_{k=0}^{l} \frac{1}{k!(v-u)^l(v'-u')^k} \sum_{t=0}^{l-k} \frac{(-)^k(l+k)!(l-k)!l!}{(l-k)!(k+t)!(l-t)!t!(l-k-t)!}(u'-u)^{l-t}(u'-v)^{k+t},$$

of which proof is as what follows: Proving the following is equivlaent with proving $\mathcal{I}_2$,

$$\sum_{s=0}^{l-k-t} \frac{(-)^{k+s+t}(l-k-t)!(l+k+s)!}{(l-s-k-t)!(s+k)!s!} = \frac{(-)^l(l+k)!l!}{(k+t)!(l-t)!}. \tag{2.81}$$

With a new notation $(l)_k = l(l+1)(l+2)\cdots(l+k-1)$, the left hand side of the above relation becomes

$$\begin{aligned}
&\sum_{s=0}^{l-k-t} \frac{(-)^{k+t}(-l+k+t)_s(l+k+1)_s(l+k)!}{(k+1)_s k!s!} \qquad (2.82)\\
=&\frac{(-)^{k+t}(l+k)!}{k!}\sum_{s=0}^{\infty}\frac{(-l+k+t)_s(l+k+1)_s}{(k+1)_s s!}\\
=&\frac{(-)^{k+t}(l+k)!}{k!}\lim_{z\to 1_-} F(-l+k+t;l+k+1;k+1;z)\\
=&\frac{(-)^{k+t}(l+k)!}{k!}\frac{\Gamma(k+1)\Gamma(-t-k)}{\Gamma(-l)\Gamma(l-t+1)} = \frac{(-)^l(l+k)!}{k!}\frac{\Gamma(k+1)\Gamma(l+1)}{\Gamma(1+t+k)\Gamma(l-t+1)}\\
=&\frac{(-)^l(l+k)!l!}{(k+t)!(l-t)!}
\end{aligned}$$

in the second line, the upper bound of summation vanishes because $(-l+k+t)_s = 0$ when $s > l-k-t$, and F is *hypergeometry series*. In the third line, I use the limit of hypergeomety function given as

$$\lim_{z\to 1_-} F(\alpha;\beta;\gamma;z) = \frac{\Gamma(\gamma)\Gamma(\gamma-\alpha-\beta)}{\Gamma(\gamma-\alpha)\Gamma(\gamma-\beta)}, \tag{2.83}$$

and also using

$$\Gamma(\epsilon-n) = (-1)^{n-1}\frac{\Gamma(-\epsilon)\Gamma(\epsilon+1)}{\Gamma(n+1-\epsilon)}. \tag{2.84}$$

With these proved identities $\mathcal{I}_1$ and $\mathcal{I}_2$, Legendre function can be written as,

$$\begin{aligned}
\hat{n}_L P_l(\nu) &= \hat{n}_L \frac{(-1)^l}{l!}\frac{(v-u)^{l+1}}{(v'-u')^l}(\frac{\partial}{\partial u})^l\Big\{\frac{(u-u')^l(u-v')^l}{(v-u)^{l+1}}\Big\} \qquad (2.85)\\
&= \hat{n}_L \frac{1}{(l!)^2}\frac{(v-u)^{l+1}}{(v'-u')^l}(\frac{\partial}{\partial u})^l(\frac{\partial}{\partial v})^l\Big\{\frac{(u-u')^l(u-v')^l}{(v-u)}\Big\}
\end{aligned}$$

$$= \frac{1}{2l!}\frac{(v-u)}{(v'-u')^l}\hat{\partial}_L\big(\frac{(u-u')^l(u-v')^l}{r}\big)\,.$$

Alternatively, the above relation also can be proved by invoking the Riemann function Martin (1951) of Euler-Poisson-Darboux equation,

$$\partial_{uv}f + \frac{l(l+1)}{(v-u)^2}f = 0\,. \tag{2.86}$$

if $P_l(\nu)$ is the Riemann function of the EPD equation, there are requirements that, first $P_l(\nu)$ itself is the solution(because the EPD equation is self-adjoint), and $\partial_u P_l(\nu) = 0$ when $v = v'$ and also $\partial_v P_l(\nu) = 0$ when $u = u'$. And this is also the case of

$$\frac{(-1)^l}{l!}\frac{(v'-u')^{l+1}}{(v-u)^l}(\frac{\partial}{\partial u'})^l\Big\{\frac{(u'-u)^l(u'-v)^l}{(v'-u')^{l+1}}\Big\}\,. \tag{2.87}$$

That is, both expressions are the Reimann function of the EPD equation and because the Reimann function is unique thus they are same.

Anyway, the expression of solution becomes

$$M(\phi)(x) = \frac{\pi}{2}\int^u du'\int_v^u dv'\frac{1}{l!(v'-u')^{l-1}}\hat{\partial}_L(\frac{(u-u')^l(u-v')^l}{r})\sigma_L(\frac{1}{2}(v'-u'),\frac{1}{2}(u'+v')) \tag{2.88}$$

$$= \frac{\pi}{2}\hat{\partial}_L\Big[r^{-1}\int^u du'\int_v^u dv'\frac{(u-u')^l(u-v')^l}{l!(v'-u')^{l-1}}\sigma_L(\frac{1}{2}(u'+v'),\frac{1}{2}(v'-u'))\Big]\,.$$

(note that I was able to place $\hat{\partial}_L$ before intergals. See Eq.(2.97)) By changing the variable

$$v' = u' + 2\,r', \tag{2.89}$$

we have arrived the generic result,

$$M(\phi)(x) = \frac{\pi}{2^{l-1}l!}\hat{\partial}_L\Big[r^{-1}\int_{-\infty}^u du'\int_{\frac{v-u'}{2}}^{\frac{u-u'}{2}} dr'\frac{(u-u')^l(u-u'-2r')^l}{l!r'^{l-1}}\sigma_L(u'+r',r')\Big]\,. \tag{2.90}$$

Multipolar retarded solution of Compact support sources

At this point, let us additionally assume that the sourece has a compact support, there exits $d > 0$ such that $\rho = 0$ when $r > d$. And let us consider $\phi(t, \mathbf{x})$ only where $r > d$. Additional change of variable as

$$u' = u + (z-1)\, r', \tag{2.91}$$

yields

$$\begin{aligned}
\phi(x) &= \frac{(-)^l \pi}{2^{l-1} l!} \hat{\partial}_L \Big[r^{-1} \int_{-1}^{+1} dz \int_0^r dr' (1-z^2)^l \, r'^{l+2} \, \sigma_L(u + zr', r') \Big], \qquad (2.92) \\
&= \frac{(-)^l \pi}{2^{l-1} l!} \hat{\partial}_L \Big[r^{-1} \int_{-1}^{+1} dz \int_0^d dr' (1-z^2)^l \, r'^{l+2} \, \sigma_L(u + zr', r') \Big], \\
&= \frac{(-)^l \pi}{2^{l-1} l!} \hat{\partial}_L \Big[r^{-1} \int_{-1}^{+1} dz \int_0^\infty dr' (1-z^2)^l \, r'^{l+2} \, \sigma_L(u + zr', r') \Big].
\end{aligned}$$

You can see that integration was dependent on r. But since, as mentioned, we are interested in $r > d$, the radial integraion interval can be extended to infinity. Re-inputting

$$\sigma_L(t, r) = \frac{(2l+1)!!}{4\pi \, l!} \int d\Omega \, \hat{n}_L \, \rho(t, \mathbf{x}), \tag{2.93}$$

yields

$$\phi(x, t) = \sum_{l=0}^{\infty} \frac{(-)^l}{l!} \partial_L \Big\{ \frac{F_L(t - r/c)}{r} \Big\} \quad \text{where} \quad r > d\,, \tag{2.94}$$

where F_L is a STF tensor such that

$$F_L(u) = \frac{(2l+1)!!}{2^{l+1} l!} \int d^3\mathbf{x}' \, \hat{x}'_L \int_{-1}^{+1} dz \, (1-z^2)^l \, \rho(u + z\, r', \mathbf{x}')\,. \tag{2.95}$$

Multipolar retarded solution of Non-compact support sources

From Eq.(2.90) again, let us find another expression for non compact support sources. Take a change of notation $u' \to s$, $r' \to x$ for usual notation, then the multipole expanded vacuum solution ϕ_3 become,

$$\phi(x, t) = \int_{-\infty}^{u} ds \int_{\frac{1}{2}(v-s)}^{\frac{1}{2}(u-s)} dx \hat{\partial}_L [r^{-1} \frac{(u-s)^l (u-s-2x)^l}{x^{l-1}}] \rho_L(x, x+s) \tag{2.96}$$

$$= \int^{u} ds \int_0^{\frac{1}{2}(u-s)} dx \hat{\partial}_L [r^{-1} \frac{(u-s)^l (u-s-2x)^l}{x^{l-1}}] \rho_L(x, x+s)$$
$$- \int^{u} ds \int_0^{\frac{1}{2}(v-s)} dx \hat{\partial}_L [r^{-1} \frac{(v-s)^l (v-s-2x)^l}{x^{l-1}}] \rho_L(x, x+s).$$

in the last line, I use the identity,

$$\hat{\partial}_L(\frac{u^i}{r}) = \hat{\partial}_L(\frac{v^i}{r}) \,, \tag{2.97}$$

where i s are integer. Defining

$$\mathcal{R}_L(\rho, s) := \rho^l \int_0^{\rho} dx \, \frac{(\rho - x)^l}{l!} \left(\frac{2}{x}\right)^{l-1} \rho_L(x, x+s) \,, \tag{2.98}$$

we have the following expression,

$$\phi(x) = \sum_l \int_{-\infty}^{u} ds \hat{\partial}_L(\frac{\mathcal{R}_L(\frac{t-r-s}{2}, s) - \mathcal{R}_L(\frac{t+r-s}{2}, s)}{r}) \,, \tag{2.99}$$

or, equivalently,

$$\phi(t,x) = \sum_l \int_r^{\infty} ds \hat{\partial}_L(\frac{\mathcal{R}_L(\frac{s-r}{2}, t-s/c) - \mathcal{R}_L(\frac{s+r}{2}, t-s/c)}{2r}) \,, \tag{2.100}$$
$$= \sum_l \int_{-r}^{r} ds \hat{\partial}_L(\frac{\mathcal{R}_L(\frac{s+r}{2}, t-s/c)}{r}) - \frac{1}{4\pi} \sum_l \frac{(-)^l}{l!} \hat{\partial}_L(\frac{R_L(t-r/c) - R_L(t+r/c)}{2r}),$$

where

$$R_L(t) := 8\pi(-)^{l+1} l! \int_{-\infty}^{t} ds \mathcal{R}_L(\frac{t-s}{2}, s) \,. \tag{2.101}$$

Or, with another change of variable as $s = t - x\,(z+1)$,

$$R_L(t) := 8\pi(-)^{l+1} l! \int_{-\infty}^{t} ds \, \big(\frac{t-s}{2}\big)^l \int_0^{\frac{t-s}{2}} dx \, \frac{(\frac{t-s}{2} - x)^l}{l!} \left(\frac{2}{x}\right)^{l-1} \rho_L(x, x+s)$$
$$= 8\pi(-)^{l+1} l! \int_{-\infty}^{t} ds \, \big(\frac{t-s}{2}\big)^l \int_0^{\frac{t-s}{2}} dx \, \frac{(\frac{t-s}{2} - x)^l}{l!} \left(\frac{2}{x}\right)^{l-1} \rho_L(x, x+s)$$
$$= 8\pi(-)^{l+1} l! \int_1^{\infty} dz \, (-x) \big(x\,(z+1)/2\big)^l \int_0^{\infty} dx \, \frac{(x(z+1)/2 - x)^l}{l!} \left(\frac{2}{x}\right)^{l-1} \rho_L(x, t-zx)$$
$$= \int_1^{\infty} dz \, \frac{1}{2^l} (1-z^2)^l \int_0^{\infty} dx \, (x)^{l+2} \, \frac{(2l+1)!!}{l!} \int d\Omega \hat{n}_L \rho(\vec{x}, t-zx)$$
$$= -\int_1^{\infty} dz \, \gamma_l(z) \int d^3x \, \hat{x}_L \, \rho(\vec{x}, t-zx) \,. \tag{2.102}$$

2.7.2 Derivation of G_L

First let us compute that

$$\partial_0 F^{0\mu}(t-r/c) = \frac{d}{c\,du} F^{0\mu}(t-r/c). \tag{2.103}$$

From the definition of F we have gotten earlier, we get

$$\begin{aligned}
&\partial_0 F^{0\mu} \qquad (2.104)\\
&= \int d^3y\,|y|^B\,\hat{y}_L \int_{-1}^{+1} dz\,\delta_l(z)\,\partial_0 \bar{\tau}^{0\mu}(t-\frac{r}{c}+\frac{z|y|}{c}, y^i) \quad (\because \partial_\nu \bar{\tau}^{\nu\mu}=0)\,,\\
&= -\int d^3y\,|y|^B\,\hat{y}_L \int_{-1}^{+1} dz\,\delta_l(z)\,\left(\frac{d}{dy^j}\bar{\tau}^{j\mu}(T(y),y^i) - \frac{\partial T(y)}{\partial y^j}\partial_T \bar{\tau}^{j\mu}(T,y^i)\right) \quad (T := t-\frac{r}{c}+\frac{z|y|}{c})\,,\\
&= \int d^3y\,\frac{\partial}{\partial y^j}(|y|^B\,\hat{y}_L)\int_{-1}^{+1} dz\,\delta_l(z)\,\bar{\tau}^{j\mu}(T,y^i) \quad \text{(integration by parts)}\,,\\
&\quad -\int d^3y\,|y|^B\,\hat{y}_L \int_{-1}^{+1} dz\,\frac{\frac{d}{dz}\delta_{l+1}(z)}{(2l+3)z}\frac{\partial T(y)}{\partial y^j}\partial_T\bar{\tau}^{j\mu}(T,y^i) \quad (\because \frac{d\delta_{l+1}}{dz} = -(2l+3)z\delta(z)_l)\,,\\
&=: G_L^\mu(t-r/c) + \int d^3y\,|y|^B\,l\,\delta_{j<k}y_{L-1>}\int_{-1}^{+1} dz\,\delta_l(z)\,\bar{\tau}^{j\mu}(T,y^i) \quad (\because \frac{\partial \hat{y}_L}{\partial y^j} = l\delta_{j<k}y_{L-1>})\,,\\
&\quad +\int d^3y\,|y|^B\,\hat{y}_L\int_{-1}^{+1} dz\,\frac{\delta_{l+1}(z)}{(2l+3)}\partial_z\left(\frac{y^j}{c|y|}\partial_T\bar{\tau}^{j\mu}(T(z),y^i)\right)\,,\\
&= G_L^\mu(t-r/c) + \int d^3y\,|y|^B\,l\,\hat{y}_{<L-1}\int_{-1}^{+1} dz\,\delta_l(z)\,\bar{\tau}^{j>\mu}(T,y^i)\,,\\
&\quad +\int d^3y\,|y|^B\,\hat{y}_L\,y^j\int_{-1}^{+1} dz\,\frac{\delta_{l+1}(z)}{(2l+3)}\left(\frac{1}{c^2}\partial_T^2\bar{\tau}^{j\mu}(T(z),y^i)\right)\,,\\
&= G_L^\mu(t-r/c) + \int d^3y\,|y|^B\,l\,\hat{y}_{<L-1}\int_{-1}^{+1} dz\,\delta_l(z)\,\bar{\tau}^{j>\mu}(T,y^i)\,,\\
&\quad +\int d^3y\,|y|^B\,\hat{y}_{Lj}\int_{-1}^{+1} dz\,\frac{\delta_{l+1}(z)}{(2l+3)}\left(\frac{1}{c^2}\partial_T^2\bar{\tau}^{j\mu}(T(z),y^i)\right) \quad (\because \hat{y}_L y_j = \hat{y}_{Lj} + \frac{l}{2l+1}|y|^2\delta_{j<i_l}y_{L-1})\,,\\
&\quad +\int d^3y\,|y|^B(\frac{l}{2l+1}\hat{y}_{<L-1})\int_{-1}^{+1} dz\,\frac{(\frac{d}{dz})^2\delta_{l+1}(z)}{(2l+3)}\left(\bar{\tau}^{j>\mu}(T(z),y^i)\right)\,,
\end{aligned}$$

$$
\begin{aligned}
&= G_L^{\mu}(t-r/c) + \int d^3y\,|y|^B\, l\,\hat{y}_{<L-1} \int_{-1}^{+1} dz\, \left(\delta_l(z) + \frac{(\frac{d}{dz})^2 \delta_{l+1}(z)}{(2l+1)(2l+3)} \right) \bar{\tau}^{j>\mu}(T, y^i)\,, \\
&\quad + \int d^3y\,|y|^B\, \hat{y}_{Lj} \int_{-1}^{+1} dz\, \frac{\delta_{l+1}(z)}{(2l+3)} \left(\frac{1}{c^2} \partial_T^2 \bar{\tau}^{j\mu}(T(z), y^i) \right)\,, \\
&= G_L^{\mu}(t-r/c) + \int d^3y\,|y|^B\, l\,\hat{y}_{<L-1} \int_{-1}^{+1} dz\, \delta_{l-1}(z)\, \bar{\tau}^{j>\mu}(T, y^i) \\
&\quad + \left(\frac{d}{cdu} \right)^2 \frac{F_{jL}^{j\mu}(t-r/c)}{2l+3} \quad \left(\because \delta_{l-1}(z) = \left(\delta_l(z) + \frac{(\frac{d}{dz})^2 \delta_{l+1}(z)}{(2l+1)(2l+3)} \right) \right)\,, \\
&= G_L^{\mu}(t-r/c) + l\, F_{<L-1}^{i_l>\mu}(t-r/c) + \left(\frac{d}{cdu} \right)^2 \frac{F_{jL}^{j\mu}(t-r/c)}{2l+3}\,.
\end{aligned}
$$

In the middle of the calculation, it was defined that

$$
G_L^{\mu}(t-r/c) = \int d^3y\, B|y|^{B-2}\, \hat{y}_L\, y_j \int_{-1}^{+1} dz\, \delta_l(z)\, \bar{\tau}^{j\mu}(t - \frac{r}{c} + \frac{z|y|}{c}, y^i). \tag{2.105}
$$

Now turn our attention to proving that the above defintion of G_L works.

$$
\begin{aligned}
&\sum_l^{\infty} \frac{(-)^l}{l!} \partial_0 \hat{\partial}_L \{ \frac{F_L^{0\mu}(t - \frac{r}{c})}{r} \} \qquad (2.106) \\
&= \sum_l^{\infty} \frac{(-)^l}{l!} \hat{\partial}_L \{ \frac{1}{r} G_L^{\mu}(t-r/c) + l\, F_{<L-1}^{i_l>\mu}(t-r/c) + \left(\frac{d}{cdu} \right)^2 \frac{F_{jL}^{j\mu}(t-r/c)}{2l+3} \}.
\end{aligned}
$$

Let us focus on the second term,

$$
\begin{aligned}
&\sum_{l=1}^{\infty} \frac{(-)^l}{(l-1)!}\, \partial_{L-1 i_l} \left(\frac{F_{<L-1}^{i_l>\mu}(t-r/c)}{r} \right) \qquad (2.107) \\
&= \sum_{l=1}^{\infty} \frac{(-)^l}{(l-1)!}\, \hat{\partial}_{L-1 i_l} \left(\frac{F_{L-1}^{i_l\mu}(t-r/c)}{r} \right) \quad \text{(STF operation is transferred to derivatives)} \\
&= -\sum_{l=0}^{\infty} \frac{(-)^l}{l!}\, \hat{\partial}_{L i_l} \left(\frac{F_L^{i_l\mu}(t-r/c)}{r} \right)
\end{aligned}
$$

Before further calculations, let us use the following statement,

$$
\hat{\partial}_{Li} f(r) = \hat{\partial}_L \partial_i f(r) - \frac{l}{2l+1} \delta_{i<i_l} \partial_{L-1>} \left((\frac{\partial}{\partial r})^2 + \frac{2}{r} \frac{\partial}{\partial r} \right) f(r). \tag{2.108}
$$

This could be straightforwardly proved being cautious about that ∂_i and ∂_r are not commutable.

In this case, since

$$\left((\frac{\partial}{\partial r})^2+\frac{2}{r}\frac{\partial}{\partial r}\right)\frac{F(t-r/c)}{r}=(\frac{d}{cdt})^2\frac{F(t-r/c)}{r}\,, \tag{2.109}$$

the second term becomes,

$$\begin{aligned}
&-\sum_{l=0}^{\infty}\frac{(-)^l}{l!}\,\hat{\partial}_{Li_l}\left(\frac{F_L^{i_l\mu}(t-r/c)}{r}\right) \qquad (2.110)\\
&=-\sum_{l=0}^{\infty}\frac{(-)^l}{l!}\,\hat{\partial}_L\partial_{i_l}\left(\frac{F_L^{i_l\mu}(t-r/c)}{r}\right)+\sum_{l=l}^{\infty}\frac{(-)^l}{(l-1)!}\frac{1}{2l+1}\partial_{L-1}(\frac{d}{c\,du})^2\left(\frac{F_{jL-1}^{j\mu}(t-r/c)}{r}\right)\\
&=-\sum_{l=0}^{\infty}\frac{(-)^l}{l!}\,\hat{\partial}_L\partial_{i_l}\left(\frac{F_L^{i_l\mu}(t-r/c)}{r}\right)-\sum_{l=0}^{\infty}\frac{(-)^l}{l!}\frac{1}{2l+3}\partial_L(\frac{d}{c\,du})^2\left(\frac{F_{jL}^{j\mu}(t-r/c)}{r}\right)
\end{aligned}$$

Thus,

$$\begin{aligned}
&\sum_{l}^{\infty}\frac{(-)^l}{l!}\partial_0\hat{\partial}_L\{\frac{F_L^{0\mu}(t-\frac{r}{c})}{r}\} \qquad (2.111)\\
&=\sum_{l}^{\infty}\frac{(-)^l}{l!}\hat{\partial}_L\{\frac{1}{r}G_L^{\mu}(t-r/c)\}-\sum_{l=0}^{\infty}\frac{(-)^l}{l!}\,\hat{\partial}_L\partial_{i_l}\left(\frac{F_L^{i_l\mu}(t-r/c)}{r}\right),
\end{aligned}$$

or

$$\begin{aligned}
&\sum_{l}^{\infty}\frac{(-)^l}{l!}\partial_\nu\hat{\partial}_L\{\frac{F_L^{\nu\mu}(t-\frac{r}{c})}{r}\} \qquad (2.112)\\
&=\sum_{l}^{\infty}\frac{(-)^l}{l!}\partial_0\hat{\partial}_L\{\frac{F_L^{0\mu}(t-\frac{r}{c})}{r}\}+\sum_{l=0}^{\infty}\frac{(-)^l}{l!}\,\hat{\partial}_L\partial_{i_l}\left(\frac{F_L^{i_l\mu}(t-r/c)}{r}\right)\\
&=\sum_{l}^{\infty}\frac{(-)^l}{l!}\hat{\partial}_L\{\frac{1}{r}G_L^{\mu}(t-r/c)\}\,.
\end{aligned}$$

Finally we get G_L. Then by the expression for v in terms of G_L, we determine v.

Chapter 3

Quasi-Keplerian parametrization of Eccentric Orbits

In this chapter, we derive fourth post-Newtonian (4PN) order contributions to Keplerian-type parametric solution for describing dynamics of non-spinning compact binaries in eccentric orbits. The underlying compact binary dynamics is described by the 4PN accurate near-zone local-in-time Arnowitt-Deser-Misner (ADM) Hamiltonian, derived in Jaranowski and Schäfer (2015). We provide explicit 4PN order expressions for various orbital elements and functions of our parametric solution in terms of the conserved orbital energy, angular momentum for a given symmetric mass ratio. Resulting parametric solution is employed to obtain an updated inspiral, merger and ring-down waveform family to model the coalescence of moderately eccentric binaries of non-spinning black holes. This work is influenced by Hinder et al. (2018).

3.1 4PN accurate Equations of Motion

We write below the local-in-time near-zone 4PN-accurate Hamiltonian in ADM-type coordinates and in the center-of-mass frame, as given by Eq. (8.41) of Jaranowski and Schäfer

(2015),

$$\mathcal{H}^{\rm local}_{\rm 4PN}(\mathbf{r},\hat{\mathbf{p}}) = \frac{\hat{\mathbf{p}}^2}{2} - \frac{1}{r} + \frac{1}{c^2}\mathcal{H}_1(\mathbf{r},\hat{\mathbf{p}}) + \frac{1}{c^4}\mathcal{H}_2(\mathbf{r},\hat{\mathbf{p}}) + \frac{1}{c^6}\mathcal{H}_3(\mathbf{r},\hat{\mathbf{p}}) + \frac{1}{c^8}\mathcal{H}_4(\mathbf{r},\hat{\mathbf{p}})\,. \tag{3.1}$$

The explicit expressions for $\mathcal{H}_1, \mathcal{H}_2$ and $\mathcal{H}_3$ which are the 1PN, 2PN and 3PN contributions given by Eqs. (7) in Memmesheimer et al. (2004) and $\mathcal{H}_4$, the 4PN order contribution, can be extracted from Eq. (8.41) in Jaranowski and Schäfer (2015),

$$\mathcal{H}_1(\mathbf{r},\hat{\mathbf{p}}) = \frac{1}{8}\,(3\eta-1)\,(\hat{\mathbf{p}}^2)^2 - \frac{1}{2}\Big\{(3+\eta)\,\hat{\mathbf{p}}^2 + \eta\,(\mathbf{n}\cdot\hat{\mathbf{p}})^2\Big\}\,\frac{1}{r} + \frac{1}{2\,r^2}\,, \tag{3.2a}$$

$$\begin{aligned}\mathcal{H}_2(\mathbf{r},\hat{\mathbf{p}}) = {}& \frac{1}{16}\left(1-5\eta+5\eta^2\right)(\hat{\mathbf{p}}^2)^3 \\ & + \frac{1}{8}\Big\{\left(5-20\eta-3\eta^2\right)(\hat{\mathbf{p}}^2)^2 - 2\eta^2(\mathbf{n}\cdot\hat{\mathbf{p}})^2(\hat{\mathbf{p}}^2) - 3\eta^2(\mathbf{n}\cdot\hat{\mathbf{p}})^4\Big\}\frac{1}{r} \\ & + \frac{1}{2}\Big\{(5+8\eta)\,\hat{\mathbf{p}}^2 + 3\eta\,(\mathbf{n}\cdot\hat{\mathbf{p}})^2\Big\}\,\frac{1}{r^2} - \frac{1}{4}\,(1+3\,\eta)\,\frac{1}{r^3},\end{aligned} \tag{3.2b}$$

$$\begin{aligned}\mathcal{H}_3(\mathbf{r},\hat{\mathbf{p}}) = {}& \frac{1}{128}\left(-5+35\eta-70\eta^2+35\eta^3\right)(\hat{\mathbf{p}}^2)^4 + \Big\{\left(-7+42\eta-53\eta^2-5\eta^3\right)(\hat{\mathbf{p}}^2)^3 \\ & + (2-3\eta)\,\eta^2(\mathbf{n}\cdot\hat{\mathbf{p}})^2\,(\hat{\mathbf{p}}^2)^2 + 3(1-\eta)\,\eta^2\,(\mathbf{n}\cdot\hat{\mathbf{p}})^4\,(\hat{\mathbf{p}}^2) - 5\eta^3\,(\mathbf{n}\cdot\hat{\mathbf{p}})^6\Big\}\,\frac{1}{16}\,\frac{1}{r} \\ & + \Big\{\frac{1}{16}\,\left(-27+136\eta+109\eta^2\right)(\hat{\mathbf{p}}^2)^2 + \frac{1}{16}(17+30\eta)\,\eta\,(\mathbf{n}\cdot\hat{\mathbf{p}})^2\,\hat{\mathbf{p}}^2 \\ & + \frac{1}{12}\,(5+43\,\eta)\,\eta\,(\mathbf{n}\cdot\hat{\mathbf{p}})^4\Big\}\,\frac{1}{r^2} \\ & + \left\{\Big[-\frac{25}{8} + \left(\frac{\pi^2}{64} - \frac{335}{48}\right)\eta - \frac{23\,\eta^2}{8}\Big]\,\hat{\mathbf{p}}^2 + \left(-\frac{85}{16} - \frac{3\,\pi^2}{64} - \frac{7\,\eta}{4}\right)\,\eta\,(\mathbf{n}\cdot\hat{\mathbf{p}})^2\right\} \\ & \times \frac{1}{r^3} + \left\{\frac{1}{8} + \Big(\frac{109}{12} - \frac{21}{32}\pi^2\Big)\eta\right\}\,\frac{1}{r^4}\,,\end{aligned} \tag{3.2c}$$

$$\mathcal{H}_4(\mathbf{r},\hat{\mathbf{p}}) = \left(\frac{7}{256} - \frac{63}{256}\,\eta + \frac{189}{256}\,\eta^2 - \frac{105}{128}\,\eta^3 + \frac{63}{256}\,\eta^4\right)(\hat{\mathbf{p}}^2)^5 \tag{3.2d}$$

$$
\begin{aligned}
&+\left\{\frac{45}{128}\,(\hat{\mathbf{p}}^2)^4-\frac{45}{16}\,(\hat{\mathbf{p}}^2)^4\,\eta+\left(\frac{423}{64}\,(\hat{\mathbf{p}}^2)^4-\frac{3}{32}\,(\mathbf{n}\cdot\hat{\mathbf{p}})^2\,(\hat{\mathbf{p}}^2)^3\right.\right.\\
&\left.-\frac{9}{64}\,(\mathbf{n}\cdot\hat{\mathbf{p}})^4\,(\hat{\mathbf{p}}^2)^2\right)\eta^2+\left(-\frac{1013}{256}\,(\hat{\mathbf{p}}^2)^4+\frac{23}{64}\,(\mathbf{n}\cdot\hat{\mathbf{p}})^2\,(\hat{\mathbf{p}}^2)^3\right.\\
&\left.+\frac{69}{128}\,(\mathbf{n}\cdot\hat{\mathbf{p}})^4\,(\hat{\mathbf{p}}^2)^2-\frac{5}{64}\,(\mathbf{n}\cdot\hat{\mathbf{p}})^6\,\hat{\mathbf{p}}^2+\frac{35}{256}\,(\mathbf{n}\cdot\hat{\mathbf{p}})^8\right)\eta^3\\
&+\left(-\frac{35}{128}\,(\hat{\mathbf{p}}^2)^4-\frac{5}{32}\,(\mathbf{n}\cdot\hat{\mathbf{p}})^2\,(\hat{\mathbf{p}}^2)^3-\frac{9}{64}\,(\mathbf{n}\cdot\hat{\mathbf{p}})^4\,(\hat{\mathbf{p}}^2)^2\right.\\
&\left.\left.-\frac{5}{32}(\mathbf{n}\cdot\hat{\mathbf{p}})^6\hat{\mathbf{p}}^2-\frac{35}{128}(\mathbf{n}\cdot\hat{\mathbf{p}})^8\right)\eta^4\right\}\frac{1}{r}\\
&+\left\{\frac{13}{8}\,(\hat{\mathbf{p}}^2)^3+\left(-\frac{791}{64}\,(\hat{\mathbf{p}}^2)^3+\frac{49}{16}\,(\mathbf{n}\cdot\hat{\mathbf{p}})^2\,(\hat{\mathbf{p}}^2)^2-\frac{889}{192}\,(\mathbf{n}\cdot\hat{\mathbf{p}})^4\,\hat{\mathbf{p}}^2\right.\right.\\
&\left.+\frac{369}{160}\,(\mathbf{n}\cdot\hat{\mathbf{p}})^6\right)\eta+\left(\frac{4857}{256}\,(\hat{\mathbf{p}}^2)^3-\frac{545}{64}\,(\mathbf{n}\cdot\hat{\mathbf{p}})^2\,(\hat{\mathbf{p}}^2)^2+\frac{9475}{768}\,(\mathbf{n}\cdot\hat{\mathbf{p}})^4\,\hat{\mathbf{p}}^2\right.\\
&\left.-\frac{1151}{128}\,(\mathbf{n}\cdot\hat{\mathbf{p}})^6\right)\eta^2+\left(\frac{2335}{256}\,(\hat{\mathbf{p}}^2)^3+\frac{1135}{256}\,(\mathbf{n}\cdot\hat{\mathbf{p}})^2\,(\hat{\mathbf{p}}^2)^2\right.\\
&\left.\left.-\frac{1649}{768}\,(\mathbf{n}\cdot\hat{\mathbf{p}})^4\,\hat{\mathbf{p}}^2+\frac{10353}{1280}\,(\mathbf{n}\cdot\hat{\mathbf{p}})^6\right)\eta^3\right\}\frac{1}{r^2}\\
&+\left\{\frac{105}{32}\,(\hat{\mathbf{p}}^2)^2+\left[\left(\frac{2749\pi^2}{8192}-\frac{589189}{19200}\right)(\hat{\mathbf{p}}^2)^2+\left(\frac{63347}{1600}-\frac{1059\pi^2}{1024}\right)(\mathbf{n}\cdot\hat{\mathbf{p}})^2\,\hat{\mathbf{p}}^2\right.\right.\\
&\left.\left.+\left(\frac{375\pi^2}{8192}-\frac{23533}{1280}\right)(\mathbf{n}\cdot\hat{\mathbf{p}})^4\right]\eta+\left[\left(\frac{18491\,\pi^2}{16384}-\frac{1189789}{28800}\right)(\hat{\mathbf{p}}^2)^2\right.\right.\\
&\left.\left.+\left(-\frac{127}{3}-\frac{4035\,\pi^2}{2048}\right)(\mathbf{n}\cdot\hat{\mathbf{p}})^2\,\hat{\mathbf{p}}^2+\left(\frac{57563}{1920}-\frac{38655\pi^2}{16384}\right)(\mathbf{n}\cdot\hat{\mathbf{p}})^4\right]\eta^2\right.\\
&\left.+\left(-\frac{553}{128}(\hat{\mathbf{p}}^2)^2-\frac{225}{64}\,(\mathbf{n}\cdot\hat{\mathbf{p}})^2\,\hat{\mathbf{p}}^2-\frac{381}{128}\,(\mathbf{n}\cdot\hat{\mathbf{p}})^4\right)\eta^3\right\}\frac{1}{r^3}\\
&+\left\{\frac{105}{32}\,\hat{\mathbf{p}}^2+\left[\left(\frac{185761}{19200}-\frac{21837\,\pi^2}{8192}\right)\hat{\mathbf{p}}^2+\left(\frac{3401779}{57600}-\frac{28691\,\pi^2}{24576}\right)(\mathbf{n}\cdot\hat{\mathbf{p}})^2\right]\eta\right.
\end{aligned}
$$

$$+\left[\left(\frac{672811}{19200}-\frac{158177\,\pi^2}{49152}\right)\hat{\mathbf{p}}^2+\left(\frac{110099\,\pi^2}{49152}-\frac{21827}{3840}\right)(\mathbf{n}\cdot\hat{\mathbf{p}})^2\right]\eta^2\Bigg\}\frac{1}{r^4}$$

$$+\left\{-\frac{1}{16}+\left(\frac{6237\,\pi^2}{1024}-\frac{169199}{2400}\right)\eta+\left(\frac{7403\,\pi^2}{3072}-\frac{1256}{45}\right)\eta^2\right\}\frac{1}{r^5}\,,$$

where $\mathbf{r}=\mathbf{R}/(GM)$, $r=|\mathbf{r}|$, $\mathbf{n}=\mathbf{r}/r$ and $\hat{\mathbf{p}}=\mathbf{P}/\mu$; $\mathbf{R}$ and $\mathbf{P}$ are the relative separation vector and its conjugate momentum vector. Because of the Hamiltonian is invariant under time trnaslation and spatial rotations, there are two conservative quantities: energy $E=\mathcal{H}^{local}_{\rm 4PN}$ and the reduced angular momentum $\hat{\mathbf{J}}=\mathbf{r}\times\hat{\mathbf{p}}$ of the binary in the center of mass frame. Hence one can restrict the motion of non-spinning compact binary to a plane and employ polar coordinates such that $\mathbf{r}=r\,(\cos\phi,\sin\phi)$. This relative motion can be obtained from the following differential equations arising from the Hamiltonian equations,

$$\dot{r}=\mathbf{n}\cdot\frac{\partial\mathcal{H}}{\partial\hat{\mathbf{p}}}\ , \tag{3.3a}$$

$$r^2\,\dot{\phi}=\left|\mathbf{r}\times\frac{\partial\mathcal{H}}{\partial\hat{\mathbf{p}}}\right|\,, \tag{3.3b}$$

where $\dot{r}=dr/dt,\dot{\phi}=d\phi/dt$ and t denotes the coordinate time scaled by $G\,M$. By introducing $s:=\frac{1}{r}$, Eq.(3.3a) is schematically written into a ninth degree polynomial,

$$\dot{r}^2\equiv\frac{1}{s^4}\left(\frac{ds}{dt}\right)^2=a_0+a_1\,s+a_2\,s^2+a_3\,s^3+a_4\,s^4+a_5\,s^5+a_6\,s^6+a_7\,s^7+a_8\,s^8+a_9\,s^9\,. \tag{3.4}$$

Note that the coefficients a_8 and a_9 contain only 4PN order contributions. A number of steps are required to obtain parametric solution to (3.4). First, we compute the two nonzero positive roots of $\dot{r}=0$ among 9 roots, of which Newtonian order contribution does not vanish. We label these two 4PN order roots as s_- and s_+ and they correspond to the turning points of our PN-accurate eccentric orbits. In other words, s_- and s_+ characterizes the pericenter and the apocenter of the underlying post-Newtonian accurate eccentric orbit and they are functions of the orbital energy, angular momentum and the

mass ratio. For the sake of completeness, we display below their 1PN accurate expressions

$$s_- = \frac{1+\sqrt{1+2\,h^2\,E}}{h^2} - \frac{1}{c^2}\frac{\left(1+\sqrt{1+2\,h^2\,E}\right)^2}{8\,h^4\,\sqrt{1+2\,h^2\,E}}\Big[-\eta-9+2\,(\eta-7)\,\sqrt{1+2\,h^2\,E}+(3\eta-1)\,\left(1+2\,h^2\,E\right)\Big], \tag{3.5a}$$

$$s_+ = \frac{1-\sqrt{1+2\,h^2\,E}}{h^2} + \frac{1}{c^2}\frac{\left(1-\sqrt{1+2\,h^2\,E}\right)^2}{8\,h^4\,\sqrt{1+2\,h^2\,E}}\Big[-\eta-9-2\,(\eta-7)\,\sqrt{1+2\,h^2\,E}+(3\eta-1)\,\left(1+2\,h^2\,E\right)\Big]. \tag{3.5b}$$

We are now in a position to parametrize 4PN order radial motion with the help of the following ansatz:

$$r = a_r\,(1-e_r\,\cos u), \tag{3.6}$$

where a_r and e_r are some 4PN order semi-major axis and radial eccentricity, respectively. This ansatz allows us to express both a_r and e_r in terms of s_- and s_+ as

$$a_r = \frac{1}{2}\frac{s_-+s_+}{s_-\,s_+}\,, \qquad e_r = \frac{s_--s_+}{s_-+\,s_+}\,. \tag{3.7}$$

and therefore to obtain 4PN order expressions for a_r and e_r^2 in terms of E, h and η in a straightforward manner.

We now move on to obtain an integral connecting the coordinate time t and s after factorising the above $(ds/dt)^2$ expression using 4PN order s_- and s_+ expressions. The resulting 4PN order integral may be written as

$$t-t_0 = \int_s^{s_-} \frac{A_0+A_1\bar{s}+A_2\bar{s}^2+A_3\bar{s}^3+A_4\bar{s}^4+A_5\bar{s}^5+A_6\bar{s}^6+A_7\bar{s}^7}{\sqrt{(s_--\bar{s})(\bar{s}-s_+)}\,\bar{s}^2}d\bar{s}\,. \tag{3.8}$$

Similialy, the angular part is to be computed from an expression for $d\phi/ds$ that includes 4PN order contributions. This expression was derived, as noted earlier, using $d\phi/ds = \dot{\phi}/\dot{s}$,

where $\dot{\phi}$ expression arises from the usual Hamiltonian equation of motion (3.3b). Influenced by our approach to tackle the radial motion, we obtain an expression for $d\phi/ds$ that is factorised by our PN-accurate two positive roots, namely s_- and s_+. The resulting expression may be written as

$$\phi - \phi_0 = \int_s^{s_-} d\bar{s}\, \frac{B_0 + B_1\,\bar{s} + B_2\,\bar{s}^2 + B_3\,\bar{s}^3 + B_4\,\bar{s}^4 + B_5\,\bar{s}^5 + B_6\,\bar{s}^6 + B_7\,\bar{s}^7}{\sqrt{(s_- - \bar{s})(\bar{s} - s_+)}} \tag{3.9}$$

where the coefficients $B_i : i = 1..7$, as expected, are some 4PN order functions of E, h and η. Noting that (3.8) and (3.9) have the same structure, what we have to do is to calculate the following form of integration

$$\int \frac{f(\bar{s})}{\sqrt{(s_- - \bar{s})\,(\bar{s} - s_+)}} d\bar{s}\,. \tag{3.10}$$

By changing of variables $\bar{s} = \frac{1}{a_r(1-e_r\,\cos\bar{u})}$ and $d\bar{s} = d\bar{u}\,\bar{s}^2\,a_r\,e_r\,\sin\bar{u}$, the above integral becomes

$$\int_0^u \frac{\sqrt{1-e_r^2}}{a_r\,(1 - e_r\,\cos u)} f(u) d\bar{u}\,,$$

where $f(\bar{u}) := f(\frac{1}{a_r(1-e_r\,\cos\bar{u})})$. Furthermore, the explict form of f of both temporal and angular integrals suggests that we need to carry out the integration of the following type,

$$I(u,n) := \int_0^u \frac{d\bar{u}}{(1 - e_r\,\cos\bar{u})^n}\,, \tag{3.11}$$

where $n \geq 1$ is an integer and $s = \frac{1}{a_r(1-e_r\,\cos u)}$. For covenience, we introduce the radial true anomaly

$$\tilde{\nu}(u) := 2\,\arctan(\sqrt{\frac{1+e_r}{1-e_r}}\tan\frac{u}{2})\,, \tag{3.12}$$

or reversely,

$$u = 2\,\arctan(\sqrt{\frac{1-e_r}{1+e_r}}\tan\frac{\tilde{\nu}}{2})\,. \tag{3.13}$$

Then the partial derivative of $I(u,n)$ with respect to u can be written in two ways

$$\frac{\partial I(u,n)}{\partial u} = \frac{1}{(1 - e_r\,\cos u)^n}\,, \tag{3.14a}$$

$$\frac{\partial I(u,n)}{\partial u} = \frac{\partial I(u(\tilde{\nu}),n)}{\partial \tilde{\nu}} \frac{\sqrt{1-e_r^2}}{1-e_r\,\cos u} \quad (\because \frac{d}{du}\tilde{\nu}(u) = \frac{\sqrt{1-e_r^2}}{1-e_r\,\cos u}). \tag{3.14b}$$

Equating them and making use of $\frac{1}{1-e_r\cos u} = \frac{1+e_r\cos\tilde{\nu}}{1-e_r^2}$ yield

$$\frac{\partial I(u(\tilde{\nu}),n)}{\partial \tilde{\nu}} = \frac{1}{\sqrt{1-e_r^2}\,(1-e_r\,\cos u)^{n-1}} = \frac{\left(1+e_r\,\cos\tilde{\nu}\right)^{n-1}}{(1-e_r^2)^{n-\frac{1}{2}}}\,, \tag{3.15}$$

by which the integration $I(u,n)$ can be obtained only via elementray integrals such as $\int d\tilde{\nu}\cos^m\tilde{\nu}$. This results in the following provisional parametric expression for the angular motion that includes 4PN order contributions as

$$\begin{aligned}\frac{2\,\pi}{\Phi}\,(\phi-\phi_0) &= \tilde{\nu} + \frac{\lambda_1}{c^2}\sin\tilde{\nu} + \frac{\lambda_2}{c^4}\sin 2\tilde{\nu} \\ &\quad + \frac{\lambda_3}{c^4}\sin 3\tilde{\nu} + \frac{\lambda_4}{c^6}\sin 4\tilde{\nu} + \frac{\lambda_5}{c^6}\sin 5\tilde{\nu} + \frac{\lambda_6}{c^8}\sin 6\tilde{\nu} + \frac{\lambda_7}{c^8}\sin 7\tilde{\nu}\,,\end{aligned} \tag{3.16}$$

where λ_i are some PN accurate functions, expressible in terms of E, h and η. We obtain our final parametrization for l and ϕ equations with the help of some true anomaly variable $v = 2\arctan\left[\left(\frac{1+e_\phi}{1-e_\phi}\right)^{1/2}\tan\frac{u}{2}\right]$ that involves a new angular eccentricity parameter e_ϕ. The plan is to introduce v in below while allowing e_ϕ to differ from e_r by some yet to be determined PN corrections. Let $y \sim \mathcal{O}(1/c^2)$ be their difference as

$$y = \frac{\left(\frac{1+e_r}{1-e_r}\right)^{1/2}}{\left(\frac{1+e_\phi}{1-e_\phi}\right)^{1/2}} - 1. \tag{3.17}$$

This leads the following PN-accurate expression for $\tilde{v}$ in terms of v

$$\begin{aligned}\tilde{\nu} &= \nu + y\sin\nu + \frac{y^2}{4}\,(-2\sin\nu + \sin 2\nu) + \frac{y^3}{12}\,(3\sin\nu - 3\sin 2\nu + \sin 3\nu) \\ &\quad + \frac{y^4}{32}\,(-4\sin\nu + 6\sin 2\nu - 4\sin 3\nu + \sin 4\nu) + \mathcal{O}(1/c^{10})\,,\end{aligned} \tag{3.18}$$

where y connects e_ϕ and e_r to 4PN order. We now express $\frac{2\pi}{\Phi}\,(\phi-\phi_0)$, given by Eq. (3.16), in terms of v and demand that there are no $\sin v$ terms to 4PN order. This requirement

uniquely determines those PN corrections y that connect e_ϕ to e_r. For example, the dominant 1PN contribution of y may be written as

$$y = -\frac{\eta\sqrt{1+2\,E\,h^2}}{2\,c^2\,h^2} + \mathcal{O}(1/c^4)\,. \tag{3.19}$$

It should be noted that we imposed such a restriction because 1PN-accurate parametric solution, derived in Damour and Deruelle (1985), supported a *Keplerian* like parametrization for the angular part with the help of v. This leads to the following parametric solution for the angular motion while incorporating 4PN order contributions:

$$\begin{aligned}\frac{2\,\pi}{\Phi}\,(\phi-\phi_0) &= \nu + \left(\frac{f_{4\phi}}{c^4}+\frac{f_{6\phi}}{c^6}+\frac{f_{8\phi}}{c^8}\right)\sin 2\nu + \left(\frac{g_{4\phi}}{c^4}+\frac{g_{6\phi}}{c^6}+\frac{g_{8\phi}}{c^8}\right)\sin 3\nu \\ &\quad + \left(\frac{i_{6\phi}}{c^6}+\frac{i_{8\phi}}{c^8}\right)\sin 4\nu + \left(\frac{h_{6\phi}}{c^6}+\frac{h_{8\phi}}{c^8}\right)\sin 5\nu \\ &\quad + \frac{k_{8\phi}}{c^8}\,\sin 6\,\nu + \frac{j_{8\phi}}{c^8}\,\sin 7\,\nu\,. \end{aligned} \tag{3.20}$$

Interestingly, the ν contributions at 2PN, 3PN and 4PN orders are supplemented by other trigonometric functions of ν and this why we call the resulting solution as the generalized quasi-Keplerian parametric solution. We will display shortly the explicit 4PN order expressions for these orbital elements and functions.

3.2 4PN accurate order of Qausi-Keplerian parametrization

Finally, we display, in its entirety, the fourth post-Newtonian accurate generalized quasi-Keplerian parametrization for a compact binary moving in an eccentric orbit in ADM-type coordinates

$$r = a_r\,(1-e_r\,\cos u)\,, \tag{3.21a}$$

$$l := n\,(t-t_0) = u - e_t\,\sin u + \left(\frac{g_{4t}}{c^4}+\frac{g_{6t}}{c^6}+\frac{g_{8t}}{c^8}\right)(\nu-u)$$

$$+\left(\frac{f_{4t}}{c^4}+\frac{f_{6t}}{c^6}+\frac{f_{8t}}{c^8}\right)\sin\nu+\left(\frac{i_{6t}}{c^6}+\frac{i_{8t}}{c^8}\right)\sin 2\,\nu+\left(\frac{h_{6t}}{c^6}+\frac{h_{8t}}{c^8}\right)\sin 3\,\nu$$
$$+\frac{k_{8t}}{c^8}\sin 4\,\nu+\frac{j_{8t}}{c^8}\sin 5\,\nu\,, \tag{3.21b}$$

$$\frac{2\,\pi}{\Phi}\,(\phi-\phi_0)=\nu+\left(\frac{f_{4\phi}}{c^4}+\frac{f_{6\phi}}{c^6}+\frac{f_{8\phi}}{c^8}\right)\sin 2\nu+\left(\frac{g_{4\phi}}{c^4}+\frac{g_{6\phi}}{c^6}+\frac{g_{8\phi}}{c^8}\right)\sin 3\nu$$
$$+\left(\frac{i_{6\phi}}{c^6}+\frac{i_{8\phi}}{c^8}\right)\sin 4\nu+\left(\frac{h_{6\phi}}{c^6}+\frac{h_{8\phi}}{c^8}\right)\sin 5\nu$$
$$+\frac{k_{8\phi}}{c^8}\sin 6\,\nu+\frac{j_{8\phi}}{c^8}\sin 7\,\nu. \tag{3.21c}$$

In what follows, we display the 4PN order expressions for the orbital elements a_r, n, Φ, and the post-Newtonian orbital functions that appear at 2PN, 3PN and 4PN orders in terms of intrinsic parameters

$$\begin{aligned}
a_r \;=\;& \frac{1}{(-2\,E)}\Bigg\{1+\frac{(-2\,E)}{4\,c^2}\,(-7+\eta)+\frac{(-2\,E)^2}{16c^4}\,\Bigg[(1+10\,\eta+\eta^2)\\
&+\frac{1}{(-2\,E\,h^2)}(-68+44\,\eta)\Bigg]+\frac{(-2\,E)^3}{192\,c^6}\,\Bigg[3-9\,\eta-6\,\eta^2\\
&+3\,\eta^3+\frac{1}{(-2\,E\,h^2)}\Big(864+\left(-3\,\pi^2-2212\right)\eta+432\,\eta^2\Big)\\
&+\frac{1}{(-2\,E\,h^2)^2}\Big(-6432+\left(13488-240\,\pi^2\right)\eta-768\,\eta^2\Big)\Bigg]\\
&+\frac{(-2\,E)^4}{3686400\,c^8}\,\Bigg[14400-57600\,\eta+28800\,\eta^2-158400\,\eta^3+14400\,\eta^4\\
&+\frac{1}{(-2\,E\,h^2)}\Big(-4147200+(-38071488+1280250\pi^2)\,\eta\\
&+\left(19038208+4030875\,\pi^2\right)\,\eta^2+4262400\,\eta^3\Big)\\
&+\frac{1}{(-2\,E\,h^2)^2}\,\Big(316800000+\left(-661398528+21132000\pi^2\right)\,\eta\\
&+\left(363371776-26908200\pi^2\right)\,\eta^2-20160000\,\eta^3\Big)
\end{aligned}$$

$$+\frac{1}{(-2\,E\,h^2)^3}\left(-1228492800+\left(2644664832-59785200\,\pi^2\right)\,\eta\right.$$
$$\left.+\left(-826707456+34613400\,\pi^2\right)\,\eta^2+13824000\,\eta^3\right)\Bigg]\Bigg\}, \tag{3.22a}$$

$$\begin{aligned} n &= (-2\,E)^{3/2}\Bigg\{1+\frac{(-2\,E)}{8\,c^2}\,(-15+\eta)+\frac{(-2\,E)^2}{128c^4}\Bigg[555+30\,\eta \\ &+11\,\eta^2+\frac{192}{\sqrt{(-2\,E\,h^2)}}\,(-5+2\,\eta)\Bigg]+\frac{(-2\,E)^3}{3072\,c^6}\Bigg[-29385 \\ &-4995\,\eta-315\,\eta^2+135\,\eta^3-\frac{16}{(-2\,E\,h^2)^{3/2}}\Bigg(10080+123\,\eta\,\pi^2 \\ &-13952\,\eta+1440\,\eta^2\Bigg)+\frac{5760}{\sqrt{(-2\,E\,h^2)}}\left(17-9\,\eta+2\,\eta^2\right)\Bigg] \\ &+\frac{(-2\,E)^4}{1474560\,c^8}\Bigg[\frac{3317760\,(-5+2\,\eta)^2}{-2\,E\,h^2}+\frac{138240}{\sqrt{(-2\,E\,h^2)}} \\ &\times\left(-1125+550\,\eta-175\,\eta^2+38\,\eta^3\right)+135\Bigg(232881 \\ &+65300\,\eta+4070\,\eta^2-460\,\eta^3+241\,\eta^4\Bigg) \\ &-\frac{80}{(-2\,E\,h^2)^{3/2}}\Bigg(-5443200+\left(10467328-150987\pi^2\right)\,\eta \\ &+\left(-3959808+32472\pi^2\right)\,\eta^2+311040\,\eta^3\Bigg) \\ &+\frac{48}{(-2\,E\,h^2)^{5/2}}\Bigg(-17297280+\left(37556864-771585\,\pi^2\right)\,\eta \\ &+\left(-13464960+236160\,\pi^2\right)\,\eta^2+403200\,\eta^3\Bigg)\Bigg]\Bigg\}, \end{aligned} \tag{3.22b}$$

$$g_{4\,t} = \frac{3\,(-2\,E)^2}{2}\left\{\frac{5-2\,\eta}{\sqrt{(-2\,E\,h^2)}}\right\}, \tag{3.22c}$$

$$g_{6\,t} = \frac{(-2\,E)^3}{192}\left\{\frac{1}{(-2\,E\,h^2)^{3/2}}\Bigg(10080+123\,\eta\,\pi^2-13952\,\eta\right.$$

$$+1440\,\eta^2\Big) + \frac{1}{\sqrt{(-2\,E\,h^2)}}\left(-3420 + 1980\,\eta - 648\,\eta^2\right)\Big\}, \tag{3.22d}$$

$$\begin{aligned} g_{8\,t} &= -\frac{(-2\,E)^4}{92160}\Big\{\frac{3}{(-2\,E\,h^2)^{5/2}}\Big(-17297280 + \big(37556864 \\ &\quad -771585\pi^2\big)\eta + 1920\left(-7013 + 123\,\pi^2\right)\eta^2 + 403200\eta^3\Big) \\ &\quad -\frac{5}{(-2\,E\,h^2)^{3/2}}\Big(-3628800 + \left(7835008 - 128847\pi^2\right)\eta \\ &\quad +36\left(-98144 + 861\pi^2\right)\eta^2 + 293760\eta^3\Big) + \frac{207360}{(-2\,E\,h^2)}\,(5 - 2\,\eta)^2 \\ &\quad +\frac{1080}{\sqrt{(-2\,E\,h^2)}}\left(-3375 + 1600\eta - 755\eta^2 + 246\eta^3\right)\Big\}, \end{aligned} \tag{3.22e}$$

$$f_{4\,t} = -\frac{1}{8}\,\frac{(-2\,E)^2}{\sqrt{(-2\,E\,h^2)}}\Big\{(4+\eta)\,\eta\,\sqrt{(1+2\,E\,h^2)}\Big\}, \tag{3.22f}$$

$$\begin{aligned} f_{6\,t} &= \frac{(-2\,E)^3}{192}\Big\{\frac{1}{(-2\,E\,h^2)^{3/2}}\,\frac{1}{\sqrt{1+2\,E\,h^2}}\Big(1728 - 4148\,\eta + 3\,\eta\,\pi^2 \\ &\quad +600\,\eta^2 + 33\,\eta^3\Big) + 3\,\frac{\sqrt{(-2\,E\,h^2)}}{\sqrt{(1+2\,E\,h^2)}}\eta\,\left(-64 - 4\,\eta + 23\,\eta^2\right) \\ &\quad +\frac{1}{\sqrt{(-2\,E\,h^2)\,(1+2\,E\,h^2)}}\Big(-1728 + 4232\,\eta - 3\,\eta\,\pi^2 \\ &\quad -627\,\eta^2 - 105\,\eta^3\Big)\Big\}, \end{aligned} \tag{3.22g}$$

$$\begin{aligned} f_{8\,t} &= -\frac{(-2\,E)^4}{14745600}\,\frac{(-2\,E\,h^2)^{3/2}}{(1+2\,E\,h^2)^{3/2}}\Big\{7200\,\eta\left(4672 + 912\,\eta\right. \\ &\quad \left.-303\,\eta^2 + 902\,\eta^3\right) + \frac{2764800}{\sqrt{(-2\,E\,h^2)}}\,\eta\,(4+\eta)\,(-5+2\eta) \\ &\quad +\frac{1}{(-2\,E\,h^2)}\Big(331776000 + 1350\left(-919776 + 2377\pi^2\right)\eta \\ &\quad +\left(568404992 + 2468925\pi^2\right)\eta^2 - 94248000\eta^3 - 16128000\eta^4\Big) \end{aligned}$$

$$
\begin{aligned}
&-\frac{5529600}{(-2\,E\,h^2)^{3/2}}\,\eta\,(4+\eta)\,(-5+2\eta)\\
&+\frac{1}{(-2\,E\,h^2)^2}\left(-2226585600+\left(10348301504-252478050\pi^2\right)\eta\right.\\
&\left.+9\left(-614377024+9064225\pi^2\right)\eta^2+383328000\eta^3+10411200\eta^4\right)\\
&+\frac{2764800}{(-2\,E\,h^2)^{5/2}}\,\eta\,\left(-20+3\eta+2\eta^2\right) \qquad (3.22\text{h})\\
&+\frac{1}{(-2\,E\,h^2)^3}\left(3607142400+2\left(-8729633504+247794225\,\pi^2\right)\eta\right.\\
&\left.+\left(9340505856-170534025\,\pi^2\right)\,\eta^2-471441600\,\eta^3+1152000\,\eta^4\right)\\
&+\frac{1}{(-2\,E\,h^2)^4}\left(-1712332800+\left(8314359104-246319350\pi^2\right)\eta\right.\\
&\left.\left.+\left(-4388287232+86487075\pi^2\right)\eta^2+184226400\eta^3-1944000\eta^4\right)\right\},
\end{aligned}
$$

$$
i_{6\,t} \;=\; \frac{(-2\,E)^3}{32}\,\eta\left\{\frac{(1+2\,E\,h^2)}{(-2\,E\,h^2)^{3/2}}\left(23+12\,\eta+6\,\eta^2\right)\right\}, \qquad (3.22\text{i})
$$

$$
\begin{aligned}
i_{8\,t} \;=\;& \frac{(-2\,E)^4}{921600}\left\{-\frac{300}{\sqrt{-2\,E\,h^2}}\,\eta\left(-8904+12207\eta+2356\eta^2+864\eta^3\right)\right.\\
&+\frac{1}{(-2\,E\,h^2)^{3/2}}\left(-1857600+\left(10986256-1072425\pi^2\right)\eta\right.\\
&\left.+\left(-38708632+3152775\pi^2\right)\eta^2+4891200\eta^3+176400\eta^4\right)\\
&+\frac{1}{(-2\,E\,h^2)^{5/2}}\left(1857600+\left(-12167056+1072425\pi^2\right)\eta\right.\\
&\left.\left.+\left(43313932-3152775\pi^2\right)\eta^2-3709200\eta^3+126000\eta^4\right)\right\}, \qquad (3.22\text{j})
\end{aligned}
$$

$$
h_{6\,t} \;=\; \frac{13\,(-2\,E)^3}{192}\eta^3\left(\frac{1+2\,E\,h^2}{-2\,E\,h^2}\right)^{3/2}, \qquad (3.22\text{k})
$$

$$
\begin{aligned}
h_{8\,t} &= \frac{(-2\,E)^4}{14745600}\left(\frac{1+2\,E\,h^2}{-2\,E\,h^2}\right)^{1/2}\eta\,\Bigg\{-3600\,\eta^2\,(-839+526\,\eta)\\
&+\frac{1}{(-2\,E\,h^2)}\Bigg(6\,\left(-9586592+405075\,\pi^2\right)\\
&+5\,\left(-21746432+2673315\,\pi^2\right)\,\eta+23416800\,\eta^2+1368000\,\eta^3\Bigg)\\
&+\frac{1}{(-2\,E\,h^2)^2}\Bigg(57519552-2430450\,\pi^2\\
&+\left(108732160-13366575\,\pi^2\right)\,\eta-23067600\,\eta^2+900000\,\eta^3\Bigg)\Bigg\}, \qquad (3.22l)
\end{aligned}
$$

$$
\begin{aligned}
\Phi &= 2\,\pi\,\Bigg\{1+\frac{3}{c^2h^2}+\frac{(-2\,E)^2}{4\,c^4}\Bigg[\frac{3}{(-2\,E\,h^2)}\,(-5+2\,\eta)\\
&+\frac{15}{(-2\,E\,h^2)^2}\,(7-2\,\eta)\Bigg]+\frac{(-2\,E)^3}{128\,c^6}\Bigg[\frac{24}{(-2\,E\,h^2)}(5-5\eta\\
&+4\eta^2)-\frac{1}{(-2\,E\,h^2)^2}\Bigg(10080-13952\,\eta+123\,\eta\,\pi^2+1440\,\eta^2\Bigg)\\
&+\frac{5}{(-2\,E\,h^2)^3}\Bigg(7392-8000\,\eta+123\,\eta\,\pi^2+336\,\eta^2\Bigg)\Bigg]\\
&-\frac{(-2\,E)^4}{73728\,c^8}\,\frac{1}{(-2\,E\,h^2)}\Bigg[-6912\,\eta^2\,(-5+4\eta)\\
&+\frac{3}{(-2\,E\,h^2)}\Bigg(-1814400+\left(5202688-106707\pi^2\right)\eta\\
&+240\left(-12944+123\pi^2\right)\eta^2+276480\eta^3\Bigg)\\
&-\frac{6}{(-2\,E\,h^2)^2}\Bigg(-17297280+\left(37556864-771585\pi^2\right)\eta\\
&+1920\left(-7013+123\pi^2\right)\eta^2+403200\eta^3\Bigg)\Bigg]\\
&+\frac{7}{(-2\,E\,h^2)^3}\Bigg(-37065600+\left(63502592-1275315\pi^2\right)\eta
\end{aligned}
$$

$$+2400\left(-6056+123\pi^2\right)\eta^2+207360\eta^3\Big)\Big]\Big\}\,, \tag{3.22m}$$

$$f_{4\,\phi} = \frac{(-2\,E)^2}{8}\,\frac{(1+2\,E\,h^2)}{(-2\,E\,h^2)^2}\,\eta\,(1-3\,\eta)\,, \tag{3.22n}$$

$$\begin{aligned} f_{6\,\phi} = {} & \frac{(-2\,E)^3}{256}\Big\{\frac{4\,\eta}{(-2\,E\,h^2)}\left(-11-40\,\eta+24\,\eta^2\right) \\ & +\frac{1}{(-2\,E\,h^2)^2}\Big(-256+1192\,\eta-49\,\eta\,\pi^2+336\,\eta^2-80\,\eta^3\Big) \\ & +\frac{1}{(-2\,E\,h^2)^3}\Big(256+49\,\eta\,\pi^2-1076\,\eta-384\,\eta^2-40\,\eta^3\Big)\Big\}\,, \end{aligned} \tag{3.22o}$$

$$\begin{aligned} f_{8\,\phi} = {} & \frac{(-2\,E)^4}{7372800}\Big\{\frac{900\,\eta}{(-2\,E\,h^2)}\Big(6844-13989\,\eta-1530\,\eta^2+1888\,\eta^3\Big) \\ & +\frac{1}{(-2\,E\,h^2)^2}\Big(9273600+2\left(-303923464+7907025\,\pi^2\right)\,\eta \\ & +\left(567130588+8219475\,\pi^2\right)\,\eta^2-26411400\eta^3+1180800\,\eta^4\Big) \\ & -\frac{2}{(-2\,E\,h^2)^3}\Big(84844800+10\left(-149381636+4263405\,\pi^2\right)\,\eta \\ & -19\,\left(-67975466+173325\,\pi^2\right)\,\eta^2-54814500\,\eta^3+2980800\,\eta^4\Big) \\ & \frac{1}{(-2\,E\,h^2)^4}\Big(177004800+\left(-2446310192+72629250\,\pi^2\right)\,\eta \\ & -15\,\left(-132716108+963535\,\pi^2\right)\,\eta^2-86679000\,\eta^3+1929600\,\eta^4\Big)\Big\}\,, \end{aligned} \tag{3.22p}$$

$$g_{4\,\phi} = -\frac{3(-2\,E)^2}{32}\frac{\eta^2}{(-2\,E\,h^2)^2}(1+2\,E\,h^2)^{3/2}\,, \tag{3.22q}$$

$$g_{6\,\phi} = \frac{(-2\,E)^3}{768}\,\sqrt{(1+2\,E\,h^2)}\Big\{-\frac{3}{(-2\,E\,h^2)}\,\eta^2\,(9-26\,\eta)$$

$$
\begin{aligned}
&-\frac{1}{(-2\,E\,h^2)^2}\,\eta\Big(220+3\,\pi^2+312\,\eta+150\,\eta^2\Big)\\
&+\frac{1}{(-2\,E\,h^2)^3}\,\eta\left(220+3\,\pi^2+96\,\eta+45\,\eta^2\right)\Big\}\,, \qquad (3.22r)
\end{aligned}
$$

$$
\begin{aligned}
g_{8\,\phi} \;=\;& \frac{(-2\,E)^4}{176947200}\,\frac{1}{\sqrt{(1+2\,E\,h^2)}}\Big\{-10800\eta^2\left(36-95\eta+1226\eta^2\right)\\
&+\frac{3\,\eta}{(-2\,E\,h^2)}\Big(-404533824+5453550\pi^2\\
&+\left(731023360+381825\,\pi^2\right)\eta-115070400\,\eta^2-9129600\,\eta^3\Big)\\
&+\frac{1}{(-2\,E\,h^2)^2}\Big(44236800+2\left(-6842155424+127907475\pi^2\right)\eta\\
&-87\left(-253902848+3210525\,\pi^2\right)\,\eta^2\\
&-2262477600\,\eta^3+39096000\,\eta^4\Big)\\
&+\frac{1}{(-2\,E\,h^2)^3}\Big(-88473600+\left(23556745280-464880750\,\pi^2\right)\eta\\
&+\left(-37649997312+561808575\,\pi^2\right)\eta^2\\
&+3436488000\eta^3-103766400\,\eta^4\Big)\\
&+\frac{1}{(-2\,E\,h^2)^4}\Big(44236800+\left(-11086035904+225426450\pi^2\right)\eta\\
&+\left(17722415616-281347425\pi^2\right)\eta^2\\
&-1527246000\eta^3+50133600\eta^4\Big)\Big\}\,, \qquad (3.22s)
\end{aligned}
$$

$$
i_{6\,\phi} \;=\; \frac{(-2\,E)^3}{128}\,\frac{(1+2\,E\,h^2)^2}{(-2\,E\,h^2)^3}\,\eta\left(5+28\,\eta+10\,\eta^2\right)\,, \qquad (3.22t)
$$

$$
i_{8\,\phi} \;=\; \frac{(-2\,E)^4}{14745600}\,\frac{\sqrt{(1+2\,E\,h^2)}}{(-2\,E\,h^2)^2}\Big\{-7200\left(440-1330\eta+700\eta^2+173\eta^3\right)
$$

$$
\begin{aligned}
&+\frac{1}{(-2\,E\,h^2)}\Bigg(175308224+1767300\pi^2\\
&+\left(-407514720-9062175\pi^2\right)\eta+70257600\eta^2-1713600\eta^3\Bigg)\\
&+\frac{1}{(-2\,E\,h^2)^2}\Bigg(-169548224+1767300\pi^2\\
&+\left(412741920-9062175\pi^2\right)\eta-58420800\eta^2+3535200\eta^3\Bigg)\Bigg\}, \qquad (3.22u)
\end{aligned}
$$

$$
h_{6\,\phi} = \frac{5\,(-2\,E)^3}{256}\,\frac{\eta^3}{(-2\,E\,h^2)^3}\,(1+2\,E\,h^2)^{5/2}\,, \qquad (3.22v)
$$

$$
\begin{aligned}
h_{8\,\phi} &= \frac{(-2\,E)^4}{6553600}\,\frac{\eta}{(-2\,E\,h^2)^2}\,(1+2\,E\,h^2)^{3/2}\Bigg\{78000\eta^2\\
&-172000\eta^3+\frac{1}{(-2\,E\,h^2)}\Bigg(8273856+11250\pi^2\\
&+\left(-24254464-579825\pi^2\right)\eta+7604000\eta^2-238400\eta^3\Bigg)\\
&+\frac{1}{(-2\,E\,h^2)^2}\Bigg(-8273856+11250\pi^2\\
&+\left(24254464-579825\pi^2\right)\,\eta-6962000\,\eta^2+490400\,\eta^3\Bigg)\Bigg\}. \qquad (3.22w)
\end{aligned}
$$

We also display below 4PN order expressions for the radial, time and angular eccentricities in ADM-like gauge

$$
\begin{aligned}
{e_r}^2 &= 1+2\,E\,h^2+\frac{(-2\,E)}{4\,c^2}\Bigg\{24-4\,\eta+5\,(-3+\eta)\,(-2\,E\,h^2)\Bigg\}\\
&+\frac{(-2\,E)^2}{8\,c^4}\Bigg\{52+2\,\eta+2\,\eta^2-\left(80-55\,\eta+4\,\eta^2\right)(-2\,E\,h^2)\\
&-\frac{8}{(-2\,E\,h^2)}\,(-17+11\,\eta)\Bigg\}+\frac{(-2\,E)^3}{192\,c^6}\Bigg\{-768-6\,\eta\,\pi^2\\
&-344\,\eta-216\,\eta^2+3(-2\,E\,h^2)\Bigg(-1488+1556\,\eta-319\,\eta^2
\end{aligned}
$$

$$
\begin{aligned}
&+4\,\eta^3\Big) - \frac{4}{(-2\,E\,h^2)}\left(588 - 8212\,\eta + 177\,\eta\,\pi^2 + 480\,\eta^2\right)\\
&+\frac{192}{(-2\,E\,h^2)^2}\left(134 - 281\,\eta + 5\,\eta\,\pi^2 + 16\,\eta^2\right)\Big\}\\
&+\frac{(-2\,E)^4}{1843200\,c^8}\Big\{-87552000 + 6\left(-8124448 + 160575\pi^2\right)\eta\\
&+\left(38809408 + 4117275\pi^2\right)\eta^2 - 1310400\eta^3\\
&+14400\left(-6432 + 9036\,\eta - 3240\,\eta^2 + 221\,\eta^3\right)(-2\,E\,h^2)\\
&+\frac{1}{(-2\,E\,h^2)}\Big(-154828800 + \left(1433661888 - 8719650\pi^2\right)\,\eta\\
&+\left(-276075584 - 34996575\,\pi^2\right)\,\eta^2 + 2707200\,\eta^3\Big)\\
&+\frac{4}{(-2\,E\,h^2)^2}\Big(-166579200 + \left(365251776 - 18585450\,\pi^2\right)\,\eta\\
&+\left(-288257984 + 24130125\pi^2\right)\,\eta^2 + 7891200\,\eta^3\Big)\\
&-\frac{48}{(-2\,E\,h^2)^3}\Big(-51187200 + \left(110194368 - 2491050\,\pi^2\right)\eta\\
&+\left(-34446144 + 1442225\,\pi^2\right)\eta^2 + 576000\,\eta^3\Big)\Big\}
\end{aligned}
\tag{3.23a}
$$

$$
\begin{aligned}
{e_t}^2 \;=\;& 1 + 2\,E\,h^2 + \frac{(-2\,E)}{4\,c^2}\Big\{-8 + 8\,\eta - (-17 + 7\,\eta)\,(-2\,E\,h^2)\Big\}\\
&+\frac{(-2\,E)^2}{8\,c^4}\Big\{8 + 4\,\eta + 20\,\eta^2 - (-2\,E\,h^2)(112 - 47\,\eta + 16\,\eta^2)\\
&-24\,\sqrt{(-2\,E\,h^2)}\,(-5 + 2\,\eta) + \frac{4}{(-2\,E\,h^2)}\,(17 - 11\,\eta)\\
&-\frac{24}{\sqrt{(-2\,E\,h^2)}}\,(5 - 2\,\eta)\Big\}\\
&+\frac{(-2\,E)^3}{192\,c^6}\Big\{24\,(-2 + 5\,\eta)\left(-23 + 10\,\eta + 4\,\eta^2\right) - 15\left(-528\right.
\end{aligned}
$$

$$+200\,\eta-77\,\eta^2+24\,\eta^3\Big)(-2\,E\,h^2)-72\,(265-193\,\eta$$

$$+46\,\eta^2)\sqrt{(-2\,E\,h^2)}-\frac{2}{(-2\,E\,h^2)}\Big(6732+117\,\eta\,\pi^2-12508\,\eta$$

$$+2004\,\eta^2\Big)+\frac{2}{\sqrt{(-2\,E\,h^2)}}\Big(16380-19964\,\eta+123\,\eta\,\pi^2$$

$$+3240\,\eta^2\Big)-\frac{2}{(-2\,E\,h^2)^{3/2}}\Big(10080+123\,\eta\,\pi^2-13952\,\eta$$

$$+1440\,\eta^2\Big)+\frac{96}{(-2\,E\,h^2)^2}\Big(134-281\,\eta+5\,\eta\,\pi^2+16\,\eta^2\Big)\Big\}$$

$$+\frac{(-2\,E)^4}{460800\,c^8}\Big\{3600\,\big(-25500+25804\,\eta-7267\,\eta^2+1236\,\eta^3$$

$$+280\,\eta^4\big)-28800\,\big(1828-563\,\eta+237\,\eta^2-84\,\eta^3$$

$$+25\,\eta^4\big)\,(-2\,E\,h^2)-10800\big(-18795+15344\eta-6303\eta^2$$

$$+1262\eta^3\Big)\,\sqrt{(-2\,E\,h^2)}+\frac{50}{\sqrt{(-2\,E\,h^2)}}\Big(-9265320$$

$$+\big(16589440-179031\pi^2\big)\,\eta+12\,\big(-620854+4305\pi^2\big)\,\eta^2$$

$$+851472\,\eta^3\Big)+\frac{1}{(-2\,E\,h^2)}\,\Big(215107200+6\big(-58544128$$

$$+595725\,\pi^2\big)\eta+\big(159273712-4409175\,\pi^2\big)\,\eta^2-19425600\eta^3\Big)$$

$$-\frac{20}{(-2\,E\,h^2)^{3/2}}\,\Big(-36918720+\big(84382336-1538535\pi^2\big)\,\eta$$

$$+30\,\big(-1188608+16359\pi^2\big)\,\eta^2+2030400\eta^3\Big)+$$

$$+\frac{1}{(-2\,E\,h^2)^2}\,\Big(-324777600+\big(765039936-16500150\pi^2\big)\,\eta$$

$$+\big(-348347776+13645725\pi^2\big)\,\eta^2+15062400\eta^3\Big)$$

$$+\frac{30}{(-2\,E\,h^2)^{5/2}}\,\Big(-17297280+\big(37556864-771585\,\pi^2\big)\,\eta$$

$$
\begin{aligned}
&+1920\left(-7013+123\,\pi^2\right)\eta^2+403200\,\eta^3\Big)\\
&-\frac{6}{(-2\,E\,h^2)^3}\Big(-51187200-6\left(-18365728+415175\,\pi^2\right)\,\eta\\
&+\left(-34446144+1442225\,\pi^2\right)\,\eta^2+576000\,\eta^3\Big)\Big\} \qquad (3.23b)\\
{e_\phi}^2 \;=\;& 1+2\,E\,h^2+\frac{(-2\,E)}{4\,c^2}\Big\{24+(-15+\eta)\,(-2\,E\,h^2)\Big\}\\
&+\frac{(-2\,E)^2}{16\,c^4}\Big\{-32+176\,\eta+18\,\eta^2-(-2\,E\,h^2)(160-30\,\eta\\
&+3\,\eta^2)+\frac{1}{(-2\,E\,h^2)}\,\left(408-232\,\eta-15\,\eta^2\right)\\
&+\frac{(-2\,E)^3}{384\,c^6}\Big\{-16032+2764\,\eta+3\,\eta\,\pi^2+4536\,\eta^2+234\,\eta^3\\
&-36\left(248-80\,\eta+13\,\eta^2+\eta^3\right)(-2\,E\,h^2)-\frac{6}{(-2\,E\,h^2)}\Big(2456\\
&-26860\,\eta+581\,\eta\,\pi^2+2689\,\eta^2+10\,\eta^3\Big)+\frac{3}{(-2\,E\,h^2)^2}\Big(27776\\
&-65436\,\eta+1325\,\eta\,\pi^2+3440\,\eta^2-70\,\eta^3\Big)\Big\}\\
&+\frac{(-2\,E)^4}{14745600\,c^8}\Big\{-2455603200+\left(-90744000-2028150\pi^2\right)\eta\\
&+\left(-111502592-2843325\pi^2\right)\eta^2+169034400\eta^3+6652800\eta^4\\
&+\frac{1}{(-2\,E\,h^2)}\Big(-4479897600+\left(8522781120+286041150\pi^2\right)\eta\\
&+\left(14865824512-178464375\pi^2\right)\eta^2-1211166000\eta^3-2325600\eta^4\Big)\\
&+\frac{1}{(-2\,E\,h^2)^2}\Big(-9570816000+\left(70136820416-2520137850\pi^2\right)\eta\\
&+\left(-60219368192+1052061525\pi^2\right)\eta^2+2090973600\eta^3-5011200\eta^4\Big)
\end{aligned}
$$

$$+\frac{1}{(-2\,E\,h^2)^3}\left(33533337600+\left(-103173396416+2712160050\pi^2\right)\eta\right.$$
$$+\left(45489430272-860961825\pi^2\right)\eta^2-1000096200\eta^3-2300400\eta^4\Big)$$
$$+(-2\,E\,h^2)\left(-740966400+342835200\eta\right.$$
$$\left.-77932800\eta^2-4393800\eta^3-1105200\eta^4\right)\Big\}. \tag{3.23c}$$

The three eccentricities e_r, e_t and e_ϕ are related by

$$\begin{aligned}
e_t &= e_r\left\{1+\frac{(-2E)}{2c^2}(-8+3\eta)+\frac{(-2E)^2}{8c^4}\frac{1}{(-2Eh^2)}\Big[-34+22\eta\right.\\
&\quad+(-60+24\eta)\sqrt{(-2Eh^2)}+\left(72-33\eta+12\eta^2\right)(-2Eh^2)\Big]\\
&\quad+\frac{(-2E)^3}{192c^6}\frac{1}{(-2Eh^2)^2}\Big[-6432+13488\eta-240\eta\pi^2\\
&\quad-768\eta^2+\Big(-10080+13952\eta-123\eta\pi^2\\
&\quad-1440\eta^2\Big)\sqrt{(-2Eh^2)}+(2700-4420\eta-3\eta\pi^2\\
&\quad+1092\eta^2)(-2Eh^2)+(9180-6444\eta+1512\eta^2)(-2Eh^2)^{3/2}\\
&\quad+\Big(-3840+1284\eta-672\eta^2+240\eta^3\Big)(-2Eh^2)^2\Big]\\
&\quad+\frac{(-2\,E)^4}{3686400\,c^8}\,\frac{1}{(-2\,E\,h^2)^3}\Big[24\Big(-51187200\\
&\quad-6\left(-18365728+415175\pi^2\right)\eta\\
&\quad+\left(-34446144+1442225\pi^2\right)\eta^2+576000\eta^3\Big)\\
&\quad+120\Big(-17297280+\left(37556864-771585\pi^2\right)\eta\\
&\quad+1920\left(-7013+123\pi^2\right)\eta^2+403200\eta^3\Big)\sqrt{(-2\,E\,h^2)}
\end{aligned}$$

$$
\begin{aligned}
&-8\left(-74332800-84\left(-2081024+46875\pi^2\right)\eta\right.\\
&\left.+\left(-90032672+4083525\pi^2\right)\eta^2+4824000\eta^3\right)\left(-2\,E\,h^2\right)\\
&-200\left(-8087040+\left(15259264-176079\pi^2\right)\eta\right.\\
&\left.+396\left(-15776+123\pi^2\right)\eta^2+501120\eta^3\right)\left(-2\,E\,h^2\right)^{3/2}\\
&+\left(87552000+6\left(-940448+234975\pi^2\right)\eta\right.\\
&\left.+\left(-57435392+3958875\pi^2\right)\eta^2+26035200\eta^3\right)\left(-2\,E\,h^2\right)^2\\
&+43200\left(-15215+12344\eta-5243\eta^2+1062\eta^3\right)\left(-2\,E\,h^2\right)^{5/2}\\
&\left.+14400\left(11392-2560\eta+1394\eta^2-685\eta^3+240\eta^4\right)\left(-2\,E\,h^2\right)^3\right]\Bigg\}, \quad (3.24a)
\end{aligned}
$$

$$
\begin{aligned}
e_\phi \;=\;& e_r\Bigg\{1+\frac{(-2E)}{2c^2}\eta+\frac{(-2E)^2}{32c^4}\frac{1}{(-2Eh^2)}\Big[136-56\eta-15\eta^2\\
&+\eta(20+11\eta)(-2Eh^2)\Big]+\frac{(-2E)^3}{768c^6}\frac{1}{(-2Eh^2)^2}\Big[31872\\
&-88404\eta+2055\eta\pi^2+4176\eta^2-210\eta^3+\Big(2256\\
&+10228\eta-15\eta\pi^2-2406\eta^2-450\eta^3\Big)(-2Eh^2)+6\eta\,(136\\
&+34\eta+31\eta^2)(-2Eh^2)^2\Big]\\
&+\frac{(-2\,E)^4}{29491200\,c^8}\,\frac{1}{(-2\,E\,h^2)^3}\Big[13877452800+\big(-60858759104\\
&+1755596850\pi^2\big)\eta+\left(32262110976-307147425\pi^2\right)\eta^2\\
&-778912200\eta^3-2300400\eta^4-4\Big(25804800
\end{aligned}
$$

$$
\begin{aligned}
&+\left(-4767433920+160819650\pi^2\right)\eta\\
&+\left(4392024832+15380475\pi^2\right)\eta^2\\
&-193980150\eta^3+3645900\eta^4\Big)\left(-2\,E\,h^2\right)\\
&+\Big(176947200+\left(-340355904+11895750\pi^2\right)\eta\\
&+\left(1113945856+34888725\pi^2\right)\eta^2\\
&-167808600\eta^3-14965200\eta^4\Big)\left(-2\,E\,h^2\right)^2\\
&+1800\,\eta\left(29696+3040\eta+4137\eta^2+2814\eta^3\right)\left(-2\,E\,h^2\right)^3\Big]\Big\}\,. \qquad \text{(3.24b)}
\end{aligned}
$$

Clearly, it is important to provide a consistency check that can ensure the correctness of these lengthy expressions for the 4PN order orbital elements and functions. We adopt two consistency checks following Memmesheimer et al. (2004). This requires us to express PN-accurate expressions for $\dot{r}^2$ and $\dot{\phi}^2$, derived using the Hamiltonian equations of motion and given by Eqs. (3.3), in terms of E, h, η and $1-e_r\cos u$ while using the fact that $r=a_r\left(1-e_r\cos u\right)$. Note that the expressions for a_r and e_r^2 were obtained from the PN accurate roots s_- and s_+, and therefore, do not involve any of our complicated integrals. In the first part of our check, we compare such an expression with the one that explicitly employed our parametric solution, namely $\dot{r}^2=\left(\frac{dr}{du}\,\frac{du}{dt}\right)^2$. This expression for $\dot{r}^2$ is found to be in total agreement with our earlier $\dot{r}^2$ expression to the 4PN order after some lengthy simplifications. Thereafter, we performed a similar check on the angular part by computing $\dot{\phi}^2=\left(\frac{d\phi}{dv}\,\frac{dv}{du}\,\frac{du}{dt}\right)^2$ in terms of E,h,η and $(1-e_r\cos u)$. We have verified that such an expression is identical to our Hamiltonian equations of motion based $\dot{\phi}^2$ expression to 4PN order. In fact, we have also performed these two checks while using $\tilde{v}$ variable based parametric solution. These computations provided us with two powerful checks on our 4PN order generalized quasi-Keplerian parametrization. Finally, we have verified that to the 3PN order, our results are in agreement with results available in Damour and Schafer

(1988); Schäfer and Wex (1993); Memmesheimer et al. (2004).

3.3 4PN-3PN Keplerian Parameter Evolution and Full Waveforms of Eccentric Binaries waveform

The 4PN accurate QKP presented here is used to extend the origianl 3PN-2PN Insprial-Ringdown-Merger code by Hinder et al. (2018) to 4PN-3PN Inspiral-Ringdown-Merger code. Since the details will be presented in the future technical paper, we just describe the relative 3PN dissipation effects schematically. We adopt $x = \left(\frac{G\,m}{c^3}\frac{\Phi}{2\pi}n\right)^{\frac{2}{3}}$,[1] and e_t to parametrize 4PN conservative dynamics instead of energy and angular momentum, and solve the following dissipative effects,

$$\frac{dx}{dt} = \dot{x}^{\rm N}(e_t) + \dot{x}^{\rm 1PN}(e_t)\,x + \dot{x}^{\rm 1.5PN}(e_t)\,x^{3/2} + \dot{x}^{\rm 2PN}(e_t)\,x^2 + \dot{x}^{\rm 2.5PN}(e_t)\,x^{2.5} + \dot{x}^{\rm 3PN}(e_t)\,x^3\,, \tag{3.25a}$$

$$\frac{de_t}{dt} = \dot{e}_t^{\rm N}(e_t) + \dot{e}_t^{\rm 1PN}(e_t)\,x + \dot{e}_t^{\rm 1.5PN}(e_t)\,x^{3/2} + \dot{e}_t^{\rm 2PN}(e_t)\,x^2 + \dot{e}_t^{\rm 2.5PN}(e_t)\,x^{2.5} + \dot{e}_t^{\rm 3PN}(e_t)\,x^3\,. \tag{3.25b}$$

Note that $\dot{x}^{\rm 1.5PN}(e_t)\,x^{3/2}$ and $\dot{e}_t^{\rm 1.5PN}(e_t)\,x^{3/2}$ (1.5PN) contributions arise from the leading order of *tail effect*.[2] And $\dot{x}^{\rm 2.5PN}(e_t)\,x^{5/2}, \dot{e}_t^{\rm 2.5PN}(e_t)\,x^{5/2}$ represent the next-leading order of the tail effect, while $\dot{x}^{\rm 3PN}(e_t)\,x^3, \dot{e}_t^{\rm 3PN}(e_t)\,x^3$ partially stand for the leading order of *tail-of-tail* effect.[3] For the detailed expressions, please see Arun et al. (2009). The resulting PN waveform is attached to Circular Merging model (Hinder et al. (2018)) after circularized enough to cover Merger and Ringdown stages. In Figure 3.1 we have shown evolution

[1] where m is the total mass of the binary

[2] The tail effect of gravitational field arises from non-linear couplings between each multipolar waves and monopolar part. Especially, the leading order of tail effect corresponds to quadrupoler wave overcoming Newtonian potential of sources to propagate out.

[3] 3PN order contribution also includes the next-next-next leading order of linear-dissipation.

of $x(t)$ and e_t for an eccentric binary with initial eccentricity of 0.3 at $x = 0.065$ which corresponds to about 30 Hz for equal mass binary composed of 10 $M_\odot$ binary. We also have shown the same quantities with (relative) Newtonian order (Red) and 2PN (Blue) for comparison with our 3PN radiation reaction. One can find that the higher PN order is, the faster it goes to plunge. Along with this tendency, the 3PN dissipation seems to correct a small portion to 2PN order dissipation at least during ~ 10 cycles just before plunge. This is a good sign to show that PN acceleration is actually converging, given that the binary has only 12 cycles before plunge (where PN theory breaks down).

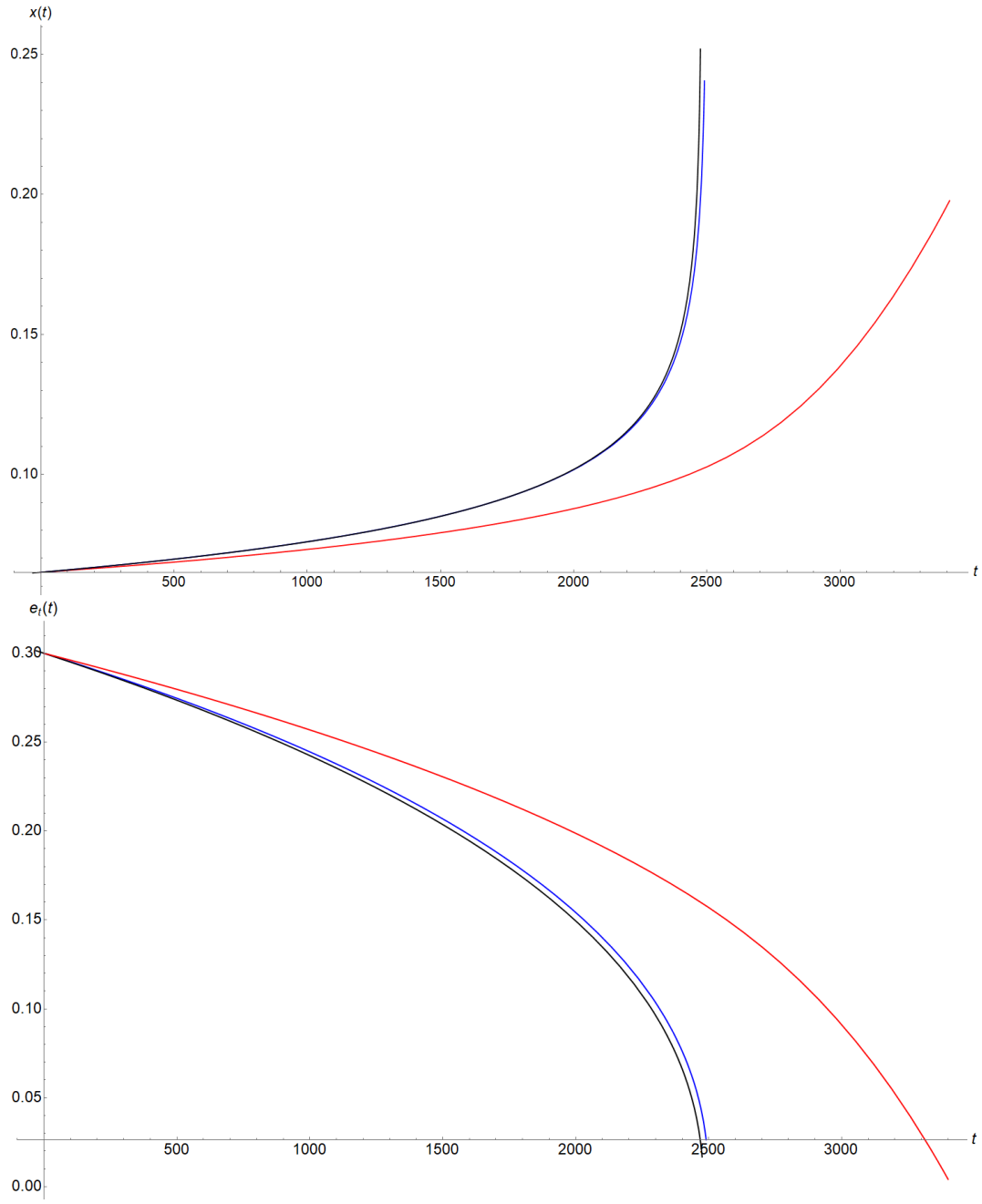

Figure 3.1 An example: Time evolution of x and e_t with the initial values $x = 0.065, e_t = 0.3$ in the accuracy of relative **3**PN, 2PN and Newtonian order radiation reaction.

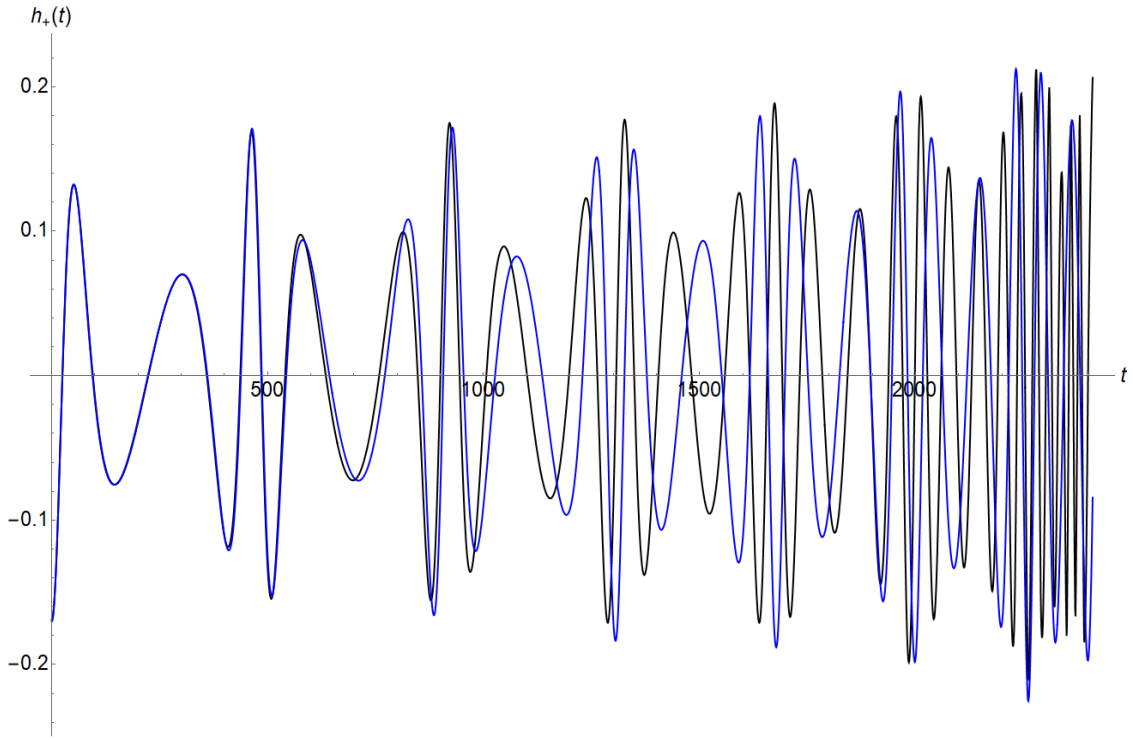

Figure 3.2 An example: h^+ with $x = 0.065, e_t = 0.3$ initially. The blue one is the 3PN waveform while the **black one** is the 4PN waveform. This presents only inspiral part.

3.4 Discussion

In this chapter, we have derived explicit expressions up to 4PN order for various orbital elements and functions of quasi-Keplerian parametric solution in terms of the conserved orbital energy and angular momentum, for black hole binaries in eccentric orbits. The evolution of the frequency and ecccentricities. Unlike the Newtonian case, two different eccentricities are required to characterize the orbit at a given time: they are r_r, e_t. Both quantities converge to 0 due to the dissipation of energy and angular momentum through gravitational radiation. The orbital evolution of the binaries can be followed until the merger phase which starts at the orbital distance of around $6Gm/c^2$ corresponding to the

inner-most stable circular orbit. The evolution of the orbital parameters such as semi-major axis, eccentricity and orbital frequency are compared with those obtained from lower-order PN calculations and are found to be similar when the orbital radius is much larger than the Schawarzschild radius and deviate toward the last phase of inspiral.
Our parametric solution can be used to compute the waveforms of gravitational waves for binaries with moderate eccentricity. (In Fig. 3.2, we have shown an example of waveforms for the same initial orbital parameters of Fig. 3.1 up to 4 PN (black line) and 3PN (blue line) We can see that the general behaviors similar but the phases deviate after about 3 cycles. As expected from the evolution of the frequency and eccentricity in Fig. 3.1, the 4PN gives faster evolution.) Our formalism cannot be used to follow the orbits during the merger phase since the PN approach breaks down. The waveforms during the merger and ringdown can be modeled with total mass of the binaries assuming that the orbit is fully circulatized before these phases based on the results of numerical relativity (mereger phase) and perturbation theory (ring-down phase) (Hinder et al. (2018)). Following the procedure by Hinder et al. (2018), we can obtain full waveforms starting from inspiral phase to merger and ring-down (IMR) for eccentrici binaries. Since most time consuming part of the inspiral phase is computed using our analytic expressions, the generation of the full waveform requires very small amount of computing time. Our scheme can be efficiently used to search for eccentric binaries from gravitational wave data. We will separately publish a paper that describes the derivation of the full waveforms and corresponding computer code.

Chapter 4

Quasi-Keplerian parametrization of Spin Precession[1]

4.1 Introduction

Under Newtonian gravity which has only mass as a source, the two body problem can be analytically solved into the well-known Kepler parametrized solution. But under the Einstein gravity which has a stress energy tensor of 10 components as its source, parameters more than mass must be considered. In the classical works Mathisson (2010); Corinaldesi and Papapetrou (1951); Dixon (1977); Bailey and Israel (1983), multipolar expansion of stress energy tensor on a generic background metric field, has been made under the assumption that matter is highly localized in space. The results, which involve mass as a monopole contribution while spin as a dipole moment, give us understanding on how masses and spin angular momenta of point particles affect the entire dynamics. Unlike Newtonian gravity, spin angular momentum produces extra gravitational effects and thus makes orbit plane of two body and spin axes precess.

[1] This chapter was published in Cho and Lee (2019).

Even though dynamics of binary systems in general relativity can be solved by numerical relativity (NR) with high accuracy, it is still worth solving the equation of motion analytically. Actually, the post-Newtonian (PN) approximation which has been well established (Blanchet (2014); Bernard et al. (2018)), provides spin precession equation (Gergely et al. (1998); Gergely (1999); Blanchet et al. (2006); Faye et al. (2006)) and the orbital evolution equations up to at least 4PN order (Damour et al. (2014); Bernard et al. (2018)). Although the PN equations can be integrated numerically with much smaller amount of computer resources than NR but analytical solution would be desirable for quick parameter estimation (Veitch et al. (2015); Farr et al. (2016)).

Until now analytic solutions have been obtained only for some limited cases such as quasi-circular, nearly aligned (Klein et al. (2013)), slowly spinning (Chatziioannou et al. (2013)) or almost equal mass (Königsdörffer and Gopakumar (2005); Tessmer (2009)). General cases with arbitrary spin can be solved up to a certain PN order in terms of elliptic functions Racine (2008) and recent works present a form of the solutions partially in terms of sine-like Jacobi elliptic function with integrating out the oscillating part of orbital motion Marsat et al. (2014); Chatziioannou et al. (2017). In this chapter, we present an analytic parametrized solution which involves both spin precession and orbital evolution for the binaries with arbitrary spins, masses and eccentricities of orbit. Namely, our solution parameterizes tilt angle of orbital planes and precession of spin angular momentum with respect to a fixed inertial frame, radial and angular motion of relative displacement of binaries and physical time evolution only via the eccentric anomaly, a Keplerian parameter that serves as an independent variable. Additionally because we express the entire parameterization in closed form witout any approximations, the solution is fully general.

This chapter is organized as follows. In §4.2, dynamics which we are going to solve is presented in terms of Hamiltonian. The Hamiltonian includes Newtonian order of orbital dynamics and the leading order of spin-orbit interaction term (linear in spin). Parameters and reference frames which we choose are also presented. In §4.3, the ways to get the

Keplerian-type parametrizations and their results are given in the following orders : Relative motion of angles between angular momenta (§4.3.1), the absolute precession of the orbital angular momentum in an inertial frame (§4.3.2), and finally, the relative position of compact binaries (§4.3.3). In §4.4, we provide an approximant for almost equal mass case and compare it with the previous work Königsdörffer and Gopakumar (2005) as a sanity check. The final secion summarized our results.

4.2 Dynamics with leading order of spin-orbit interaction

4.2.1 The Hamiltonian

In *Arnowitt-Deser-Misner*(ADM) type cooridnate Arnowitt et al. (2008) and with the *Newton-Wigner-Pryce* supplementary spin condition Newton and Wigner (1949); Pryce (1948), the (reduced) Hamiltonian H for compact bianary systems composed of two stars with masses m_1 and m_2, is as follows Wex (1995),

$$H = \frac{\boldsymbol{p}^2}{2} - \frac{1}{r} + \frac{1}{c^2\, r^3} \boldsymbol{L} \cdot \boldsymbol{S}_{\text{eff}}\,, \tag{4.1}$$

where c is the speed of light, $\boldsymbol{r} = \frac{\boldsymbol{R}}{G\,(m_1+m_2)}$, $\boldsymbol{p} = \frac{\boldsymbol{\mathcal{P}}\,(m_1+m_2)^2}{m_1\, m_2}$ with $\boldsymbol{R}$ and $\boldsymbol{\mathcal{P}}$ being relative position vector and conjugate momentum, respectively. The orbital angular momentum $\boldsymbol{L}$ and effective spin S_{eff} are defined as

$$\boldsymbol{L} = \boldsymbol{r} \times \boldsymbol{p}\,, \tag{4.2}$$

and

$$\boldsymbol{S}_{\text{eff}} = \delta_1\, \boldsymbol{S}_1 + \delta_2\, \boldsymbol{S}_2\,. \tag{4.3}$$

Here $\boldsymbol{S}_1$ and $\boldsymbol{S}_2$ are spin vectors of m_1 and m_2 and the waiting factors of δ_1 and δ_2 are,

$$\delta_1 = 2\,\frac{m_1\, m_2}{M^2}\left(1 + \frac{3}{4}\frac{m_2}{m_1}\right)\,, \tag{4.4a}$$

$$\delta_2 = 2\,\frac{m_1\,m_2}{M^2}\left(1+\frac{3}{4}\frac{m_1}{m_2}\right)\,. \tag{4.4b}$$

For a consistent post-Newtonian approximation, we need to include the first correction of orbital dynamics (1PN) but intentionally exclude it because 1PN correction to orbital motion does not affect the spin precession at the leading order and bringing the 1PN correction into the result is expected to be straightforward Königsdörffer and Gopakumar (2005); Damour and Deruelle (1985).

The equation of motion is given by Poisson bracket,

$$\dot{\boldsymbol{r}} := \frac{d\boldsymbol{r}}{dt} = \{\boldsymbol{r},\, H\}\,. \tag{4.5}$$

Likewise the corresponding angular momentum and spin precession equations are given as

$$\frac{d\boldsymbol{L}}{dt} = \{\boldsymbol{L},\, H\} = \frac{1}{c^2\,r^3}\,\boldsymbol{S}_{\rm eff}\times\boldsymbol{L}\,, \tag{4.6a}$$

$$\frac{d\boldsymbol{S}_1}{dt} = \{\boldsymbol{S}_1,\, H\} = \frac{\delta_1}{c^2\,r^3}\,\boldsymbol{L}\times\boldsymbol{S}_1\,, \tag{4.6b}$$

$$\frac{d\boldsymbol{S}_2}{dt} = \{\boldsymbol{S}_2,\, H\} = \frac{\delta_2}{c^2\,r^3}\,\boldsymbol{L}\times\boldsymbol{S}_2\,, \tag{4.6c}$$

by invoking the fact that angular momentum is a generator of rotations *i.e.*

$$\{S_i, S_j\} = \epsilon_{ijk}\,S_k\,. \tag{4.7}$$

From the evolution of angular momentum and spins, we can find several conserved quantities that can be exploited in deriving the dynamical solutions. First, the magnitudes of the angular momenta are conserved because

$$\frac{d(\boldsymbol{L}\cdot\boldsymbol{L})}{dt} = \frac{2}{c^2\,r^3}\,\boldsymbol{L}\cdot(\boldsymbol{S}_{\rm eff}\times\boldsymbol{L}) = 0\,, \tag{4.8a}$$

$$\frac{d(\boldsymbol{S}_1\cdot\boldsymbol{S}_1)}{dt} = \frac{2\,\delta_1}{c^2\,r^3}\,\boldsymbol{S}_1\cdot(\boldsymbol{L}\times\boldsymbol{S}_1) = 0\,, \tag{4.8b}$$

$$\frac{d(\boldsymbol{S}_2\cdot\boldsymbol{S}_2)}{dt} = \frac{2\,\delta_2}{c^2\,r^3}\,\boldsymbol{S}_2\cdot(\boldsymbol{L}\times\boldsymbol{S}_2) = 0\,. \tag{4.8c}$$

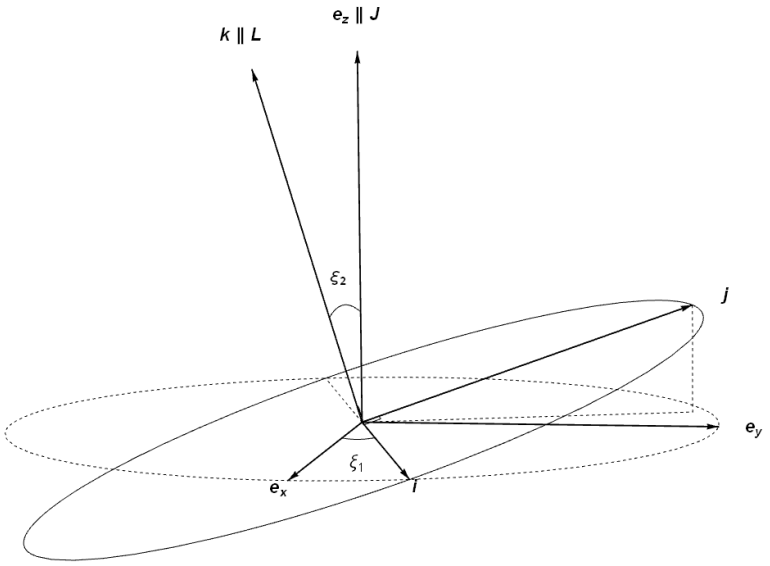

Figure 4.1 Two bases are displayed : The inertial frame ($\boldsymbol{e}_x$, $\boldsymbol{e}_y$, $\boldsymbol{e}_z$) and the non-inertial frame ($\boldsymbol{i}$, $\boldsymbol{j}$, $\boldsymbol{k}$). The total angular momentum $\boldsymbol{J}$ is parallel to $\boldsymbol{e}_z$, and the orbital angular momentum $\boldsymbol{L}$ to $\boldsymbol{k}$. The non-inertial frame is constructed by rotating the inertial frame around z-axis by ξ_1 and then around x-axis by ξ_2, so that ξ_1 and ξ_2 determine the orientation of $\boldsymbol{L}$.

Also in the absence of the angular momentum loss from the binary system, the *total angular momentum* $\boldsymbol{J} = \boldsymbol{L} + \boldsymbol{S}_1 + \boldsymbol{S}_2$ is conserved. Without loss of generality we can define the z-axis of the inertial frame to be aligned with $\boldsymbol{J}$ while the the orthogonal axes x and y can be chosen arbitrarily on the plane perpendicular to z-axis as shown in Fig. 4.1.

At the same time, we define an orthonormal non inertial frame $(\boldsymbol{i}, \boldsymbol{j}, \boldsymbol{k})$,

$$\begin{pmatrix} \boldsymbol{i} \\ \boldsymbol{j} \\ \boldsymbol{k} \end{pmatrix} = \Lambda \begin{pmatrix} \boldsymbol{e}_x \\ \boldsymbol{e}_y \\ \boldsymbol{e}_z \end{pmatrix} \tag{4.9}$$

where Λ is the Euler matrix as shown below

$$\Lambda = \begin{pmatrix} \cos\xi_1 & \sin\xi_1 & 0 \\ -\sin\xi_1\,\cos\xi_2 & \cos\xi_1\,\cos\xi_2 & \sin\xi_2 \\ \sin\xi_1\sin\xi_2 & -\cos\xi_1\sin\xi_2 & \cos\xi_2 \end{pmatrix} . \tag{4.10}$$

The geometric meaning of the Euler matrix is presented in Fig. 4.1.

Next, we define the angles γ, κ_1 and κ_2 in the range of $[0,\,\pi]$ such that

$$\cos\gamma := \frac{\boldsymbol{S}_1 \cdot \boldsymbol{S}_2}{S_1\;S_2}\,, \tag{4.11a}$$

$$\cos\kappa_1 := \frac{\boldsymbol{L} \cdot \boldsymbol{S}_1}{L\;S_1}\,, \tag{4.11b}$$

$$\cos\kappa_2 := \frac{\boldsymbol{L} \cdot \boldsymbol{S}_2}{L\;S_2}\,, \tag{4.11c}$$

as illustrated in Fig. 4.2.

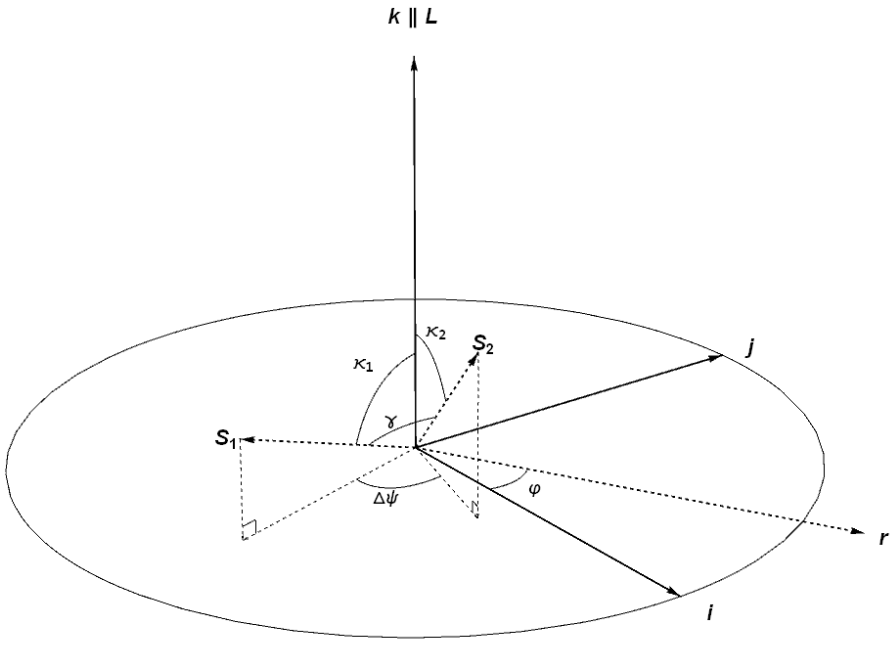

Figure 4.2 The geometry of spin and angular momentum vectors, and the inertial frame.

The rates of changes of these angles are given via Eq.(4.6) *i.e.*

$$\frac{d\cos\gamma}{dt} = \frac{\delta_1-\delta_2}{c^2\,r^3\,S_1\,S_2}\boldsymbol{L}\cdot(\boldsymbol{S}_1\times\boldsymbol{S}_2)\,, \tag{4.12a}$$

$$\frac{d\cos\kappa_1}{dt} = \frac{\delta_2}{c^2\,r^3\,S_1\,L}\boldsymbol{L}\cdot(\boldsymbol{S}_1\times\boldsymbol{S}_2)\,, \tag{4.12b}$$

$$\frac{d\cos\kappa_2}{dt} = -\frac{\delta_1}{c^2\,r^3\,S_2\,L}\boldsymbol{L}\cdot(\boldsymbol{S}_1\times\boldsymbol{S}_2)\,. \tag{4.12c}$$

By observing their common factor $\boldsymbol{L}\cdot(\boldsymbol{S}_1\times\boldsymbol{S}_2)$, we can define new conserved quantities σ_1, σ_2 as follows

$$\sigma_1 := \cos\gamma - \frac{L}{S_2}\frac{\delta_1-\delta_2}{\delta_2}\cos\kappa_1\,, \tag{4.13a}$$

$$\sigma_2 := \cos\kappa_2 + \frac{\delta_1}{\delta_2}\frac{S_1}{S_2}\cos\kappa_1\,. \tag{4.13b}$$

Note that if $\delta_1-\delta_2=0$, or equal mass case, then $\sigma_1=\cos\gamma$ implying that the angle γ between $\boldsymbol{S}_1$ and $\boldsymbol{S}_2$ is conserved.

Through straightforward vector algebra, one can show that

$$\boldsymbol{L}\cdot(\boldsymbol{S}_1\times\boldsymbol{S}_2) = L\,S_1\,S_2\,\sin\kappa_1\sin\kappa_2\sin\Delta\psi\,,$$

where $\Delta\psi$ is an angle between the projection of $\boldsymbol{S}_1$ and $\boldsymbol{S}_2$ onto x-y plane of the non-inertial frame where $\boldsymbol{L}$ is along with z-axis (See Fig. 4.2). It has the following relation with the others,

$$\cos\Delta\psi = \frac{\cos\gamma-\cos\kappa_1\,\cos\kappa_2}{\sin\kappa_1\,\sin\kappa_2}\,. \tag{4.14}$$

When either $\sin\kappa_1=0$ or $\sin\kappa_2=0$, $\Delta\psi$ is not defined in the geometric sense. But physically we can extend the definition of $\Delta\psi$ properly. For example let us assume that $\kappa_1=0$ and $\sin\kappa_2\neq0$ at the initial time t_0. Then, during an infinitesimal time interval dt, $d\boldsymbol{S}_1=0$ because $|\frac{d\boldsymbol{S}_1}{dt}|\sim|\boldsymbol{L}\times\boldsymbol{S}_1|\sim\sin\kappa_1=0$. On the other hand, $d\boldsymbol{L}=\boldsymbol{L}(t_0+dt)-\boldsymbol{L}(t_0)=-\frac{dt\,\delta_2}{c^2\,r^3}\boldsymbol{L}\times\boldsymbol{S}_2$. Therefore the square of the $d\boldsymbol{L}$ is given as

$$\big|\boldsymbol{L}(t_0+dt)-\boldsymbol{L}(t_0)\big|^2 = dt^2\,\left(\frac{L\,S_2\,\delta_2\,\sin\kappa_2}{c^2\,r^3}\right)^2\,. \tag{4.15}$$

Because $\boldsymbol{L}(t_0)$ and $\boldsymbol{S}_1(t_0)$ are aligned and $\boldsymbol{S}_1(t_0 + dt) = \boldsymbol{S}_1(t_0)$, the infinitesimal change of κ_1 is the angle between $\boldsymbol{L}(t_0 + dt)$ and $\boldsymbol{L}(t_0)$. Thus the right hand side of Eq.(4.15) is

$$2\,L^2\,(1 - \cos d\kappa_1) = L^2\,d\kappa_1^2\, + O(d\kappa_1^3). \tag{4.16}$$

Since κ_1 can only increase during dt, we get $\frac{d\kappa_1}{dt} = \frac{\delta_2\,S_2\,\sin\kappa_2}{c^2\,r^3}$. Thus by setting $\sin\Delta\psi = -1$, replacing the vectorial expression $\boldsymbol{L}\cdot(\boldsymbol{S}_1 \times \boldsymbol{S}_2)$ in Eqs.(4.12) to the algebraic expression $L\,S_1\,S_2\,\sin\kappa_1 \sin\kappa_2 \sin\Delta\psi$ becomes valid even in the case of $\kappa_1 = 0$. Likewise we arrive at same extension $\sin\Delta\psi = -1$ when $\kappa_2 = \pi$ (with $\sin\kappa_1 \neq 0$), while $\sin\Delta\psi = 1$ in the case of $\kappa_1 = \pi$ ($\sin\kappa_2 \neq 0$) and $\kappa_2 = 0$ ($\sin\kappa_1 \neq 0$). Mathematically, this kind of extension is nothing but taking the limit of $\sin\kappa_{1,2} \to 0$ along the physically preferred paths. If $\sin\kappa_1 = 0$ and $\sin\kappa_2 = 0$ are both satisfied at some point, since every angle becomes constant, we do not need to define $\Delta\psi$.

We have three time dependent variables $\kappa_1(t)$, $\kappa_2(t)$ and $\gamma(t)$ to solve and two conserved quantities, σ_1 and σ_2. So, if we determine a numerical value of any one angle (say κ_1), the others are determined automatically by the initially fixed values of σ_1 and σ_2. This fact allows the relations of Eqs.(4.12), where κ_1, κ_2 and γ are non-linearly entangled, to be expressed in a single variable equation, for example κ_1. This specific choice of κ_1 is followed from the fact that γ is not a good parameter. As mentioned earlier, γ fails to parametrize the dynamics when mass ratio becomes close to 1. Choosing γ as a paramter was used in Kesden et al. (2015), and we can see that there are divergences as $q \to 1$ in the equations (7a) and (7b) in Kesden et al. (2015).

4.3 The Keplerian-type parametrization

4.3.1 The Keplerian-type parametrization of the Angles

In this subsection, we solve the Eqs.(4.12). We reduce the common factor $\boldsymbol{L}\cdot(\boldsymbol{S}_1\times\boldsymbol{S}_2)$, using σ_1 and σ_2, into single variable ($\cos\kappa_1$) dependent expression,

$$\frac{\boldsymbol{L}\cdot(\boldsymbol{S}_1\times\boldsymbol{S}_2)}{L\,S_1\,S_2}=\sin\kappa_1\sin\kappa_2\sin\Delta\psi \tag{4.17}$$

$$\begin{aligned}
&=\pm\sqrt{1-\cos^2\kappa_1-\cos^2\kappa_2-\cos^2\gamma+2\cos\gamma\cos\kappa_1\cos\kappa_2}\\
&=\frac{\pm}{\delta_2\,S_2}\Big\{-2\,\delta_1\,L\,S_1(\delta_1-\delta_2)\cos^3\kappa_1-\big[L^2\,(\delta_1-\delta_2)^2+2\,\delta_2\,L\,\sigma_2\,S_2\,(\delta_2-\delta_1)\\
&\quad+\delta_1^2\,S_1^2+2\,\delta_1\,\delta_2\,\sigma_1\,S_1\,S_2+\delta_2^2\,S_2^2\big]\,\cos^2\kappa_1 \qquad (4.18)\\
&\quad+2\,\delta_2\,S_2\left[L\,\sigma_1\,(\delta_2-\delta_1)+\sigma_2\,(\delta_1S_1+\delta_2\sigma_1S_2)\right]\cos\kappa_1-\delta_2^2\,S_2^2\,(\sigma_1^2+\sigma_2^2-1)\Big\}^{1/2}.
\end{aligned}$$

The sign of $\boldsymbol{L}\cdot(\boldsymbol{S}_1\times\boldsymbol{S}_2)$ is determined by the sign of $\sin\Delta\psi$. For simplicity, let us denote $\cos\kappa_1=x$ and factorize the expression inside the square root in terms of its 3rd polynomial roots of $x=(x_1,x_2,x_3)$ and introduce a coefficient $A:=2\,L\,S_1\,\delta_1\,(\delta_2-\delta_1)$ to simplify the above equation as

$$\frac{\boldsymbol{L}\cdot(\boldsymbol{S}_1\times\boldsymbol{S}_2)}{L\,S_1\,S_2}=\frac{\pm}{\delta_2\,S_2}\sqrt{A\,(x-x_1)(x-x_2)(x-x_3)}\,. \tag{4.19}$$

Before proceeding integrations, one needs to clarify the existence of the real roots of x. Here is a brief proof: Let us assume that there is no instance such that $\kappa_1(t)$, $\kappa_2(t)$ and $\gamma(t)$ satisfy $\boldsymbol{L}\cdot(\boldsymbol{S}_1\times\boldsymbol{S}_2)=0$ during evolutions. This assumption says that if $\boldsymbol{L}\cdot(\boldsymbol{S}_1\times\boldsymbol{S}_2)>0$ initially this inequalitiy always holds by virtue of continuity. Also the followings hold forever, $\frac{d\cos\kappa_1}{dt}>0$, $\frac{d\cos\gamma}{dt}>0$ (if $\delta_1>\delta_2$) and $\frac{d\cos\kappa_2}{dt}<0$. Then we are able to find a real value T such that $\cos\kappa_1>0$, $\cos\gamma>0$ and $\cos\kappa_2<0$ at times $t>T$ unless $\frac{d\cos\kappa_1}{dt}\to 0+$, $\frac{d\cos\gamma}{dt}\to 0+$ and $\frac{d\cos\kappa_2}{dt}\to 0-$ fast enough as $t\to\infty$. But we exclude this dissipative possibility because governing dynamics is symmetric under the reflection of $t\to -t$.

Meanwhile the time derivative of $\boldsymbol{L}\cdot(\boldsymbol{S}_1\times\boldsymbol{S}_2)$ is

$$\begin{aligned}&\frac{d\boldsymbol{L}\cdot(\boldsymbol{S}_1\times\boldsymbol{S}_2)}{dt}\\ =&\frac{-2\cos\kappa_1+2\cos\gamma\,\cos\kappa_2}{\boldsymbol{L}\cdot(\boldsymbol{S}_1\times\boldsymbol{S}_2)}\,\frac{d\cos\kappa_1}{dt}\\ +&\frac{-2\cos\kappa_2+2\cos\gamma\,\cos\kappa_1}{\boldsymbol{L}\cdot(\boldsymbol{S}_1\times\boldsymbol{S}_2)}\,\frac{d\cos\kappa_2}{dt}\\ +&\frac{-2\cos\gamma+2\cos\kappa_1\,\cos\kappa_2}{\boldsymbol{L}\cdot(\boldsymbol{S}_1\times\boldsymbol{S}_2)}\,\frac{d\cos\gamma}{dt}\,.\end{aligned}\tag{4.20}$$

It is obvious that $\frac{d\boldsymbol{L}\cdot(\boldsymbol{S}_1\times\boldsymbol{S}_2)}{dt}<0$ when $t>T$. Similarly we can estimate its second time derivative and we can decompose it into two components *i.e.* $\frac{d^2\boldsymbol{L}\cdot(\boldsymbol{S}_1\times\boldsymbol{S}_2)}{dt^2}=\hat{A}(t)+\hat{B}(t)\,\dot{r}$ where $\hat{A}(t)<0$, $\hat{B}(t)>0$ but $\dot{r}$ oscillates sinusoidally between positive and negative values with zero averaged value *i.e.* $\frac{1}{2\pi}\int_0^{2\pi}du\,\dot{r}=0$. Thus in much longer time scale than one orbital period, the absolute value of $\frac{d\boldsymbol{L}\cdot(\boldsymbol{S}_1\times\boldsymbol{S}_2)}{dt}$ increases, *i.e.* decreasing of $\boldsymbol{L}\cdot(\boldsymbol{S}_1\times\boldsymbol{S}_2)$ accelerates. This suggests that at some point $\boldsymbol{L}\cdot(\boldsymbol{S}_1\times\boldsymbol{S}_2)$ will pass zero, or $\boldsymbol{L}\cdot(\boldsymbol{S}_1\times\boldsymbol{S}_2)>0$ cannot hold forever. This is contradictory to the assumption. Likewise another assumption that $\boldsymbol{L}\cdot(\boldsymbol{S}_1\times\boldsymbol{S}_2)<0$ also encounters the same contradiction. Finally we come to the conclusion that whatever the initial condition is, binary systems eventually meet the configuration which corresponds to $\boldsymbol{L}\cdot(\boldsymbol{S}_1\times\boldsymbol{S}_2)=0$. Actually this happens twice, once when $\boldsymbol{L}\cdot(\boldsymbol{S}_1\times\boldsymbol{S}_2)$ is increasing or once when it is decreasing. Let us match cosine value of these two κ_1 values to x_2 and x_3. Then it is obvious that they are real and the absolute values are less than or equal to 1. Additionally, from the fact that cubic polynomicals of which all coefficients are real, cannot have two real roots and a single complex root, we can conclude that x_1 is also real. Note that our assumption does not include the equal mass case, *i.e.*, $\delta_1=\delta_2$ in the above proof. Since there is no reason for any discontinuity toward the equal mass case, we can extend the validity of our formalism to $\delta_1=\delta_2$ although we need a special caution in applying the formalism presented below when two masses become very close. The case of nearly equal mass is treated separately in §4.4.

Without loss of generality, we assume that $A > 0$ and $x_2 \leq \cos\kappa_1 \leq x_3$, because it must be non negative within the square root as illustrated in Fig. 4.3.

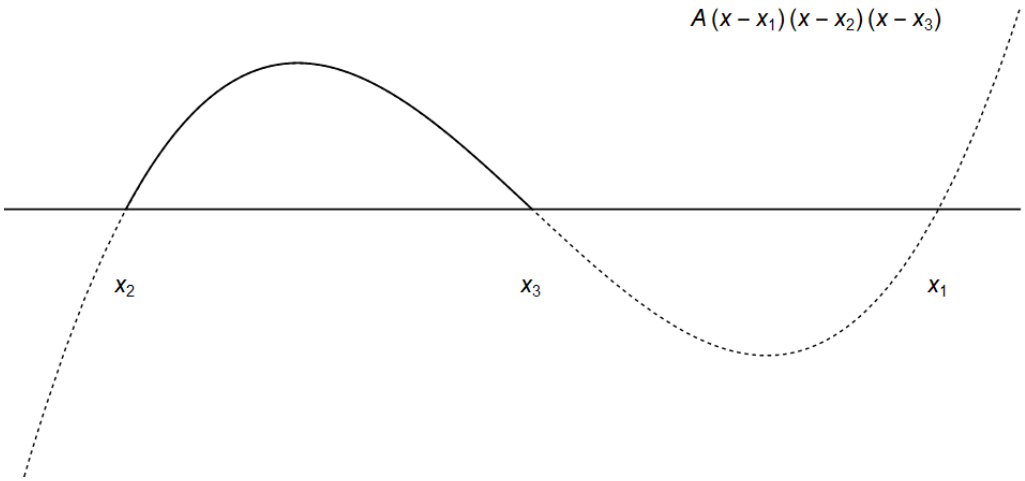

Figure 4.3 The shape of the function inside the square-root of Eq.(4.17).

Eq.(4.12b) becomes,

$$\frac{dx}{dt} = \frac{\pm}{c^2\, r^3}\sqrt{A(x-x_1)(x-x_2)(x-x_3)}\,, \tag{4.21}$$

or,

$$\frac{d\cos\kappa_1}{\sqrt{A(\cos\kappa_1 - x_1)(\cos\kappa_1 - x_2)(\cos\kappa_1 - x_3)}} = \frac{\pm\, dt}{c^2\, r^3}. \tag{4.22}$$

It is enough that r is given in the Newtonian order, because we restrict the spin orbit interaction only up to the leading order. In Newtonian order we can use the well known expressions of $r = a\,(1 - e\,\cos u)$ and $n\,(t - t_0) = u - e\,\sin u$, where u is the eccentric anomaly, n is the mean angular speed and t is physical time with an initial value t_0 when $u = 0$, a is the semi-major axis of the ellipse, and e is the eccentricity. Thus the right hand side of Eq.(4.22) can be integrated to

$$(r.h.s) = \int du \frac{dt}{du}\frac{\pm 1}{c^2\, r^3}$$

$$
\begin{aligned}
&= \alpha \pm \frac{\nu + e\sin\nu}{c^2\, n\, a^3\, (1-e^2)^{3/2}}\,, \\
&= \alpha \pm \frac{\nu + e\sin\nu}{c^2\, L^3} + O(\frac{1}{c^3}),
\end{aligned} \tag{4.23}
$$

where we use the Newtonian expression of the magnitude of the orbital angular momentum $L = n^{\frac{1}{3}}\, a\, (1-e^2)^{\frac{1}{2}} + O(\frac{1}{c})$ with $\nu = 2\,\arctan(\sqrt{\frac{1+e}{1-e}}\,\tan\frac{u}{2})$ and α refers to proper initial value which will be defined later. Note that the given expression of Eq.(4.23) is somewhat deceiving. Because the $\pm$ sign in front of ν dependent term changes as $\cos\kappa_1$ passes its maximum x_3 or minimum x_2. For example, if $\cos\kappa_1$ arrives at x_3 when $\nu = \nu_3$, then when $\nu > \nu_3$ it would be better if right hand side of Eq.(4.23) is written as

$$
\alpha + 2\,\frac{\nu_3 + e\sin\nu_3}{c^2\, L^3} - \frac{\nu + e\sin\nu}{c^2\, L^3}\,, \tag{4.24}
$$

hence it has a periodic structure behind and more complicated feature than presented in Eq.(4.23). But as we can see later, the presented expression of Eq.(4.23) will be justified. Now let us solve the left hand side of Eq.(4.22) keeping in mind that $x_2 \le x \le x_3 < x_1$,

$$
\begin{aligned}
(l.h.s) &= \frac{dx}{\sqrt{A(x-x_1)(x-x_2)(x-x_3)}} \\
&= \frac{dx}{\sqrt{A(x_1-x_2)}\sqrt{\frac{x_1-x}{x_1-x_2}}\sqrt{x-x_2}\sqrt{x_3-x_2}\sqrt{\frac{x_3-x}{x_3-x_2}}} \\
&= \frac{\frac{1}{\sqrt{x_3-x_2}}\frac{1}{\sqrt{x-x_2}}dx}{\sqrt{A(x_1-x_2)}\sqrt{1-\frac{x_3-x_2}{x_1-x_2}\frac{x-x_2}{x_3-x_2}}\sqrt{1-\frac{x-x_2}{x_3-x_2}}}.
\end{aligned} \tag{4.25}
$$

Since $0 \le \frac{x-x_2}{x_3-x_2} \le 1$, we can introduce a new variable y defined through

$$
\sin^2 y = \frac{x-x_2}{x_3-x_2} \tag{4.26}
$$

which is restricted to $0 \le y \le \frac{\pi}{2}$. Then the last line of the Eq.(4.25) becomes

$$
\frac{\frac{1}{\sqrt{x_3-x_2}}\frac{1}{\sqrt{x-x_2}}dx}{\sqrt{A(x_1-x_2)}\sqrt{1-\frac{x_3-x_2}{x_1-x_2}\sin^2 y}\,\cos y} \tag{4.27}
$$

$$= \frac{2\,dy}{\sqrt{A(x_1 - x_2)}\sqrt{1 - \frac{x_3 - x_2}{x_1 - x_2}\sin^2 y}}\,.$$

Identifying this integral as the Elliptic Integral of the first kind F,

$$F(\phi,\, k) := \int^{\phi} \frac{d\theta}{\sqrt{1 - k^2\,\sin^2\theta}}\,, \tag{4.28}$$

the Eq.(4.27) can be written in the following compact form

$$\frac{2}{\sqrt{A(x_1 - x_2)}}\,F\left(\arcsin\sqrt{\frac{\cos\kappa_1 - x_2}{x_3 - x_2}}, \sqrt{\frac{x_3 - x_2}{x_1 - x_2}}\right)\,. \tag{4.29}$$

There could be other possible forms instead of Eq.(4.29) but, under the assumption of $x_2 \le \cos\kappa_1 \le x_3$, the above form is well defined.

Finally by integrating both sides of Eq.(4.22), Keplerian parametrization of $\cos\kappa_1$ can be obtained as,

$$\begin{aligned}\cos\kappa_1 \;&=\; x_2 + (x_3 - x_2)\,\mathrm{sn}^2(\Upsilon\,,\,\beta) \\ &= x_2\,\mathrm{cn}^2(\Upsilon\,,\,\beta) + x_3\,\mathrm{dn}^2(\Upsilon\,,\,\beta)\,,\end{aligned} \tag{4.30}$$

where $\Upsilon = \frac{\sqrt{A(x_1 - x_2)}}{2}(\alpha + \frac{\nu + e\sin\nu}{c^2\,L^3})$, $\beta = \sqrt{\frac{x_3 - x_2}{x_1 - x_2}}$ and sn, cn and dn are the sine, cosine and tangent like Jacobi elliptic functions Whittaker and Watson (2009).

It is worth pointing out that $\pm$ sign which was supposed to be inside the definition of Υ according to Eq.(4.23), is removed. Because of symmetric property, $\mathrm{sn}^2(X, b) = \mathrm{sn}^2(-X, b)$, we have a freedom to choose definition of Υ among four cases of $\pm\frac{\sqrt{A(x_1 - x_2)}}{2}(\alpha \pm \frac{\nu + e\sin\nu}{c^2\,L^3})$. Firstly, we have chosen $\frac{\sqrt{A(x_1 - x_2)}}{2}(\pm\alpha + \frac{\nu + e\sin\nu}{c^2\,L^3})$ so that the sign of ν dependent term is positive. And we make $\pm$ sign in front of α be absorbed into the definition of α. That is,

$$\alpha = \pm\frac{2}{\sqrt{A(x_1 - x_2)}}\,F\left(\arcsin\sqrt{\frac{\cos\kappa_{1(0)} - x_2}{x_3 - x_2}},\, \beta\right)\,, \tag{4.31}$$

where $\cos\kappa_{1(0)}$ is an initial value of $\cos\kappa_1$ when $t = t_0$, or $u = 0$. The $\pm$ sign is determined as : $+$ for the case that $\frac{d\cos\kappa_1}{dt} > 0$ initially while $-$ for $\frac{d\cos\kappa_1}{dt} < 0$ initially. Lastly, as we have seen, the expression of Eq.(4.23) could not capture its oscillating feature. But we

do not need to be concerned of it since the final form of our solution Eq.(4.30) trivially captures the feature. Taking Eq.(4.24) as an example again, the reflection symmetry of sn, $\mathrm{sn}(X+b,d)=\mathrm{sn}(X-b,d)$ when sn has its maximum or minimum at X, allows (here we intentionally omit $\frac{\sqrt{A(x_1-x_2)}}{2}$ and β)

$$\begin{aligned}&\mathrm{sn}\left(\alpha+2\frac{\nu_3+e\sin\nu_3}{c^2\,L^3}-\frac{\nu+e\sin\nu}{c^2\,L^3}\right)\\ =&\mathrm{sn}\left(\alpha+\frac{\nu+e\sin\nu}{c^2\,L^3}\right)\end{aligned}\tag{4.32}$$

so that our solution is justified to be valid independent of duration.

In the case of $A<0$ *i.e.* $m_1<m_2$, the form of our solution is still valid with rearranging the order of the roots as $x_1<x_3\leq x_2$. Also in the case of no dynamics *i.e.* $\frac{d\cos\kappa_1}{dt}=0$ all the time, our solution is valid with $x_2=x_3$. In the case of $A=0$ *i.e.* $m_1=m_2$, our solution is still valid with $x_1\to\infty$ and thus $\beta=0$.

Additionally, because the sine-like Jacobian elliptic function $\mathrm{sn}(\Upsilon,\beta)$ is periodic, we can get the period of the precessional motion. Let N be the number of orbital cycles. During N cycles, Υ increases as

$$\Delta\Upsilon_N=\frac{\sqrt{A(x_1-x_2)}\,\pi\,N}{c^2\,L^3}\tag{4.33}$$

while $\mathrm{sn}^2(\Upsilon,\beta)$ has a following period Whittaker and Watson (2009),

$$\Delta\Upsilon_P=\pi\,\mathcal{F}_{2,1}\left(\frac{1}{2},\frac{1}{2};1;\beta^2\right).\tag{4.34}$$

So $\Delta\Upsilon_P=\Delta\Upsilon_N$ yields the number of cycles $N=N_{\mathrm{prec}}$ of the binary system during one period of precession,

$$N_{\mathrm{prec}}=\mathcal{F}_{2,1}\left(\frac{1}{2},\frac{1}{2};1;\beta^2\right)\frac{c^2\,L^3}{\sqrt{A\,(x_1-x_2)}}\tag{4.35}$$

where $\mathcal{F}_{2,1}$ is a hypergeometric function.

Furthermore, invoking the definitions of σ_1 and σ_2, we can get the relationship between γ, κ_1 and κ_2

$$\cos\gamma=\sigma_1+\frac{L}{S_2}\frac{\delta_1-\delta_2}{\delta_2}\cos\kappa_1\,,\tag{4.36a}$$

$$\cos\kappa_2 = \sigma_2 - \frac{\delta_1}{\delta_2}\frac{S_1}{S_2}\cos\kappa_1\,. \tag{4.36b}$$

Now, in the non-inertial frame where the orbital angular momentum is fixed as $\boldsymbol{L} = (0,0,L)$, we have a parametrization on how the spin angular momentums evolve around $\boldsymbol{L}$.

In the non inertial frame, each angular momentum is expressed as,

$$\boldsymbol{J} = \Lambda^{-1,T}\begin{pmatrix}0\\0\\J\end{pmatrix}_i = \begin{pmatrix}0\\J\,\sin\xi_2\\J\,\cos\xi_2\end{pmatrix}_n\,, \tag{4.37a}$$

and

$$\boldsymbol{L} = \begin{pmatrix}0\\0\\L\end{pmatrix}_n\,, \tag{4.37b}$$

$$\boldsymbol{S}_1 = S_1\begin{pmatrix}\sin\kappa_1\cos\xi_3\\\sin\kappa_1\sin\xi_3\\\cos\kappa_1\end{pmatrix}_n\,, \tag{4.37c}$$

$$\boldsymbol{S}_2 = S_2\begin{pmatrix}\sin\kappa_2\cos(\xi_3+\Delta\psi)\\\sin\kappa_2\sin(\xi_3+\Delta\psi)\\\cos\kappa_2\end{pmatrix}_n\,, \tag{4.37d}$$

where $\Lambda^{-1,T}$ is the inverse matrix of the transpose of Λ and the subscripts n and i refer to non-inertial and inertial frame respectively, where components of vector are described. Since $\boldsymbol{J} = \boldsymbol{L} + \boldsymbol{S}_1 + \boldsymbol{S}_2$, we get the following three relations

$$0 \;=\; S_1\,\sin\kappa_1\,\cos\xi_3 + S_2\,\sin\kappa_2\,\cos(\xi_3+\Delta\psi) \tag{4.38a}$$

$$J\,\sin\xi_2 \;=\; S_1\,\sin\kappa_1\,\sin\xi_3 + S_2\,\sin\kappa_2\,\sin(\xi_3+\Delta\psi) \tag{4.38b}$$

$$J\,\cos\xi_2 = L + S_1\cos\kappa_1 + S_2\cos\kappa_2\,. \tag{4.38c}$$

Fom Eq.(4.38c), we get $\cos\xi_2$ in terms of $\cos\kappa_1$,

$$\begin{aligned}\cos\xi_2 &= \frac{1}{J}(L + S_1\cos\kappa_1 + S_2\cos\kappa_2)\,, \\ &= \frac{L+S_2\sigma_2}{J} - \frac{S_1\,(\delta_1-\delta_2)}{J\delta_2}\cos\kappa_1\,.\end{aligned} \tag{4.39}$$

On the other hands, from Eq.(4.38a) and Eq.(4.38b), we get the expression for ξ_3

$$\begin{pmatrix} \sin\xi_3 \\ \cos\xi_3 \end{pmatrix} = \begin{pmatrix} \frac{S_1\,\sin\kappa_1 + S_2\,\cos\Delta\psi\,\sin\kappa_2}{J\,\sin\xi_2} \\ \frac{S_2\,\sin\Delta\psi\,\sin\kappa_2}{J\,\sin\xi_2} \end{pmatrix}, \tag{4.40}$$

with Eq.(4.14),

$$\sin\xi_3 = \frac{S_1\,\sin^2\kappa_1 + S_2\,(\cos\gamma - \cos\kappa_1\,\cos\kappa_2)}{J\,\sin\kappa_1\,\sin\xi_2}. \tag{4.41}$$

This completes parametrization of all relative angles in Kepelerian type.

4.3.2 The Keplerian-type Parametrization of the Orbital Angular Momentum

Now, we are in the position to solve a Keplerian parametrization of ξ_1. The easiest way is to get components of $\frac{d\boldsymbol{L}}{dt}$ in the non inertial frame, and solve Eq.(4.6a), also in the non inertial frame.

Starting from the inertial-expression of $\frac{d\boldsymbol{L}}{dt}$, we can get components of $\frac{d\boldsymbol{L}}{dt}$ in the non-inertial frame ,

$$\begin{aligned}\frac{d\boldsymbol{L}}{dt} &= L\,\frac{d\boldsymbol{k}}{dt} \\ &= L\begin{pmatrix} \cos\xi_1\,\sin\xi_2\,\dot{\xi}_1 + \sin\xi_1\,\cos\xi_2\,\dot{\xi}_2 \\ \sin\xi_1\,\sin\xi_2\,\dot{\xi}_1 - \cos\xi_1\,\cos\xi_2\,\dot{\xi}_2 \\ -\sin\xi_2\,\dot{\xi}_2 \end{pmatrix}_i\end{aligned} \tag{4.42}$$

$$= L \begin{pmatrix} \sin\xi_2\,\dot{\xi}_1 \\ -\dot{\xi}_2 \\ 0 \end{pmatrix}_n .$$

From the componential expression of Eq.(4.6a) in the non-inertial frame, we get

$$\begin{pmatrix} \sin\xi_2\,\dot{\xi}_1 \\ -\dot{\xi}_2 \\ 0 \end{pmatrix}_n = \frac{1}{c^2\,r^3} \begin{pmatrix} S_1\,\delta_1\,\sin\kappa_1\,\sin\xi_3 + S_2\,\delta_2\,\sin\kappa_2\,\sin(\xi_3+\Delta\psi) \\ -S_1\,\delta_1\,\sin\kappa_1\,\cos\xi_3 - S_2\,\delta_2\,\sin\kappa_2\,\cos(\xi_3+\Delta\psi) \\ 0 \end{pmatrix}_n . \quad (4.43)$$

The first row in the equation can be written in terms of $\cos\kappa_1$ using the relations Eqs.(4.36) and (4.38),

$$\dot{\xi}_1 =: \frac{1}{c^2\,r^3}\left(\frac{\beta_1}{\cos\kappa_1+\alpha_1} - \frac{\beta_2}{\cos\kappa_1+\alpha_2}\right), \quad (4.44)$$

where α_1, α_2, β_1 and β_2 are defined as follows

$$\alpha_1 = -\frac{\delta_2\,(J+L+S_2\,\sigma_2)}{S_1\,(\delta_1-\delta_2)}, \quad (4.45a)$$

$$\alpha_2 = -\frac{\delta_2\,(-J+L+S_2\,\sigma_2)}{S_1\,(\delta_1-\delta_2)}, \quad (4.45b)$$

$$\beta_1 = -\frac{L^2\,\delta_1 + J^2\,\delta_2 + S_1\,(\delta_1-\delta_2)(S_1+S_2\,\sigma_1) + L\,S_2\,\delta_1\,\sigma_2 + J\left[L+(\delta_1+\delta_2)+S_2\,\sigma_2\,\delta_2\right]}{2\,S_1\,(\delta_1-\delta_2)}, \quad (4.45c)$$

$$\beta_2 = -\frac{L^2\,\delta_1 + J^2\,\delta_2 + S_1\,(\delta_1-\delta_2)(S_1+S_2\,\sigma_1) + L\,S_2\,\delta_1\,\sigma_2 - J\left[L+(\delta_1+\delta_2)+S_2\,\sigma_2\,\delta_2\right]}{2\,S_1\,(\delta_1-\delta_2)}. \quad (4.45d)$$

The integration can be written as, again with $x = \cos\kappa_1$,

$$\int d\xi_1 = \pm \int \frac{dx}{\sqrt{A\,(x-x_1)\,(x-x_2)\,(x-x_3)}}\left(\frac{\beta_1}{x+\alpha_1} - \frac{\beta_2}{x+\alpha_2}\right). \quad (4.46)$$

At this point, we encounter similar issue discussed around Eq.(4.23). The sign of $\frac{dx}{dt}$ oscillates during evolution and this makes the integration messy. To resolve this, we use y introduced in Eq.(4.26) again but imposing that y increases as t increases instead of restricting the range of y. (In fact, by comparing with Eq.(4.30), $y = \mathrm{am}(\Upsilon, \beta)$.) Then, the integration can be written without the $\pm$ sign as

$$\int d\xi_1 = \int \frac{2\,dy}{\sqrt{A(x_1-x_2)}\sqrt{1-\frac{x_3-x_2}{x_1-x_2}\sin^2 y}} \left(\frac{\frac{\beta_1}{\alpha_1+x_2}}{1-\frac{x_2-x_3}{\alpha_1+x_2}\sin^2 y} - \frac{\frac{\beta_2}{\alpha_2+x_2}}{1-\frac{x_2-x_3}{\alpha_2+x_2}\sin^2 y} \right). \tag{4.47}$$

The above integration is identified as the Elliptic integral of the third kind Whittaker and Watson (2009), denoted as Π,

$$\Pi\,(a,\,b,\,c) := \int_0^b \frac{1}{\sqrt{1-c^2\,\sin^2\theta}} \frac{d\theta}{1-a\,\sin^2\theta}\,. \tag{4.48}$$

Therefore

$$\xi_1 - \xi_{1(0)} = \frac{2}{\sqrt{A\,(x_1-x_2)}} \Big(\frac{\beta_1\,\Pi\,(\frac{x_2-x_3}{\alpha_1+x_2},\,\mathrm{am}(\Upsilon,\,\beta),\,\beta)}{\alpha_1+x_2} - \frac{\beta_2\,\Pi\,(\frac{x_2-x_3}{\alpha_2+x_2},\,\mathrm{am}(\Upsilon,\,\beta),\,\beta)}{\alpha_2+x_2} \Big), \tag{4.49}$$

where $\xi_{1(0)}$ is an initially determined parameter and am denotes the Jacobi amplitude.
Up to now Keplerian parametrization for evolution of angular momentum has been derived in the inertial frame. Especially, the orbital angular momentum $\boldsymbol{L}$ dynamics is totally determined by Eqs.(4.49) and (4.39) up to leading order precession. The last step is a parametrization of relative motion of binaries up to the leading order of spin-orbit interaction.

4.3.3 Keplerian-type Parametrization of the relative motion of binaries

From the Hamiltonian Eq.(4.1), the equation governing $\boldsymbol{r}$ is

$$\dot{\boldsymbol{r}} = \frac{\partial H}{\partial \boldsymbol{p}} = \boldsymbol{p} + \frac{1}{c^2\,r^3}\,(\delta_1\,\boldsymbol{S}_1 + \delta_2\,\boldsymbol{S}_2) \times \boldsymbol{r}\,, \tag{4.50}$$

or,

$$\boldsymbol{p} = \dot{\boldsymbol{r}} - \frac{1}{c^2\, r^3}\left(\delta_1\, \boldsymbol{S}_1 + \delta_2\, \boldsymbol{S}_2\right) \times \boldsymbol{r}. \tag{4.51}$$

As can be seen from Fig. 4.1, $\boldsymbol{r}$ can be written,

$$\boldsymbol{r} = \begin{pmatrix} r\cos\varphi \\ r\sin\varphi \\ 0 \end{pmatrix}_n . \tag{4.52}$$

To get an explicit expression for $\dot{\boldsymbol{r}}$, we must take time derivative of $\boldsymbol{r}$ in the inertial frame, and bring it back to the non-inertial frame using the Euler matrix,

$$\dot{\boldsymbol{r}} = \begin{pmatrix} \dot{r}\,\cos\varphi - r\,\sin\varphi\,(\dot{\xi}_1\,\cos\xi_2 + \dot{\varphi}) \\ \dot{r}\,\sin\varphi + r\,\cos\varphi\,(\dot{\xi}_1\,\cos\xi_2 + \dot{\varphi}) \\ r\,(-\dot{\xi}_1\,\sin\xi_2\,\cos\varphi + \dot{\xi}_2\,\sin\varphi) \end{pmatrix}_n . \tag{4.53}$$

Now we have all ingredients (Eqs.(4.37) and (4.53)) to express the vector identity $\boldsymbol{L} = \boldsymbol{r}\times\boldsymbol{p}$ in non-inertial frame components,

$$\begin{pmatrix} 0 \\ 0 \\ L \end{pmatrix}_n = \boldsymbol{L} = \boldsymbol{r}\times\boldsymbol{p} = \begin{pmatrix} -\frac{D}{r}\,\sin\varphi \\ \frac{D}{r}\,\cos\varphi \\ r^2\,\frac{d\varphi}{dt} + r^2\,\cos\xi_2\,\dot{\xi}_1 - \frac{S1\,\delta_1\,\cos\kappa_1 + S2\,\delta_2\,\cos\kappa_2}{c^2\,r} \end{pmatrix}_n , \tag{4.54}$$

where

$$D = r^3\left(-\sin\varphi\,\dot{\xi}_2 + \sin\xi_2\,\cos\varphi\,\dot{\xi}_1\right) \tag{4.55}$$

$$-\frac{1}{c^2}\Bigg\{\cos\varphi\left(S_1\,\delta_1\,\sin\kappa_1\sin\xi_3 + S_2\,\delta_2\,\sin\kappa_2\,\sin(\xi_3+\Delta\psi)\right)$$

$$-\sin\varphi\left(S_1\,\delta_1\,\cos\xi_3\,\sin\kappa_1 + S_2\,\delta_2\,\cos(\xi_3+\Delta\psi)\,\sin\kappa_2\right)\Bigg\}. \tag{4.56}$$

Note that D trivially vanishes as Eq.(4.54) requires as Eq.(4.43) is satisfied.

The third component of $\boldsymbol{L}$ reads to the following equation

$$\begin{aligned}\frac{d\varphi}{dt} &= \frac{L}{r^2} + \frac{1}{c^2\, r^3}\,(S_1\,\delta_1\,\cos\kappa_1 + S_2\,\delta_2\,\cos\kappa_2) - \cos\xi_2\,\dot{\xi}_1\,, \\ &= \frac{L}{r^2}\,(1 - \frac{\delta_1+\delta_2}{c^2\, r}) + \frac{1}{c^2\, r^3}\,(\frac{\beta_1}{\alpha_1+\cos\kappa_1} + \frac{\beta_2}{\alpha_2+\cos\kappa_1})\,.\end{aligned} \tag{4.57}$$

For perturbatively consistent integration of $\frac{d\varphi}{dt}$, we need 1.5PN accurate r expression. It is because $\frac{d\varphi}{dt}$ depends on r from Newtonian order while we want to get φ with an accuracy of 1.5PN. For a moment, we need to find the Keplerian parametrization of r. Using $\boldsymbol{p}^2 = \dot{r}^2 + \frac{L^2}{r^2}$ and $H = E$,

$$\dot{r}^{\,2} = 2\,E + \frac{2}{r} - \frac{L^2}{r^2} - \frac{2\,(\boldsymbol{L}\cdot\boldsymbol{S}_{\rm eff})}{c^2\, r^3}\,. \tag{4.58}$$

Note that $\boldsymbol{L}\cdot\boldsymbol{S}_{\rm eff}$ is a constant with the following simplification

$$\begin{aligned}\boldsymbol{L}\cdot\boldsymbol{S}_{\rm eff} &= \boldsymbol{L}\cdot(\delta_1\,\boldsymbol{S}_1 + \delta_2\,\boldsymbol{S}_2) \\ &= \delta_1\,L\,S_1\,\cos\kappa_1 + \delta_2\,L\,S_2\,\cos\kappa_2 \\ &= \delta_2\,L\,S_2\,\sigma_2\,.\end{aligned} \tag{4.59}$$

Eq.(4.58) is easily integrated (Damour and Deruelle (1985)) and the radial motion is described, up to leading order of spin-orbit coupling, as

$$r = a_r\,(1 - e_r\,\cos u)\,, \tag{4.60a}$$

$$n\,(t - t_0) = u - e_t\,\sin u\,, \tag{4.60b}$$

where

$$a_r = -\frac{1}{2\,E}(1 - \frac{2\,\delta_2\,S_2\,\sigma_2}{L}\,\frac{E}{c^2})\,, \tag{4.60c}$$

$$n = (-2\,E)^{3/2}\,, \tag{4.60d}$$

$$e_r^2 = 1 + 2\,E\,L^2 + 8\,(1 + E\,L^2)\,\frac{\delta_2\,S_2\,\sigma_2}{L}\,\frac{E}{c^2}\,, \tag{4.60e}$$

$$e_t^2 = 1 + 2\,E\,L^2 + \frac{4\,\delta_2\,S_2\,\sigma_2}{L}\,\frac{E}{c^2}\,. \tag{4.60f}$$

Now let us go back to Eq.(4.57). We've already known that the integration of the second term of right hand side of Eq.(4.57) is the Elliptic integral of the thrid kind and the integration of the first term is easily done via Eq.(4.60),

$$\varphi - \varphi_0 = (1+k)\,\bar{\nu} + \frac{2\,\beta_1\,\Pi(\frac{x_2-x_3}{\alpha_1+x_2},\,\mathrm{am}(\Upsilon,\beta),\,\beta)}{\sqrt{A\,(x_1-x_2)}(\alpha_1+x_2)} + \frac{2\,\beta_2\,\Pi(\frac{x_2-x_3}{\alpha_2+x_2},\,\mathrm{am}(\Upsilon,\beta),\,\beta)}{\sqrt{A\,(x_1-x_2)}(\alpha_2+x_2)}\,, \tag{4.61a}$$

where

$$k = \frac{-1}{c^2\,L^2}\left(\delta_1 + \delta_2 + 3\frac{\delta_2\,S_2\,\sigma_2}{L}\right)\,, \tag{4.61b}$$

$$\bar{\nu} = 2\,\arctan\left(\sqrt{\frac{1+e_\varphi}{1-e_\varphi}}\,\tan\frac{u}{2}\right)\,, \tag{4.61c}$$

$$e_\varphi^2 = 1 + 2\,E\,L^2 + 4\,(\delta_1+\delta_2)\,(1+2\,E\,L^2)\,\frac{E}{c^2} + 4\,(3+4\,E\,L^2)\,\frac{\delta_2\,S_2\,\sigma_2}{L}\frac{E}{c^2}\,, \tag{4.61d}$$

and φ_0 is an initially given value.

In principle, we have all parametrizations for describing the Newtonian orbital motion with the leading order of spin-orbit coupling. In the inertial frame, it is written as

$$\boldsymbol{r} = r\begin{pmatrix} \cos\xi_1\,\cos\varphi - \sin\xi_1\,\cos\xi_2\,\sin\varphi \\ \sin\xi_1\,\cos\varphi + \cos\xi_1\,\cos\xi_2\,\sin\varphi \\ \sin\varphi\,\sin\xi_2 \end{pmatrix}_i\,. \tag{4.62}$$

4.4 Almost equal mass Approximation

In this section, we restrict our parametrizations in the case of $\delta_2 - \delta_1 \sim 0$, and provide the simpler version trucated at the order of $O((\delta_2-\delta_1)^2)$. Such a limiting case was considered by Tessmer (2009) but the result was not provided in a closed form. Here we provide it

only by elementary functions. In the exactly equal mass case, the solution was derived by Königsdörffer and Gopakumar (2005) analytically so that we have a chance to compare directly.

For the purpose of expansion for nearly same mass binaries, we choose a dimensionless parameter δ,

$$\delta := \delta_2 - \delta_1 = \frac{3}{2}\,\frac{m_1 - m_2}{M} \tag{4.63}$$

which is assumed to be non-negative (*i.e.* $m_1 \geq m_2$). The targeted approximant is achieved straightforwardly by changing of variable $\delta_2 \to \delta + \delta_1$ and expanding it in terms of δ up to the first order. We should be careful about the fact that, since $A\,(x-x_1)(x-x_2)(x-x_3)$ becomes the 2nd order polynomial in the case of equal mass, x_1 should blow up as $\delta \to 0$ and indeed by concrete calculation, it turns out that $x_1 = \frac{1}{\delta}\,\frac{\delta_1\left(S_1^2+2\sigma_1\,S_1\,S_2+S_2^2\right)}{2\,L\,S_1} + O(\delta^0)$. And we further find that

$$\frac{x_2 - x_3}{\alpha_1 + x_2} = -\delta\,\frac{2\,S_1\,S_2\,\sqrt{\left(1-\sigma_1^2\right)\left(S_1^2+2\sigma_1 S_1 S_2+\left(1-\sigma_2^2\right)S_2^2\right)}}{\delta_1\,\left(S_1^2+2\sigma_1 S_1 S_2+S_2^2\right)(J+L+\sigma_2 S_2)} + O(\delta^2)\,, \tag{4.64}$$

$$\frac{x_2 - x_3}{\alpha_2 + x_2} = -\delta\,\frac{2\,S_1\,S_2\,\sqrt{\left(1-\sigma_1^2\right)\left(S_1^2+2\sigma_1 S_1 S_2+\left(1-\sigma_2^2\right)S_2^2\right)}}{\delta_1\,\left(S_1^2+2\sigma_1 S_1 S_2+S_2^2\right)(-J+L+\sigma_2 S_2)} + O(\delta^2)\,, \tag{4.65}$$

$$\beta = \delta\,\frac{4\,L\,S_1\,S_2\,\sqrt{\left(1-\sigma_1^2\right)\,\left(S_1^2+2\sigma_1 S_1 S_2+\left(1-\sigma_2^2\right)S_2^2\right)}}{\delta_1\,\left(S_1^2+2\sigma_1 S_1 S_2+S_2^2\right)^2} + O(\delta^2)\,. \tag{4.66}$$

In order to get the Keplerian parametrizations for ξ_1 and φ expanded up to the first order in δ, it is essential to get the first order approximant of the type $\Pi(\mathcal{A},\,\mathrm{am}(\Upsilon,\beta),\,\beta)$. With $\mathcal{A} \sim O(\delta^1)$, $\beta \sim O(\delta^1)$ and $\Upsilon \sim O(\delta^0)$, we have

$$\Pi(\mathcal{A},\,\mathrm{am}(\Upsilon,\beta),\,\beta) = \left(1+\frac{\mathcal{A}}{2}\right)\,\Upsilon - \frac{\mathcal{A}}{4}\,\sin 2\Upsilon + O(\delta^2)\,. \tag{4.67}$$

Then it staightforwardly follows that

$$\xi_1 - \xi_{1(0)} = \Xi_1\,\hat{\Upsilon} + \,\Xi_2\,\sin 2\hat{\Upsilon} + O(\delta^2)\,, \tag{4.68}$$

where

$$\Xi_1 = \frac{2J}{\sqrt{S_1^2 + 2\sigma_1 S_1 S_2 + S_2^2}} + \delta \frac{2\,J\,S_2\,(\sigma_1 S_1 + S_2)}{\delta_1\left(S_1^2 + 2\sigma_1\,S_1\,S_2 + S_2^2\right)^{3/2}}\,, \tag{4.69}$$

$$\Xi_2 = -\delta \frac{J\,\sqrt{1-\sigma_1^2}\,S_1\,S_2^2\,\sigma_2}{\delta_1\,(S_1^2 + 2\sigma_1\,S_1\,S_2 + S_2^2)^{3/2}\sqrt{S_1^2 + 2\,\sigma_1\,S_1\,S_2 + (1-\sigma_2^2)\,S_2^2}}\,, \tag{4.70}$$

and $\hat{\Upsilon}$ is the truncated one,

$$\hat{\Upsilon} = \alpha + \frac{\delta_1\,\sqrt{S_1^2 + S_2^2 + 2\,S_1\,S_2\,\sigma_1}}{2\,c^2\,L^3}\,(\nu + e\,\sin\nu). \tag{4.71}$$

Similarly, Eq.(4.61a) is expanded to

$$\varphi - \varphi_0 = (1+\hat{k})\,\hat{\nu} + \Phi_1\,\hat{\Upsilon}\;+\;\Phi_2\,\sin 2\hat{\Upsilon} + O(\delta^2)\,, \tag{4.72}$$

where

$$\Phi_1 = \frac{2L}{\sqrt{S_1^2 + 2\sigma_1 S_1 S_2 + S_2^2}} + \delta \frac{2\,L\,S_1\,(S_1 + \sigma_1 S_2)}{\delta_1\,\left(S_1^2 + 2\sigma_1 S_1 S_2 + S_2^2\right)^{3/2}}\,, \tag{4.73a}$$

$$\Phi_2 = \delta \frac{(J^2 - L^2 - L\,S_2\,\sigma_2)\,\sqrt{1-\sigma_1^2}\,S_1\,S_2}{\delta_1\,(S_1^2 + 2\sigma_1\,S_1\,S_2 + S_2^2)^{3/2}\sqrt{S_1^2 + 2\,\sigma_1\,S_1\,S_2 + (1-\sigma_2^2)\,S_2^2}}\,, \tag{4.73b}$$

$$\hat{k} = -\frac{\delta_1\,(2\,L + 3\,\sigma_2\,S_2)}{c^2 L^3} + \delta\,\frac{(-L - 3\,\sigma_2\,S_2)}{c^2 L^3}\,, \tag{4.73c}$$

$$\begin{aligned}\hat{e}^{\,2} &= 1 + 2\,E\,L^2 + \frac{4\delta_1\,E\,\left(4\,E\,L^3 + 4\,E\,L^2\sigma_2 S_2 + 2L + 3\sigma_2 S_2\right)}{c^2 L} \\ &\quad + \delta\,\frac{4\,E\,\left(2\,E\,L^3 + 4\,E\,L^2\sigma_2 S_2 + L + 3\sigma_2 S_2\right)}{c^2 L}\,,\end{aligned} \tag{4.73d}$$

with $\hat{\nu} = 2\,\arctan\left(\sqrt{\frac{1+\hat{e}}{1-\hat{e}}}\,\tan\frac{u}{2}\right)$. Note that $\hat{k}$, $\hat{e}$ are just approximants of k and e_φ in Eqs.(4.61) truncated at the order of $O(\delta^2)$.

4.4.1 Equal mass binaries limit

From this we can easily compare the leading terms with the results of Königsdörffer and Gopakumar (2005), which deals with equal mass case. By setting $\delta = 0$, the expression for

ξ_1 becomes,

$$\xi_1 - \xi_{1(0)} = \frac{J\,\delta_1}{c^2\,L^3}\,(\nu + e\,\sin\nu)\,. \tag{4.74}$$

Similarly,

$$\begin{aligned}\varphi - \varphi_0 = &\left(1 - \frac{\delta_1\,(2L + 3\,S_2\,\sigma_2)}{c^2\,L^3}\right)\,\hat{\nu}\,|_{\delta=0} \\ &+ \frac{\delta_1}{c^2\,L^2}\,(\nu + e\,\sin\nu)\,.\end{aligned} \tag{4.75}$$

Since the followings hold perturbatively,

$$\begin{aligned}&2\arctan\left(a\,(1+b)\right) \\ =&2\arctan\left(a\right) + b\,\sin\left(2\arctan\left(a\right)\right) + O(b^2)\,,\end{aligned} \tag{4.76}$$

and

$$\begin{aligned}&\sqrt{\frac{1+(a+b)}{1-(a+b)}} \\ =&\sqrt{\frac{1+a}{1-a}}\,\left(1 + \frac{b}{1-a^2}\right) + O(b^2)\end{aligned} \tag{4.77}$$

we can make some part of φ more compact by introducing

$$\begin{aligned}\bar{\nu}' &:= \hat{\nu}\,|_{\delta=0} + \frac{\delta_1}{c^2\,L^2}\,e\,\sin\nu \\ &=\,2\,\arctan\left(\sqrt{\frac{1+\hat{e}}{1-\hat{e}}}\,\tan\frac{u}{2}\,(1 + \frac{\delta_1}{c^2\,L^2}e)\right) + O(\frac{1}{c^4})\,, \\ &=:\,2\,\arctan\left(\sqrt{\frac{1+e'}{1-e'}}\,\tan\frac{u}{2}\right) + O(\frac{1}{c^4})\,.\end{aligned} \tag{4.78}$$

Now we arrive the compact form in the accuracy of $O(\frac{1}{c^4})$ such that

$$\varphi - \varphi_0 = (1 + k')\,\bar{\nu}' + O(\frac{1}{c^4}), \tag{4.79}$$

where

$$k' = -\frac{\delta_1}{c^2\,L^2}\,(1+3\frac{S_2\,\sigma_2}{L})\,, \tag{4.80a}$$

$$\bar{\nu}' = 2\,\arctan\left(\sqrt{\frac{1+e'}{1-e'}}\,\tan\frac{u}{2}\right)\,, \tag{4.80b}$$

$$e'^{\,2} = 1+2\,E\,L^2+4\,\delta_1\,(1+2\,E\,L^2)\frac{E}{c^2} \tag{4.80c}$$

$$+\,4\,(3+4\,E\,L^2)\frac{\delta_1\,S_2\,\sigma_2}{L}\,\frac{E}{c^2}\,.$$

These results are coincident with the results of Königsdörffer and Gopakumar (2005).

4.5 Conclusion

We have solved the spin precession equation and the Newtonian orbital motion in ADM gauge for binary system with arbitrary spins, mass ratio and eccentricity up to leading order of spin orbit coupling. We arrived at quasi-Keplerian parametric solutions in a simple closed form. The elliptic functions are essential in our parametrizations and they have been thoroughly speculated by mathematicians. So our solutions are expected to give us systematic and mathematically deep understandings on how rotating bodies move in gravitational field. On the other hand, numerical computations for the elliptic functions are rather expensive compared to the elementary functions. However, our rough numercial estimations suggest that a couple of the constants defined in this paper such as β, $\frac{x_2-x_3}{\alpha_1+x_2}$ tend to be very small in almost all initial configurations, implying that we would be able to re-express the elliptic functions in terms of the elementary functions without significant numercial errors. This could be our future work.

We also expect that the solutions presented here can be directly used to get efficient ready-to-use time domain gravitational waveform templates modulated by spin precession and swings of orbital plane, which would be useful in analyzing the gravitational wave data. Furthermore, the result of this paper will provide useful knowledges to com-

plete phenomenological models such as *effective-one-body* which requires both numerical calibrations and analytic solutions.

Chapter 5

Quasi-Keplerian parametrization of Hyperbolic Encounter[1]

5.1 Introduction

Interesting astrophysical scenarios involving strong gravitational fields usually require accurate and efficient ways of describing orbital dynamics of compact binaries. These scenarios include gravitational wave (GW) events, observed by the advanced LIGO -Virgo interferometers Abbott et al. (2016a), labeled GW150914, GW151226, GW170104, GW170608, GW170814, and GW170817 Abbott et al. (2016c,b, 2017a,b,c,d). The first five are associated with the coalescence of black hole (BH) binaries while GW170817 involved a merging neutron star binary. Orbital dynamics of compact binaries inspiraling due to the emission of GWs can be accurately described by the PN approximation to general relativity Blanchet (2014). In this approximation, orbital dynamics of non-spinning compact binaries is provided as corrections to Newtonian equations of motion in powers of $(v/c)^2 \sim G\,m/(c^2\,r)$, where v, m, and r are the velocity, total mass and relative separa-

[1] This chapter was published in Cho et al. (2018).

tion of the binary. At present, conservative orbital dynamics of compact binaries have been computed to the fourth PN order which provides $(v/c)^8$ accurate general relativity based corrections to Newtonian description (see for examples Porto and Rothstein (2017); Damour and Jaranowski (2017); Foffa et al. (2017); Bernard et al. (2017); Damour et al. (2016) and their many references for a glimpse of this herculean effort from various approaches). Interestingly, it is possible to obtain a Keplerian-type parametric solution to PN-accurate orbital dynamics of compact binaries in non-circular orbits. This was demonstrated by Damour and Deruelle for 1PN-accurate compact binary orbital dynamics, relevant for both eccentric and hyperbolic orbits Damour and Deruelle (1985). They introduced three eccentricities so that the parametrization looks 'Keplerian' even at 1PN order. These computations were extended to 2PN and 3PN orders by Schäfer and his collaborators which led to the generalized quasi-Keplerian parametric solution for compact binaries in precessing eccentric orbits Damour and Schafer (1988); Schäfer and Wex (1993); Memmesheimer et al. (2004). This solution plays an important role in the on-going efforts to model GWs from merging BH binaries in eccentric orbits Hinder et al. (2010); Huerta et al. (2017). This is due to the use of certain GW phasing formalism, developed in Damour et al. (2004); Königsdörffer and Gopakumar (2006), for describing the inspiral part of eccentric binary coalescence. This formalism employs Keplerian-type parametric solution to model orbital and periastron precession timescale variations present in the two GW polarization states $h_+(t)$ and $h_\times(t)$. These features are crucial to obtain $h_+(t)$ and $h_\times(t)$ from compact binaries inspiraling along PN-accurate eccentric orbits in an accurate and efficient manner Tanay et al. (2016). Additionally, high precision radio observations of binary pulsars employ an accurate relativistic 'timing formula' Damour and Deruelle (1986); Damour and Taylor (1992) which requires 1PN-accurate Keplerian type parametric solution for compact binaries moving in precessing eccentric orbits Damour and Deruelle (1985). This timing formula is crucial to test both the predictions of general relativity and the viability of alternate theories of gravity in strong field situations present in our

galaxy Stairs (2003). In this chapter, we derive from first principles parametric solution to 3PN accurate conservative orbital dynamics of compact binaries moving in hyperbolic orbits. This parametric solution is given both in Arnowitt, Deser, and Misner (ADM)-type and modified harmonic (MH) coordinates. The reason that we adpat both gauges is that ADM is useful for comparing with numerical data from numerical relativity (NR) simulations which make use of ADM formalism, and MH is proper for constructing GW waveforms. The associated orbital elements and functions are provided as PN-accurate functions of the conserved orbital energy, angular momentum and the symmetric mass ratio. The correctness of our solutions is verified by comparing 3PN-accurate expressions for the radial and angular velocities arising from our solutions with their counterparts, computed directly from the orbital dynamics. Additionally, we develop a modified analytic continuation prescription to obtain our 3PN-accurate Keplerian type parametric solution for hyperbolic orbits from its eccentric versions, available in Memmesheimer et al. (2004). This is a desirable feature as we are essentially providing an additional test on the correctness of lengthy expressions present in Memmesheimer et al. (2004) which are, as noted earlier, required to construct templates for eccentric inspirals. We also obtain temporally evolving GW polarization states for compact binaries in 3.5PN-accurate hyperbolic orbits. This is achieved by allowing orbital elements and functions of our 3PN accurate Keplerian type parametric solution to vary due to 1PN-accurate radiation reaction effects, relevant for hyperbolic orbits Königsdörffer and Gopakumar (2006); De Vittori et al. (2014). Our efforts are motivated by the observation that compact binaries in unbound orbits are plausible GW sources for both the ground and space based GW observatories. It turned out that such rare events are expected to occur in globular clusters and galactic nuclear clusters or plausibly in dense clusters of primordial black holes Kocsis et al. (2006); García-Bellido and Nesseris (2018). Moreover, hyperbolic encounters may create bound binaries having very high eccentricities Hansen (1972); Walker and Will (1979). It was argued that plausible detection rates for such eccentric binaries may become comparable to that for

isolated compact binary coalescences O'Leary et al. (2009). Interestingly, such hyperbolic GW events involving neutron stars may even be accompanied by electro-magnetic flares Tsang (2013). The present effort should provide accurate gravitational waveforms for hyperbolic passages that can be adapted in to the LSC Algorithm Library Suite of the LIGO Scientific Collaboration.

5.2 Derivation of Keplerian type parametric solution for compact binaries in hyperbolic orbits

We first provide detailed derivation of 1PN-accurate Keplerian type parametric solution for compact binaries in hyperbolic orbits. This procedure explicitly demonstrates why one requires three eccentricities to obtain the desired solution, computed by employing certain analytic continuation arguments in Damour and Deruelle (1985). The 3PN extension of Sec. 5.2.1 is detailed in Sec. 5.2.2.

5.2.1 1PN-accurate qusi-Keplerian parametrization for hyperbolic orbits

We begin by displaying 1PN-accurate expressions for the radial and angular motion

$$\left(\frac{dr}{dt}\right)^2 = a_0 + a_1\, s + a_2\, s^2 + a_3\, s^3\,, \tag{5.1a}$$

$$\frac{d\phi}{dt} = d_0\, s^2 + d_1\, s^3\,, \tag{5.1b}$$

where both radial and temporal variables are scaled by $G\,m$ Damour and Deruelle (1985). This allows us to introduce a variable $s = 1/r$ where $r = |\boldsymbol{R}|/(G\,m)$ and $\boldsymbol{R}$ is the relative separation vector such that $\boldsymbol{R} = R\,(\cos\phi, \sin\phi, 0)$. The constant coefficients, a_0, a_1, a_2, a_3, d_0 and d_1, are given in terms of certain conserved orbital energy ($\tilde{E}$) and

angular momentum ($\tilde{J}$) as

$$a_0 = \frac{2\tilde{E}}{\mu} + \frac{1}{c^2}\frac{(2\tilde{E})^2}{\mu^2}\frac{-3+9\eta}{4}\,, \tag{5.2a}$$

$$a_1 = 2 - \frac{1}{c^2}\frac{2\tilde{E}}{\mu}(6-7\eta)\,, \tag{5.2b}$$

$$a_2 = -\frac{\tilde{J}^2}{G^2m^2\mu^2} - \frac{1}{c^2}\Big(\frac{2\tilde{E}\tilde{J}^2}{G^2m^2\mu^3}(3\eta-1) + (-10+5\eta)\Big)\,, \tag{5.2c}$$

$$a_3 = \frac{1}{c^2}\frac{\tilde{J}^2}{G^2m^2\mu^2}(8-3\eta)\,, \tag{5.2d}$$

$$d_0 = \frac{\tilde{J}}{Gm\mu} + \frac{1}{c^2}\frac{2\tilde{E}\tilde{J}}{G^2m^2\mu^3}\frac{-1+3\eta}{2}\,, \tag{5.2e}$$

$$d_1 = \frac{1}{c^2}\frac{\tilde{J}}{Gm\mu}(-4+2\eta)\,, \tag{5.2f}$$

where $\tilde{E}$ and $\tilde{J}$ stand for the 1PN-accurate conserved orbital energy and angular momentum while μ and η denote the usual reduced mass and symmetric mass ratio. It should be obvious that these coefficients take simpler forms in terms certain reduced orbital energy and angular momentum variables, defined as $E = \tilde{E}/\mu, h = \tilde{J}/(G\,m\,\mu)$. Additionally, we let $E > 0$ as we are interested in hyperbolic orbits in this paper.

Influenced by Damour and Deruelle (1985), wee tackle the radial motion by introducing certain *conchoidal* transformation

$$r = \bar{r} + \frac{a_3}{2\,a_2'} \tag{5.3}$$

where $\frac{a_3}{2\,a_2'} \sim O(\frac{1}{c^2})$ and $\lim_{c\to 0} a_2'$ gives a_2. It is fairly straightforward to recast the above radial equation in terms of $\bar{r}$ as

$$\begin{aligned}\left(\frac{d\bar{r}}{dt}\right)^2 &= a_0 + \frac{a_1}{\bar{r}} + \frac{a_2}{\bar{r}^2} - \frac{a_1a_3}{2\bar{r}^2} - \frac{a_3}{\bar{r}^3} + \frac{a_3}{\bar{r}^3} + O(\frac{1}{c^4})\,,\\ &= a_0 + \frac{a_1}{\bar{r}} + \frac{\bar{a}_2}{\bar{r}^2} + O(\frac{1}{c^4})\,,\end{aligned} \tag{5.4}$$

where $\bar{a}_2 = a_2 - \frac{a_1 a_3}{2a_2'}$ while consistently neglecting terms $\mathcal{O}(\frac{1}{c^4})$. To solve the above equation, we introduce an angular parameter u such that

$$\frac{du}{dt} = \frac{1}{a_4\,\bar{r}} > 0 \quad ; \quad a_4 > 0. \tag{5.5}$$

This leads to

$$\left(\frac{d\bar{r}}{du}\right)^2 = a_4^2\left(a_0\bar{r}^2 + a_1\bar{r} + \bar{a}_2\right)\,. \tag{5.6}$$

Clearly, we require $(a_0\,\bar{r}^2 + a_1\,\bar{r} + a_2') > 0$ and this allows us to write

$$\begin{aligned} \pm a_4\,du &= \frac{d\bar{r}}{\sqrt{a_0\bar{r}^2 + a_1\bar{r} + \bar{a}_2}} \\ &= \frac{d\bar{R}}{\sqrt{\bar{a}_2 - \frac{a_1^2}{4a_0} + a_0(\bar{r} + \frac{a_1}{2a_0})^2}}\,. \end{aligned} \tag{5.7}$$

For hyperbolic motion, we observe that $\left(\bar{a}_2 - a_1^2/(4\,a_0)\right)$ is indeed negative. Therefore, we re-write this equation as

$$\pm a_4\left(\sqrt{-\bar{a}_2 + \frac{a_1^2}{4a_0}}\right)\,du = \frac{d\bar{r}}{\sqrt{-1 + \frac{4a_0^2}{a_1^2 - 4\bar{a}_2 a_0}(\bar{r} + \frac{a_1}{2a_0})^2}}\,. \tag{5.8}$$

We now introduce u' such that $\cosh u' = \sqrt{\frac{4a_0^2}{a_1^2 - 4\bar{a}_2 a_0}}(\bar{r} + \frac{a_1}{2a_0})$ which allows us to write the above equation as

$$\pm a_4\,\sqrt{a_0}du = du'\,. \tag{5.9}$$

We let $a_4 = \frac{1}{\sqrt{a_0}}$ to ensure that $\cosh u' = \cosh(\pm u) = \cosh u$. This leads to the following equations for $\bar{r}$ and therefore r:

$$\bar{r} = -\frac{a_1}{2a_0} + \sqrt{\frac{a_1^2 - 4\bar{a}_2 a_0}{4a_0^2}}\,\cosh u\,, \tag{5.10a}$$

$$r = -\frac{a_1}{2a_0} + \frac{a_3}{2a_2'} + \sqrt{\frac{a_1^2 - 4\bar{a}_2 a_0}{a_0^2}}\,\cosh u\,,$$

$$= \left(\frac{a_1}{2a_0} - \frac{a_3}{2a_2'}\right) \left\{-1 + \left(\frac{a_1}{2a_0} - \frac{a_3}{2a_2'}\right)^{-1} \times \sqrt{\frac{a_1^2 - 4\bar{a}_2 a_0}{4a_0^2}} \cosh u \right\}. \tag{5.10b}$$

We now we identify $\left(\frac{a_1}{2a_0} - \frac{a_3}{2a_1'}\right)$ with a_r and the coefficient of $\cosh u$ with e_r. The 1PN-accurate expression for e_r is therefore given by

$$e_r = \left(\frac{a_1}{2a_0} - \frac{a_3}{2a_2'}\right)^{-1} \sqrt{\frac{a_1^2 - 4\bar{a}_2 a_0}{a_1^2}}\,,$$
$$= (1 + \frac{a_0 a_3}{a_1 a_2'})\sqrt{1 - \frac{4\bar{a}_2 a_0}{a_1^2}} + O(\frac{1}{c^3})\,. \tag{5.11}$$

Invoking Eqs. (5.2), the parametric equation for r may be summarized as

$$r = a_r\ (e_r\ \cosh u - 1)\ , \tag{5.12a}$$

$$a_r = \frac{1}{2E} + \frac{1}{c^2}(\frac{7}{4} - \frac{\eta}{4})\,, \tag{5.12b}$$

$$e_r^2 = 1 + 2Eh^2 + \frac{1}{c^2}(2E)\big(-44 + 19\eta + 2Eh^2(\frac{1}{2} - \frac{\eta}{2})\big)\,, \tag{5.12c}$$

We have verified that expressions for a_r is identical to Eq. (7.4) in Damour and Deruelle (1985), obtained by invoking the argument of analytic continuation.

To obtain 1PN accurate Kepler equation, we turn to Eq. (5.5) for the angular variable u and integrate it to obtain

$$\sqrt{a_0}(t - t_0) = \int \bar{r} du\,,$$
$$= \int du \left\{-\frac{a_1}{2a_0} + \sqrt{\frac{a_1^2 - 4\bar{a}_2 a_0}{4a_0^2}} \cosh u\right\}, \tag{5.13}$$
$$= \left(-\frac{a_1}{2a_0} u + \sqrt{\frac{a_1^2 - 4\bar{a}_2 a_0}{4a_0^2}} \sinh u\right).$$

It is straightforward to re-write the above equation in the more familiar form,namely

$$n(t-t_0) = e_t \sinh u - u\,, \quad \text{where} \tag{5.14a}$$

$$n = \frac{2a_0^{\frac{3}{2}}}{a_1}\,, \tag{5.14b}$$

$$e_t = \sqrt{1 - \frac{4\bar{a}_2 a_0}{a_1^2}}\,. \tag{5.14c}$$

Using Eqs. (5.2), we can express these orbital elements in terms of the conserved E, h and η as

$$n = (2E)^{\frac{3}{2}} + \frac{1}{c^2}(2E)^{\frac{5}{2}}\frac{15-\eta}{8}\,, \tag{5.15a}$$

$$\begin{aligned} e_t^2 &= 1 + 2Eh^2 \\ &\quad + \frac{1}{c^2}(2E)\big(-18 + 8\eta + 2Eh^2(\frac{17}{4} - \eta\frac{7}{4})\big)\,. \end{aligned} \tag{5.15b}$$

The above expressions are also identical to those given in Damour and Deruelle (1985). We are now in a position to deal with the angular motion. Influenced by Damour and Deruelle (1985), we take another conchoidal transformation

$$\tilde{r} = r - \frac{d_1}{2d_0}\,. \tag{5.16}$$

With the help of our expression for r, we have

$$\tilde{r} = \tilde{a}(\tilde{e}\cosh u - 1)\,, \tag{5.17}$$

where $\tilde{a} = a_r - \frac{d_1}{2d_0}$ and $\tilde{e} = \frac{a_r e_r}{\tilde{a}}$. In terms of $\tilde{r}$, the 1PN-accurate equation for the angular motion, given in Eqs. (5.1), takes the simpler Newtonian form:

$$\frac{d\phi}{dt} = \frac{d_0}{\tilde{r}^2}\,. \tag{5.18}$$

With the help of our 1PN-accurate Kepler Equation, this leads to

$$\frac{d\phi}{du} = \frac{d_0}{n\,\tilde{a}^2}\frac{(e_t\cosh u - 1)}{(\tilde{e}\cosh u - 1)^2}\,. \tag{5.19}$$

We introduce $e_\phi = 2\,\tilde{e} - e_t$ and this allows us to simplify $(e_t \cosh u - 1)/((\tilde{e}\cosh u - 1)^2)$ to $1/(e_\phi \cosh u - 1)$ modulo the neglected $\mathcal{O}(1/c^4)$ terms. Integrating the resulting $d\phi/du = d_0/(n\,\tilde{a}^2\,(e_\phi \cosh u - 1))$ expression gives us

$$\begin{aligned}
\phi - \phi_0 &= \frac{d_0}{n\tilde{a}^2} \int \frac{du}{e_\phi \cosh u - 1}\,, \\
&= \frac{d_0}{n\tilde{a}^2} \int \frac{du}{(e_\phi - 1)\cosh^2 \frac{u}{2} + (e_\phi + 1)\sinh^2 \frac{u}{2}}\,, \\
&= \frac{d_0}{n\left(\sqrt{e_\phi^2 - 1}\right)\,\tilde{a}^2} \int \frac{du \sqrt{\frac{e_\phi+1}{e_\phi-1}} \frac{1}{\cosh^2 \frac{u}{2}}}{1 + \frac{e_\phi+1}{e_\phi-1}\tanh^2 \frac{u}{2}}\,, \\
&= \frac{d_0}{n\,\tilde{a}^2\,\sqrt{e_\phi^2 - 1}}\, 2 \arctan\Big(\sqrt{\frac{e_\phi + 1}{e_\phi - 1}} \tanh \frac{u}{2}\Big)\,. \qquad (5.20)
\end{aligned}$$

We now introduce K such that

$$\phi - \phi_0 = K \times 2 \arctan\Big(\sqrt{\frac{e_\phi + 1}{e_\phi - 1}} \tanh \frac{u}{2}\Big)\,, \quad \text{where} \qquad (5.21a)$$

$$K = \frac{d_0}{n\,\tilde{a}^2\,\sqrt{e_\phi^2 - 1}}\,, \qquad (5.21b)$$

It is straightforward to express K and e_ϕ in terms of the conserved quantities like E and h and we have

$$K = 1 + \frac{1}{c^2}\frac{34 - 15\eta + (2Eh^2)(-8 + 3\eta)}{2h^2}\,, \qquad (5.22a)$$

$$\begin{aligned}
e_\phi^2 &= 1 + 2Eh^2 \qquad (5.22b) \\
&\quad + \frac{1}{c^2}(2E)\Big(-34 + 15\eta + 2Eh^2\big(\frac{-47}{4} + \frac{21}{4}\eta\big)\Big)\,.
\end{aligned}$$

We have verified that Eqs. (5.12), (5.14, (5.15), (5.21) and (5.22) indeed are identical to their counterparts in Damour and Deruelle (1985), obtained by invoking the arguments of analytic continuation. In the next subsection, we extend these calculations to 3PN order.

5.2.2 3PN-accurate qusi-Keplerian parametrization for hyperbolic orbits

The plan is to derive from first principles a 3PN-accurate Keplerian-type parametric solution for compact binaries in hyperbolic orbits. We are attempting the 3PN extension of Sec. 5.2.1, as it is not straightforward to obtain a hyperbolic version of the 3PN-accurate generalized quasi-Keplerian parametrization for compact binaries in eccentric orbits, detailed in Memmesheimer et al. (2004), simply by invoking the analytic continuation arguments of Damour and Deruelle (1985). The main difficulty with analytic continuation is due to the structure of 3PN-accurate (eccentric) Kepler Equation, given by Eq. (19b) in Memmesheimer et al. (2004), which reads

$$\begin{aligned} l \equiv \quad & n'\,(t-t_0) = u' - e_t\,\sin u' + \left(\frac{g_{4t'}}{c^4}+\frac{g_{6t'}}{c^6}\right)\,(v'-u') \\ & + \left(\frac{f_{4t'}}{c^4}+\frac{f_{6t'}}{c^6}\right)\,\sin v' + \frac{i_{6t'}}{c^6}\,\sin 2\,v' + \frac{h_{6t'}}{c^6}\,\sin 3\,v'\,, \end{aligned} \tag{5.23}$$

where n', u' and v' stand for the mean motion, eccentric and true anomalies of an eccentric orbit, and where the orbital functions $g_{4t'}$, $g_{6t'}$, $f_{4t'}$, $f_{6t'}$, $i_{6t'}$, $h_{6t'}$ are PN-accurate functions of the conserved energy, angular momentum and the symmetric mass ratio η. It is customary to employ the following exact expression for $(v'-u')$, derived in Königsdörffer and Gopakumar (2006):

$$v'-u' = 2\tan^{-1}\left(\frac{\beta'_\phi\sin u'}{1-\beta'_\phi\cos u'}\right)\,, \tag{5.24}$$

where $\beta'_\phi = (1-\sqrt{1-e_\phi^2})/e_\phi$. A close inspection reveals that it is certainly problematic to apply the usual analytic continuation arguments of Damour and Deruelle (1985), namely, to let $u' \to \imath v$ and allow $\sqrt{-E} \to \imath\sqrt{E}$ to obtain the hyperbolic version of an exact expression for $v'-u'$. Additionally, the presence of $(-2\,E\,h^2)^{\frac{1}{2}}$ and its multiples in the explicit expressions for $n', g_{4t'}$ and $g_{6t'}$, as given by Eqs. (20) of Memmesheimer et al. (2004), introduces further complications while trying to achieve hyperbolic versions

of these expressions.

These considerations prompted us to obtain hyperbolic versions of Eqs. (19), (20) and (21) of Memmesheimer et al. (2004) (describing the radial and angular motion in an eccentric binary, as well as the Kepler equation) with the help of ab-initio computations. It turned out that these detailed computations enabled us to devise a modified version of the standard analytic continuation arguments, in order to extract hyperbolic counterparts of the expressions in Memmesheimer et al. (2004). This allowed us to check the correctness of our computations and to confirm the validity of Memmesheimer et al. (2004). An additional way of checking the lengthy expressions in Memmesheimer et al. (2004) is highly desirable, as this work is usually invoked for the GW phasing of compact binaries inspiraling along eccentric orbits.

We begin by tackling the hyperbolic radial part of the 3PN-accurate Keplerian-type parametric solution. The input for our calculation is the following 3PN-accurate expression for $\dot{r}^2$, symbolically written as

$$\begin{aligned}\dot{r}^2 \equiv& \frac{1}{s^4}\left(\frac{ds}{dt}\right)^2 \\ =& a_0 + a_1 s + a_2 s^2 + a_3 s^3 + a_4 s^4 + a_5 s^5 + a_6 s^6 + a_7 s^7 \,,\end{aligned} \tag{5.25}$$

where explicit functional forms of the coefficients a_i are given by Eqs. (A1) and (A3) of Memmesheimer et al. (2004), for the ADM-type and modified harmonic gauges, respectively. We observe that in the Newtonian limit the right hand side of Eq. (5.25) is a second order polynomial in s and therefore admits two roots. It is straightforward to obtain 3PN-accurate versions of these two real-valued roots, even in the case of hyperbolic orbits. Subsequently, we factorize the 3PN-accurate expression for $\dot{r}^2$ with the help of the two roots s_+ and s_-. This leads to

$$(t - t_0) = \int \frac{ds\ \left(b_0 + b_1 s + b_2 s^2 + b_3 s^3 + b_4 s^4 + b_5 s^5\right)}{s^2\sqrt{(s_+ - s)(s - s_-)}} \,, \tag{5.26}$$

where we used the parametric equation $r = a_r(e_r \cosh u - 1)$. The explicit functional forms for the coefficients b_i may be found in Eqs. (A2) and (A4) of Memmesheimer et al. (2004).

Note the factorization of the denominator and how it differs from Eq. (9) of Memmesheimer et al. (2004). This is because for hyperbolic orbits we find the roots $s_+ > 0$ and $s_- < 0$, which allows us to introduce $r = a_r(e_r \cosh u - 1)$. The above integral leads to

$$\begin{aligned} t - t_0 = {} & c_0' \, (e_r \sinh u - u) + c_1' \, u + \frac{c_2' \, \nu'}{\sqrt{e_r^2 - 1}} \\ & + \frac{c_3'}{(e_r^2-1)^{3/2}} \left(\nu' + e_r \sin \nu' \right) \\ & + \frac{c_4'}{(e_r^2-1)^{5/2}} \left(\frac{e_r^2+2}{2} \nu' + 2 e_r \sin \nu' + \frac{e_r^2}{4} \sin 2\nu' \right) \\ & + \frac{c_5'}{(e_r^2-1)^{7/2}} \left[(1 + \frac{3e_r^2}{2}) \nu' + (3e_r + \frac{3}{4} e_r^3) \sin \nu' \right. \\ & \left. + \frac{3e_r^2}{4} \sin 2\nu' + \frac{e_r^3}{12} \sin 3\nu' \right] , \end{aligned} \tag{5.27}$$

where $c_i' = b_i / (a_r^{i-1} \sqrt{-s_+ \, s_-})$ and $\nu' = 2 \frac{1}{\sqrt{e_r^2-1}} \arctan(\sqrt{\frac{e_r+1}{e_r-1}} \tanh \frac{u}{2})$. The above equation can be re-written as

$$\begin{aligned} t - t_0 = {} & c_0 \sinh u - c_1 \, u + c_2 \nu' + c_3 \sin \nu' \\ & + c_4 \sin 2\nu' + c_5 \sin 3\nu' \, , \end{aligned} \tag{5.28}$$

with explicit relations between the coefficients c_is and c_i's given in Sec. 5.6.

It is straightforward to deduce that the coefficient c_3 of $\sin \nu'$ in Eq. (5.28) begins at 1PN order. Therefore, the above result deviates from our 1PN-accurate Keplerian-type parametric solution, derived in the previous section. It turns out that a suitable change of the ν' variable can remedy this undesirable feature, which will be addressed later.

We turn our attention to the angular motion. The relevant ingredient of the calculation is $d\phi/ds = \dot{\phi}/\dot{s}$, which may be symbolically written as

$$\frac{d\phi}{ds} = - \frac{d_0 + d_1 s + d_2 s^2 + d_3 s^3 + d_4 s^4 + d_5 s^5}{\sqrt{(s_+ - s)(s - s_-)}} \, , \tag{5.29}$$

where the coefficients d_i are listed in Eqs. (A2) and (A4) in Memmesheimer et al. (2004) (there denoted as B_i), for ADM-type and modified harmonic gauges, respectively. This

leads to

$$\phi - \phi_0 = \int du \left(\frac{e'_0}{r} + \frac{e'_1}{r^2} + \frac{e'_2}{r^3} + \frac{e'_3}{r^4} + \frac{e'_4}{r^5} + \frac{e'_5}{r^6} \right), \tag{5.30}$$

where $e'_i = d_i/(a_r^{i+1}\sqrt{-s_+ s_-})$. The above expression can be integrated to obtain

$$\begin{aligned} \phi - \phi_0 = {} & e_0 \nu' + e_1 \sin \nu' + e_2 \sin 2\nu' + e_3 \sin 3\nu' \\ & + e_4 \sin 4\nu' + e_5 \sin 5\nu' \,. \end{aligned} \tag{5.31}$$

As expected, the coefficients e_i are certain PN-accurate expressions and are given as functions of e'_i in Sec. 5.6. We observe that the coefficient of $\sin \nu'$ in Eq. (5.31), namely e_1, begins at 1PN order. Therefore, the above functional form for the angular motion $\phi - \phi_0$ also deviates from our 1PN-accurate angular solution, given by Eq. (5.21).

It is possible to correct this undesirable feature by introducing a certain PN accurate true anomaly $\nu = 2 \arctan\left[\left(\frac{e_\phi + 1}{e_\phi - 1} \right)^{1/2} \tanh \frac{u}{2} \right]$, defined with the help of the *angular eccentricity* e_ϕ. This eccentricity parameter deviates from e_r at PN orders by yet to be computed PN corrections. It is easy to obtain the following 3PN accurate expression for ν' in terms of ν

$$\begin{aligned} \nu' = {} & \nu + (f' - \frac{f'^2}{2} + \frac{f'^3}{4}) \sin \nu \\ & + (\frac{f'^2}{4} - \frac{f'^3}{4}) \sin 2\,\nu + \frac{f'^3}{12} \sin 3\,\nu \,, \end{aligned} \tag{5.32}$$

where f' should provide PN corrections connecting e_ϕ and e_r. We invoke the above relation in our $\phi - \phi_0$, given by Eq. (5.31), and demand that there be no $\sin \nu'$ terms to 3PN order. The resulting 3PN-accurate parametric solution for the angular motion indeed reproduces Eq. (5.31) when restricted to 1PN order. This procedure uniquely provides the PN corrections that connect e_ϕ to e_r, and the resulting final parametrization for the angular motion reads

$$\frac{2\pi}{\Phi}(\phi - \phi_0) = \nu + (\frac{f_{4\phi}}{c^4} + \frac{f_{6\phi}}{c^6}) \sin 2\,\nu + (\frac{g_{4\phi}}{c^4} + \frac{g_{6\phi}}{c^6}) \tag{5.33}$$

$$\times \sin 3\,\nu + \frac{h_{6\phi}}{c^6}\sin 4\,\nu + \frac{i_{6\phi}}{c^6}\sin 5\,\nu\,.$$

We are now in a position to re-parametrize our 3PN accurate expression for $t - t_0$, given by Eq. (5.28), in terms of ν with a procedure similar to the one outlined above. This also ensures that we recover our Keplerian-type parametric expression for $l(u)$ at 1PN order. The improved expression for the 3PN-accurate Kepler equation reads

$$\begin{aligned}\frac{2\pi}{P}(t-t_0) =& e_t \sinh u - u + (\frac{f_{4t}}{c^4} + \frac{f_{6t}}{c^6})\,\nu + (\frac{g_{4t}}{c^4} \\ &+ \frac{g_{6t}}{c^6})\sin\nu + \frac{h_{6t}}{c^6}\sin 2\,\nu + \frac{i_{6t}}{c^6}\sin 3\,\nu\,.\end{aligned} \tag{5.34}$$

We observe that the transformation from ν' to ν ensures that the coefficients of ν terms appear only at the 2PN and 3PN orders.

Collecting various results, we display in full the third post-Newtonian accurate generalized quasi-Keplerian parametrization for compact binaries in hyperbolic orbits as

$$r = a_r\,(e_r\,\cosh u - 1)\,, \tag{5.35a}$$

$$\begin{aligned}\frac{2\pi}{P}(t-t_0) &= e_t \sinh u - u + (\frac{f_{4t}}{c^4} + \frac{f_{6t}}{c^6})\,\nu + (\frac{g_{4t}}{c^4} + \frac{g_{6t}}{c^6})\sin\nu \\ &+ \frac{h_{6t}}{c^6}\sin 2\,\nu + \frac{i_{6t}}{c^6}\sin 3\,\nu\,,\end{aligned} \tag{5.35b}$$

$$\begin{aligned}\frac{2\pi}{\Phi}(\phi-\phi_0) &= \nu + (\frac{f_{4\phi}}{c^4} + \frac{f_{6\phi}}{c^6})\sin 2\,\nu \\ &+ (\frac{g_{4\phi}}{c^4} + \frac{g_{6\phi}}{c^6})\sin 3\,\nu + \frac{h_{6\phi}}{c^6}\sin 4\,\nu + \frac{i_{6\phi}}{c^6}\sin 5\,\nu\,,\end{aligned} \tag{5.35c}$$

where $\nu = 2\,\tan^{-1}\left[\left(\frac{e_\phi+1}{e_\phi-1}\right)^{1/2}\tanh\frac{u}{2}\right]$. Note that the 3PN-accurate expressions for the orbital elements $a_r, e_r^2, P = 2\pi/n, e_t^2, \Phi$, and e_ϕ^2 and the orbital functions $g_{4t}, g_{6t}, f_{4t}, f_{6t}, i_{6t}, h_{6t}, f_{4\phi}, f_{6\phi}, g_{4\phi}, g_{6\phi}$ and $h_{6\phi}$ are functions of E, h and η. Their 3PN-accurate expressions in the modified harmonic coordinates arise from Eqs. (A3) and (A4) of Memmesheimer et al. (2004) and are

given by

$$
\begin{aligned}
a_r =& \frac{1}{(2\,E)}\Bigg\{1+\frac{(2\,E)}{4\,c^2}\,(7-\eta)+\frac{(2\,E)^2}{16c^4}\,\Bigg[(1+\eta^2)\\
&+\frac{1}{(2\,E\,h^2)}(64-112\,\eta)\Bigg]+\frac{(2\,E)^3}{192\,c^6}\,\Bigg[-3+3\,\eta-3\,\eta^3\\
&+\frac{1}{(2\,E\,h^2)}\left(768+\left(123\,\pi^2-\frac{215408}{35}\right)\eta+1344\,\eta^2\right)\\
&+\frac{1}{(2\,E\,h^2)^2}\left(6144+\left(-\frac{704096}{35}+492\,\pi^2\right)\eta+1728\,\eta^2\right)\Bigg]\Bigg\}, \qquad (5.36a)
\end{aligned}
$$

$$
\begin{aligned}
{e_r}^2 =& 1+2\,E\,h^2+\frac{(2\,E)}{4\,c^2}\Big\{-24+4\,\eta+5\;(-3+\eta)\,(2\,E\,h^2)\Big\}\\
&+\frac{(2\,E)^2}{8\,c^4}\Big\{60+148\,\eta+2\,\eta^2+\left(80-45\,\eta+4\,\eta^2\right)(2\,E\,h^2)\\
&+\frac{8}{(2\,E\,h^2)}\,(-16+28\,\eta)\Big\}+\frac{(2\,E)^3}{6720\,c^6}\Big\{2\,(1680-(90632+4305\pi^2)\eta+33600\eta^2)\\
&+4\,\eta^3\Big)\;-\frac{80}{(2\,E\,h^2)}\left(1008+(-21130+861\pi^2)\,\eta+2268\,\eta^2\right)\\
&-\frac{16}{(2\,E\,h^2)^2}\Big((53760+(-176024+4305\pi^2)\,\eta+15120\,\eta^2)\Big)\Big\}, \qquad (5.36b)
\end{aligned}
$$

$$
\begin{aligned}
n =& (2\,E)^{3/2}\Big\{1-\frac{(2\,E)}{8\,c^2}\;(-15+\eta)+\frac{(2\,E)^2}{128c^4}\Big[555+30\,\eta+11\,\eta^2\Big]\\
&+\frac{(2\,E)^3}{1024\,c^6}\Big[653+111\eta+7\eta^2+3\eta^3\Big]\Big\}, \qquad (5.36c)
\end{aligned}
$$

$$
\begin{aligned}
{e_t}^2 =& \;1+2\,E\,h^2+\frac{(2\,E)}{4\,c^2}\Big\{8-8\,\eta+(17-7\,\eta)\,(2\,E\,h^2)\Big\}\\
&+\frac{(2\,E)^2}{8\,c^4}\Big\{4\,(3+18\,\eta+5\,\eta^2)+(2\,E\,h^2)(112-47\,\eta+16\,\eta^2)\\
&+\frac{16}{(2\,E\,h^2)}\,(-4+7\,\eta)\Big\}+\frac{(2\,E)^3}{840\,c^6}\Big\{-70(42-830\,\eta+321\,\eta^2+30\,\eta^3)
\end{aligned}
$$

$$
\begin{aligned}
&- \frac{525}{8}(2Eh^2)(-528 + 200\,\eta - 77\,\eta^2 + 24\,\eta^3) \\
&- \frac{3}{4(2\,E\,h^2)}\left(73920 + (-260272 + 4305\pi^2)\,\eta + 61040\,\eta^2\right) \\
&- \frac{1}{(2\,E\,h^2)^2}\left(53760 + (-176024 + 4305\pi^2)\,\eta + 15120\,\eta^2\right)\Bigg\}, \qquad (5.36d)
\end{aligned}
$$

$$
f_{4\,t} = \frac{3\,(2\,E)^2}{2}\left\{\frac{5 - 2\,\eta}{\sqrt{(2\,E\,h^2)}}\right\}, \qquad (5.36e)
$$

$$
\begin{aligned}
f_{6\,t} =& \frac{(2\,E)^3}{192(2Eh^2)^{\frac{3}{2}}}\Bigg\{\Bigg(10080 + 123\,\eta\,\pi^2 - 13952\,\eta \\
&+ 1440\,\eta^2\Bigg) + (2Eh^2)36\left(95 - 55\,\eta + 18\,\eta^2\right)\Bigg\}, \qquad (5.36f)
\end{aligned}
$$

$$
g_{4\,t} = -\frac{1}{8}\,\frac{(2\,E)^2}{\sqrt{(2\,E\,h^2)}}\left\{(-15 + \eta)\,\eta\,\sqrt{(1 + 2\,E\,h^2)}\right\}, \qquad (5.36g)
$$

$$
\begin{aligned}
g_{6\,t} =& \frac{(2\,E)^3}{2240(2Eh^2)^{\frac{3}{2}}\sqrt{1 + 2Eh^2}}\Bigg\{35(2Eh^2)^2\eta\left(23\eta^2 - 175\eta + 297\right) \\
&+ (2Eh^2)\left(22400 + (49321 - 1435\pi^2)\eta - 27300\eta^2 + 1225\eta^3\right) \\
&+ 385\,\eta^3 - 20965\eta^2 + \left(-1435\pi^2 + 43651\right)\eta + 22400\Bigg\}, \qquad (5.36h)
\end{aligned}
$$

$$
h_{6\,t} = \frac{(2\,E)^3}{16}\,\eta\left\{\frac{(1 + 2\,E\,h^2)}{(2\,E\,h^2)^{3/2}}\left(116 - 49\eta + 3\eta^2\right)\right\}, \qquad (5.36i)
$$

$$
i_{6\,t} = \frac{(2\,E)^3}{192}\eta^3\left(\frac{1 + 2\,E\,h^2}{2\,E\,h^2}\right)^{3/2}\left(23 - 73\eta + 13\eta^2\right), \qquad (5.36j)
$$

$$
\Phi = 2\,\pi\left\{1 + \frac{3}{c^2h^2} + -\frac{3(2E)^2}{4(2Eh^2)^2c^4}\Big[-35 + 10\eta + (2Eh^2)\big(-5 + 2\eta\big)\Big]\right.
$$

$$+\frac{(2\,E)^3}{128\,c^6(2Eh^2)^3}\Big[36960+(615\pi^2-40000)\eta+1680\eta^2$$
$$+(2Eh^2)(10080+123\eta\pi^2-13952\eta+1440\eta^2)$$
$$+(2Eh^2)^2\big(120-120\eta+96\eta^2\big)\Big]\Big\}, \tag{5.36k}$$

$$f_{4\,\phi}=\frac{(2\,E)^2}{8}\,\frac{(1+2\,E\,h^2)}{(2\,E\,h^2)^2}\,(1+19\,\eta-3\,\eta^2)\,, \tag{5.36l}$$

$$f_{6\,\phi}=\frac{(2\,E)^3}{26880(2Eh^2)^3}\Big\{67200+(994704-30135\pi^2)\,\eta-335160\eta^2-4200\eta^3$$
$$+280(2Eh^2)^2(3+506\,\eta-357\,\eta^2+36\,\eta^3) \tag{5.36m}$$
$$+(2Eh^2)\big(60480+(991904-30135\eta^2)\eta-428400\eta^2+8400\eta^3\big)\Big\},$$

$$g_{4\,\phi}=\frac{(1-3\eta)(2\,E)^2}{32}\,\frac{\eta}{(2\,E\,h^2)^2}(1+2\,E\,h^2)^{3/2}\,, \tag{5.36n}$$

$$g_{6\,\phi}=\frac{(2\,E)^3}{768}\,\frac{\sqrt{(1+2\,E\,h^2)}}{(2Eh^2)^3}\,\eta\Big\{36161-1435\pi^2-28525\,\eta+525\,\eta^2 \tag{5.36o}$$
$$+35(2Eh^2)^2(14-49\,\eta+26\,\eta^2)+(2Eh^2)(35706-1435\pi^2-27510\eta+1750\eta^2)\Big\},$$

$$h_{6\,\phi}=\frac{(2\,E)^3}{192}\,\frac{(1+2\,E\,h^2)^2}{(2\,E\,h^2)^3}\,\eta\left(82-57\,\eta+15\,\eta^2\right)\,, \tag{5.36p}$$

$$i_{6\,\phi}=\frac{(2\,E)^3}{256}\,\eta\frac{1-5\eta+5\eta^2}{(2\,E\,h^2)^3}\,(1+2\,E\,h^2)^{5/2}\,, \tag{5.36q}$$

$${e_\phi}^2=1+2\,E\,h^2+\frac{(2\,E)}{4\,c^2}\Big\{-24+(-15+\eta)\,(2\,E\,h^2)\Big\}$$
$$+\frac{(2\,E)^2}{16\,c^4(2Eh^2)}\Big\{-416+91\eta+15\eta^2+2(2Eh^2)\big(-20+17\eta+9\eta^2\big)$$

$$
\begin{aligned}
&+ (2Eh^2)^2\big(160 - 31\eta + 3\eta^2\big)\Big\} \\
&- \frac{(2\,E)^3}{13440\,c^6(2Eh^2)^2}\Big\{2956800 + (-5627206 + 81795\pi^2)\,\eta - 14490\eta^2 - 7350\eta^3 \\
&- (2Eh^2)^2(584640 + (17482 + 4305\pi^2)\,\eta + 7350\,\eta^2 - 8190\eta^3) \\
&+ 420(2Eh^2)^3(744 - 248\,\eta + 31\,\eta^2 + 3\,\eta^3) \qquad (5.36r) \\
&+ 14(2Eh^2)(36960 + 7(-48716 + 615\pi^2)\,\eta - 225\,\eta^2 + 150\,\eta^3)\Big\}\,.
\end{aligned}
$$

Let us recall that both the radial and temporal coordinates are scaled by $G\,m$, and that the expressions for a_r and n are therefore given by $a_r = 1/(2\,E)$ and $n = (2\,E)^{3/2}$ at the Newtonian order. The three eccentricities e_r, e_t and e_ϕ, which differ from each other from the first post-Newtonian order, are related by

$$
\begin{aligned}
e_t \;=\;& e_r\left\{1 + \frac{(2E)}{2c^2}(8 - 3\eta) + \frac{(2E)^2}{c^4}\frac{1}{(2Eh^2)}\left[8 - 14\,\eta + \big(36 - 19\,\eta + 6\,\eta^2\big)\,(Eh^2)\right]\right. \\
&+\frac{(2E)^3}{3360\,c^6}\frac{1}{(2Eh^2)^2}\Big[-420\,(2\,E\,h^2)^2\,\big(10\eta^3 - 34\eta^2 + 65\eta - 160\big) + E\,h^2\big(105840\eta^2 \\
&+\big(4305\pi^2 - 354848\big)\,\eta + 87360\big) + 30240\,\eta^2 \\
&\left.+\big(8610\pi^2 - 352048\big)\,\eta + 107520\Big]\right\}, \qquad (5.37a)
\end{aligned}
$$

$$
\begin{aligned}
e_\phi \;=\;& e_r\left\{1 - \frac{(2E)}{2c^2}\eta - \frac{(2E)^2}{32c^4}\frac{1}{(2Eh^2)}\left[160 + 357\eta - 15\eta^2 - \eta(-1 + 11\eta)(2Eh^2)\right]\right. \\
&+\frac{(2E)^3}{8960c^6}\frac{1}{(2Eh^2)^2}\Big[-70(2Eh^2)^2\,\eta\,\big(31\eta^2 - \eta - 1\big) + 5\,(2Eh^2)\big(-1050\,\eta^3 \\
&+31304\,\eta^2 + \big(1435\pi^2 - 36546\big)\,\eta + 4928\big) + 2450\,\eta^3 + 166110\,\eta^2 + \big(18655\pi^2 \\
&\left.-1854\big)\,\eta - 412160\Big]\right\}. \qquad (5.37b)
\end{aligned}
$$

These relations allow one to choose a specific eccentricity parameter to describe a PN accurate hyperbolic orbit. Following the above detailed procedure, it is straightforward to obtain 3PN-accurate expressions for the above listed quantities also in an ADM-type gauge. The 3PN-accurate Keplerian-type parametric solution arises from Eqs. (A1) and (A2) of Memmesheimer et al. (2004) and is structurally identical to Eqs. (5.35). This is expected as Eqs. (A1), (A2) and (A3) and (A4) of Memmesheimer et al. (2004) are polynomials of the same degree though their coefficients are different. The ADM versions of Eqs. (5.36) are listed in Appendix 5.4.

We are now in a position to explore the possibility of obtaining our 3PN-accurate hyperbolic solution from its eccentric counterpart through analytic continuation. A close inspection of our results reveals that the 3PN-accurate expression for the orbital element n in Eqs. (5.36), is structurally different from its eccentric counterpart, given by Eq. (25c) of Memmesheimer et al. (2004). Moreover, the structure of the relevant two Kepler equations is different (compare Eq. (19b) of Memmesheimer et al. (2004) with our Eq. (5.35b)). Therefore, it is reasonable to expect that additional arguments may be required to obtain *practically viable* analytic continuation arguments for extracting our main results from that of Memmesheimer et al. (2004). We begin from the eccentric Kepler equation, given by Eq. (24b) of Memmesheimer et al. (2004), which may be written as

$$\begin{aligned} l &= \frac{2\pi}{P_e}\,(t-t_0) = u' - e_t\,\sin u' \\ &\quad + \left(\frac{g'_{4t}}{c^4}+\frac{g'_{6t}}{c^6}\right)(\nu'-u') + \left(\frac{f'_{4t}}{c^4}+\frac{f'_{6t}}{c^6}\right)\sin\nu' + \frac{i'_{6t}}{c^6}\,\sin 2\,\nu' + \frac{h'_{6t}}{c^6}\,\sin 3\,\nu'\,, \end{aligned} \tag{5.38}$$

where *primed* variables denote an eccentric binary and P_e stands for the 3PN-accurate orbital period of an eccentric binary. The presence of the term $\nu'-u' \equiv 2\tan^{-1}\left(\beta'_\phi \sin u'/(1-\beta'_\phi\cos u')\right)$ in the above Kepler equation, where $\beta_\phi = (1-\sqrt{1-e_\phi^2})/e_\phi$, leads to certain imaginary terms while adapting the usual argument of analytic continuation, namely $u' \to \imath v$ and

$\sqrt{-E} \to \imath\sqrt{E}$, to obtain its hyperbolic version Damour and Deruelle (1985).

At 1PN order, the above arguments ensure that the expression for P_e becomes a purely imaginary quantity, i.e., $\imath P_{\rm hyp}$ and that $u' - e_t \sin u'$ becomes $\imath v - \mathrm{e}_t \sin(\imath v)$. This guarantees that $(P_e)(u' - e_t \sin u')/(2\,\pi)$ leads to $(P_{\rm hyp})(e_t \sinh v - v)/(2\,\pi)$. This observation influenced us to consider an expression for $(t - t_0)$, as given by Eq. (5.38), rather than $l = n(t - t0)$, while invoking the usual arguments for analytic continuation (AAC) . It is easy to show that the 3PN-accurate eccentric expression for n gives a complex quantity rather than a purely imaginary one under the AAC. This is essentially due to the presence of $(-2\,E\,h^2)$ terms present in Eq. (25c) in Memmesheimer et al. (2004). Similar arguments also apply to the terms $u' - e_t \sin u' + (\frac{g'_{4t}}{c^4} + \frac{g'_{6t}}{c^6})\,(\nu' - u')$ in the 3PN-accurate eccentric Kepler Equation under the AAC. However, the product of $P_e/2\,\pi$ and the above terms while substituting $u' \to \imath v$ and $\sqrt{-E} \to \imath\sqrt{E}$ becomes a real quantity and can be identified with $(P/2\,\pi) \times [e_t \sinh u - u + (\frac{f_{4t}}{c^4} + \frac{f_{6t}}{c^6})\,\nu]$. Here, $P/(2\,\pi)$ is the PN-accurate inverse of n, given by our Eqs. (5.36). It should be noted that this procedure ensures that the complex quantities that we encountered while applying the AAC in Eq. (5.38) are now properly handled to obtain our 3PN-accurate hyperbolic solution. Let us emphasize that we were able to formulate this reasoning mainly because of the availability of our 3PN-accurate hyperbolic solution, obtained from our detailed ab-initio computations. In other words, it is rather difficult to extract a 3PN-accurate orbital element n for hyperbolic orbits from its eccentric version simply by invoking the arguments for analytic continuation of Damour and Deruelle (1985). We require re-definitions of certain terms in the eccentric Kepler equation to obtain its hyperbolic version through analytic continuation. These re-definitions, however, can be worked out if the actual hyperbolic solution is available, computed from first principles as done in this paper. Finally, we observe that all other eccentric orbital elements and functions transition smoothly into their hyperbolic counterparts while employing the AAC. The extraction of our 3PN-accurate hyperbolic solution from its eccentric counterpart, as noted earlier, provides an additional test for the

correctness of the lengthy expressions present in Memmesheimer et al. (2004).

We have also adapted for our purposes a consistency check which was devised in Memmesheimer et al. (2004) to test the fidelity of the 3PN-accurate eccentric parametrization and its PN-accurate orbital elements and functions. The idea is to compute 3PN-accurate expressions for $\dot{r}^2$ and $\dot{\phi}^2$ using our parametric solution, via $\dot{r}^2 = \left(\frac{dr}{du}\,\frac{du}{dt}\right)^2$ and $\dot{\phi}^2 = \left(\frac{d\phi}{dv}\,\frac{dv}{du}\,\frac{du}{dt}\right)^2$. These lengthy 3PN-accurate expressions are first obtained in terms of E, h, η and $(e_r\,\cosh u - 1)$ and are later converted in terms of E, h, η and r while using our 3PN-accurate expression for $r = a_r(E, h, \eta)\,(e_r\,\cos hu - 1)$. A detailed check is provided by comparing these parametric expressions for $\dot{r}^2$ and $\dot{\phi}^2$ with those extracted from Eqs. (A3) and (A4) in Memmesheimer et al. (2004). Note that these equations arise from the 3PN-accurate expressions for the orbital energy and angular momentum as evident by examining Eqs. (22) and (23) and the associated discussions in Memmesheimer et al. (2004). We have verified that the above two sets of 3PN-accurate expressions for $\dot{r}^2$ and $\dot{\phi}^2$ in terms E, h, η and r are identical to each other in the case of hyperbolic orbits. Let us emphasize that this check is very sensitive to the structure of the parametric solution and the explicit PN-accurate expressions for the various orbital elements and functions. Therefore, the complete agreement to 3PN order between the parametric and Hamiltonian-based sets of $\dot{r}^2$ and $\dot{\phi}^2$ expressions – along with our improved analytic continuation relations – provide powerful checks on our 3PN-accurate generalized quasi-Keplerian parametrization for compact binaries in hyperbolic orbits. Additionally, we have verified that our results are in agreement with Damour and Deruelle (1985) at 1PN order. In what follows, we apply our 3PN-accurate Keplerian type parametric solution to obtain time-domain gravitational waveforms for compact binaries in hyperbolic orbits while incorporating effects of GW emission.

5.3 GW polarization states for compact binaries in 3.5PN-accurate hyperbolic orbits

This section presents an efficient prescription to obtain temporally evolving GW polarization states for compact binaries moving in fully 3.5PN-accurate hyperbolic orbits. Clearly, this requires us to prescribe a way of incorporating the dissipative effects of GW emission appearing at 2.5PN and 3.5PN orders into our 3PN-accurate orbital dynamics. With the help of Damour et al. (2004); Königsdörffer and Gopakumar (2006); De Vittori et al. (2014), this is pursued in steps which we will briefly outline below. We begin by considering the following expressions for the quadrupolar (or Newtonian) order GW polarization states, $h_+|_Q$ and $h_\times|_Q$, for compact binaries in non-circular orbits, available in De Vittori et al. (2014), which read

$$\begin{aligned} h_+|_{\rm Q} =& -\frac{G\,m\,\eta}{c^4\,R}\times \\ & \left\{\left(1+C_\theta^2\right)\left[\left(z+r^2\dot{\phi}^2-\dot{r}^2\right)\cos 2\phi \right.\right. \\ & \left.\left. +2r\dot{r}\dot{\phi}\sin 2\phi\right]+S_\theta^2\left(z-r^2\dot{\phi}^2-\dot{r}^2\right)\right\}, \end{aligned} \tag{5.39a}$$

$$\begin{aligned} h_\times|_{\rm Q} =& -2\frac{G\,m\,\eta}{c^4\,R}C_\theta\times \\ & \left\{\left(z+r^2\dot{\phi}^2-\dot{r}^2\right)\sin 2\phi-2r\dot{r}\dot{\phi}\cos 2\phi\right\}. \end{aligned} \tag{5.39b}$$

The parameter z is related to the radial coordinate of the orbit by $z=G\,m/r$, while R is the radial distance to the source, and $C_\theta=\cos\theta$, $S_\theta=\sin\theta$ with θ being the orbital inclination. Obviously, the temporal evolutions of $h_+|_Q(t)$ and $h_\times|_Q(t)$ require a prescription for evolving $r, \dot{r}=\mathrm{d}r/\mathrm{d}t, \phi$ and $\dot{\phi}=\mathrm{d}\phi/\mathrm{d}t$ in time.

In the next step, we obtain fully 3PN-accurate parametric expressions for the dynamical variables appearing in the above expressions for $h_+|_Q(t)$ and $h_\times|_Q(t)$. This requires parametric expressions not only for r and ϕ, available in the previous section, but also for $\dot{r}$ and $\dot{\phi}$. We obtain 3PN-accurate parametric expressions for $\dot{r}$ and $\dot{\phi}$ by noting that

$\dot{r} = (dr/du)\times(du/dt)$ and $\dot{\phi} = (d\phi/d\nu)\times(d\nu/du)\times(du/dt)$. These expressions are provided in terms of a certain gauge-invariant dimensionless PN expansion parameter $\xi = \frac{G\,m\,n}{c^3}$, where $n = \frac{2\pi}{P}$ as defined in Eq. (5.36c), the *time eccentricity* e_t and the eccentric anomaly u. The dynamical variables have to derived carefully, as we introduced scaled coordinates in the previous section. Our particular choice of variables is influenced by the ease with which we can specify various initial conditions during the numerical construction of GW templates. To obtain 3PN-accurate temporal evolutions of $r, \dot{r}, \phi$ and $\dot{\phi}$, we also need to express the right-hand side of the 3PN-accurate Kepler equation in terms of ξ and e_t.

The third step involves including the effects of GW emission during hyperbolic passages. This is accomplished by providing differential equations for $d\xi/dt$ and de_t/dt, whose derivation is influenced by Damour et al. (2004); Königsdörffer and Gopakumar (2006). These equations, as expected, incorporate radiation reaction effects entering the orbital dynamics at 2.5PN and 3.5PN orders. Through a numerical solution of the Kepler equation along with these two coupled differential equations for ξ and e_t, we obtain the fully 3.5PN-accurate temporal evolution for $r, \dot{r}, \phi$ and $\dot{\phi}$. This enables us to construct $h_+|_Q(t)$ and $h_\times|_Q(t)$ for compact binaries in 3.5PN-accurate hyperbolic orbits. Finally, we provide a 3PN accurate expression for ξ in terms of a certain PN-accurate gauge-dependent impact parameter b and time eccentricity e_t, as it is very convenient to characterize hyperbolic orbits through their impact parameters and eccentricities. Thus, we obtain ready-to-use GW templates for compact binaries in PN-accurate hyperbolic orbits.

In the following, we provide explicit expressions for various dynamical variables in terms of ξ, e_t and u that will be required for obtaining $h_+|_Q(t)$ and $h_\times|_Q(t)$. For the sake of readability, we will only explicitly list the 1PN-accurate expressions for these dynamical variables, given in terms of ξ, e_t and u as

$$r(u) = \frac{Gm}{c^2}\frac{1}{\xi^{2/3}}(e_{\rm t}\cosh u - 1)\left\{1 + \xi^{2/3}\,\frac{2\eta - 18 - (6-7\eta)e_{\rm t}\cosh u}{6\,(e_{\rm t}\cosh u - 1)}\right\}\,, \quad \text{(5.40a)}$$

$$\dot{r}(u) = \xi^{1/3} \frac{c\, e_{\rm t} \sinh u}{e_{\rm t} \cosh u - 1} \left\{ 1 - \xi^{2/3} \frac{6 - 7\eta}{6} \right\} \,, \tag{5.40b}$$

$$\phi(u) - \phi_0 = 2 \arctan \left[\left(\frac{e_\phi + 1}{e_\phi - 1} \right)^{1/2} \tanh u/2 \right] \left\{ 1 + \xi^{2/3} \frac{3}{e_{\rm t}^2 - 1} \right\} \,, \tag{5.40c}$$

$$\dot{\phi}(u) = \frac{n \sqrt{e_{\rm t}^2 - 1}}{(e_{\rm t} \cosh u - 1)^2} \left\{ 1 - \xi^{2/3} \, \frac{\left[3 - (4 - \eta)\, e_{\rm t}^2 + (1 - \eta)\, e_{\rm t} \cosh u \right]}{\left(e_{\rm t}^2 - 1 \right) \left(e_{\rm t} \cosh u - 1 \right)} \right\} \,. \tag{5.40d}$$

The lengthy 3PN-accurate versions of these expressions are provided in Appendix 5.5. It should be obvious that temporal evolutions for the 3PN version of above equations, namely Eqs. (5.40), require a 3PN-accurate Kepler equation in terms of ξ and e_t that connects l and u. This 3PN-accurate equation in MH gauge is given by

$$l = n(t - t_0) = l_{\rm N} + l_{\rm 1PN} + l_{\rm 2PN} + l_{\rm 3PN} \,, \tag{5.41a}$$

$$l_{\rm N} = e_t \sinh u - u \,, \tag{5.41b}$$

$$l_{\rm 1PN} = 0 \,, \tag{5.41c}$$

$$l_{\rm 2PN} = \frac{\xi^{4/3}}{8\sqrt{e_t^2 - 1}} \Big[12\nu(5 - 2\eta) - e_t(\eta - 15)\eta \sin \nu \Big] \,, \tag{5.41d}$$

$$\begin{aligned} l_{\rm 3PN} = {} & \frac{\xi^2}{6720(e_t^2 - 1)^{3/2}(e_t \cosh u - 1)} \Bigg\{ 35\nu \Big\{ 96 e_t^2 \Big[\eta(11\eta - 29) + 30 \Big] \\ & + \eta(960\eta + 123\pi^2 - 13184) + 8640 \Big\} (e_t \cosh u - 1) \\ & + 840 e_t \sqrt{e_t^2 - 1} (\eta - 4) \sinh u \Big[e_t(\eta - 15)\eta \cos \nu + 24\eta - 60 \Big] \\ & + e_t \sin \nu \, (e_t \cosh u - 1) \Bigg[\eta \Big\{ 70 e_t^2 \Big[\eta(39\eta - 239) + 7 \Big] \\ & - 4 \Big[70\eta \, (\eta + 222) - 35967 \Big] - 4305 \, \pi^2 \Big\} + 70 e_t \eta \Big\{ e_t \Big[\eta(13\eta - 73) + 23 \Big] \\ & \times \cos 2\nu + 12 \Big[\eta \, (3\,\eta - 49) + 116 \Big] \, \cos \nu \Big\} + 67200 \Bigg] \Bigg\} \,. \end{aligned} \tag{5.41e}$$

The above equation allows us to adapt Mikkola's method, developed to numerically solve the classical Kepler equation for hyperbolic orbits as detailed in Sec. 4 of Mikkola (1987).

Mikkola's very effecient and computationally inexpensive approach approximates the classical Kepler equation as a cubic polynomial in an auxiliary variable $s(u)$, finding its roots and substantially reducing the error of the initial guess through a fourth-order extension of Newton's method. We employ Mikkola's procedure in an iterative manner to tackle PN corrections to the classic Kepler equation appearing at 2PN and 3PN orders. It should be noted that our 3PN-accurate Kepler equation is identical to the classical (Newtonian) Kepler equation at 1PN order, which is only possible due to the use of the time eccentricity e_t as a parameter to specify the orbit. To solve above 3PN-accurate Kepler equation, we tackle the 1PN-accurate Kepler equation, namely $l = n(t - t_0) = e_t \sinh u - u$, using Mikkola's original prescription and obtain a 1PN-accurate expression for $u(l)$.
This method requires us to express l in terms of a new variable $s' = \sinh \frac{u}{3}$,

$$l = e_t \left(3s' + 4s'^3\right) - 3 \ln(s' + \sqrt{1 + s'^2}) \,, \tag{5.42}$$

and truncating it to the third order in s',

$$l = 3(1 - e_t)s' + (4e_t + \frac{1}{2})\, s'^3 \,. \tag{5.43}$$

This third order polynomial can be solved in a closed form, say, $s' = s'(l\,;\, e_t)$. To minimize the error, replacing s' to

$$\omega(l) := s'(l) + \frac{0.071 s'(l)^5}{(1 + 0.45 s'(l)^2)(1 + 4 s'(l)^2) e_t}.$$

Now we can get the most accurate solution,

$$u(l) \; = l - e_t \left(3\omega(l) + 4\omega(l)^3\right). \tag{5.44}$$

The accuracy of the solution can further improved by the use of Newton method as noted in Mikkola (1987).
This allows us to express numerically the 2PN and 3PN corrections that appear on the right-hand side of Eq. (5.41) in terms of $(\,\xi, e_t, l\,)$. We now introduce a certain parameter l' such that $l' = l - l_{4,6}$, where $l_{4,6}$ are the 2PN and 3PN corrections present in Eq. (5.41)

which are evaluated using 1PN-accurate $u(l)$. The 3PN accurate $u(l)$ is obtained, as expected, by solving $l' = e_t \sinh u - u$, once again employing Mikkola's method. In this way, we pursue an accurate and efficient solution to our 3PN accurate Kepler equation which allows us to compute the 3PN-accurate temporal evolutions for the dynamical variables present in our expressions for $h_+|_Q(t)$ and $h_\times|_Q(t)$. We note, in passing, that to obtain these 3PN-accurate expressions for $r, \dot{r}, \phi$ and $\dot{\phi}$, we have used unique 3PN-accurate expressions that provide $2\,E$ and h in terms of ξ and e_t by inverting the relevant expressions present in our parametric solution. Further, we have also employed 3PN-accurate relations that provide e_r and e_ϕ in terms of e_t, ξ and η. We are now in a position to discuss how GW emission effects are incorporated.

GW emission influences binary dynamics at 2.5PN and 3.5PN orders, and we incorporate these effects by adapting the phasing formalism developed for eccentric binaries (detailed in Damour et al. (2004); Königsdörffer and Gopakumar (2006)) to hyperbolic encounters. This requires us to compute time derivatives of the 1PN-accurate expressions for the conserved orbital energy and angular momentum of binaries in non-circular orbits, given by Eqs. (3.35) and (3.36) in Blanchet and Schaefer (1989). These time derivatives are obtained using PN-accurate equations of motion that include both conservative and reactive terms to 1PN order, e.g., given by Eq. (3.34) of Blanchet and Schaefer (1989) and Eqs. (28), (29) of Königsdörffer and Gopakumar (2006). The resulting expressions for dE/dt and dh/dt are adapted for hyperbolic orbits with the help of our 1PN-accurate parametric expressions for the dynamical variables $r, \dot{r}$ and $\dot{\phi}$, expressed in terms of n, e_t, u. Using our 1PN-accurate expressions for $n = 2\,\pi/P$ and e_t^2 in terms of the conserved orbital energy and angular momentum, dE/dt and dh/dt then lead to the desired equations for dn/dt and de_t/dt in modified harmonic gauge:

$$\begin{aligned}\frac{dn}{dt} &= \frac{8c^6\eta\,\xi^{\frac{11}{3}}}{5\,G^2\,m^2\,\beta^6}\left[35(1-e_t^2)+49\beta+32\beta^2+6\beta^3-9\beta e_t^2\right] \\ &\quad+\frac{2c^6\eta}{35\beta^9}\xi^{\frac{13}{3}}\Big\{\beta^6(180-588\eta)+\beta^5(1340-5852\eta)\end{aligned}$$

$$
\begin{aligned}
&+2\beta^4\Big[9e_t^2(21\eta-1)-8589\eta+1003\Big]+35\beta^3\Big[e_t^2\\
&\times(244\eta-5)-684\eta+21\Big]+35\beta^2(e_t^2-1)\Big[9e_t^2\\
&\times(2\eta-17)+454\eta+193\Big]-21\beta(e_t^2-1)^2(140\eta\\
&+657)+5880(e_t^2-1)^3\Big\}\,, \qquad (5.45a)
\end{aligned}
$$

$$
\begin{aligned}
\frac{de_t}{dt} \;=\;& \frac{8\,c^3\,\eta\,(e_t^2-1)}{15\,G\,m\,\beta^6\,e_t}\xi^{\frac{8}{3}}\Big[35(1-e_t^2)+(49-9e_t^2)\beta+17\beta^2\\
&+3\beta^3\Big]-\frac{2c^3\eta}{315\beta^9 e_t}\xi^{\frac{10}{3}}\Big\{-17640(-1+e_t^2)^4+63\beta\\
&\times(-1+e_t^2)^3(657+140\eta)-105\beta^2(-1+e_t^2)^2\Big[13\\
&\times+454\eta+9e_t^2(3+2\eta)\Big]-\beta^4(-1+e_t^2)\Big[36825\\
&-53060\eta+9e_t^2(-2169+560\eta)\Big]+6\beta^6\Big[360-553\eta\\
&+e_t^2(-444+637\eta)\Big]-28\beta^3(-1+e_t^2)\Big[29(63-95\eta)\\
&+e_t^2(-1767+1105\eta)\Big]+\beta^5\Big[10215-18088\eta+e_t^2\\
&\times(-12735+20608\eta)\Big]\Big\}\,. \qquad (5.45b)
\end{aligned}
$$

where $\beta = e_t \cosh u - 1$. We have verified that these expressions can also be obtained by the usual calculations based on balance arguments. In this approach, one differentiates our 1PN-accurate expressions for n and e_t while using 1PN-accurate expressions for the far-zone fluxes, given for example by Eqs. (17) and (18) of Junker and Schaefer (1992), to replace the time derivatives of the conserved energy and angular momentum variables. The resulting expressions for dn/dt and de_t/dt, adapted for 1PN-accurate hyperbolic orbits, were found to be identical to Eqs. (5.45a) and (5.45b).

It is rather convenient to characterize hyperbolic binaries in terms of an impact parameter b, as these GW events are qualitatively similar to scattering processes. We define a PN-accurate impact parameter b such that $b\,\mathrm{v}_\infty = |\boldsymbol{r}\times\ \mathbf{v}|$ when $|\boldsymbol{r}| \to \infty$, while v_∞ stands for

the relative velocity at infinity Blanchet and Schaefer (1989). The explicit 3PN-accurate expression for b in terms of ξ and e_t in modified harmonic gauge reads

$$
\begin{aligned}
b =& \frac{Gm}{c^2}\frac{\sqrt{e_{\rm t}^2-1}}{\xi^{2/3}}\Bigg\{1-\xi^{2/3}\left(\frac{\eta-1}{e_{\rm t}^2-1}+\frac{7\eta-6}{6}\right) \\
&+\xi^{4/3}\left[1-\frac{7}{24}\eta+\frac{35}{72}\eta^2+\frac{3-16\eta}{2(e_t^2-1)}+\frac{7-12\eta-\eta^2}{2(e_t^2-1)^2}\right] \\
&+\xi^2\left[-\frac{2}{3}+\frac{87}{16}\eta-\frac{437}{144}\eta^2+\frac{49}{1296}\eta^3+\right. \\
&+\frac{36-378\eta+140\eta^2+3\eta^3}{24(e_t^2-1)}+\frac{1}{6720(e_t^2-1)^2}\big\{248640 \\
&+(-880496+12915\pi^2)\,\eta+40880\,\eta^2+3920\,\eta^3\big\} \\
&+\frac{1}{1680(e_t^2-1)^3}\big\{73080+(-228944+4305\pi^2)\eta \\
&\left.+47880\eta^2+840\eta^3\big\}\right]\Bigg\}\,.
\end{aligned}
\tag{5.46}
$$

At 1PN order, we are in agreement with De Vittori et al. (2014). This variable is essentially invoked to allow for an easy visualization of the trajectories of hyperbolic binaries.

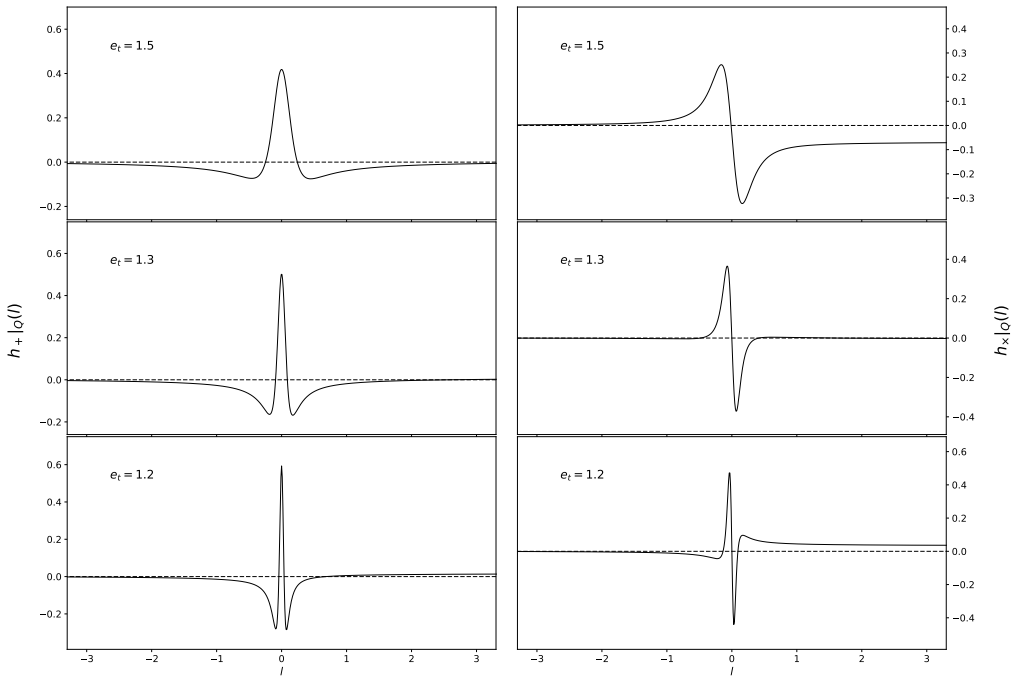

Figure 5.1 Scaled $H_+|_Q(l)$ and $H_\times|_Q(l)$ plots for non-spinning compact binaries with total mass $m = 20\,M_\odot$ and mass ratio $q = 1$. We let the eccentricity e_t take three values 1.5, 1.3 and 1.2, while choosing an impact parameter $b \sim 30\,Gm/c^2$ and inclination angle $\theta = \frac{\pi}{4}$. We observe the expected linear memory effect in the cross polarization state.

With above inputs, it is possible to obtain temporally evolving Newtonian (quadrupolar) GW polarization states, $h_+|_Q(t)$ and $h_\times|_Q(t)$, associated with compact binaries in 3.5PN-accurate hyperbolic orbits. It is convenient to numerically solve a system of three coupled differential equations, namely $dn/dt, de_t/dt$ and $dl/dt = n$. The resulting values of parameters n, e_t and l at a given epoch are then employed to obtain a 3PN-accurate value for $u(l)$ by the application of Mikkola's method as described above. With a knowledge of n, e_t, l

and u, we can then evaluate our 3PN-accurate expressions for $r, \dot{r}, \phi$ and $\dot{\phi}$. Thus, we are able to numerically provide $h_+|_Q(t)$ and $h_\times|_Q(t)$ from compact binaries in 3.5PN-accurate hyperbolic orbits. In the following, we discuss plots that demonstrate the approach and point out a feature of the waveforms previously not mentioned in the literature. In Fig. 5.1, we plot scaled quadrupolar GW polarization states, $H_+|_Q(l)$ and $H_\times|_Q(l)$, for hyperbolic passages with $b \sim 30\,G\,m/c^2$ for compact binaries having $m = 20\,M_\odot$ and $\eta = \frac{1}{4}\,(q = 1)$, while allowing e_t to take three different values. Here, $H_+|_Q(l)$ and $H_\times|_Q(l)$ denotes waveforms that have been scaled by $G\,m/c^2\,R$. We observe, as expected, the linear memory effect for the cross polarization De Vittori et al. (2014). We display in Fig. 5.2 the trajectories of compact binaries under the influence of Newtonian and fully 3.5PN-accurate orbital dynamics (respectively in black and red) and their associated $H_\times|_Q(l)$. For these, we have chosen $e_t = 1.1$ while we let the impact parameter b take two different values, namely, $\sim 50\,G\,m/c^2$ and $\sim 106\,G\,m/c^2$. These particular v values were chosen to highlight the effect of PN corrections compared to the familiar Newtonian hyperbolic orbit. We observe that the periastron advance forces the 3.5PN-accurate orbital trajectory to cross its earlier path, a feature which is absent in the Newtonian system. Additionally, this feature disappears for large impact parameter values. This is expected, as the periastron advance is small for configurations with a large impact parameter, which results in Newtonian-like trajectories. We have also verified that the PN corrections in $\Phi/2\,\pi$ indeed converge to its 1PN value in above cases; this ensures that the crossing of the trajectory is a physical effect. Interestingly, this PN effect leads to sharper GW polarization states, and it will be interesting to explore possible data analysis implications for such hyperbolic passages.

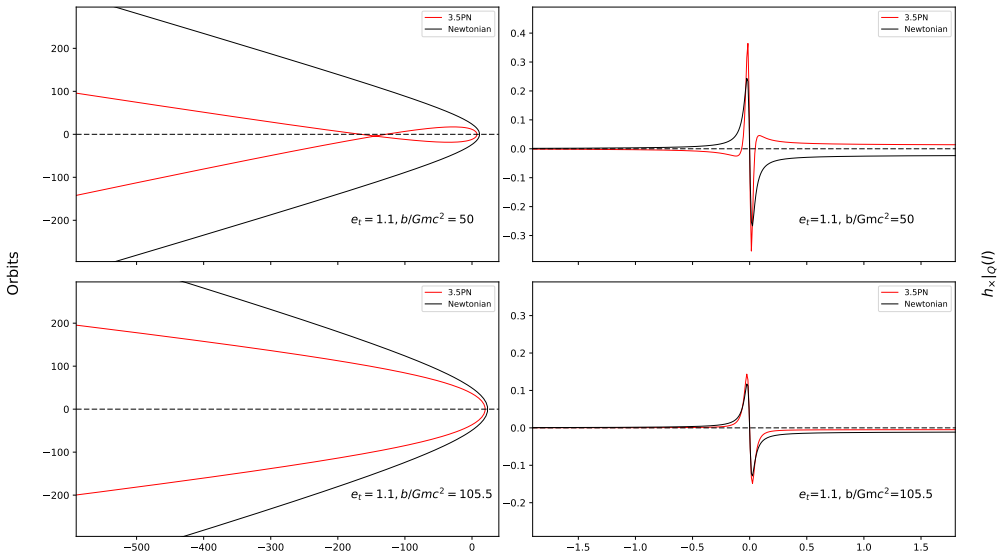

Figure 5.2 Trajectories and the associated scaled $H_\times|_Q(l)$ for hyperbolic compact binaries, with a choice of two different impact parameters b, eccentricity $e_t = 1.1$, total mass $m = 20M_\odot$, mass ratio $q = 1$, and inclination angle $\theta = \frac{\pi}{4}$. For the trajectories, we adopt the geometric unit system. Newtonian and 3.5PN-accurate hyperbolic orbits are denoted by black and red lines, respectively. The orbital trajectory of the relativistic system is clearly different, especially for hyperbolic passages with smaller b values, which is attributed to the advance of periastron. Relativistic effects also change the nature of the waveforms, as evident from the associated $h_\times|_Q(l)$ plots.

5.4 Generalized quasi-Keplerian parametrization for hyperbolic compact binaries in ADM-type gauge

We follow exactly the same procedure, detailed in Sec. 5.2.2, while using Eqs. (A1) and (A2) of Memmesheimer et al. (2004) to derive the 3PN accurate hyperbolic parametrization in ADM-type gauge. The third post-Newtonian accurate generalized quasi-Keplerian parametrization, in ADM coordinates, for hyperbolic compact binaries is given by

$$r = a_r \left(e_r \cosh u - 1\right) , \tag{5.47a}$$

$$\begin{aligned} \frac{2\pi}{P}(t-t_0) &= e_t \sinh u - u + (\frac{f_{4t}}{c^4} + \frac{f_{6t}}{c^6})\,\nu + (\frac{g_{4t}}{c^4} + \frac{g_{6t}}{c^6}) \sin\nu + \\ &\quad \frac{h_{6t}}{c^6}\sin 2\,\nu + \frac{i_{6t}}{c^6}\sin 3\,\nu\,, \end{aligned} \tag{5.47b}$$

$$\begin{aligned} \frac{2\pi}{\Phi}(\phi-\phi_0) &= \nu + (\frac{f_{4\phi}}{c^4} + \frac{f_{6\phi}}{c^6}) \sin 2\,\nu + (\frac{g_{4\phi}}{c^4} + \frac{g_{6\phi}}{c^6}) \sin 3\,\nu \\ &\quad + \frac{h_{6\phi}}{c^6}\sin 4\,\nu + \frac{i_{6\phi}}{c^6}\sin 5\,\nu\,, \end{aligned} \tag{5.47c}$$

where $\nu = 2\,\tanh^{-1}\left[\left(\frac{e_\phi+1}{e_\phi-1}\right)^{1/2}\tan\frac{u}{2}\right]$. The explicit 3PN accurate expressions for the orbital elements and functions of the generalized quasi-Keplerian parametrization, in ADM coordinates, read

$$\begin{aligned} a_r &= \frac{1}{(2\,E)}\Bigg\{1 + \frac{(2\,E)}{4\,c^2}\,(7-\eta) + \frac{(2\,E)^2}{16c^4}\Bigg[(1+10\,\eta+\eta^2) \\ &\quad + \frac{1}{(2\,E\,h^2)}(68-44\,\eta)\Bigg] + \frac{(2\,E)^3}{192\,c^6}\Bigg[-3+9\,\eta+6\,\eta^2 \\ &\quad -3\,\eta^3 + \frac{1}{(2\,E\,h^2)}\Bigg(864 + \left(-3\,\pi^2 - 2212\right)\eta + 432\,\eta^2\Bigg) \\ &\quad + \frac{1}{(2\,E\,h^2)^2}\Bigg(6432 - \left(13488 - 240\,\pi^2\right)\eta + 768\,\eta^2\Bigg)\Bigg]\Bigg\}\,, \end{aligned} \tag{5.48a}$$

$$
\begin{aligned}
{e_r}^2 &= 1 + 2\,E\,h^2 + \frac{(2\,E)}{4\,c^2}\Big\{-24 + 4\,\eta + 5\,\left(-3+\eta\right)\left(2\,E\,h^2\right)\Big\} \\
&\quad + \frac{(2\,E)^2}{8\,c^4}\Big\{52 + 2\,\eta + 2\,\eta^2 + \left(80 - 55\,\eta + 4\,\eta^2\right)\left(2\,E\,h^2\right) \\
&\quad + \frac{8}{(2\,E\,h^2)}\left(-17 + 11\,\eta\right)\Big\} + \frac{(2\,E)^3}{192\,c^6}\Big\{768 + 6\,\eta\,\pi^2 \\
&\quad + 344\,\eta + 216\,\eta^2 + 3(2\,E\,h^2)\Big(-1488 + 1556\,\eta - 319\,\eta^2 \\
&\quad + 4\,\eta^3\Big) - \frac{4}{(2\,E\,h^2)}\Big(588 - 8212\,\eta + 177\,\eta\,\pi^2 + 480\,\eta^2\Big) \\
&\quad - \frac{192}{(2\,E\,h^2)^2}\Big(134 - 281\,\eta + 5\,\eta\,\pi^2 + 16\,\eta^2\Big)\Big\}, \qquad (5.48b) \\
n &= (2\,E)^{3/2}\Big\{1 + \frac{(2\,E)}{8\,c^2}\,\left(-15+\eta\right) + \frac{(2\,E)^2}{128c^4}\Big[555 + 30\,\eta + 11\,\eta^2\Big] \\
&\quad + \frac{(2\,E)^3}{1024\,c^6}\Big[653 + 111\eta + 7\eta^2 + 3\eta^3\Big]\Big\}, \qquad (5.48c) \\
{e_t}^2 &= 1 + 2\,E\,h^2 + \frac{(2\,E)}{4\,c^2}\,\Big\{8 - 8\,\eta + (17 - 7\,\eta)\,(2\,E\,h^2)\Big\} \\
&\quad + \frac{(2\,E)^2}{8\,c^4}\Big\{8 + 4\,\eta + 20\,\eta^2 + (2\,E\,h^2)(112 - 47\,\eta + 16\,\eta^2) \\
&\quad + \frac{4}{(2\,E\,h^2)}\,(-17 + 11\,\eta)\,\Big\} + \frac{(2\,E)^3}{192\,c^6}\Big\{24\,\left(2 - 5\,\eta\right)\left(-23 + 10\,\eta + 4\,\eta^2\right) \\
&\quad - 15\,\Big(-528 + 200\,\eta - 77\,\eta^2 + 24\,\eta^3\Big)(2\,E\,h^2) \\
&\quad - \frac{2}{(2\,E\,h^2)}\Big(6732 + 117\,\eta\,\pi^2 - 12508\,\eta + 2004\,\eta^2\Big)
\end{aligned}
$$

$$-\frac{96}{(2\,E\,h^2)^2}\left(134-281\,\eta+5\,\eta\,\pi^2+16\,\eta^2\right)\Bigg\}, \tag{5.48d}$$

$$f_{4\,t} = \frac{3\,(2\,E)^2}{2}\left\{\frac{5-2\,\eta}{\sqrt{(2\,E\,h^2)}}\right\}, \tag{5.48e}$$

$$f_{6\,t} = \frac{(2\,E)^3}{192(2Eh^2)^{\frac{3}{2}}}\Bigg\{\Bigg(10080+123\,\eta\,\pi^2-13952\,\eta$$

$$+1440\,\eta^2\Bigg)+(2Eh^2)36\left(95-55\,\eta+18\,\eta^2\right)\Bigg\}, \tag{5.48f}$$

$$g_{4\,t} = -\frac{1}{8}\,\frac{(2\,E)^2}{\sqrt{(2\,E\,h^2)}}\left\{(4+\eta)\,\eta\,\sqrt{(1+2\,E\,h^2)}\right\}, \tag{5.48g}$$

$$g_{6\,t} = \frac{(2\,E)^3}{192(2Eh^2)^{\frac{3}{2}}\sqrt{1+2Eh^2}}\Bigg\{3(2Eh^2)^2\eta\left(23\eta^2-4\eta-64\right)$$

$$+(2Eh^2)\left(105\eta^3+627\eta^2+\left(3\pi^2-4232\right)\eta+1728\right)$$

$$+33\eta^3+600\eta^2+\left(3\pi^2-4148\right)\eta+1728\Bigg\}, \tag{5.48h}$$

$$h_{6\,t} = \frac{(2\,E)^3}{32}\,\eta\left\{\frac{(1+2\,E\,h^2)}{(2\,E\,h^2)^{3/2}}\left(23+12\,\eta+6\,\eta^2\right)\right\}, \tag{5.48i}$$

$$i_{6\,t} = \frac{13\,(2\,E)^3}{192}\eta^3\left(\frac{1+2\,E\,h^2}{2\,E\,h^2}\right)^{3/2}, \tag{5.48j}$$

$$\Phi = 2\,\pi\left\{1+\frac{3}{c^2h^2}+-\frac{3(2E)^2}{4(2Eh^2)^2c^4}\left[-35+10\eta+(2Eh^2)\big(-5+2\eta\big)\right]\right.$$

$$+\frac{(2\,E)^3}{128\,c^6(2Eh^2)^3}\Bigg[36960+(615\pi^2-40000)\eta+1680\eta^2$$

$$+(2Eh^2)(10080+123\eta\pi^2-13952\eta+1440\eta^2)$$

$$\left.+(2Eh^2)^2\big(120-120\eta+96\eta^2\big)\Bigg]\right\}, \tag{5.48k}$$

$$f_{4\,\phi} = \frac{(2\,E)^2}{8}\,\frac{(1+2\,E\,h^2)}{(2\,E\,h^2)^2}\,\eta\,(1-3\,\eta)\,, \tag{5.48l}$$

$$\begin{aligned} f_{6\,\phi} = {} & \frac{(2\,E)^3}{256(2Eh^2)^3}\Big\{256+(-1076+49\pi^2)\eta-384\eta^2-40\eta^3 \\ & +4(2Eh^2)^2\eta(-11-40\eta+24\eta^2)+(2Eh^2)\big(256+(-1192+49\pi^2)\eta \\ & -336\eta^2+80\eta^3\big)\Big\}, \end{aligned} \tag{5.48m}$$

$$g_{4\,\phi} = -\frac{3(2\,E)^2}{32}\,\frac{\eta^2}{(2\,E\,h^2)^2}(1+2\,E\,h^2)^{3/2}\,, \tag{5.48n}$$

$$\begin{aligned} g_{6\,\phi} = {} & \frac{(2\,E)^3}{768}\,\frac{\sqrt{(1+2\,E\,h^2)}}{(2Eh^2)^3}\,\eta\Big\{220+3\pi^2+96\eta+45\eta^2 \\ & +3(2Eh^2)^2\eta(-9+26\eta)+(2Eh^2)(220+3\pi^2+312\eta+150\eta^2)\Big\}, \end{aligned} \tag{5.48o}$$

$$h_{6\,\phi} = \frac{(2\,E)^3}{128}\,\frac{(1+2\,E\,h^2)^2}{(2\,E\,h^2)^3}\,\eta\left(5+28\,\eta+10\,\eta^2\right)\,, \tag{5.48p}$$

$$i_{6\,\phi} = \frac{5\,(2\,E)^3}{256}\,\frac{\eta^3}{(2\,E\,h^2)^3}\,(1+2\,E\,h^2)^{5/2}\,, \tag{5.48q}$$

$$\begin{aligned} {e_\phi}^2 = {} & 1+2\,E\,h^2+\frac{(2\,E)}{4\,c^2}\Big\{-24+(-15+\eta)\,(2\,E\,h^2)\Big\} \\ & +\frac{(2\,E)^2}{16\,c^4(2Eh^2)}\Big\{-408+232\eta+15\eta^2+(2Eh^2)\big(-32+176\eta+18\eta^2\big) \\ & +(2Eh^2)^2\big(160-30\eta+2\eta^2\big)\Big\} \\ & -\frac{(2\,E)^3}{384\,c^6(2Eh^2)^2}\Big\{3\big(27776+(-65436+1325\pi^2)\eta+3440\eta^2-70\eta^3\big) \\ & +36(2Eh^2)^3(248-80\eta+13\eta^2+\eta^3) \end{aligned}$$

$$+6(2Eh^2)(2456+(-26860+581\pi^2)\eta+2689\eta^2+10\eta^3)$$

$$+(2Eh^2)^2(-16032+(2764+3\pi^2)\eta+4536\eta^2+234\eta^3)\Big\}. \tag{5.48r}$$

$$\begin{aligned}
a_r &= \frac{1}{(-2E)}\Big\{1+\frac{(-2E)}{4\,c^2}\,(-7+\eta)+\frac{(-2E)^2}{16c^4}\Big[1+\eta^2\\
&\quad+\frac{16}{(-2Eh^2)}(-4+7\,\eta)\Big]+\frac{(-2E)^3}{6720\,c^6}\,\Big[105-105\,\eta\\
&\quad+105\,\eta^3+\frac{1}{(-2Eh^2)}\Big(26880+4305\,\pi^2\eta-215408\,\eta\\
&\quad+47040\,\eta^2\Big)-\frac{4}{(-2Eh^2)^2}\Big(53760-176024\,\eta+4305\,\pi^2\eta\\
&\quad+15120\,\eta^2\Big)\Big]\Big\}, \qquad (5.49a)\\
{e_r}^2 &= 1+2Eh^2+\frac{(-2E)}{4\,c^2}\Big\{24-4\,\eta+5\,(-3+\eta)\,(-2Eh^2)\Big\}\\
&\quad+\frac{(-2E)^2}{8c^4}\Big\{60+148\,\eta+2\,\eta^2-(-2Eh^2)\left(80-45\,\eta+4\,\eta^2\right)\\
&\quad+\frac{32}{(-2Eh^2)}(4-7\,\eta)\Big\}+\frac{(-2E)^3}{6720\,c^6}\Big\{-3360+181264\,\eta\\
&\quad+8610\,\pi^2\eta-67200\,\eta^2+105(-2Eh^2)\,\Big(-1488+1120\,\eta\\
&\quad-195\,\eta^2+4\,\eta^3\Big)-\frac{80}{(-2Eh^2)}\Big(1008-21130\,\eta+861\,\pi^2\eta\\
&\quad+2268\,\eta^2\Big)+\frac{16}{(-2Eh^2)^2}\Big(53760-176024\,\eta+4305\,\pi^2\eta\\
&\quad+15120\,\eta^2\Big)\Big\}, \qquad (5.49b)\\
n &= (-2E)^{3/2}\Big\{1+\frac{(-2E)}{8\,c^2}\,(-15+\eta)+\frac{(-2E)^2}{128\,c^4}\,\Big[555+30\,\eta
\end{aligned}$$

$$
\begin{aligned}
&+11\,\eta^2+\frac{192}{\sqrt{(-2Eh^2)}}(-5+2\,\eta)\Big]+\frac{(-2E)^3}{3072\,c^6}\Big[-29385\\
&-4995\,\eta-315\,\eta^2+135\,\eta^3+\frac{5760}{\sqrt{(-2Eh^2)}}(17-9\,\eta+2\,\eta^2)\\
&-\frac{16}{(-2Eh^2)^{3/2}}\Big(10080-13952\,\eta+123\,\pi^2\eta+1440\,\eta^2\Big)\Big]\Big\}, \qquad (5.49c)\\
{e_t}^2 \;=\;& 1+2Eh^2+\frac{(-2E)}{4\,c^2}\Big\{-8+8\,\eta-(-2Eh^2)(-17+7\,\eta)\Big\}\\
&+\frac{(-2E)^2}{8\,c^4}\Big\{12+72\,\eta+20\,\eta^2-24\sqrt{(-2Eh^2)}\,(-5+2\,\eta)\\
&-(-2Eh^2)(112-47\,\eta+16\,\eta^2)-\frac{16}{(-2Eh^2)}(-4+7\,\eta)\\
&+\frac{24}{\sqrt{(-2Eh^2)}}(-5+2\,\eta)\Big\}+\frac{(-2E)^3}{6720\,c^6}\Big\{23520-464800\,\eta\\
&+179760\,\eta^2+16800\,\eta^3-2520\,\sqrt{(-2Eh^2)}(265-193\,\eta\\
&+46\,\eta^2)-525(-2Eh^2)\Big(-528+200\,\eta-77\,\eta^2+24\,\eta^3\Big)\\
&-\frac{6}{(-2Eh^2)}\Big(73920-260272\,\eta+4305\,\pi^2\eta+61040\,\eta^2\Big)\\
&+\frac{70}{\sqrt{(-2Eh^2)}}\Big(16380-19964\,\eta+123\,\pi^2\eta+3240\,\eta^2\Big)\\
&+\frac{8}{(-2Eh^2)^2}\Big(53760-176024\,\eta+4305\,\pi^2\eta+15120\,\eta^2\Big)\\
&-\frac{70}{(-2Eh^2)^{3/2}}\Big(10080-13952\,\eta+123\,\pi^2\eta+1440\,\eta^2\Big)\Big\}, \qquad (5.49d)\\
g_{4\,t} \;=\;& -\frac{3(-2E)^2}{2}\Big\{\frac{1}{\sqrt{(-2Eh^2)}}(-5+2\,\eta)\Big\}, \qquad (5.49e)\\
g_{6\,t} \;=\;& \frac{(-2E)^3}{192}\Big\{\frac{1}{(-2Eh^2)^{3/2}}\Big(10080-13952\,\eta+123\,\pi^2\eta\\
&+1440\,\eta^2\Big)+\frac{1}{\sqrt{(-2Eh^2)}}(-3420+1980\,\eta-648\,\eta^2)\Big\}, \qquad (5.49f)
\end{aligned}
$$

$$f_{4\,t} = -\frac{(-2E)^2}{8}\left\{\frac{\sqrt{1+2Eh^2}}{\sqrt{(-2Eh^2)}}\eta\,(-15+\eta)\right\}, \tag{5.49g}$$

$$\begin{aligned} f_{6\,t} = {} & \frac{(-2E)^3}{2240}\left\{\frac{1}{(-2Eh^2)^{3/2}\sqrt{1+2Eh^2}}\Big(22400+43651\,\eta\right. \\ & -1435\,\pi^2\eta-20965\,\eta^2+385\,\eta^3\Big) \\ & +\frac{1}{\sqrt{(-2Eh^2)}\sqrt{1+2Eh^2}}\Big(-22400-49321\,\eta \\ & \left.+27300\,\eta^2+1435\,\pi^2\eta-1225\,\eta^3\Big)\right. \\ & \left.+\frac{35\,\sqrt{(-2Eh^2)}}{\sqrt{1+2Eh^2}}\,\eta\,(\,297-175\,\eta+23\,\eta^2)\right\}, \end{aligned} \tag{5.49h}$$

$$i_{6\,t} = \frac{(-2E)^3}{16}\left\{\frac{1+2Eh^2}{(-2Eh^2)^{3/2}}\,\eta\left(116-49\,\eta+3\,\eta^2\right)\right\}, \tag{5.49i}$$

$$h_{6\,t} = \frac{(-2E)^3}{192}\left\{\left(\frac{1+2Eh^2}{(-2Eh^2)}\right)^{3/2}\eta\,\left(23-73\,\eta+13\,\eta^2\right)\right\}, \tag{5.49j}$$

$$\begin{aligned} \Phi = {} & 2\,\pi\left\{1+\frac{3}{h^2c^2}+\frac{(-2E)^2}{4\,c^4}\left[\frac{3}{(-2Eh^2)}(-5+2\,\eta)\right.\right. \\ & \left.-\frac{15}{(-2Eh^2)^2}(-7+2\,\eta)\right]+\frac{(-2E)^3}{128\,c^6}\left[\frac{5}{(-2Eh^2)^3}\Big(7392\right. \\ & \left.-8000\,\eta+336\,\eta^2+123\,\pi^2\eta\Big)+\frac{24}{(-2Eh^2)}(5-5\,\eta+4\,\eta^2)\right. \\ & \left.\left.-\frac{1}{(-2Eh^2)^2}\Big(10080-13952\,\eta+123\,\pi^2\eta+1440\,\eta^2\Big)\right]\right\}, \end{aligned} \tag{5.49k}$$

$$f_{4\,\phi} = \frac{(-2E)^2}{8}\left\{\frac{1+2Eh^2}{(-2Eh^2)^2}\left(1+19\,\eta-3\,\eta^2\right)\right\}, \tag{5.49l}$$

$$\begin{aligned} f_{6\,\phi} = {} & \frac{(-2E)^3}{26880}\left\{\frac{1}{(-2Eh^2)^3}\Big(67200+994704\,\eta-30135\,\pi^2\eta\right. \\ & \left.-335160\,\eta^2-4200\,\eta^3\Big)+\frac{1}{(-2Eh^2)^2}\Big(-60480-991904\,\eta\right. \\ & \left.+30135\,\pi^2\eta+428400\,\eta^2-8400\,\eta^3\Big)+\frac{1}{(-2Eh^2)}\Big(840\right. \end{aligned}$$

$$+141680\,\eta - 99960\,\eta^2 + 10080\,\eta^3\Big)\Big\}, \tag{5.49m}$$

$$g_{4\,\phi} = -\frac{(-2E)^2}{32}\Big\{\frac{\left(1+2Eh^2\right)^{3/2}}{(-2Eh^2)^2}\,\eta\,(-1+3\,\eta)\Big\}, \tag{5.49n}$$

$$\begin{aligned} g_{6\,\phi} = {} & \frac{(-2E)^3}{8960}\,\frac{1}{\sqrt{1+2Eh^2}}\Big\{-35\,\eta\,(14-49\,\eta+26\,\eta^2) \\ & -\frac{1}{(-2Eh^2)}\,\eta\Big(-36196+1435\,\pi^2+29225\,\eta-2660\,\eta^2\Big) \\ & +\frac{1}{(-2Eh^2)^2}\,\eta\Big(-71867+2870\,\pi^2+56035\,\eta-2275\,\eta^2\Big) \\ & -\frac{1}{(-2Eh^2)^3}\,\eta\Big(-36161+1435\,\pi^2+28525\,\eta-525\,\eta^2\Big)\Big\}, \end{aligned} \tag{5.49o}$$

$$i_{6\,\phi} = \frac{(-2E)^3}{192}\Big\{\frac{(1+2Eh^2)^2}{(-2Eh^2)^3}\,\eta\,(82-57\,\eta+15\,\eta^2)\Big\}, \tag{5.49p}$$

$$h_{6\,\phi} = \frac{(-2E)^3}{256}\Big\{\frac{(1+2Eh^2)^{5/2}}{(-2Eh^2)^3}\,\eta\,(1-5\,\eta+5\,\eta^2)\Big\}, \tag{5.49q}$$

$$\begin{aligned} {e_\phi}^2 = {} & 1+2Eh^2+\frac{(-2E)}{4\,c^2}\Big\{24+(-2Eh^2)(-15+\eta)\Big\} \\ & +\frac{(-2E)^2}{16c^4}\Big\{-40+34\,\eta+18\,\eta^2-(-2Eh^2)(160 \\ & -31\,\eta+3\,\eta^2)-\frac{1}{(-2Eh^2)}(-416+91\,\eta+15\,\eta^2)\Big\} \\ & +\frac{(-2E)^3}{13440\,c^6}\Big\{-584640-17482\,\eta-4305\,\pi^2\eta-7350\,\eta^2 \\ & +8190\,\eta^3-420(-2Eh^2)\Big(744-248\,\eta+31\,\eta^2+3\,\eta^3\Big) \\ & -\frac{14}{(-2Eh^2)}\Big(36960-341012\,\eta+4305\,\pi^2\eta-225\,\eta^2 \\ & +150\,\eta^3\Big)-\frac{1}{(-2Eh^2)^2}\Big(-2956800+5627206\,\eta \\ & -81795\,\pi^2\eta+14490\,\eta^2+7350\,\eta^3\Big)\Big\}. \end{aligned} \tag{5.49r}$$

5.5 Fully 3PN-accurate expressions for the dynamical variables that appear in the expressions for $h_+|_Q(l)$ and $h_\times|_Q(l)$

Extending the results we listed in Eq. (5.40), we provide 3PN-accurate expressions for $r, \dot{r}, \phi$ and $\dot{\phi}$ in terms of ξ, e_t and η in modified harmonic gauge. The orbital separation reads

$$r \;=\; r_{\rm N} + r_{\rm 1PN} + r_{\rm 2PN} + r_{\rm 3PN}\,, \tag{5.50a}$$

where

$$r_{\rm N} \;=\; \frac{Gm}{c^2}\,\frac{1}{\xi^{2/3}}\,(e_t\,\cosh u - 1)\,, \tag{5.50b}$$

$$r_{\rm 1PN} \;=\; r_{\rm N}\times\frac{\xi^{2/3}}{6(e_t\cosh u-1)}\Big[(7\,\eta-6)\,e_t\,\cosh u + 2(\eta-9)\Big]\,, \tag{5.50c}$$

$$\begin{aligned} r_{\rm 2PN} \;=\; & r_{\rm N}\times\frac{\xi^{4/3}}{72(e_t^2-1)\,(e_t\cosh u-1)}\Big[(e_t^2-1)\,e_t\,(35\,\eta^2-231\,\eta+72)\,\cosh u \\ & -2e_t^2\,(4\,\eta^2+15\,\eta+36)+8\,\eta^2+534\eta-216\Big]\,, \end{aligned} \tag{5.50d}$$

$$\begin{aligned} r_{\rm 3PN} \;=\; & r_{\rm N}\times\frac{\xi^2}{181440(e_t^2-1)^2(e_t\cosh u-1)}\Bigg\{280\,e_t^4(16\,\eta^3+90\,\eta^2-81\,\eta+432) \\ & +140(e_t^2-1)^2e_t\,(49\,\eta^3-3933\,\eta^2\,+7047\,\eta-864)\,\cosh u \\ & -e_t^2\Big[8960\,\eta^3+3437280\,\eta^2+81(1435\,\pi^2-134336)\,\eta+3144960\Big] \\ & +4480\,\eta^3-761040\,\eta^2-348705\,\pi^2\,\eta+12143736\,\eta-4233600\Bigg\}\,. \end{aligned} \tag{5.50e}$$

The angular variable of the 3PN-accurate motion is given by

$$\phi \;=\; \phi_{\rm N} + \phi_{\rm 1PN} + \phi_{\rm 2PN} + \phi_{\rm 3PN}\,, \tag{5.51a}$$

where

$$\phi_{\rm N} = \nu\,, \tag{5.51b}$$

$$\begin{aligned}\phi_{\rm 1PN} = {} & \frac{\xi^{2/3}}{(e_t^2-1)\,(e_t\cosh u-1)}\Big[e_t\,\sqrt{e_t^2-1}\,(4-\eta)\,\sinh u \\ & +3\,\eta\,(e_t\,\cosh u-1)\Big]\,,\end{aligned} \tag{5.51c}$$

$$\begin{aligned}\phi_{\rm 2PN} = {} & \frac{\xi^{4/3}}{192(e_t^2-1)^{5/2}(e_t\cosh u-1)^2}\Bigg\{e_t\,(e_t^2-1)\,\Bigg[2\Big\{e_t^2\,\Big[384-\eta(7\eta+275)\Big] \\ & +4\Big[\eta(\eta+137)-792\Big]\Big\}\sinh u+e_t\Big\{e_t^2\Big[\eta(55\eta-109)+384\Big] \\ & -4\Big[\eta(13\eta+41)-600\Big]\Big\}\sinh 2u\Bigg]+6\sqrt{e_t^2-1}(e_t\cosh u-1)^2 \\ & \times\Big\{e_t^3(1-3\eta)\eta\sin 3\nu-8\nu\Big[e_t^2(26\eta-51)+28\eta-78\Big] \\ & +4e_t^2\Big[(19-3\eta)\eta+1\Big]\sin 2\nu\Big\}\Bigg)\,,\end{aligned} \tag{5.51d}$$

$$\begin{aligned}\phi_{\rm 3PN} = {} & \frac{\xi^2}{53760(e_t^2-1)^{7/2}(e_t\cosh u-1)^3}\Bigg(\sqrt{e_t^2-1}(e_t\cosh u-1)^3 \\ & \times\Bigg(2\,e_t^2\Bigg\{\Bigg[280\,e_t^2\Big\{\eta\,\Big[\eta\,(93\,\eta-781)+886\Big]+24\Big\} \\ & +\eta\Big\{32\Big[35\eta(9\eta-395)+36877\Big]-30135\pi^2\Big\}+84000\Bigg]\sin 2\nu \\ & +e_t\eta\Bigg[\Big\{35e_t^2\Big[\eta(129\eta-137)+33\Big]+4\Big[35\eta(51\eta-727)+28302\Big]\end{aligned} \tag{5.51e}$$

$$-4305\pi^2\Big\}\sin 3\nu + 35e_t\Big\{3e_t\Big[5(\eta-1)\eta+1\Big]\sin 5\nu + 4\Big[3\eta(5\eta-19)+82\Big]$$

$$\times\sin 4\nu\Big\}\Big]\Big\} + 420\nu\Big\{16(65e_t^4+320e_t^2+56)\eta^2 + \Big[123\,\pi^2(e_t^2+4)$$

$$-32(55e_t^4+870e_t^2+793)\Big]\eta + 96(26e_t^4+293e_t^2+190)\Big\}\Big)$$

$$+e_t(e_t^2-1)\sinh u\Big\{-70e_t^6\eta\Big[\eta(71\eta+61)-639\Big] + 1680e_t^4(\eta-4)\cosh^2 u$$

$$\times\Big\{3e_t\eta(3\eta-1)\cos 3\nu + 8\Big[\eta(3\eta-19)-1\Big]\cos 2\nu\Big\}$$

$$+e_t^4\Big[\eta\Big\{4\Big[70\eta(125\eta-507)-462853\Big]-4305\pi^2\Big\}+3933440\Big]$$

$$+1680e_t^2(\eta-4)\Big\{3e_t\eta(3\eta-1)\cos 3\nu + 8\Big[\eta(3\eta-19)-1\Big]\cos 2\nu\Big\}$$

$$+e_t^2\Big\{6\eta\Big[140\eta(25\eta-397)+1435\pi^2-917424\Big]+7947520\Big\}$$

$$+4e_t\cosh u\Big\{-70e_t^4\Big\{\eta\Big[\eta(39\eta-719)+2279\Big]-3072\Big\}$$

$$+840e_t^2(\eta-4)\Big\{3e_t(1-3\eta)\eta\cos 3\nu + 8\Big[(19-3\eta)\eta+1\Big]\cos 2\nu\Big\}$$

$$+e_t^2\Big[\eta\Big\{8\Big[35(232-53\eta)\eta+186959\Big]+4305\pi^2\Big\}-2983680\Big]$$

$$-20\Big[323904-\eta\Big\{4\Big[7\eta(\eta+45)+56013\Big]-861\pi^2\Big\}\Big]\Big\}$$

$$+e_t^2\Big\{-70e_t^4\eta\Big[\eta(71\eta+61)-639\Big]+e_t^2\Big[\eta\Big\{4\Big[35\,\eta$$

$$\times(229\eta - 1173) - 384978\Big] - 4305\pi^2\Big\} + 3646720\Bigg]$$

$$+20\Bigg[\eta\Big\{861\pi^2 - 4\Big[14\eta(9\eta - 25) + 54025\Big]\Big\} + 280000\Bigg]\Bigg\}\cosh 2u$$

$$+40\Big[\eta(1456\eta + 861\pi^2 - 253508) + 396480\Big]\Big\}\Bigg)\,, \tag{5.51f}$$

with $\nu = 2\arctan(\sqrt{\frac{e_t^2+1}{e_t^2-1}}\tanh\frac{u}{2})$ as before. Furthermore, we require explicit expressions for the first time derivatives $\dot{r}$ and $\dot{\phi}$ to compute GW waveforms from binaries in hyperbolic orbits, namely,

$$\dot{r} = \dot{r}_{\rm N} + \dot{r}_{\rm 1PN} + \dot{r}_{\rm 2PN} + \dot{r}_{\rm 3PN}\,, \tag{5.52a}$$

$$\dot{r}_{\rm N} = \xi^{1/3}\frac{c\,e_t\,\sinh u}{e_t\cosh u - 1}\,, \tag{5.52b}$$

$$\dot{r}_{\rm 1PN} = \dot{r}_{\rm N}\times\frac{\xi^{2/3}}{6}\,(7\eta - 6)\,, \tag{5.52c}$$

$$\begin{aligned}\dot{r}_{\rm 2PN} = {}& \dot{r}_{\rm N}\times\frac{\xi^{4/3}}{72(e_t\cosh u - 1)^2}\Big\{9e_t(\eta - 15)\eta\,\cos\nu \\ & +e_t\Big[7\eta(5\eta - 33) + 72\Big]\cosh u(e_t\cosh u - 2) \\ & +5\eta(7\eta - 3) - 468\Big\}\,,\end{aligned} \tag{5.52d}$$

$$\begin{aligned}\dot{r}_{\rm 3PN} = {}& \dot{r}_{\rm N}\times\frac{\xi^2}{181440(e_t^2-1)^{3/2}(e_t\cosh u - 1)^3} \\ & \times\Bigg\{3780(e_t^2-1)^{3/2}(7\eta - 6)(e_t\cosh u - 1)\Big[e_t(\eta - 15)\eta\cos\nu + 24\eta \\ & -60\Big] + 140(e_t^2-1)^{3/2}(49\eta^3 - 3933\eta^2 + 7047\eta - 864)(e_t\cosh u - 1)^3\end{aligned}$$

$$
\begin{aligned}
&-27\Big[-840(e_t^2-1)e_t^2\eta(\eta^2-19\eta+60)\sin\nu\sinh u-840\sqrt{e_t^2-1}e_t^3\\
&\times\eta(\eta^2-19\eta+60)\cos\nu\sinh^2 u+840\sqrt{e_t^2-1}e_t^3\eta(\eta^2-19\eta+60)\cos\nu\\
&\times\cosh^2 u+\sqrt{e_t^2-1}e_t\cosh u\Big\{e_t\Big[35(65e_t^2-32)\eta^3-525(27e_t^2+88)\eta^2\\
&+(-315e_t^2-4305\pi^2+93468)\eta+67200\Big]\cos\nu+35\Big[3e_t^3\eta(13\,\eta^2-73\,\eta+23)\,\cos 3\nu\\
&+24e_t^2\eta(3\eta^2-49\eta+116)\cos 2\nu+1056e_t^2\,\eta^2-2784\,e_t^2\,\eta+2880\,e_t^2+384\,\eta^2\\
&+123\pi^2\eta-9440\eta+2880\Big]\Big\}-\sqrt{e_t^2-1}\Big\{e_t\Big[35(65e_t^2-8)\eta^3\\
&-105(135e_t^2+592)\eta^2-3\,(105e_t^2+1435\pi^2-47956)\eta+67200\Big]\cos\nu\\
&+35\Big[3e_t^3\eta(13\eta^2-73\eta+23)\cos 3\nu+24e_t^2\eta(3\eta^2-49\eta+116)\,\cos 2\nu\\
&+480e_t^2\,\eta^2+960e_t^2\eta-2880e_t^2+960\eta^2\\
&+123\pi^2\eta-13184\eta+8640\Big]\Big\}\Big]\Big\}\,, \qquad (5.52e)
\end{aligned}
$$

as well as

$$\dot\phi = \dot\phi_{\rm N}+\dot\phi_{\rm 1PN}+\dot\phi_{\rm 2PN}+\dot\phi_{\rm 3PN}\,, \qquad (5.53a)$$

$$\dot\phi_{\rm N} = \frac{n\sqrt{e_t^2-1}}{(e_t\cosh u-1)^2}\,, \qquad (5.53b)$$

$$\dot\phi_{\rm 1PN} = \dot\phi_{\rm N}\times\frac{\xi^{2/3}}{(e_t^2-1)(e_t\cosh u-1)}\Big[e_t^2(\eta-4)+e_t(\eta-1)\cosh u-3\Big]\,, \qquad (5.53c)$$

$$\dot\phi_{\rm 2PN} = \dot\phi_{\rm N}\times\frac{\xi^{4/3}}{192(e_t^2-1)^2(e_t\cosh u-1)^2}\Big\{-6e_t^4\cosh^2 u\Big[3e_t\eta(3\eta-1)\cos 3\nu$$

$$+8(3\eta^2-19\eta-1)\cos 2\nu\Big]-e_t^2\Big[e_t^2\,(103\eta^2+131\eta-72)$$

$$-4(25\eta^2-223\eta+60)\Big]\cosh 2u+2e_t\cosh u\Big[55e_t^4\eta^2-109e_t^4\eta+384e_t^4$$

$$+18e_t^3\eta(3\eta-1)\cos 3\nu+48e_t^2(3\eta^2-19\eta-1)\cos 2\nu-45e_t^2\eta^2$$

$$+1359e_t^2\eta-432e_t^2-4\eta^2+796\eta-576\Big]+3\Big[-7e_t^4\eta^2-291e_t^4\eta$$

$$+312e_t^4-18e_t^3\eta^2\cos 3\nu+6e_t^3\eta\cos 3\nu+16e_t^2(-3\eta^2+19\eta+1)\cos 2\nu$$

$$+8(e_t^2-1)^2e_t(\eta-15)\eta\cos\nu+4e_t^2\eta^2-476e_t^2\eta-768e_t^2-256\eta+768\Big]\Big\}, \qquad (5.53d)$$

$$\dot{\phi}_{3\mathrm{PN}} = \dot{\phi}_{\mathrm{N}}\times\frac{\xi^2}{107520(e_t^2-1)^3(e_t\cosh u-1)^3}\Bigg(140\eta\Big\{16\Big[3\eta(5\eta-19)+82\Big]$$

$$\times\cos 4\nu+15e_t\Big[5(\eta-1)\eta+1\Big]\cos 5\nu\Big\}\cosh^3 u\,e_t^7$$

$$+4\Bigg\{3e_t\eta\Bigg[-525\Big[5(\eta-1)\eta+1\Big]\cos 5\nu\,e_t^2-560\Big[3\eta(5\eta-19)+82\Big]$$

$$\times\cos 4\nu e_t+2\Big\{-35\Big[\eta\,(93\eta+19)-15\Big]e_t^2-8\Big[35\eta(21\eta-344)+13941\Big]$$

$$+4305\pi^2\Big\}\cos 3\nu\Bigg]-4\Bigg[\eta\Big\{280(75\eta^2-595\eta+436)e_t^2$$

$$+16\Big[35\eta(9\eta-697)+65879\Big]-30135\pi^2\Big\}+77280\Bigg]\cos 2\nu\Bigg\}\cosh^2 u\,e_t^4$$

$$+\Bigg[70\Big\{\eta\Big[\eta(291\eta+1865)-2639\Big]+1344\Big\}e_t^4+\Big\{\eta\Big[140(10271-475\eta)\eta$$

$$+30135\pi^2-4218008\Big]+934080\Big\}e_t^2-240(5521\eta+56)+140\eta\Big[16\,\eta\,(13\eta+24)$$

$$+615\pi^2\Big]\Big]\cosh 3u e_t^3+2\Big\{-3\eta\Big\{35\Big[\eta(129\eta-137)+33\Big]e_t^2$$

$$+1540\eta(3\eta-59)-4305\pi^2+109848\Big\}\cos 3\nu\, e_t^3-2\Big[280\Big\{\eta\Big[\eta\,(93\,\eta-781)$$

$$+886\Big]+24\Big\}e_t^2+(-338240\eta-30135\pi^2+928064)\eta+70560\Big]\cos 2\nu\, e_t^2$$

$$-70(71e_t^6-572e_t^4-260e_t^2+32)\eta^3-70(61e_t^6+14900e_t^4+44228e_t^2+10336)\eta^2$$

$$+6720(138e_t^4-377e_t^2-214)+\Big[44730e_t^6+518508e_t^4+8417056e_t^2-4305(e_t^2+8)^2\pi^2$$

$$+8203040\Big]\eta\Big\}\cosh 2u\, e_t^2+\cosh u\Big(-70\Big\{\eta\Big[\eta(319\eta-8163)$$

$$+16997\Big]-30144\Big\}e_t^6+\Big[\eta\Big\{55965\pi^2-4\Big[35\eta(1331\eta-56471)$$

$$+953852\Big]\Big\}-7627200\Big]e_t^4+2\Big\{2\Big[280\Big\{\eta\Big[\eta(93\eta-781)+886\Big]$$

$$+24\Big\}e_t^2+(-338240\eta-30135\pi^2+928064)e_t+70560\Big]\cos 2\nu$$

$$+3e_t\eta\Big\{35\Big[\eta(129\eta-137)+33\Big]e_t^2+1540\eta(3\eta-59)-4305\pi^2$$

$$+109848\Big\}\cos 3\nu\Big\}\cosh 2u\, e_t^4+56\Big\{\eta\Big[10(24299-83\,\eta)\,\eta+10455\,\pi^2-739322\Big]$$

$$+130320\Big\}e_t^2+2\Big(e_t\Big(2\Big\{280\Big\{\eta\Big[\eta(57\eta-193)-506\Big]+24\Big\}$$

$$\times e_t^4 + \Bigg[\eta\Big\{16\Big[35\eta(243\eta - 2791) + 136754\Big] - 30135\pi^2\Big\} + 57120\Bigg] e_t^2$$

$$+6\Bigg[\eta\Big\{16\Big[35\eta(9\eta - 679) + 64444\Big] - 30135\pi^2\Big\} + 79520\Bigg]\Bigg\}\cos 2\nu$$

$$+3e_t\eta\Bigg\{\Bigg[35\Big[\eta(25\eta + 447) - 151\Big]e_t^4 + \Big\{2\Big[35\eta(413\eta - 1669) + 58109\Big]$$

$$-4305\pi^2\Big\}e_t^2 + 8\Big[70\eta(61\eta - 1015) + 83261\Big] - 25830\pi^2\Bigg]\cos 3\nu$$

$$+70e_t\Big\{16\left[3\,\eta\,(5\eta - 19) + 82\right]\cos 4\nu + 15e_t\left[5(\eta - 1)\eta + 1\right]\cos 5\nu\Big\}\Bigg\}\Bigg)$$

$$-8\,(e_t^2 - 1)^2\Bigg[\eta\Big\{35\left[5\eta(13\eta - 81) - 9\right]e_t^2 - 4\Big[70\eta(7\eta + 117) - 20217\Big]$$

$$-4305\pi^2\Big\} + 67200\Bigg]\cos\nu\Bigg)e_t + 320\Big[\eta(7028\eta + 3444\pi^2 - 123467) + 42000\Big]\Bigg)e_t$$

$$+2\Bigg(-70(71e_t^4 - 542e_t^2 - 744)\eta^3\,e_t^4$$

$$+\Bigg(8\Bigg[\eta\Big\{35\Big[\eta(17\eta + 507) - 2889\Big]e_t^2 - 4\Big[70\eta(\eta + 231) - 45417\Big]$$

$$-4305\pi^2\Big\} + 67200\Bigg]\cos\nu\,(e_t^2 - 1)^2 + e_t(-2\Bigg\{280\Big\{\eta\Big[\eta(57\eta - 193)$$

$$-506\Big] + 24\Big\}e_t^4 + \Bigg[\eta\Big\{16\Big[35\eta(93\eta - 1601) + 106234\Big] - 30135\pi^2\Big\}$$

$$+57120\Bigg]e_t^2 + 64(30787\eta + 2625) + 70\eta\Big[16\eta(9\eta - 643) - 861\pi^2\Big]\Bigg\}\cos 2\nu$$

$$+e_t\eta\Bigg\{3\Bigg[-35\Big[\eta(25\eta+447)-151\Big]\,e_t^4+\Big\{4305\pi^2-2\Big[35\eta(227\eta-1707)$$

$$+59159\Big]\Big\}e_t^2+2\Big[280(327-19\eta)\eta+4305\pi^2-109988\Big]\Bigg]\cos 3\nu+70\,e_t$$

$$\times\Big\{-16\Big[3\eta(5\eta-19)+82\Big]\cos 4\nu-15e_t\Big[5(\eta-1)\eta+1\Big]\cos 5\nu\Big\}\Bigg\}$$

$$-840\sqrt{e_t^2-1}(\eta-4)\Big\{64e_t\Big[\eta(3\eta-19)-1\Big]\cos\nu(e_t\cosh u-1)^2$$

$$+36e_t^2\eta(3\eta-1)\cos 2\nu(e_t\cosh u-1)^2+\eta\Big[(19\eta+111)e_t^4+9(3\eta-1)$$

$$\times(e_t\cosh 2u-4\cosh u)e_t^3+(70\eta-258)e_t^2-8(\eta-15)\Big]\Big\}\sin\nu\sinh u)\Bigg)e_t$$

$$-70(61e_t^8+11454e_t^6+57640e_t^4+45184e_t^2+1536)\eta^2+6720(34e_t^6-e_t^4$$

$$-188e_t^2-600)+\Big[44730e_t^8+263008e_t^6+4781712e_t^4+17066880e_t^2$$

$$-4305(e_t^6+10e_t^4+84e_t^2+40)\pi^2+6482560\Big]\eta\Bigg)\Bigg)\,. \tag{5.53e}$$

5.6 Relations between coefficients in the parametrization of $t-t_0$ and $\phi-\phi_0$

Our 3PN-accurate Keplerian-type parametric solution, derived from first principles, relies on explicit expressions for certain coefficients c_i, c_i' and e_i, e_i' to parametrize the radial and angular motion, respectively. In Sec. II.B, we have used the following explicit relations between coefficients c_i and $c_i' = b_i/(a_r^{i-1}\sqrt{-s_+\,s_-})$ to obtain the parametric solution for $t-t_0$ in Eq. (5.28) from Eq. (5.27).

$$c_0 = c_0'\,e_r\,, \tag{5.54a}$$

$$c_1 = c_0' - c_1' \,, \tag{5.54b}$$

$$c_2 = \frac{c_2'}{(e_r^2-1)^{1/2}} + \frac{c_3'}{(e_r^2-1)^{3/2}} + \frac{c_4'\,(e_r^2+2)}{2\,(e_r^2-1)^{5/2}} + \frac{c_5'}{(e_r^2-1)^{7/2}}(1+\frac{3e_r^2}{2}) \,, \tag{5.54c}$$

$$c_3 = \frac{c_3'\,e_r}{(e_r^2-1)^{3/2}} + \frac{2\,c_4'\,e_r}{(e_r^2-1)^{5/2}} + \frac{c_5'}{(e_r^2-1)^{7/2}}\,(3\,e_r + \frac{3}{4}\,e_r^3) \,, \tag{5.54d}$$

$$c_4 = \frac{c_4'\,e_r^2}{4\,(e_r^2-1)^{5/2}} + \frac{3\,c_5'\,e_r^2}{4\,(e_r^2-1)^{7/2}} \,, \tag{5.54e}$$

$$c_5 = \frac{c_5'\,e_r^3}{12\,(e_r^2-1)^{7/2}} \,. \tag{5.54f}$$

Also in Sec. II.B, the parametric solution for $\phi - \phi_0$ in Eq. (5.31) was obtained from Eq. (5.30) by using explicit relations between the coefficients e_i and $e_i' = d_i/(a_r^{i+1}\sqrt{-s_+s_-})$, namely:

$$\begin{aligned} e_0 =& \frac{e_0'}{(e_r{}^2-1)^{1/2}} + \frac{e_1'}{(e_r{}^2-1)^{3/2}} + \frac{e_2'\left(e_r{}^2+2\right)}{2\,(e_r{}^2-1)^{5/2}} + \frac{e_3'\,(3e_r{}^2+2)}{2\,(e_r{}^2-1)^{7/2}} \\ &+ \frac{e_4'\left(3e_r{}^4+24e_r{}^2+8\right)}{8\,(e_r{}^2-1)^{9/2}} + \frac{e_5'\left(15e_r{}^4+40e_r{}^2+8\right)}{8\,(e_r{}^2-1)^{11/2}}, \end{aligned} \tag{5.55a}$$

$$\begin{aligned} e_1 =& \frac{e_1'e_r}{(e_r{}^2-1)^{3/2}} + \frac{2e_2'e_r}{(e_r{}^2-1)^{5/2}} + \frac{3e_3'\left(e_r{}^2+4\right)e_r}{4\,(e_r{}^2-1)^{7/2}} + \frac{e_4'\left(3e_r{}^2+4\right)e_r}{(e_r{}^2-1)^{9/2}} \\ &+ \frac{5e_5'\left(e_r{}^4+12e_r{}^2+8\right)e_r}{8\,(e_r{}^2-1)^{11/2}} \,, \end{aligned} \tag{5.55b}$$

$$e_2 = \frac{e_2'e_r{}^2}{4\,(e_r{}^2-1)^{5/2}} + \frac{3e_3'e_r{}^2}{4\,(e_r{}^2-1)^{7/2}} + \frac{e_4'\left(e_r{}^2+6\right)e_r{}^2}{4\,(e_r{}^2-1)^{9/2}} + \frac{5e_5'\left(e_r{}^2+2\right)e_r{}^2}{4\,(e_r{}^2-1)^{11/2}} \,, \tag{5.55c}$$

$$e_3 = \frac{e_3'e_r{}^3}{12\,(e_r{}^2-1)^{7/2}} + \frac{e_4'e_r{}^3}{3\,(e_r{}^2-1)^{9/2}} + \frac{5e_5'\left(e_r{}^2+8\right)e_r{}^3}{48\,(e_r{}^2-1)^{11/2}} \,, \tag{5.55d}$$

$$e_4 = \frac{e_4'e_r{}^4}{32\,(e_r{}^2-1)^{9/2}} + \frac{5e_5'e_r{}^4}{32\,(e_r{}^2-1)^{11/2}} \,, \tag{5.55e}$$

$$e_5 = \frac{e_5'e_r{}^5}{80\,(e_r{}^2-1)^{11/2}} \,. \tag{5.55f}$$

5.7 Comparisons with Numerical Relativity

Our PN waveforms and numerical relativity (NR) waveforms are compared as Fig.5.3 for an illustrative example. The NR waveform was generated in the same way of Bae et al. (2017). The two waveforms seem to make an agreement. Note that this comparison was not made neither in quantitative nor in algorithmic manner.

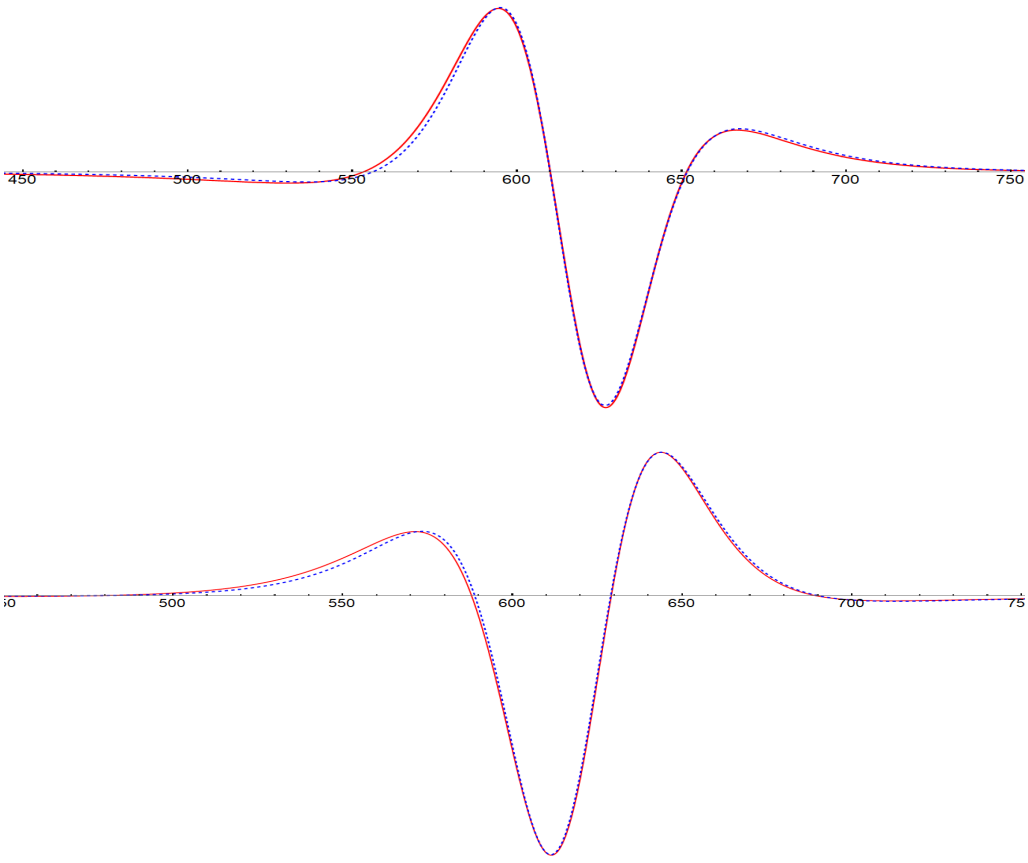

Figure 5.3 Comparison of $\psi 4$ between numerical relativity simulation results and our hyperbolic waveform. The above one is real-valued part and the below one is imaginary part with $h = 5.6$ and $E = 0$ initially.

5.8 Conclusions

In this chapter, we provided 'ready-to-use' time-domain GW polarization templates for compact binaries moving in fully 3.5PN-accurate hyperbolic orbits. A crucial input for constructing these waveforms is our *ab-initio* derivation of 3PN-accurate Keplerian type parametric solution for compact binaries in hyperbolic orbits. Our effort extended to 3PN order the classic 1PN result of Damour and Deruelle,obtained by the argument of analytic continuation Damour and Deruelle (1985). Additionally, we provided two critical checks to verify the correctness of our solution and its lengthy 3PN-accurate expressions. We incorporated the effects of GW emission, occurring at 2.5PN and 3.5PN orders in the orbital dynamics, by adapting for hyperbolic orbits GW phasing formalism for eccentric inspirals, detailed in Damour et al. (2004); Königsdörffer and Gopakumar (2006). This is how we constructed our PN-accurate GW templates, namely temporally evolving GW polarization states, for hyperbolic encounters.

The present effort should be useful in a number of on-going investigations. Our templates are being implemented in the LSC Algorithm Library Suite (LALSuite). This is to explore the possibility of searching for the presence o such GW events in the interferometric data streams in the near future. We list the following plausible astrophysical considerations for initiating such efforts. It was pointed out that such encounters involving neutron stars can give rise to certain resonant shattering flares in the electromagnetic sector due to strong tidal interactions between neutron stars during hyperbolic encounters, though event rates are expected to be low Tsang (2013). Very recently, it was argued that aLIGO relevant GW burst events may occur during hyperbolic encounters of Primordial Black Holes in dense clusters García-Bellido and Nesseris (2018). Therefore, it should be of some interest to explore the search sensitivity and the possible false alarm rates of hyperbolic GW events by adapting such an effort for eccentric inspirals Tiwari et al. (2016).

The present computation will be crucial to obtain fully 3PN-accurate expressions for radiated energy and angular momentum fluxes associated with hyperbolic encounters. which

are only available to 1PN-order Blanchet and Schaefer (1989); Junker and Schaefer (1992). Currently, these computations are being extended to 3PN order Boetzel et al. (2018). These investigation is expected to complement efforts that focus on the scatterings of test particles by black hole space-time Hopper and Cardoso (2018); Bini and Geralico (2017); Hopper (2018). It will also be desirable to adapt Bini and Damour (2012, 2017) for exploring our GW burst signals using the framework of effective-one-body formalism.

Chapter 6

Summary and Future Works

In order to build reliable and accurate GW waveforms efficiently, post-Newtonian formalism is the most important method. The PN efforts are two-fold: (1) Reducing Einstein's field equations to PN equations of motion, and (2) Solving the PN equations and getting GW waveforms. This thesis has presented some of the hitherto most accurate and efficient ongoing efforts of the latter.

In the chapter 3, we derived fourth post-Newtonian (4PN) order contributions to Keplerian-type parametric solution for describing dynamics of non-spinning compact binaries in eccentric orbits. The underlying compact binary dynamics is described by the 4PN accurate near-zone local-in-time ADM Hamiltonian. We provide explicit expressions up to 4PN order for various orbital elements and functions of our parametric solution in terms of the conserved orbital energy, angular momentum for a given symmetric mass ratio. The resulting parametric solution is employed to obtain an updated inspiral, merger and ring-down waveform family to model the coalescence of non spinning black hole binaries in moderately eccentric orbits. Our parametric solution can be used to compute the waveforms of gravitational waves for binaries with moderate eccentricity. Our formalism cannot be used to follow the orbits during the merger phase since the PN approach breaks down. The waveforms during the merger and ringdown can be modeled with total mass of the

binaries assuming that the orbit is fully circulatized before these phases based on the results of numerical relativity (mereger phase) and perturbation theory (ring-down phase) (Hinder et al. (2018)). Following the procedure by Hinder et al. (2018), we have obtained full waveforms starting from inspiral phase to merger and ring-down (IMR) for eccentrici binaries. Since most time consuming part of the inspiral phase is computed using our analytic expressions, the generation of the full waveform requires very small amount of computing time. Our scheme can be efficiently used to search for eccentric binaries from gravitational wave data. We will separately publish a paper that describes the derivation of the full waveforms and corresponding computer code.

In the chapter 4, we have solved the spin precession equation and the Newtonian orbital motion in ADM gauge for binary system with arbitrary spins, mass ratio and eccentricity, up to leading order of spin orbit coupling. We arrived at quasi-Keplerian parametric solutions in a simple closed form. The elliptic functions are essential in our parametrizations and they have been thoroughly speculated by mathematicians. So our solutions are expected to give us systematic and mathematically deep understandings on how rotating bodies move in gravitational field.

In the chapter 5, we provided formalism for the computations of 'ready-to-use' time-domain GW polarization templates for compact binaries moving in fully 3.5PN-accurate hyperbolic orbits. A crucial input for constructing these waveforms is our *ab-initio* derivation of 3PN-accurate Keplerian type parametric solution for compact binaries in hyperbolic orbits. Our effort extended to 3PN order of the classic 1PN result by the argument of analytic continuation Damour and Deruelle (1985). Additionally, we provided two critical checks to verify the correctness of our solution and its lengthy 3PN-accurate expressions. We incorporated the effects of GW emission, occurring at 2.5PN and 3.5PN orders in the orbital dynamics, by adapting hyperbolic orbits GW phasing formalism for eccentric inspirals, detailed in Damour et al. (2004); Königsdörffer and Gopakumar (2006). This is how we constructed our PN-accurate GW templates, namely temporally evolving GW

polarization states, for hyperbolic encounters. The present computation will be crucial to obtain fully 3PN-accurate expressions for radiated energy and angular momentum fluxes associated with hyperbolic encounters. which are only available to 1PN-order Blanchet and Schaefer (1989); Junker and Schaefer (1992). Currently, these computations are being extended to 3PN order by Boetzel et al. (2018). Such an extension is expected to complement the efforts that focus on the scatterings of test particles by black hole space-time (Hopper and Cardoso (2018); Bini and Geralico (2017); Hopper (2018)). It will also be desirable to adapt the scheme of Bini and Damour (2012, 2017) for exploring our GW burst signals using the framework of effective-one-body formalism.

In near future, what we have presented is planned to be extended to more general cases. The first one could be gravitational waveforms from eccenctirc binaries of spinning compact objects, which would be the most generic binaries we are likely to meet. The phase correction due to the leading order of spin-orbit interaction, was calculated in the chpater 4, but we did not present explicit expressions of gravitational waveforms. It is because the leading order spin-orbit interaction is not enough to build reliable GW waveforms, since at least, the leading order of spin-spin interaction is also required even for moderately spinning objects (Gergely (1999)). However, the spin-precession equations containing spin-spin interaction is known to be non-integrable and hence hard to integrate them. In many literatures (Kesden et al. (2015); Klein et al. (2013)), averaging spin precession equations with respect to orbit period is usually adopted to solve the spin-precession equations, but the averaging method does not mathematically gaurantee that it holds after a long time (in this case, longer than spin-precession time scale). Thus we should examine the reliabilty of the averaging method as well as look for integrating the spin precession equations without averaging.

The second one is to get conditions for caputring of binaries, *i.e.* transitions from hyperbolic orbits to elliptic orbits. It could be estimated as what follows: (1) Assume that a binary is captured *i.e.* initial eccentricity is almost unity. (2) Expand Eq.(5.45a) and

Eq.(5.45b) around $e_t = 1$ (e_t is a time-eccentricity). (3) Integrate the expanded dissipative equations around $e_t = 1$ and periastron $u = 0$. (4) Then we might get the conditions for the gravitational capturing.

In the long-term perspective, we still have a long way to go as described illustratively below. In the chapter 1, we have introduced the slow time $\hat{t} = \epsilon\, t$. The small parameter $\epsilon = \frac{\dot{\omega}}{\omega^2}$, is formally the order of $\frac{1}{c^5}$. The radiation-reaction scale of $\hat{t} \sim \frac{1}{\omega}$, $t_r \sim \frac{\omega}{\dot{\omega}}$ is in the order of $t_r \sim \mathcal{O}(c^8)$. Hence, integrating PN equations of motion for (non-spinning) compact binaries as long as $t \sim t_r$ is given as

$$\ddot{\mathbf{x}} = \sum_{n=0}^{\infty} \frac{1}{c^n} \ddot{\mathbf{x}}_{(n)}\,, \tag{6.1}$$

$$\begin{aligned} \delta\mathbf{x} &\sim \int^{t_r} dt \int^{t_r} dt\, \ddot{\mathbf{x}} \sim t_r^2 \int^1 d\tilde{t} \int^1 d\tilde{t} \sum_{n=0}^{\infty} \frac{1}{c^n} \ddot{\mathbf{x}}_{(n)}\,, \\ &\sim \int^1 d\tilde{t} \int^1 d\tilde{t} \sum_{n=0}^{\infty} c^{16-n}\, \ddot{\mathbf{x}}_{(n)}\,. \end{aligned} \tag{6.2}$$

Note that, for instance, the phase correction due to $n = 8$ (4PN) order contribution in the acceleration, is not small but numerically very large $\sim \mathcal{O}(c^8)$. Furthermore, even $n = 16$ (8PN) order contribution can not be neglected but gives a moderate correction ($\sim \mathcal{O}(c^0)$) proportional to square of integration time. The higher than 8PN order terms could be ignored.

This 8PN journey will be very exhausting. From the birth of Einstein's field equations to the calculation of state-of-the-art 4PN correction, it has taken about 90 years. However, since this requirement of the intensively high order contributions does not come from the need of knowledge on the PN acceleration but from the long-term evolution, hence, we can partially focus on dissipative contributions, which lead to secular drifting, to the relative 5.5PN order. This could be acheived via MPM theory. As recent progresses, one can find 4.5PN accurate the 'tails-of-tails-of-tails' radiative moments in Marchand et al. (2016), and

the 4PN accurate the source quadrupole moment in terms of post-Newtonian sources in Marchand et al. (2020) in BDI formalism. Although we have not considered in this thesis, the traditional phasing formalism (Damour et al. (2004); Königsdörffer and Gopakumar (2006)) is expected to be re-formulated in such a high order flux. Furthermore, the effects of spin to the flux to the higher order also should be considered and the equations of motion for spinning compact binaries has been well developed, which can be found in Porto et al. (2011); Blanchet et al. (2011); Bohé et al. (2013) as examples. On the other hand, although extending the osculating QKP parametrization method to spinning compact binaries is very crucial because of their chaotic behaviour (Huang and Wu (2016)), but it still remains so out of reach that phasing formalism with the additional time scale (time scale of spin-precession) for spinning compact binaries, has not even been reliably constructed.

We are expecting that what has been presented in this thesis could be a cornerstone of extension to compeleting the higher order phase corrections as well as extending the phasing formalism for spinning compact binaries.

Bibliography

Abbott, B. P., Abbott, R., Abbott, T. D., Abernathy, M. R., Acernese, F., Ackley, K., Adams, C., Adams, T., Addesso, P., Adhikari, R. X., et al. (2016a). GW150914: The Advanced LIGO Detectors in the Era of First Discoveries. *Physical Review Letters*, 116(13):131103.

Abbott, B. P., Abbott, R., Abbott, T. D., Abernathy, M. R., Acernese, F., Ackley, K., Adams, C., Adams, T., Addesso, P., Adhikari, R. X., et al. (2016b). GW151226: Observation of Gravitational Waves from a 22-Solar-Mass Binary Black Hole Coalescence. *Physical Review Letters*, 116(24):241103.

Abbott, B. P., Abbott, R., Abbott, T. D., Abernathy, M. R., Acernese, F., Ackley, K., Adams, C., Adams, T., Addesso, P., Adhikari, R. X., et al. (2016c). Observation of Gravitational Waves from a Binary Black Hole Merger. *Physical Review Letters*, 116(6):061102.

Abbott, B. P., Abbott, R., Abbott, T. D., Acernese, F., Ackley, K., Adams, C., Adams, T., Addesso, P., Adhikari, R. X., Adya, V. B., and et al. (2017a). GW170104: Observation of a 50-Solar-Mass Binary Black Hole Coalescence at Redshift 0.2. *Physical Review Letters*, 118(22):221101.

Abbott, B. P., Abbott, R., Abbott, T. D., Acernese, F., Ackley, K., Adams, C., Adams, T., Addesso, P., Adhikari, R. X., Adya, V. B., and et al. (2017b). GW170608: Observation

of a 19 Solar-mass Binary Black Hole Coalescence. *ApJ*, 851:L35.

Abbott, B. P., Abbott, R., Abbott, T. D., Acernese, F., Ackley, K., Adams, C., Adams, T., Addesso, P., Adhikari, R. X., Adya, V. B., and et al. (2017c). GW170814: A Three-Detector Observation of Gravitational Waves from a Binary Black Hole Coalescence. *Physical Review Letters*, 119(14):141101.

Abbott, B. P., Abbott, R., Abbott, T. D., Acernese, F., Ackley, K., Adams, C., Adams, T., Addesso, P., Adhikari, R. X., Adya, V. B., and et al. (2017d). GW170817: Observation of Gravitational Waves from a Binary Neutron Star Inspiral. *Physical Review Letters*, 119(16):161101.

Arnowitt, R., Deser, S., and Misner, C. W. (2008). Republication of: The dynamics of general relativity. *Gen. Relativ. Gravit.*, 40(9):1997–2027.

Arun, K. G., Blanchet, L., Iyer, B., and Sinha, S. (2009). Third post-Newtonian angular momentum flux and the secular evolution of orbital elements for inspiralling compact binaries in quasi-elliptical orbits. *Phys. Rev. D*, 80(12):124018.

Bae, Y. B., Lee, H. M., Kang, G., and Hansen, J. (2017). Gravitational radiation driven capture in unequal mass black hole encounters. *Phys. Rev. D*, 96(8).

Bailey, I. and Israel, W. (1983). Lagrangian Dynamics of Spinning Particles and Polarized Media in General Relativity. *Commun. Math. Phys.*, 588(1):577–588.

Bernard, L., Blanchet, L., Bohé, A., Faye, G., and Marsat, S. (2017). Energy and periastron advance of compact binaries on circular orbits at the fourth post-Newtonian order. *Phys. Rev. D*, 95(4):044026.

Bernard, L., Blanchet, L., Faye, G., and Marchand, T. (2017). Center-of-Mass Equations of Motion and Conserved Integrals of Compact Binary Systems at the Fourth Post-Newtonian Order. *Phys. Rev. D*, 97(4).

Bernard, L., Blanchet, L., Faye, G., and Marchand, T. (2018). Center-of-mass equations of motion and conserved integrals of compact binary systems at the fourth post-Newtonian order. *Phys. Rev. D*, 97(4):044037.

Bini, D. and Damour, T. (2012). Gravitational radiation reaction along general orbits in the effective one-body formalism. *Phys. Rev. D*, 86(12):124012.

Bini, D. and Damour, T. (2017). Gravitational scattering of two black holes at the fourth post-Newtonian approximation. *Phys. Rev. D*, 96(6):064021.

Bini, D. and Geralico, A. (2017). Hyperbolic-like elastic scattering of spinning particles by a Schwarzschild black hole. *General Relativity and Gravitation*, 49:84.

Blanchet, L. (1987). Radiative Gravitational Fields in General Relativity: Ii. Asymptotic Behaviour At Future Null Infinity. *Proc. R. Soc. London, Ser. A Math. Phys. Sci.*, 409(1837):383–399.

Blanchet, L. (1993). Time-asymmetric structure of gravitational radiation. *Phys. Rev. D*, 47(10):4392–4420.

Blanchet, L. (1998). On the multipole expansion of the gravitational field. *Class. Quantum Gravity*, 15(7):1971–1999.

Blanchet, L. (2014). Gravitational Radiation from Post-Newtonian Sources and Inspiralling Compact Binaries. *Living Rev. Relativ.*, 17.

Blanchet, L., Buonanno, A., and Faye, G. (2006). Higher-order spin effects in the dynamics of compact binaries. II. Radiation field. *Phys. Rev. D*, 74(10):104034.

Blanchet, L., Buonanno, A., and Faye, G. (2011). Tail-induced spin-orbit effect in the gravitational radiation of compact binaries. Technical Report 6.

Blanchet, L. and Damour, T. (1986). Radiative gravitational fields in general relativity I. General structure of the field outside the source. *Philos. Trans. R. Soc. London. Ser. A, Math. Phys. Sci.*, 320(1555):379–430.

Blanchet, L. and Schaefer, G. (1989). Higher order gravitational radiation losses in binary systems. *MNRAS*, 239:845–867.

Boetzel, Y., Cho, G., and Gopakumar, A. (2018). *To be published.*

Bohé, A., Marsat, S., and Blanchet, L. (2013). Next-to-next-to-leading order spin-orbit effects in the gravitational wave flux and orbital phasing of compact binaries. Technical Report 13.

Bondi, H., Van der Burg, M., and Metzner, A. (1962). Gravitational waves in general relativity, VII. Waves from axi-symmetric isolated system. *Proc. R. Soc. London. Ser. A. Math. Phys. Sci.*, 269(1336):21–52.

Chatziioannou, K., Klein, A., Cornish, N., and Yunes, N. (2017). Analytic Gravitational Waveforms for Generic Precessing Binary Inspirals. *Phys. Rev. Lett.*, 118(5):051101.

Chatziioannou, K., Klein, A., Yunes, N., and Cornish, N. (2013). Gravitational waveforms for precessing, quasicircular compact binaries with multiple scale analysis: Small spin expansion. *Phys. Rev. D*, 88(6):063011.

Cho, G., Gopakumar, A., Haney, M., and Lee, H. M. (2018). Gravitational waves from compact binaries in post-Newtonian accurate hyperbolic orbits. *Phys. Rev. D*, 98(2).

Cho, G. and Lee, H. M. (2019). Analytic Keplerian-type parametrization for general spinning compact binaries with leading order spin-orbit interactions. *Phys. Rev. D*, 100(4).

Corinaldesi, E. and Papapetrou, A. (1951). Spinning Test-Particles in General Relativity. II. Technical Report 1097.

Damour, T. and Deruelle, N. (1985). General relativistic celestial mechanics of binary systems. I. The post-Newtonian motion. *Ann. Inst. Henri Poincaré Phys. Théor., Vol. 43, No. 1, p. 107 - 132*, 43:107–132.

Damour, T. and Deruelle, N. (1985). General relativistic celestial mechanics of binary systems. I. The post-Newtonian motion. *Ann. l'Institut Henri Poincare*, 43(1):107–132.

Damour, T. and Deruelle, N. (1986). General relativistic celestial mechanics of binary systems. II. The post-Newtonian timing formula. *Ann. Inst. Henri Poincaré Phys. Théor., Vol. 44, No. 3, p. 263 - 292*, 44:263–292.

Damour, T., Gopakumar, A., and Iyer, B. R. (2004). Phasing of gravitational waves from inspiralling eccentric binaries. *Phys. Rev. D*, 70(6):064028.

Damour, T. and Jaranowski, P. (2017). Four-loop static contribution to the gravitational interaction potential of two point masses. *Phys. Rev. D*, 95(8).

Damour, T., Jaranowski, P., and Schäfer, G. (2014). Nonlocal-in-time action for the fourth post-Newtonian conservative dynamics of two-body systems. *Phys. Rev. D*, 89(6):064058.

Damour, T., Jaranowski, P., and Schäfer, G. (2016). Conservative dynamics of two-body systems at the fourth post-Newtonian approximation of general relativity. *Phys. Rev. D*, 93(8):084014.

Damour, T. and Schafer, G. (1988). Higher-order relativistic periastron advances and binary pulsars. *Nuovo Cimento B Serie*, 101:127–176.

Damour, T. and Taylor, J. H. (1992). Strong-field tests of relativistic gravity and binary pulsars. *Phys. Rev. D*, 45:1840–1868.

De Vittori, L., Gopakumar, A., Gupta, A., and Jetzer, P. (2014). Gravitational waves from spinning compact binaries in hyperbolic orbits. *Phys. Rev. D*, 90(12):124066.

Dixon, W. (1977). Dynamics of Extended Bodies in General Relativity. *Proc. Boy. Soc. Lond. A*, 8(3):197–217.

Farr, B., Berry, C. P. L., Farr, W. M., Haster, C.-J., Middleton, H., Cannon, K., Graff, P. B., Hanna, C., Mandel, I., Pankow, C., Price, L. R., Sidery, T., Singer, L. P., Urban, A. L., Vecchio, A., Veitch, J., and Vitale, S. (2016). Parameter estimation on gravitational waves from neutron-star binaries with spinning components. *Astrophys. J.*, 825(2):116.

Faye, G., Blanchet, L., and Buonanno, A. (2006). Higher-order spin effects in the dynamics of compact binaries. I. Equations of motion. *Phys. Rev. D*, 74(10):104033.

Faye, G., Marsat, S., Blanchet, L., and Iyer, B. R. (2012). The third and a half-post-Newtonian gravitational wave quadrupole mode for quasi-circular inspiralling compact binaries. Technical Report 17.

Foffa, S., Mastrolia, P., Sturani, R., and Sturm, C. (2017). Effective field theory approach to the gravitational two-body dynamics at fourth post-Newtonian order and quintic in the Newton constant. *Phys. Rev. D*, 95(10).

García-Bellido, J. and Nesseris, S. (2018). Gravitational wave energy emission and detection rates of Primordial Black Hole hyperbolic encounters. *Phys. Dark Universe*, 21:61–69.

Gergely, L., Perjés, Z. I., and Vasúth, M. (1998). Spin effects in gravitational radiation back reaction. III. Compact binaries with two spinning components. *Phys. Rev. D*, 58(12):124001.

Gergely, L. Á. (1999). Spin-spin effects in radiating compact binaries. *Phys. Rev. D*, 61(2):024035.

Hansen, R. O. (1972). Post-Newtonian Gravitational Radiation from Point Masses in a Hyperbolic Kepler Orbit. *Phys. Rev. D*, 5:1021–1023.

Hinder, I., Herrmann, F., Laguna, P., and Shoemaker, D. (2010). Comparisons of eccentric binary black hole simulations with post-Newtonian models. *Phys. Rev. D*, 82(2):024033.

Hinder, I., Kidder, L. E., and Pfeiffer, H. P. (2018). Eccentric binary black hole inspiral-merger-ringdown gravitational waveform model from numerical relativity and post-Newtonian theory. *Phys. Rev.*, D98(4):044015.

Hopper, S. (2018). Unbound motion on a Schwarzschild background: Practical approaches to frequency domain computations. *Phys. Rev. D*, 97(6):064007.

Hopper, S. and Cardoso, V. (2018). Scattering of point particles by black holes: Gravitational radiation. *Phys. Rev. D*, 97(4):044031.

Huang, L. and Mei, L. (2019). Symplectic integrators for post-Newtonian Lagrangian dynamics. *Phys. Rev. D*, 100(2):024057.

Huang, L. and Wu, X. (2016). Second post-Newtonian Lagrangian dynamics of spinning compact binaries. *Eur. Phys. J. C*, 76(9).

Huerta, E. A., Kumar, P., Agarwal, B., George, D., Schive, H. Y., Pfeiffer, H. P., Haas, R., Ren, W., Chu, T., Boyle, M., Hemberger, D. A., Kidder, L. E., Scheel, M. A., and Szilagyi, B. (2017). Complete waveform model for compact binaries on eccentric orbits. *Phys. Rev. D*, 95(2).

Jaranowski, P. and Schäfer, G. (2015). Derivation of local-in-time fourth post-Newtonian ADM Hamiltonian for spinless compact binaries. *Phys. Rev. D*, 92(12).

Junker, W. and Schaefer, G. (1992). Binary systems - Higher order gravitational radiation damping and wave emission. *MNRAS*, 254:146–164.

Kesden, M., Gerosa, D., O'Shaughnessy, R., Berti, E., and Sperhake, U. (2015). Effective Potentials and Morphological Transitions for Binary Black Hole Spin Precession. *Phys. Rev. Lett.*, 114(8):081103.

Klein, A., Cornish, N., and Yunes, N. (2013). Gravitational waveforms for precessing, quasicircular binaries via multiple scale analysis and uniform asymptotics: The near spin alignment case. *Phys. Rev. D*, 88(12):124015.

Kocsis, B., Gáspár, M. E., and Márka, S. (2006). Detection Rate Estimates of Gravity Waves Emitted during Parabolic Encounters of Stellar Black Holes in Globular Clusters. *ApJ*, 648:411–429.

Königsdörffer, C. and Gopakumar, A. (2005). Post-Newtonian accurate parametric solution to the dynamics of spinning compact binaries in eccentric orbits: The leading order spin-orbit interaction. *Phys. Rev. D*, 71(2):024039.

Königsdörffer, C. and Gopakumar, A. (2006). Phasing of gravitational waves from inspiralling eccentric binaries at the third-and-a-half post-Newtonian order. *Phys. Rev. D*, 73(12):124012.

Lubich, C., Walther, B., and Bruegmann, B. (2010). Symplectic Integration of Post-Newtonian Equations of Motion with Spin. *Phys. Rev. D*, 81(10).

Marchand, T., Bernard, L., Blanchet, L., and Faye, G. (2017). Ambiguity-Free Completion of the Equations of Motion of Compact Binary Systems at the Fourth Post-Newtonian Order. *Phys. Rev. D*, 97(4).

Marchand, T., Blanchet, L., and Faye, G. (2016). Gravitational-wave tail effects to quartic non-linear order. Technical Report 24.

Marchand, T., Henry, Q., Larrouturou, F., Marsat, S., Faye, G., and Blanchet, L. (2020).

The mass quadrupole moment of compact binary systems at the fourth post-Newtonian order. Technical report.

Marsat, S., Bohé, A., Blanchet, L., and Buonanno, A. (2014). Next-to-leading tail-induced spin–orbit effects in the gravitational radiation flux of compact binaries. *Class. Quantum Gravity*, 31(2):025023.

Martin, M. H. (1951). Riemann's Method and the Problem of Cauchy. *Bull. Am. Math. Soc.*, 57(4):238–249.

Mathisson, M. (2010). Republication of: The mechanics of matter particles in general relativity. *Gen. Relativ. Gravit.*, 42(4):989–1010.

Memmesheimer, R.-M., Gopakumar, A., and Schäfer, G. (2004). Third post-Newtonian accurate generalized quasi-Keplerian parametrization for compact binaries in eccentric orbits. *Phys. Rev. D*, 70(10):104011.

Mikkola, S. (1987). A cubic approximation for Kepler's equation. *Celestial Mechanics*, 40:329–334.

Newton, T. D. and Wigner, E. P. (1949). Localized States for Elementary Systems. *Rev. Mod. Phys.*, 21(3):400–406.

O'Leary, R. M., Kocsis, B., and Loeb, A. (2009). Gravitational waves from scattering of stellar-mass black holes in galactic nuclei. *MNRAS*, 395:2127–2146.

Porto, R. A. (2016). The Effective Field Theorist's Approach to Gravitational Dynamics. *Phys. Rep.*, 633:1–104.

Porto, R. A., Ross, A., and Rothstein, I. Z. (2011). Spin induced multipole moments for the gravitational wave flux from binary inspirals to third Post-Newtonian order. *J. Cosmol. Astropart. Phys.*, 2011(3).

Porto, R. A. and Rothstein, I. Z. (2017). Apparent ambiguities in the post-Newtonian expansion for binary systems. *Phys. Rev. D*, 96(2).

Poujade, O. and Blanchet, L. (2002). Post-Newtonian approximation for isolated systems calculated by matched asymptotic expansions. *Phys. Rev. D*, 65(12).

Pryce, M. H. L. (1948). The mass-centre in the restricted theory of relativity and its connexion with the quantum theory of elementary particles. *Proc. R. Soc. London. Ser. A. Math. Phys. Sci.*, 195(1040):62–81.

Racine, É. (2008). Analysis of spin precession in binary black hole systems including quadrupole-monopole interaction. *Phys. Rev. D*, 78(4):044021.

Sachs, R. (1962). Gravitational waves in general relativity VIII. Waves in asymptotically flat space-time. *Proc. R. Soc. London. Ser. A. Math. Phys. Sci.*, 270(1340):103–126.

Schäfer, G. and Jaranowski, P. (2018). Hamiltonian formulation of general relativity and post-Newtonian dynamics of compact binaries. *Living Rev. Relativ.*, 21(1).

Schäfer, G. and Wex, N. (1993). Second post-Newtonian motion of compact binaries. *Physics Letters A*, 174:196–205.

Stairs, I. H. (2003). Testing General Relativity with Pulsar Timing. *Living Reviews in Relativity*, 6:5.

Tanay, S., Haney, M., and Gopakumar, A. (2016). Frequency and time-domain inspiral templates for comparable mass compact binaries in eccentric orbits. *Phys. Rev. D*, 93(6):064031.

Tessmer, M. (2009). Gravitational waveforms from unequal-mass binaries with arbitrary spins under leading order spin-orbit coupling. *Phys. Rev. D*, 80(12):124034.

Tiwari, V., Klimenko, S., Christensen, N., Huerta, E. A., Mohapatra, S. R. P., Gopakumar, A., Haney, M., Ajith, P., McWilliams, S. T., Vedovato, G., Drago, M., Salemi, F., Prodi, G. A., Lazzaro, C., Tiwari, S., Mitselmakher, G., and Da Silva, F. (2016). Proposed search for the detection of gravitational waves from eccentric binary black holes. *Phys. Rev. D*, 93(4):043007.

Tsang, D. (2013). Shattering Flares during Close Encounters of Neutron Stars. *ApJ*, 777:103.

Veitch, J., Raymond, V., Farr, B., Farr, W., Graff, P., Vitale, S., Aylott, B., Blackburn, K., Christensen, N., Coughlin, M., Del Pozzo, W., Feroz, F., Gair, J., Haster, C. J., Kalogera, V., Littenberg, T., Mandel, I., O'Shaughnessy, R., Pitkin, M., Rodriguez, C., Röver, C., Sidery, T., Smith, R., Van Der Sluys, M., Vecchio, A., Vousden, W., and Wade, L. (2015). Parameter estimation for compact binaries with ground-based gravitational-wave observations using the LALInference software library. *Phys. Rev. D*, 91(4):042003.

Walker, M. and Will, C. M. (1979). Relativistic Kepler problem. I. Behavior in the distant past of orbits with gravitational radiation damping. *Phys. Rev. D*, 19:3483–3494.

Wex, N. (1995). The second post-Newtonian motion of compact binary-star systems with spin. *Class. Quantum Gravity*, 12(4):983–1005.

Whittaker, E. and Watson, G. (2009). *A course of modern analysis: an introduction to the general theory of infinite processes and of analytic functions; with an account of the principal transcendental functions (3rd edition, 1920).*

요 약

정확한 중력파 파형을 빠르게 추출해내는 일은 이론과 관측 모두에게서 중요하다. 포스트-뉴토니안 (PN) 이론은 쌍성계의 운동과 그로부터 방출되는 중력파의 파형을 계산하는 데에 유일한 해석적 방법론을 제공한다. 그러나 긴 시간의 중력파 파형을 얻기 위해서 적분 가능하지 않는 포스트-뉴토니안 운동방정식을 풀어야하는 것은 자명한 일이 아니다. 이것을 해결하기 위해, 준 케플러 매개화와 상수 변분법이 널리 도입된다. 본고를 통해서, 우리는 다음의 세 가지 경우에 대하여 준 케플러 매개화와 중력파 파형을 계산하는 효율적인 알고리즘을 제공한다.

첫째로, 우리는 자전하지 않는 밀집 쌍성계의 타원 궤도 운동에 대하여, 네번째 섭동 정확도 (4PN)로 준 케플러 매개화를 유도하였다. 이에 바탕이 되는 운동 방정식은, Arnowitt-Deser-Misner (ADM) 좌표계에서 유도된, 시간에 국소적인 4PN 해밀토니안에 의해 기술되었다. 우리는 쌍성계의 타원 궤도를 기술하는 요소들을 에너지, 각운동량 그리고 질량비에 의존하는 명시적인 매개화의 형태로 제공한다. 그 결과, 우리가 구한 해는 적당한 이심율을 가지는 타원 궤도의 쌍성계가 서로 가까워지다가 하나로 충돌하는 전과정을 기술하는데 응용된다.

둘째로, 우리는 ADM 좌표계에서 자전하는 쌍성계의 보존 운동에 대한 완전한 준 케플러 매개화를 제공한다. 이 해는 임의의 이심율, 질량비 그리고 자전 각운동량의 일반적인 구성에 대해, 자전에 의한 효과의 일차 근사하에, 운동을 기술할 수 있다. 우리의 결과에 따라서 중력파 파형은 높은 정확도로 빠르게 계산될 수 있다.

세번째로, 우리는 세번째 섭동 정확도로 자전하지 않는 밀집 쌍성계의 쌍곡선 충돌에 대한 준 케플러 매개화를 유도하였다. 우리는 쌍성계의 쌍곡선 궤도를 기술하는 요소들을 에너지, 각운동량 그리고 질량비에 의존하는 명시적인 매개의 표현을, ADM 좌표계와 harmonic 좌표계에서 제공한다. 우리는 또한 이전에 독립적으로 계산된 타원 궤도의 해를 이용한 검산을 제공한다. 우리의 준 케플러 매개 해를 이용하여 쌍곡선 궤도에서 방출되는 중력파의 파형을 3.5PN 정확도로 계산한다. 그리고 마지막으로 우리의 결과를 개선할 수 있는 방법들에 대해서도 의논한다.

주요어: 포스트-뉴토니안 이론– 밀접성 쌍성계의 동역학 – 중력파

학 번: 2014-21341